NBSIR 87-3575

Measurement of the Setting Time and Strength of Concrete by the Impact-Echo Method

Stephen P. Pessiki
Nicholas J. Carino

U.S. DEPARTMENT OF COMMERCE
National Bureau of Standards
National Engineering Laboratory
Center for Building Technology
Structures Division
Gaithersburg, MD 20899

July 1987

U.S. DEPARTMENT OF COMMERCE

NATIONAL BUREAU OF STANDARDS

NBSIR 87-3575

MEASUREMENT OF THE SETTING TIME AND STRENGTH OF CONCRETE BY THE IMPACT-ECHO METHOD

Stephen P. Pessiki
Nicholas J. Carino

July 1987

ABSTRACT

   Tests were performed to evaluate the feasibility of using the impact-echo method to determine setting time and monitor strength development of concrete. In the impact-echo method, the test object is subjected to point impact and the surface displacement adjacent to the impact point is monitored. From the measured displacement waveform and the thickness of the object, the P-wave velocity is determined. Changes in the P-wave velocity with time reveal information about the development of mechanical properties.

   Setting time tests were made on concrete mixtures of two water-cement ratios and with and without set-controlling admixtures. A strong correlation was found between the time of initial setting of mortars sieved from the concrete, as determined by penetration resistance (ASTM C 403), and the time when the P-wave velocity began to increase. Two approaches for using the impact-echo method to define the setting time of concrete are presented.

   Tests were performed to examine the relationship between P-wave velocity, as determined by the impact-echo method, and the compressive strength of concrete. At early ages (up to about 3 days at standard temperature), the relationship was independent of curing temperature and water cement ratio.

   It is concluded that the impact-echo method is a promising technique for nondestructively monitoring the development of mechanical properties in concrete from initial setting to ages of several days.

KEYWORDS: Concrete; compressive strength, early-age, impact-echo method, nondestructive testing, mortar, setting time, wave propagation.

TABLE OF CONTENTS

LIST OF TABLES

LIST OF FIGURES

CHAPTER 1
INTRODUCTION

1.0 INTRODUCTION

The purpose of this research was to evaluate a new test method for measuring the setting time and strength of concrete. The technique uses transient stress waves and is called the impact-echo method. This technique has previously been used for flaw detection in hardened concrete (10,31). In this method, stress waves are introduced into a test object by mechanical impact on its surface. The multiple reflections (echoes) of the stress waves from the boundaries of the object are monitored and used to determine the wave velocity. The change in wave velocity with age is related to setting and strength gain.

1.1 BACKGROUND

Upon initial mixing, fresh concrete is a fluid-like material. Through the physical and chemical processes collectively termed hydration, the fresh concrete gradually changes from this fluid-like material into a hardened mass. Figure 1.1 is an idealization of the early-age strength development of concrete. As can be seen in the figure, strength gain does not begin immediately after mixing. Instead, there is an induction period, during which the concrete remains fluid-like. After this induction period the concrete gradually increases in stiffness. This increase in stiffness occurs during what is known as the setting period. By the end of the setting period the concrete has changed to a rigid state, but still has little appreciable strength. Appreciable strength gain begins during the hardening period, after setting has occurred.

Setting is a gradual stiffening process, and it is difficult to define precisely when setting begins and when it has ended. The practical approach that has been adopted in standard test methods is based on monitoring the development of resistance to penetration by specified test needles. The times required to reach different levels of penetration resistance are used to define initial and final setting times of paste or mortar specimens. Since arbitrary levels of penetration resistance are used in these definitions, the setting times correspond to arbitrary levels of stiffening rather than to the start and end of some physical or chemical process. However, setting times based on penetration resistance are very useful in studying the effects of pertinent factors on the setting behavior of cementitious systems. The technique addressed by this research is an alternative to tests based on penetration resistance.

The need for being able to measure the setting time of concrete in-place can be understood with reference to Figure 1.1. Shown in the figure as a dashed line is a similar strength development curve, but with a delayed setting time. Such a delay could be caused by reduced temperature or by chemical admixtures. It is seen that the delay in setting also causes a delay in the subsequent strength gain and may have a great effect on the value of strength at a very early age. As an example, consider the strengths indicated by each curve at the time, t_1, indicated with a dashed line in the figure. Although the shapes of the two strength development curves are similar, the

1

concrete with a delayed setting time has a much lower strength at this age. Thus, detection of an unexpected delay in setting time may influence early construction operations such as the time of formwork removal, slipforming, or transfer of prestressing. Further, the ability to measure concrete setting times in-place can be used as a means of quality control when set-controlling admixtures are being used. The ability to determine when a concrete has set can also be used to reduce formwork pressures from freshly placed concrete. Pressures on tall wall forms can be reduced if earlier placed lifts have set prior to the placement of later lifts. Lastly, the ability to monitor the setting behavior of concrete may be used to determine when finishing operations can proceed.

Currently, there is no standard test (either a field or a laboratory test) for measuring the setting time of concrete that is performed on the concrete itself. The existing concrete setting time test, ASTM C 403 Standard Test Method for Time of Setting of Concrete Mixtures by Penetration Resistance (3), is performed on mortar sieved from the concrete. The resistance offered by the sieved mortar to penetration by various diameter needles is measured. Initial and final setting times are defined by penetration resistances of 500 and 4000 psi (3.5 and 27.6 MPa), respectively. Clearly, any definition of setting time based on some measure of strength (whether performed on paste, mortar, or concrete) must be arbitrary, because the strength development is a gradual process.

The penetration resistance setting time test is based on a soil testing technique adapted by Tuthill and Cordon for studying retarding admixtures (35) in concrete. Tuthill and Cordon concluded that the vibration limit of concrete, or point during the setting process when it can no longer be made plastic by revibration, is reached when the sieved mortar reaches a penetration resistance of 500 psi. Further, they concluded that at a penetration resistance of 4000 psi, the accompanying concrete had a strength of about 100 psi. The 4000 psi penetration resistance was the limit of their penetration device.

There are two limitations to using the penetration resistance test to define the setting time of concrete. First, the test is not performed on the concrete itself. Differences between the behavior of the concrete and sieved mortar are reported in Chapter 4. Second, it is not an in-place test, but is performed on small prepared specimens. Such specimens generally do not experience the same temperature and moisture conditions as the concrete in the structure, and thus are not necessarily representative of the concrete in the structure.

The ability to determine in-place concrete strength can be used to improve construction safety and economy. Reliable measurements of in-place strength can be used to determine when it is safe to remove formwork, transfer prestressing, apply post-tensioning, and to terminate curing. In-place strength information allows each of these operations to begin safely at the earliest possible time, leading to more economical and efficient construction.

Because of the importance of these safety and economic considerations, many methods of estimating in-place strength already exist. These methods include; rebound hammer (ASTM C 805), probe penetration (ASTM C 803), pullout (ASTM C 900), ultrasonic pulse velocity, maturity (recently adopted as an ASTM Standard Test Method), and cast-in-place cylinders (ASTM C 873) (3). A review of each of these methods, discussing their underlying principles and limitations can be found in Reference (1). As will be explained, the

impact-echo method offers another alternative means for estimating concrete strength at early ages.

1.2 OBJECTIVES OF RESEARCH

The objectives of this study project were to experimentally evaluate the usefulness of the impact-echo technique as a means to;

1. define and measure the setting time of concrete
2. estimate the strength of concrete

The work is presented as a first step towards reliable in-place setting time measurement and strength estimation tests for concrete using the impact-echo method.

1.3 SCOPE

Chapter 2 reviews previous work that used stress wave propagation to monitor the setting behavior and strength gain of concrete.

Background information is presented in Chapter 3. The experimental set-up and technique for making impact-echo velocity measurements is described, and the fundamentals of wave propagation in elastic solids are reviewed. As will be discussed, the setting time and strength experiments were performed using cylindrical concrete specimens. Thus, Chapter 3 also discusses the vibrations of a cylinder caused by impact. The importance of the frequency content of the impact on the resulting cylinder vibrations is examined.

Chapter 4 presents the results of the setting time study. The adaptation of the impact-echo technique for measurements on early-age mortar and concrete is discussed. Results of impact-echo velocity measurements made on prepared mortar and concrete specimens are presented. In these tests, the development of wave velocity was monitored from the time of initial casting up to ages of about 12 hours. A simple model is used to explain the wave velocity in the concrete in terms of the velocities in the paste and aggregate. Two approaches for using the impact-echo method to define and measure the setting time of concrete are presented.

Chapter 5 presents the results of the compressive strength study. The influence of changes in curing temperature, water to cement (w-c) ratio, and aggregate content on the relationship between compressive strength and wave velocity are discussed. As will be discussed, strength-velocity tests were made as early as 6 hours after initial mixing and continued up to an age of about 28 days.

Chapter 6 summarizes the important results and conclusions of the research, discusses applications, and outlines future research needs.
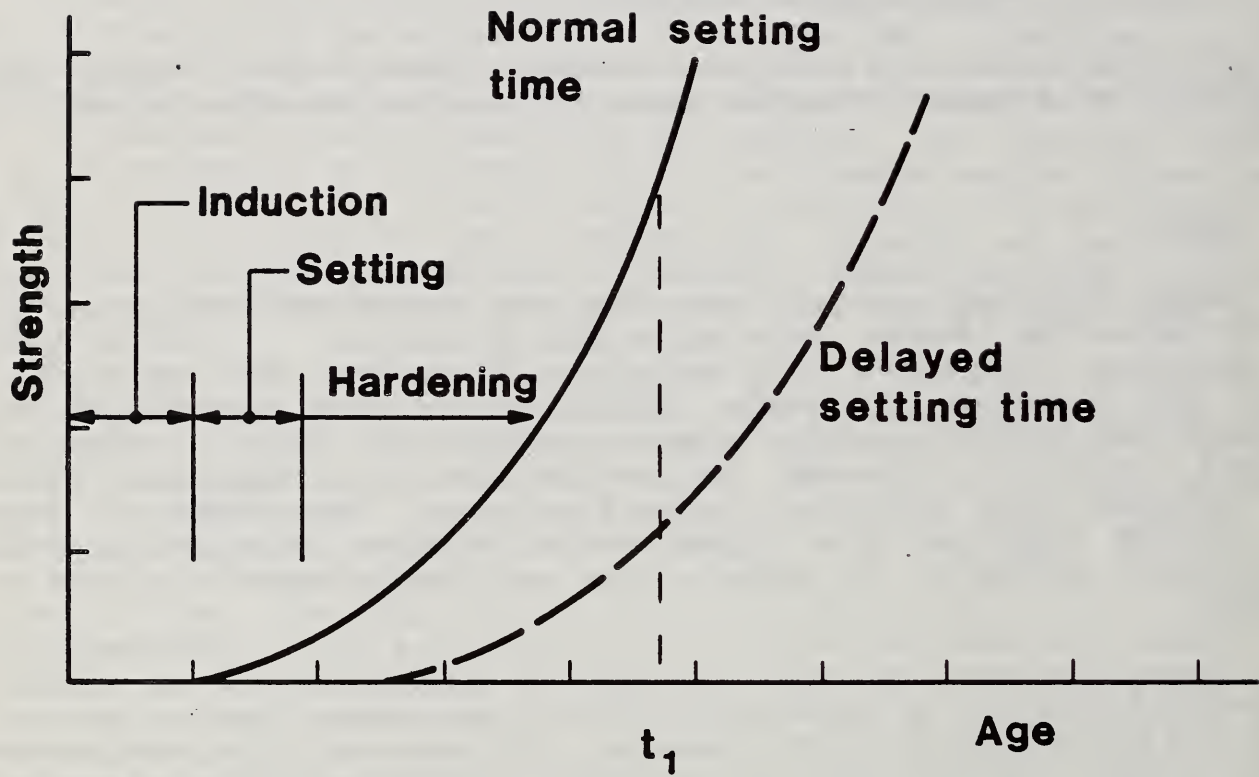
Figure 1.1   Idealization of the early-age strength development of concrete

CHAPTER 2
LITERATURE REVIEW

2.0 INTRODUCTION

Stress wave propagation has been used in the past to study the setting behavior and strength gain of concrete. The testing method used is the ultrasonic pulse velocity technique, which can briefly be described as follows. A pulse, or short train of stress waves, is introduced into a test object at one surface by a transmitting transducer (source). The arrival of this pulse is detected at a second location with a receiving transducer (receiver). The time interval between the initiation and reception of the pulse is measured, and the pulse velocity is determined by dividing this time interval by the known distance between the source and the receiver.

The present study uses a stress wave propagation method known as the impact-echo technique, which differs from the pulse velocity technique in the following manner. The pulse velocity technique is a through transmission method; the source and receiver are generally located on opposite sides of a test object. In the impact-echo technique, the source and receiver are located on the same surface of the test object. Stress waves are introduced at the source. The periodicity of multiple reflections of these stress waves within the boundaries of the test object, along with the dimensions of the object, are used to calculate wave velocity.

The two methods are similar in that both are stress wave propagation testing techniques. Thus, this chapter reviews previous work that used the ultrasonic pulse velocity method to monitor setting behavior and strength gain of concrete. Section 2.2 reviews work related to setting behavior, and Section 2.3 reviews work related to compressive strength.

2.1 PULSE VELOCITY AND SETTING

Many attempts were reported in the late 1940's and early 1950's on the measurement of pulse velocity in early-age concrete (4,14,15,19,20,21,38). These investigations examined the influence of variables such as mixture proportions, curing temperature, etc. on the development of pulse velocity. It was not until 1957 that the penetration resistance test (ASTM C 403) became a standard test method for measuring the setting time of concrete. Thus most of these early studies compared the results of pulse velocity measurements to setting time measurements performed on cement pastes. More recent work (12) has compared the development of pulse velocity and penetration resistance in mortar sieved from concrete.

Jones (19,20) and Arndt (4) reported some of the earliest attempts to monitor the development of pulse velocity in concrete. From the results presented by Jones it appears the earliest measurements were obtained at about 10 hours after initial mixing, and the corresponding pulse velocities ranged from 1200 to 1600 m/s. As will be shown in Chapter 4, the values of these earliest measurements are high compared to the earliest measurements obtained in the present study.

Arndt presented curves showing the development of pulse velocity in concretes made with three different cements and cured at two different temperatures. He reported that the pulse velocity-age curves reflect the

5

influence of temperature on setting time, as well as differences in setting times occurring between the different cements. Arndt did not evaluate the curves insofar as defining a setting time, but presented them to show the usefulness of the pulse velocity method as a means of "describing the processes" occurring during setting.

One of the earliest reported efforts specifically directed at evaluating the usefulness of the pulse velocity method as a means of determining the setting time of concrete was reported by Whitehurst (38). Whitehurst monitored the development of pulse velocity for several concretes, and compared the results with setting times of cement pastes determined by Gillmore needles (ASTM C 266) (2). Whitehurst used 100 mm x 100 mm x 400 mm beam specimens, the 400 mm dimension being the transmission length. The concrete mixtures were very stiff with slumps ranging from 3 to 6 mm. The stiff mixtures were used so that the ends of the beam molds could be removed after casting and the transmitting and receiving transducers placed directly against the fresh concrete. Even with these stiff mixes, successful measurements could not be made for the first two to four hours after mixing, depending on the cement used. Figure 2.1 shows typical results from Whitehurst's experiments. Whitehurst measured initial velocities of 1200 m/s. He reported that during the period from 4-1/2 to 8-1/2 hours after initial mixing there was a rapid increase in pulse velocity. After this period of dramatic increase, there was a decrease in the rate of velocity increase. The elapsed time from initial mixing to when the rate of velocity increase slowed was taken by Whitehurst as the setting time of the concrete. These setting times were in good agreement with setting times measured using the Gillmore needles. Whitehurst also reported that in all tests the signals received during the setting period (first 8 hours) were very weak. Attempts to perform the tests on concretes with wetter consistencies were unsuccessful because cracks developed in the beams when the end plates of the forms were removed.

Cheesman (14,15) also reported results from a study of the development of pulse velocity with time in concrete. Cheesman tested 100 mm slump concretes placed in 100 mm x 100 mm x 510 mm molds. Measurements were made through the 100 mm dimension as early as 10 minutes after mixing. The transmitting and receiving transducers were placed against rubber windows fitted into the specimen molds. Cheesman noted that the use of these windows lowered the measured pulse velocities. For the concretes tested, the pulse velocity did not increase as rapidly, or stop increasing as abruptly as observed by Whitehurst. Cheesman stated that because of this more gradual development of pulse velocity, it was difficult to correlate inflection points in the pulse velocity development curves to setting time measurements made on cement pastes with Vicat needles (ASTM C 191) (2).

Casson and Domone (12) monitored the development of pulse velocity and penetration resistance in mortar sieved from concrete. Pulse velocities were determined through a 30 mm path length. While detailed comparisons were not presented, Casson and Domone concluded that the effectiveness of admixtures on setting times could be assessed using pulse velocity measurements. In addition, they reported results of pulse velocity measurements through concrete, using a 300 mm path length. They reported that it was only after hydration created a "semi-viscous/plastic paste matrix" that successful measurements could be made. The earliest measurements made ranged from 1000 to 2000 m/s.

6

2.2 PULSE VELOCITY AND COMPRESSIVE STRENGTH

Many researchers have studied the relationship between pulse velocity and compressive strength. In these studies, the effect of the following variables on the pulse velocity-compressive strength relationship have been investigated:

- curing temperature
- content, type, and maximum size of coarse aggregate
- water to cement (w-c) ratio
- moisture content
- air content

A report by Sturrup, Vecchio, and Caratin (33) provides a comprehensive review of these investigations. The following sections focus on work performed to study the effects of curing temperature, w-c ratio, and aggregate content, type, and size.

2.2.1 Curing Temperature

The work by Elvery and Ibrahim (16) is probably the most extensive recent investigation into the variables influencing the relationship between pulse velocity and early-age compressive strength. The experiments were performed using 100 mm cubes. The cubes were placed in curing cabinets immediately after casting to allow them to reach the specified temperature as quickly as possible.

To compare the influence of different variables upon the pulse velocity-compressive strength relationship, the test data were divided into four ranges, and separate statistical analyses were made for each range. The four ranges were delineated at the following compressive strengths: range A, 0.05 to 0.30 MPa; range B, 0.30 to 2.00 MPa; range C, 2.00 to 15.00 MPa; range D, 15 to 60 MPa.

Elvery and Ibrahim concluded that curing temperature does not influence the relationship between pulse velocity and compressive strength in ranges C and D, but that temperature did have some influence in ranges A and B.

Sturrup, Vecchio, and Caratin (33) presented pulse velocity-strength curves for concretes cured at 10, 21, and 32 °C. They concluded that curing temperature does affect the pulse velocity-compressive strength relationship, but they did not generalize about how it affects the relationship.

The results of these studies seem to show that the influence of curing temperature upon the pulse velocity-compressive strength relationship is uncertain.

2.2.2 Water-Cement Ratio

The relationship between pulse velocity and compressive strength has been found to be independent of w-c ratio (8,9,16,21). Elvery and Ibrahim (16) reported that changes in w-c ratio had even less influence on the pulse velocity-compressive strength relationship than changes in curing temperature. Jones (21) pointed out that an increase in w-c ratio increases the number of water voids present in concrete. These voids decrease both

7

compressive strength and pulse velocity, and the relationship between the two apparently is unchanged.

2.2.3 Content, Type, and Maximum Size of Coarse Aggregate

It is clear from the results of previous work that an increase in aggregate content produces a higher pulse velocity for a given compressive strength (6,16,19,21). Since normal weight coarse aggregate has a higher elastic modulus than cement paste (for moderate w-c ratios), increasing the aggregate content of concrete would be expected to increase the pulse velocity. This is discussed further in Section 4.3.

Changes in pulse velocity-compressive strength relationships caused by changes in aggregate type have been reported (21,33). An aggregate with a higher elastic modulus can be expected to lead to a higher pulse velocity for a given aggregate content.

Many researchers have reported that concretes made with a larger maximum aggregate size exhibit a lower compressive strength for a given pulse velocity (6,8,9,33). Bullock and Whitehurst (6) demonstrated this for concretes tested at an age of 28 days. This effect, however, was attributed largely to an increased percentage of coarse aggregate in a properly proportioned concrete when a larger size aggregate is used, leading to a higher velocity. Byfors (8) reported that this effect is greater at earlier ages than later ages.

2.3 SUMMARY

It is apparent that one difficulty encountered in using the ultrasonic pulse velocity technique to monitor the setting behavior of concrete is that it is difficult to make measurements at very early ages. It appears that a certain degree of hydration is needed before successful measurements can be made. There does appear to be some correlation between the development of pulse velocity in concrete and the results of setting time tests performed on cement pastes.

The influence of changes in curing temperatures on the relationship between pulse velocity and compressive strength is uncertain. The pulse velocity-compressive strength relationship has been found to be independent of w-c ratio, and an increase in aggregate content was found to lead to higher pulse velocity for a given compressive strength. Lastly, an aggregate with a higher elastic modulus will lead to higher pulse velocity for a given aggregate content.
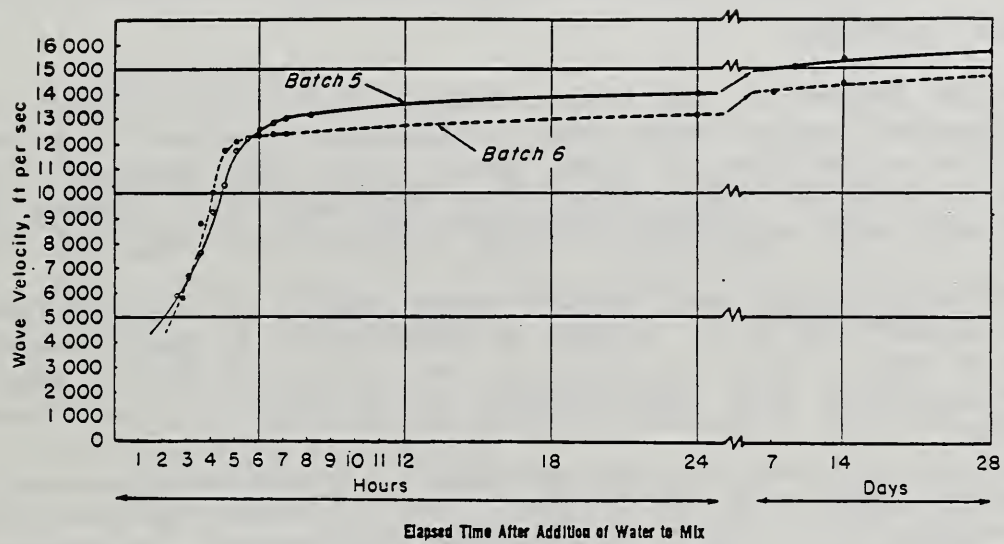
Figure 2.1   Development of pulse velocity with time (38).

9

CHAPTER 3
BACKGROUND

3.0 INTRODUCTION

This chapter presents background information needed for the remainder of the report. The experimental technique for making impact-echo measurements is explained in Section 3.1; adaptation of the method for use on early age concrete is discussed in Chapter 4. The setting time and strength experiments were performed using cylindrical concrete specimens. In order to interpret the impact-echo measurements, the vibration of a cylinder caused by impact has to be understood; this is explained in Section 3.2. In Section 3.2 it will be seen that one of the factors that determines the velocity of stress waves within a solid is the elastic modulus. Therefore, Section 3.3 discusses the development of elastic modulus in cement paste.

3.1 IMPACT-ECHO TECHNIQUE

As stated in Chapter 1, the test technique used in this study involves introducing transient stress waves into a cylindrical specimen by mechanical impact. Multiple reflections of these waves within the boundaries of the cylinder were monitored and used to calculate wave velocity. Changes in this wave velocity with age were monitored and related to setting and strength gain.

The impact sources were small steel spheres ranging in diameter from 5.56 to 12.7 mm (0.22 to 0.50 in.). To make a measurement, a sphere was dropped from a height of 200 mm (7.9 in.) onto the top surface of the cylinder. The stress waves introduced into the cylinder by the impact are discussed in Section 3.2.1.1.

The resulting vibrations were monitored with a receiving transducer, also located on the top surface of the cylinder. The transducer used in the study is shown in Figure 3.1. It is a broadband displacement transducer that responds to normal surface displacement (29). The transducer was originally developed for acoustic emission testing of metals, so a thin lead strip was inserted between the piezoelectric element and the cylinder surface to complete the transducer circuit.

The time-history of the surface displacement detected by the transducer is called a displacement waveform. Figure 3.2 (a) shows a typical displacement waveform obtained from a 152 mm diameter by 152 mm deep hardened concrete cylinder. The waveform is a digital record comprised of 1024 points recorded at a sampling frequency of 500 kHz (sampling interval of 2 us). Thus the duration of the recorded response is 1024 x 2 us = 0.002048 seconds.

The waveform in Figure 3.2 (a) is composed of the surface displacement plus a low frequency oscillation attributed to the resonance of the transducer. The effects of transducer resonance can be reduced by using a high pass filter, which strongly attenuates that part of a signal below a specific threshold frequency. A filter was used in some instances in the setting time and strength studies, and is discussed further in those respective chapters.

Multiple reflections of stress waves from the boundaries of the cylinder give the displacement waveform shown in Figure 3.2 (a) a periodic nature. The

periodicity of the reflections contained in the waveform was revealed by transforming the time-domain waveform into the frequency domain using the principle of the Fourier transform (32). The principle behind the transformation is that the displacement waveform can be constructed by the superposition of sine curves of varying amplitudes and frequencies, with appropriate phase shifts. The transformation of the waveform in Figure 3.2 (a) results in the frequency spectrum shown in Figure 3.2 (b). The frequencies of the large amplitude sine curves in the displacement waveform appear as large amplitude peaks in the frequency spectrum. Thus, peaks in the frequency spectrum reveal the frequencies of the multiple reflections within the cylinder. As will be explained in Section 3.2.3, the peak with the lowest frequency in the spectrum (above the peak attributed to transducer resonance) and the specimen height were used to compute the velocity of stress waves within the specimen. The transformation from the time domain to the frequency domain was made using the Fast Fourier Transform (FFT) technique (32).

In digital signal analysis, the frequency interval in the frequency spectrum, Δf (difference between adjacent frequency values), is

$$\Delta f = f_S / N \hspace{4cm} (3.1)$$

where f_S is the sampling frequency. N is the number of points in the record, which is dependent on the data acquisition device. Thus, as the sampling frequency increases (providing greater resolution in the displacement waveform), for a fixed value of N, the frequency interval in the frequency spectrum increases. For the example in Figure 3.2, the frequency interval is 500 kHz/1024 = 0.488 kHz.

A unity gain amplifier which was connected close to the transducer was used. This amplifier allowed the signal produced by the transducer to be measured without reducing its voltage.

The experimental set-up is shown in Figure 3.3. Data acquisition and processing, such as the FFT, were done using a digital processing oscilloscope with a maximum sampling frequency of 500 kHz. The oscilloscope was equipped with two disk drives for permanent data storage, and was interfaced with a plotter so that displacement waveforms and frequency spectra could be plotted.

3.2 VIBRATION OF A CYLINDER CAUSED BY IMPACT

Interpretation of the impact-echo tests on cylindrical concrete specimens requires an understanding of the response of a cylinder to impact. An unsupported cylinder has stress free surfaces and would be able to vibrate freely in space. Clearly, this condition can not be realized in the laboratory, because the cylinder must be supported in some manner. As a result, certain boundary displacements are constrained and surface stresses can arise. However, support can be provided in such a way that effects on the resulting vibrations are negligible, and vibrations can thus be considered to approximate those of a free cylinder.

To understand the response of a cylinder during an impact-echo test requires an understanding of impact. Thus, Section 3.2.1 discusses the details of impact, examining the stress waves generated by impact, as well as

11

the force-time function, contact time, and frequency content of impact between a sphere and a solid. To help understand the response of a cylinder to impact, previous experimental work studying the mode shapes and frequencies of vibration of solid cylinders under the action of constant driving frequencies is reviewed in Section 3.2.2. Section 3.2.3 reports the results of an experimental investigation into the vibration of a cylinder during the impact-echo test, examining the effects of the frequency content of the impact on the resulting vibrations.

3.2.1 Elastic Impact on a Solid

3.2.1.1 Stress Waves Generated by Impact

Three types of waves are generated by impact on the surface of an elastic solid; a surface wave, a dilatational wave, and a distortional wave. The surface wave, also known as the Rayleigh or R-wave, propagates along the surface of the solid, whereas the dilatational and distortional waves propagate into the solid. Dilatational waves are also known as primary or P-waves, and distortional waves are also known as secondary, shear or S-waves. The shape of the wavefronts of each wave type depends upon the impact source. For the point source impact considered in this study, the P- and S-waves radiate from the impact point into the solid along spherical wavefronts, while the R-wave propagates along the surface in a circular pattern. The wavefronts associated with each wave type caused by point impact are shown schematically in Figure 3.4.

Each type of wave can be characterized by the direction of particle motion of the medium through which the wave is propagating, relative to the direction of wave propagation. In P-waves, particle motion is parallel to the direction of wave propagation, as illustrated in Figure 3.5 (a). P-waves are associated with either tensile or compressive stresses parallel to the propagation direction. S-waves are characterized by particle motion transverse to the direction of wave propagation, as illustrated in Figure 3.5 (b). S-waves are associated with shearing stresses, and thus cannot propagate through a medium with zero shear rigidity. In R-waves, the particles move in an elliptical pattern as the wave propagates along the surface of the solid. This is illustrated in Figure 3.5 (c).

The velocity of propagation of stress waves through an infinite elastic medium depends upon the elastic modulus of the material E, Poisson's ratio v, and the material density ρ. The P-wave velocity can vary depending on the dimensions of the solid relative to the wavelength of the propagating wave. In an infinite elastic solid, the P-wave velocity C_p is given (34) by the equation

$$C_p = \sqrt{\frac{E(1-v)}{(1+v)(1-2v)}} \qquad (3.2)$$

For rod-like structures free to expand laterally, the stress component

12

perpendicular to the axis of the rod becomes negligible, and the P-wave velocity approaches what is termed the longitudinal rod velocity (34),

$$c_p = \sqrt{\frac{E}{\rho}} \ .$$
(3.3)

The S-wave velocity in an infinite elastic medium, c_s, is given (34) by the equation

$$c_s = \sqrt{\frac{G}{\rho}}$$
(3.4)

The shear rigidity G can be written as

$$G = \frac{E}{2 \ (\ 1 + \upsilon \ )}$$
(3.5)

Thus, the S-wave velocity is given by the equation

$$c_s = \sqrt{\frac{E}{2 \ \rho \ (\ 1 + \upsilon \ )}}$$
(3.6)

The ratio of S- to P-wave velocities can be expressed in terms of Poisson's ratio as

$$\frac{c_s}{c_p} = \sqrt{\frac{(\ 1 - 2 \upsilon \ )}{2 \ (\ 1 - \upsilon \ )}}$$
(3.7)

The R-wave velocity, c_r, is approximated (37) by the equation

$$c_r = \frac{0.87 + 1.12 \ \upsilon}{1 + \upsilon} \ c_s$$
(3.8)

In early age concrete, the values of E and υ are changing continuously with time. Hence c_p, c_s, and c_r, and their relative values are also changing with time. However, as stated in the introduction, the purpose of this

13

section is to provide a basic understanding of the vibration of a cylinder caused by impact. Attention is thus focused on a hardened concrete cylinder. It has been shown that the principles of elastic wave propagation can be applied to hardened concrete (31).

The P-wave generated by impact on the surface of a concrete cylinder initially propagates as a compression wave. When this wave is incident on a free surface, reflection occurs. The stresses associated with a reflected P-wave change sign, i.e., a P-wave propagating as a compression wave is reflected as a tension wave, and a tension wave is reflected as a compression wave. In addition to the reflected P-wave, an incident P-wave also generates an S-wave by a process called mode conversion. Similarly, an S-wave incident on a free surface is reflected as an S-wave and a mode converted P-wave. A more complete discussion of the reflection and mode conversion of stress waves can be found in References (23) and (24).

3.2.1.2 Force-Time Function and Contact Time of the Elastic Impact of a Sphere on a Plate

The impact of interest is that of steel spheres, ranging in diameter from 5.56 to 12.7 mm, dropped onto the surface of a cylindrical concrete specimen.

The elastic impact of a sphere on a solid can be described using the Hertz theory of elastic impact. In this theory, the force-time function of the impact is a half-cycle sine curve (17):

$$F(t) = F_{max} \sin\left(\frac{\pi t}{t_c}\right) \quad ; \quad 0 \leq t \leq t_c \tag{3.9}$$

Fmax is the maximum force exerted during the impact, and t_c is the contact time of the impact. This force time function is shown in Figure 3.6.

Using Hertz elastic theory, it has been shown that for E and for hardened concrete with a P-wave velocity of 4000 m/s (36 x 10^9 N/m^2 (5.2 x 10^3 psi) and 0.2), the contact time of a steel sphere dropped onto a concrete specimen is (31)

$$t_c = 0.00858 \, R \, / \, (h)^{0.1} \tag{3.10}$$

where R is the radius of the sphere and h is the drop height, both in meters. Thus the contact time is directly proportional to the sphere diameter, and relatively insensitive to changes in drop height. Experimental contact times may be longer than predicted by eq. (3.10) because of inelastic behavior in the concrete. The inelastic behavior can result from local crushing of the cement paste at the point of impact.

3.2.1.3 Frequency Content of Impact

Using the Fourier transformation, the force-time function in Figure 3.6 is equivalent to the summation of continuous sinusoidally varying force-time functions with different frequencies. Thus a range of frequencies is imparted into an object by impact. The frequency content of this force-time function is revealed by examination of its frequency spectrum as shown in Figure 3.7 (31). The amplitude and frequency axes of the spectrum are expressed in terms of the contact time. It is seen that there are "zeroes" in the frequency spectrum, occurring at frequencies of $1.5/(t_c)$, $2.5/(t_c)$, etc. The most significant contributions of energy imparted by the impact are at frequencies below the first zero in the spectrum. Using Figure 3.7, the frequency content for a given contact time can be determined. For example, for a 60 us contact time, the first zero in the frequency spectrum occurs at $1.5/(60$ us$) = 25$ kHz. It can be seen that as the contact time becomes shorter (smaller sphere), the range of frequencies containing significant energy increases. As will be shown in Section 3.2.3, the frequency content of the impact determines the modes of vibration that can be excited.

3.2.2 Mode Shapes of Vibration of a Free Cylinder

When a cylinder is subjected to impact it will vibrate. As it vibrates, each frequency of vibration has associated with it a deformed shape, or mode shape. The response of the cylinder to impact is the superposition of each of these mode shapes. Theoretically, a cylinder of given dimensions has an infinite number of mode shapes. An understanding of the modes of vibration of a cylinder is helpful in interpreting the results of the impact-echo tests.

An experimental study of the mode shapes and natural frequencies of vibration of solid, isotropic, elastic cylinders was performed by McMahon (25). McMahon was able to experimentally determine the frequency and approximate mode shapes of 20 of the lowest 22 modes of vibration of solid aluminum and steel cylinders. McMahon studied 3- and 4-in. diameter cylinders with thickness to radius ratios (T/r) ranging from 0.201 to 3.29 for aluminum, and 0.205 to 2.48 for steel. In the discussions to follow, the T/r ratio is referred to as the aspect ratio. The cylinders were placed on a 2 in. diameter cylindrical ceramic shell and driven at various frequencies. In order to determine the approximate mode shapes of vibration, McMahon sprinkled fine sand on the top surface of the cylinder, and statically charged lucite shavings on the vertical surface. When the cylinder was driven at a natural frequency, the sand and lucite particles moved to the locations of nodes which are locations of minimum velocity.

Figure 3.8, from McMahon, shows the approximate form of vibration of 20 of the first 22 modes of vibration. Solid lines in the plan sketches of the top surfaces indicate the approximate locations of nodal lines, and arrows indicate the directions traced by sand particles during the vibration. The dashed lines in the cross-sections indicate the approximate mode shapes. Modes are grouped by their circumferential order n, or degree of symmetry with respect to rotation about the axis of the cylinder. The first mode of vibration was identified by McMahon as the flexural mode, and the second mode as the longitudinal or rod mode.

15

Figure 3.9, adapted from McMahon, shows the experimentally determined frequencies of the first six modes of circumferential order 0 (symmetric about the axis of the cylinder) for various aspect ratios of the aluminum and steel cylinders. Frequencies are expressed as a dimensionless frequency parameter $\omega r/C$, where C is the longitudinal rod velocity. From this figure it is seen that the fundamental mode (lowest frequency mode) of vibration changes with the aspect ratio. For a small aspect ratio, i.e., a thin disk, the flexural mode (mode 1) is the fundamental mode of vibration. Above an aspect ratio of approximately 1.5, the rod mode (mode 2) becomes the fundamental mode.

It is also seen from Figure 3.9 that, for any given aspect ratio, the values of the frequency parameters determined for the aluminum and steel cylinders are about the same. Thus the frequency parameters are not greatly affected by changes in Poisson's ratio. This was confirmed in theoretical work by Hutchinson (18). Thus the frequency parameters, $\omega r/C$, of the first four axially symmetric modes of a hardened concrete cylinder, for an aspect ratio of 2, were estimated from Figure 3.9. This was done by determining the frequency parameters for aluminum ($\upsilon = 0.344$) and steel ($\upsilon = 0.293$) cylinders with an aspect ratio of 2, and making a linear extrapolation to the concrete cylinder based on an assumed Poisson's ratio of 0.20. The results of this extrapolation are presented in Table 3.1. It is noted that for an aspect ratio of 2, the rod mode (mode 2) is the fundamental mode of vibration. The frequency ratios of the first four axially symmetric modes, also presented in Table 3.1, are therefore expressed in terms of the frequency of the rod mode. These ratios will be used to help interpret the results of the experimental study presented in the next section.

3.2.3 Experimental Study of the Vibration of a Free Cylinder Caused by Impact

In the experimental studies by McMahon, the cylinders were subjected to excitation by a continuously applied driving frequency, and as a result, a single mode of vibration was observed. However, in the vibration of a cylinder caused by impact, several modes are excited at once. This is because energy is imparted to the cylinder over a range of frequencies and it is possible to simultaneously excite more than one mode of vibration. The resulting cylinder vibration is the superposition of each of these modes. As the duration of the impact becomes shorter, the energy imparted to the cylinder is distributed over a wider range of frequencies, and therefore higher modes of vibration are expected in the response.

To confirm the expected influence of contact time, the vibration of a cylinder caused by impact was studied experimentally. A 152-mm diameter by 152-mm thick (aspect ratio = 2) hardened concrete cylinder was used in the study. As in the McMahon study, the cylinder was not completely "free", but instead rested on a rubber mesh, isolating the cylinder from the supporting table.

Impact was generated by dropping steel spheres onto the center of the top surface of the specimen. The resulting surface displacements were monitored with the displacement transducer positioned at half the radius.

Two spheres with diameters of 12.7 and 5.56 mm were used. The contact times for these two spheres, calculated from eq. (3.10) are approximately 60 and 30 us, respectively. The frequency content for these two contact times, based on the half-cycle sine curve force-time function (Figure 3.4), are shown

16

in Figure 3.10. The first zero frequencies in the spectra occur at 25 and 50 kHz for 60 and 30 us impacts, respectively.

The waveform shown in Figure 3.11 (a) is the experimentally recorded top surface displacement caused by the impact of the 12.7 mm ball (t_c = 60 us). The record consists of 1024 data points, recorded at a sampling frequency of 500 kHz. The time interval between peaks in the waveform, Δt, is interpreted as the time between successive arrivals of the P-wave at the top surface of the cylinder, as it is multiply reflected between the top and bottom surfaces of the cylinder. The mode shape associated with the multiple P-wave arrivals is the rod mode identified by McMahon, which as noted earlier is the fundamental mode for the given aspect ratio. The path length traveled by the multiply reflected P-wave between successive arrivals at the top surface is 2T. Hence the P-wave velocity in the concrete cylinder can be calculated as

$$C_p = \frac{2\,T}{\Delta t} \qquad (3.11)$$

The periodicity of the multiply reflected P-wave can be obtained by computing the frequency spectrum of the waveform. Figure 3.11 (b) is the frequency spectrum of the displacement waveform shown in Figure 3.11 (a). The dominant peak in the spectrum at 12.695 kHz is the frequency f_p of successive arrivals of the multiply reflected P-wave. Hence the time interval between successive arrivals is

$$f_p = \frac{1}{\Delta t} \qquad (3.12)$$

Substituting eq. (3.12) into eq. (3.11) leads to

$$C_p = 2\,T\,f_p \qquad (3.13)$$

From Table 3.1 the frequency parameter $\omega r/C$ for this lowest mode of vibration was estimated to equal 1.48. Again it is noted that this parameter is approximate, based on an assumed Poisson's ratio for concrete and extrapolation from McMahon's experimental results. Substituting $\omega = 2\pi f$ and $T/2 = r$, and solving for C, the rod velocity, leads to C = 2.12 T f, as compared to $C_p = 2\,T\,f_p$, given by eq. (3.13). The reason for this difference is unclear.

In this study eq. (3.13) was used to convert frequency to wave velocity. From eq. (3.13), the P-wave velocity in the concrete cylinder was calculated as C_p = 2 x 0.152 m x 12.695 kHz = 3860 m/s. This velocity was checked by determining the velocity through the specimen using the pulse velocity method (ASTM C 597) (3). The P-wave velocity determined by the pulse velocity method was 4300 m/s, which is about 11 % higher than the velocity value measured by

17

the impact-echo method. This difference between the P-wave velocities measured by the two methods was expected, and has been demonstrated by others (27,31). The reason for this difference remains unknown.

However, it is clear that the frequency of the fundamental mode of vibration that was excited by the impact can be used to monitor the development of P-wave velocity.

Also present in the spectrum in Figure 3.11 (b) is a peak at 18.555 kHz due to a higher mode of vibration, and a peak at 0.977 kHz due to the natural vibration of the transducer. The frequency ratio 18.555/12.695 = 1.46 agrees closely with the 1.48 ratio of the third and second modes estimated from McMahon's results (Table 3.1). Other smaller amplitude frequency peaks may be due to other modes excited by the impact.

Figure 3.12 (a) is the top surface displacement caused by the impact of the 5.56 mm ball. This waveform is more difficult to interpret in the time domain than the waveform caused by the 12.7 mm ball. This is because the smaller ball, having a shorter contact time, imparted significant energy at higher frequencies into the specimen, thus exciting additional higher modes of vibration. The superposition of these higher modes resulted in the increased number of perturbations in the waveform. The corresponding frequency spectrum shown in Figure 3.12 (b) reveals the frequencies of the higher modes excited by the impact.

A comparison of the frequency spectra reveals that both the 60- and 30-us contact times excited modes of vibration with frequencies of 12.695 and 18.555 kHz. Further, Figure 3.12 (b) has a large amplitude peak at 24.414 kHz which is absent from Figure 3.11 (b). The 24.414 kHz mode of vibration could not be excited by the 60-us impact because the frequency content of the impact is zero at 25 kHz (refer to Figure 3.10). Thus, as expected, the frequency content of the impact determines which modes can be excited, and the resulting vibration of the cylinder is the superposition of each of these modes. Long duration impacts, containing a narrow range of low frequencies, excite only lower modes of vibration. In contrast, short duration impacts, containing a broader range of higher frequencies, excite additional higher modes of vibration.

Lastly, the frequency of the fundamental mode of vibration, as indicated by the computed frequency spectra, remained unchanged, regardless of the duration of the impact. In the setting time and strength development studies reported in later chapters, the results of impact-echo tests were analyzed in the frequency domain. The specimens used in those studies had an aspect ratio greater than 1.5. Thus the lowest frequency peak in the frequency spectrum (excluding peaks attributed to transducer resonance) was used to compute the P-wave velocity according to eq. (3.13).

3.3 DEVELOPMENT OF ELASTIC MODULUS IN CEMENT PASTE

In Section 3.2 it was seen that stress wave velocities within a solid depend upon the elastic modulus. The elastic modulus of early-age concrete increases with age as the paste matures. The discussion presented in this section gives a possible explanation for how the elastic modulus in cement paste increases as the paste matures.

Upon initial mixing, cement paste consists of solid particles (cement grains) suspended in a fluid (mixing water). This is shown schematically in

18

Figure 3.13 (a). The relative volumes of cement and water are proportional to the areas shown in the figure. Shown on the surface of each cement grain is an initial coating of hydration product that formed when the cement and water first came into contact. The hydration products formed are cement gel and calcium hydroxide. Cement gel is the name given to the hydrates, predominantly calcium silicate hydrate, formed during the hydration process. The cement gel is composed of solid particles and interstitial spaces called gel pores (28). For the purposes of this discussion, only the gel products are represented in Figure 3.13 (a).

The fresh cement paste remains in the state shown in Figure 3.13 (a) for a period of time called the induction or dormant period. This period generally lasts from 1 to 3 hours. The end of the induction period is marked by a rapid increase in hydration. Several mechanisms for the end of the induction period have been proposed and are summarized by Bye (7).

Figure 3.13 (b) shows the post-induction period structure of the cement paste. As can be seen in the figure, an initial skeletal framework has been established by the gel. As hydration proceeds, the volume of gel product increases, filling in the water-filled spaces. However, the volume occupied by the gel is less than the initial volume occupied by the unhydrated cement and mixing water. Thus some of the water-filled space will empty if additional water is not supplied externally. In this example, additional water is supplied externally, so the voids remain water-filled.

Figure 3.13 (c) shows the paste structure at a later stage of hydration. Both the volume of gel product and the degree of interlocking have increased. The remaining volume of water-filled voids create small cavities called capillary pores.

Lastly, Figure 3.13 (d) shows the structure of the cement paste at an advanced stage of hydration. The gel products occupy most of the initial paste volume. Shown in the figure are small remains of unhydrated cement and the capillary pores mentioned above.

It is seen from the above discussion that two changes take place in the structure of the hydrating cement paste. First, the volume of voids in the paste decreases. Second, the degree of interlocking between gel product increases. These two changes are the result of gel growth in the volume established by the initial cement and water mixture.

Prior to the end of the induction period, stress waves in the cement paste propagate through a fluid-solid mixture. Once an initial skeletal framework has been established, the stress waves propagate through a porous saturated solid composed of unreacted cement and hydration product, the relative proportions of each changing as the paste matures. The propagation of stress waves in fluid-solid mixtures and porous saturated solids is discussed in Reference (30).

For the purposes of this study, the cement paste is considered from a macroscopic viewpoint. It is treated as an elastic solid with an elastic modulus that increases as the paste matures. Hydration reduces the porosity of the paste and increases the degree of interlocking between hydration products (Figures 3.13 (b) and (c)), thus increasing the elastic modulus of the paste.

Consider as a second example a cement paste with a higher w-c ratio, shown in Figures 3.14 (a) through (d). The percentage of cement hydrated in each figure is the same as shown for the lower w-c ratio mixture in Figures 3.13 (a) through (d). Comparison of these figures reveals that at any degree

19

of hydration a greater degree of interlocking exists between the cement grains of the low w-c ratio paste as compared to the high w-c ratio paste. This is because the cement grains of the low w-c ratio paste are initially closer to each other than are the grains of the high w-c ratio paste. Thus at any degree of hydration, the low w-c paste will probably exhibit a higher elastic modulus.

Further, if hydration proceeds at the same rate in both the low and high w-c ratio pastes, the elastic modulus will probably develop at a faster rate in the low w-c ratio paste, and attain a higher long-term value.

It was seen in Section 3.2 that the P-wave velocity also depends upon Poisson's ratio. In fresh concrete, it may approach a value of 0.5 (fluid). As the concrete matures, it decreases to a value of about 0.20 for mature, hardened concrete.

3.4 SUMMARY

This chapter presented background information needed for the remainder of the report. First, the experimental set-up and general procedure used to make impact-echo velocity measurements was described. Next, the stress waves generated by impact on the surface of a solid were reviewed, and the force-time function, contact time, and frequency content of impact between a sphere and a plate were discussed.

The vibration of a cylinder caused by impact was explained. It was shown that the modes of vibration excited by the impact depended upon the frequency content of the impact, which in turn depended upon the contact time. Further, it was shown that the frequency of the fundamental mode of vibration remained the same, regardless of the contact time.

It was shown that for a cylinder with an aspect ratio of 2, the fundamental mode of vibration is the rod mode. The P-wave velocity can be obtained from the cylinder height T and the measured frequency of the rod mode f_p. For this study, the P-wave velocity was computed using:

$$c_p = 2 T f_p \qquad (3.13)$$

Lastly, the development of elastic modulus in maturing cement paste was discussed. The increase in elastic modulus as hydration proceeded was attributed to the reduction of porosity of the paste, and to the increased degree of interlocking between hydration products.

Table 3.1 Frequency parameters for a cylinder (aspect ratio = 2)

i	ALUMINUM	STEEL	CONCRETE*	For Concrete w_i / w_2
1	1.81	1.78	1.73	1.169
2	1.45	1.46	1.48	1
3	2.22	2.21	2.19	1.480
4	1.94	1.91	1.86	1.257

*Estimated from McMahon [25] for Poisson's ratio = 0.2
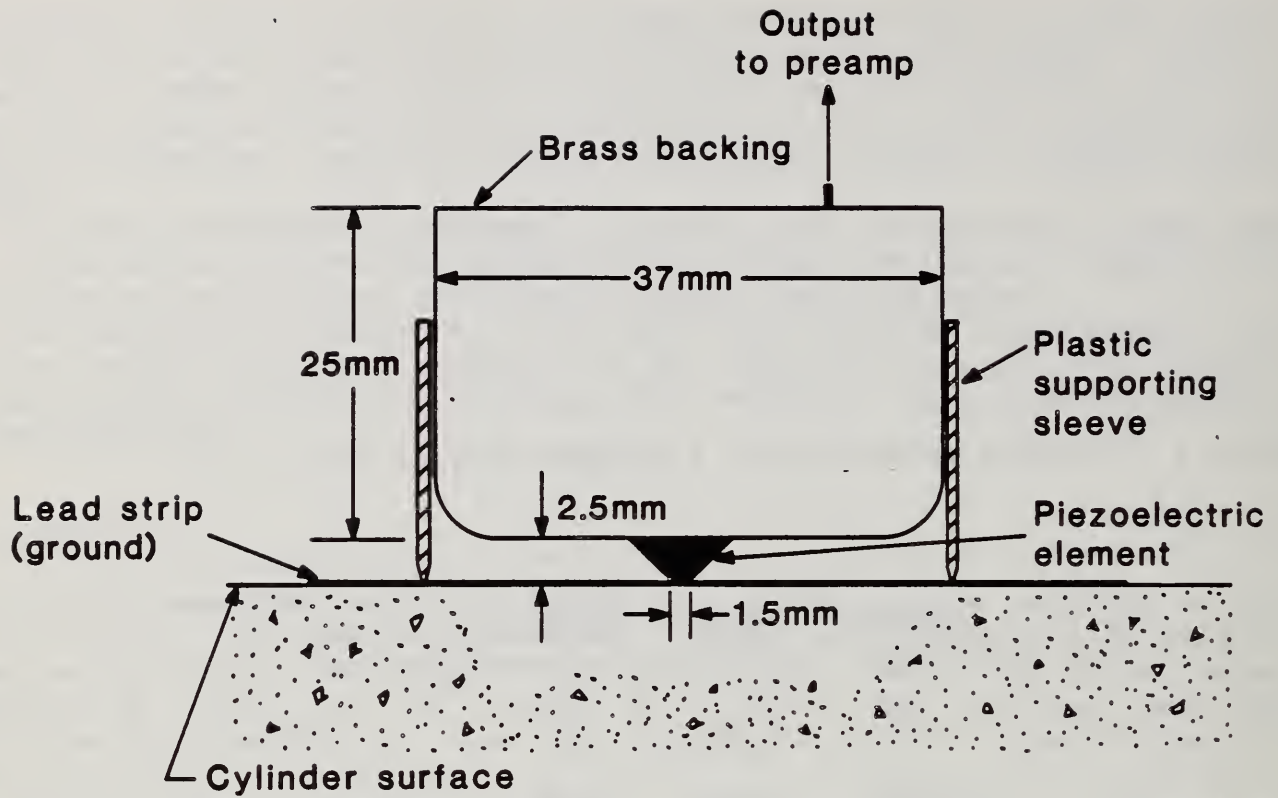
Figure 3.1   Displacement transducer
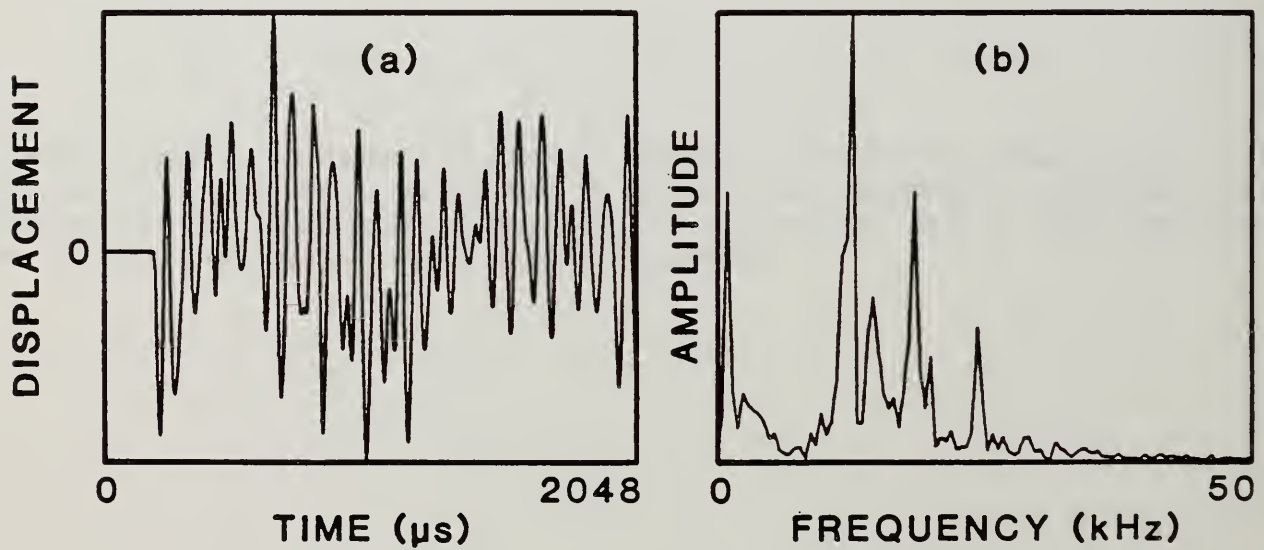
Figure 3.2   Typical impact-echo measurement: a) surface displacement
waveform; and, b) frequency spectrum

22
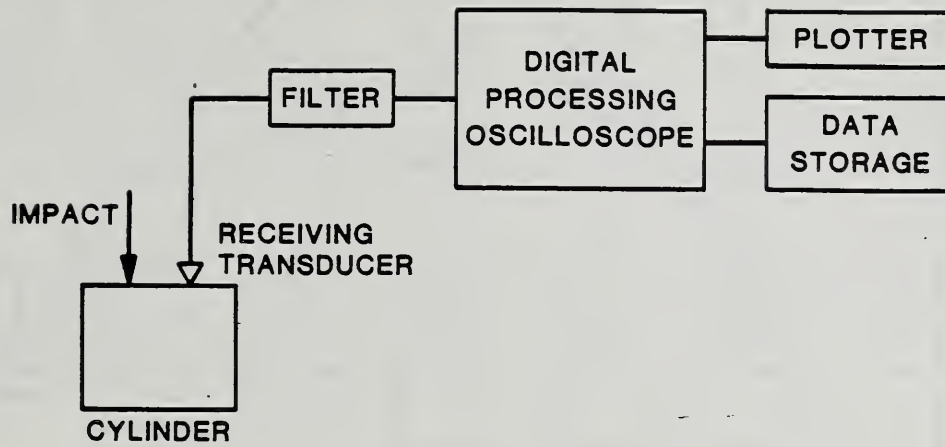
Figure 3.3   Schematic of experimental set-up
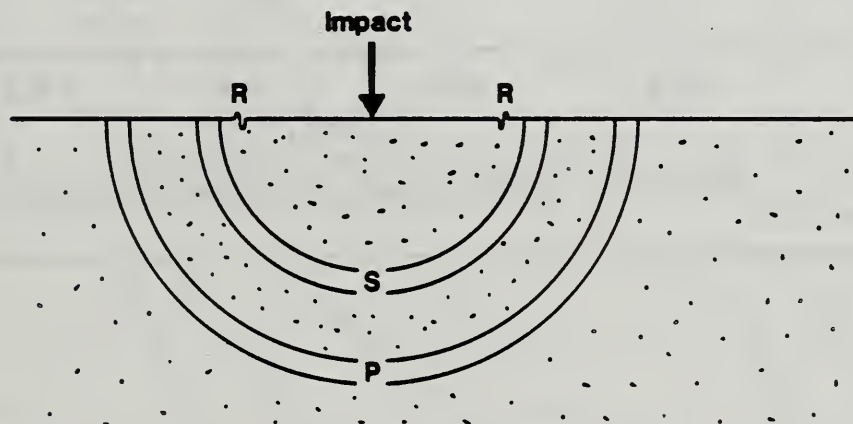
Figure 3.4   Wavefronts of P-, S- and R-waves caused by point impact
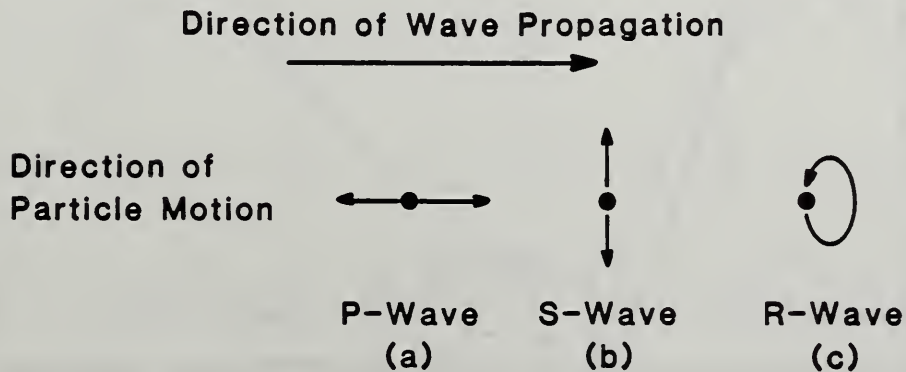
Figure 3.5   Characterization of P-, S-, and R-waves: a) P-wave;
b) S-wave; and, c) R-wave

23
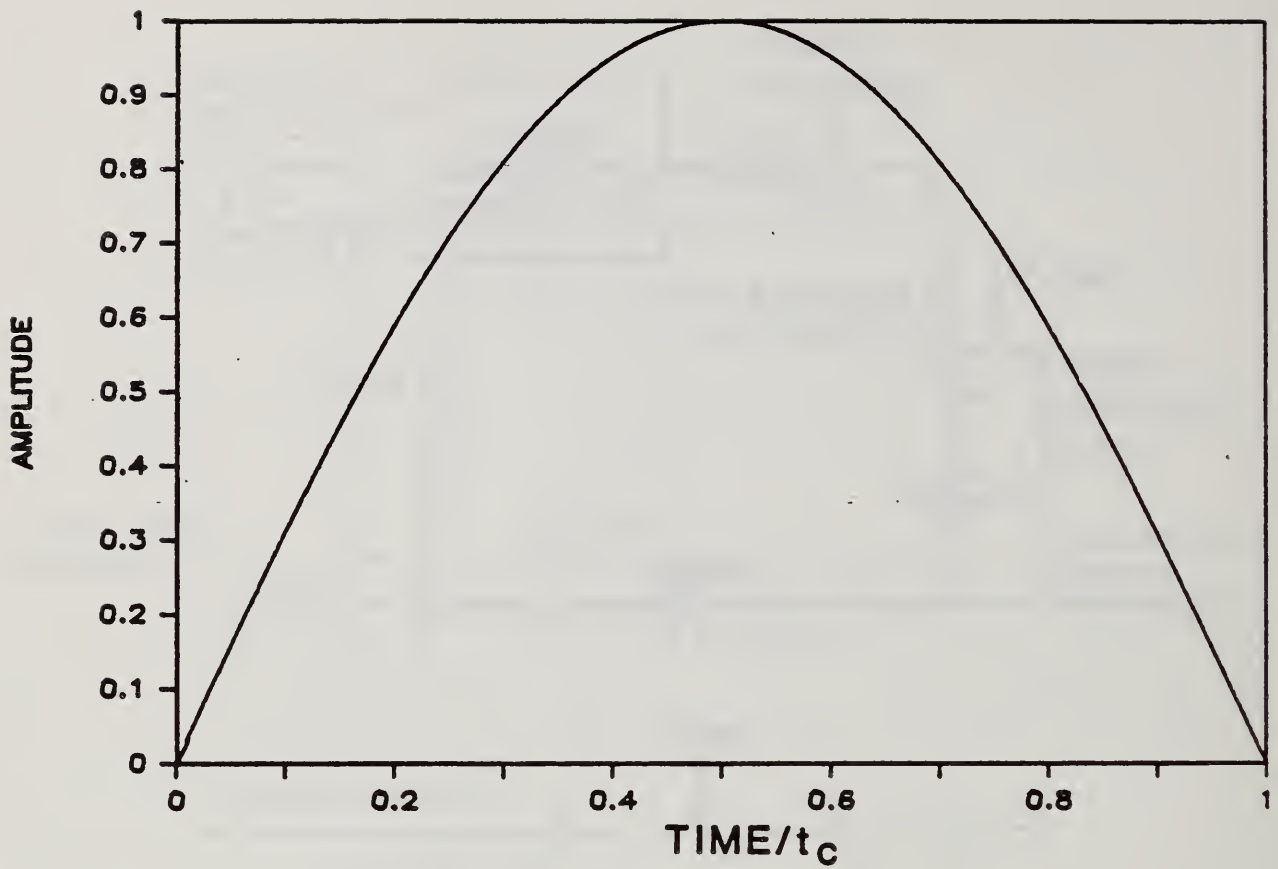
Figure 3.6   Force-time function of the elastic impact of a sphere on a solid (31)
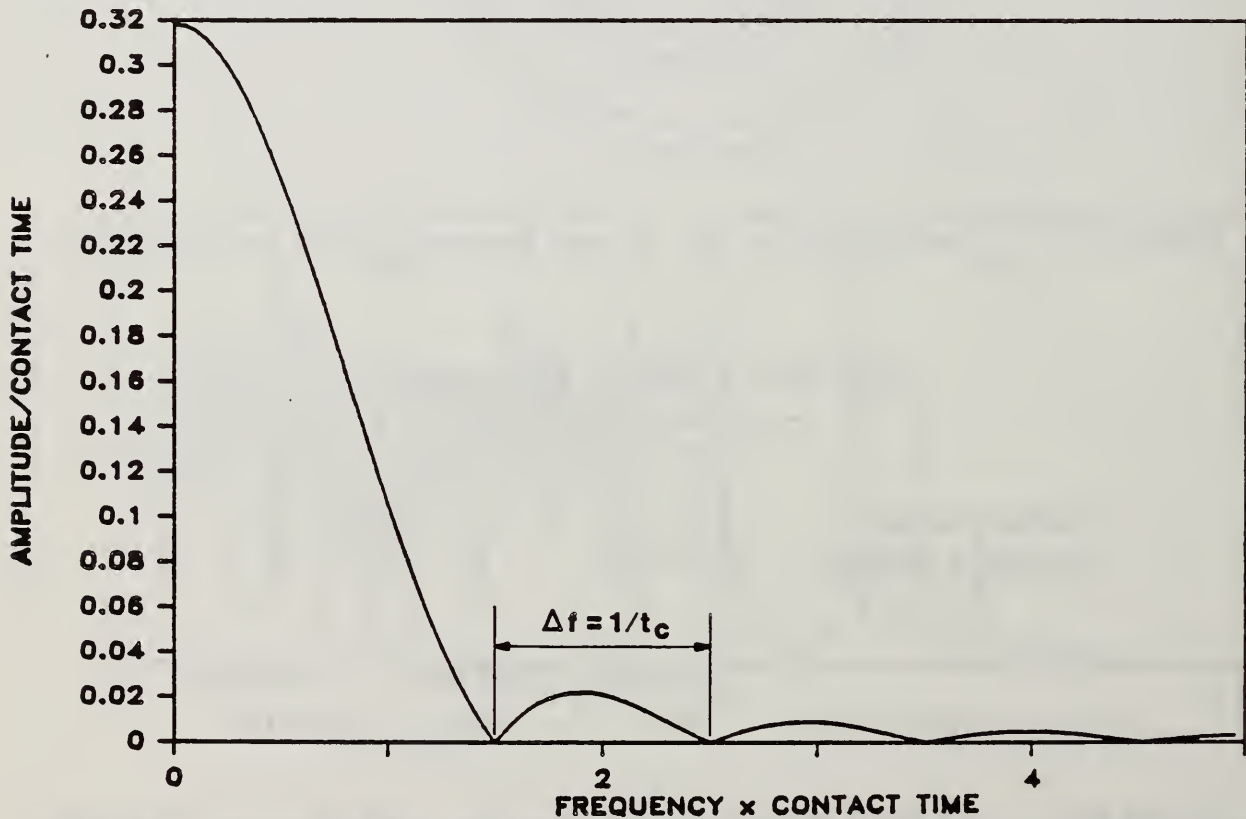
Figure 3.7   Frequency content of the force-time function shown in Figure 3.6 (31)

24
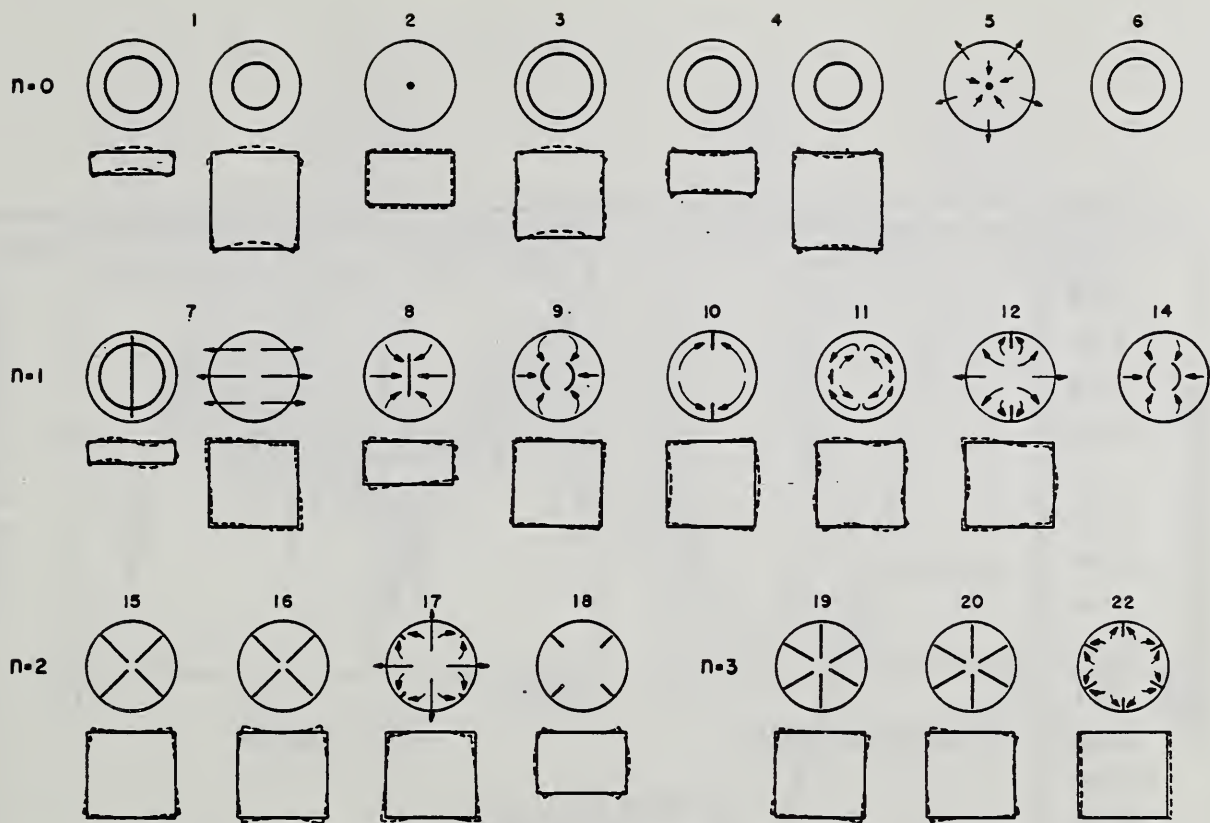
Figure 3.8   Approximate form of vibration of 20 of the first 22 modes of vibration of solid cylinders (25)
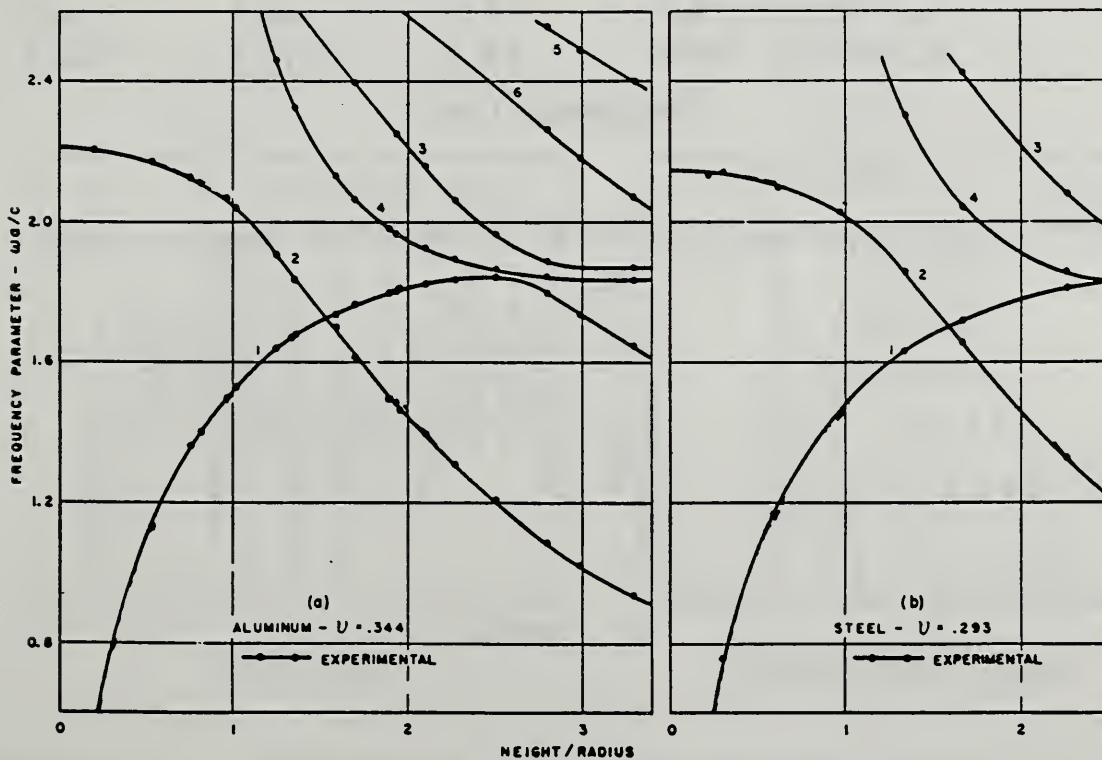
Figure 3.9   Frequencies of the first six modes of vibration circumferential order 0 (25)

25
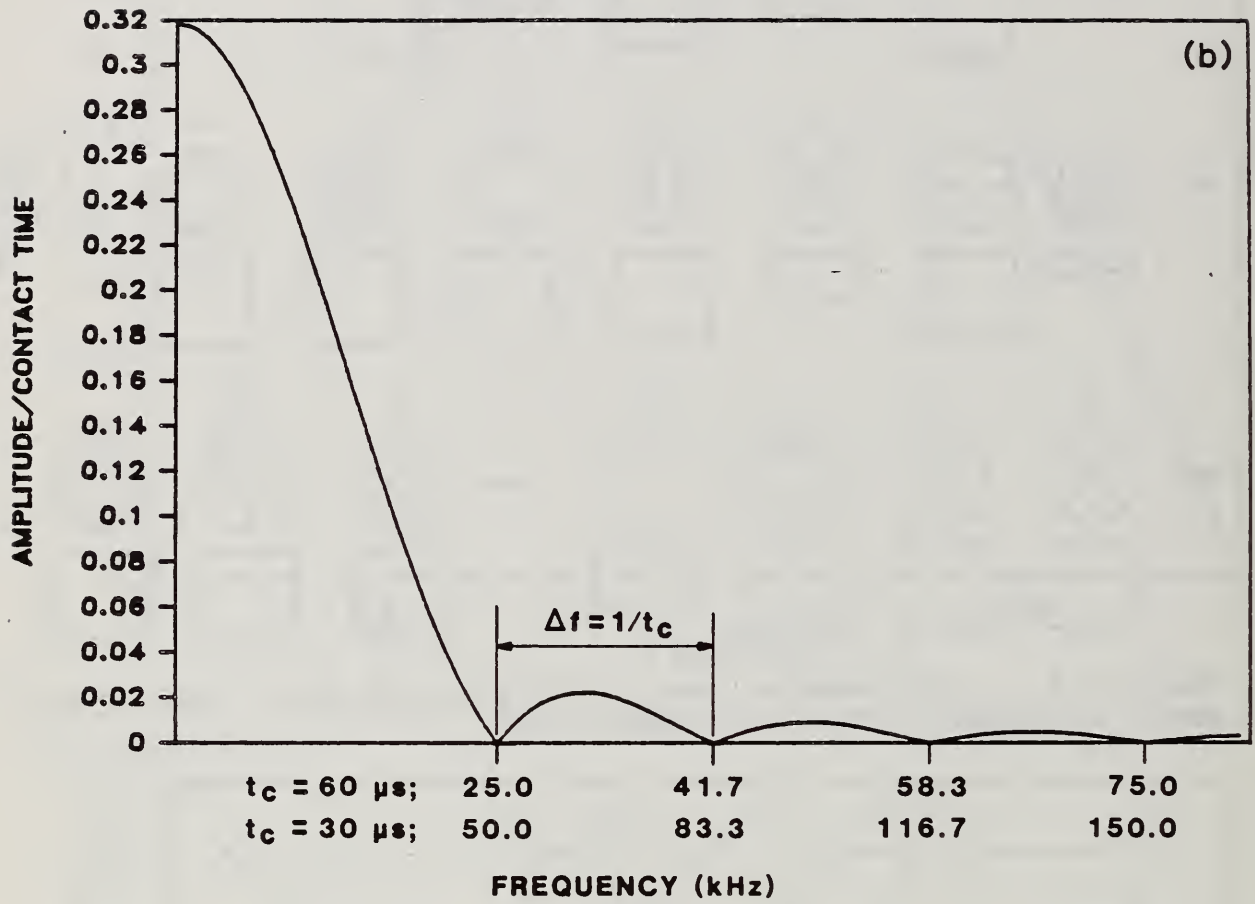
Figure 3.10   Frequency content of 60 and 30 us duration impacts

26
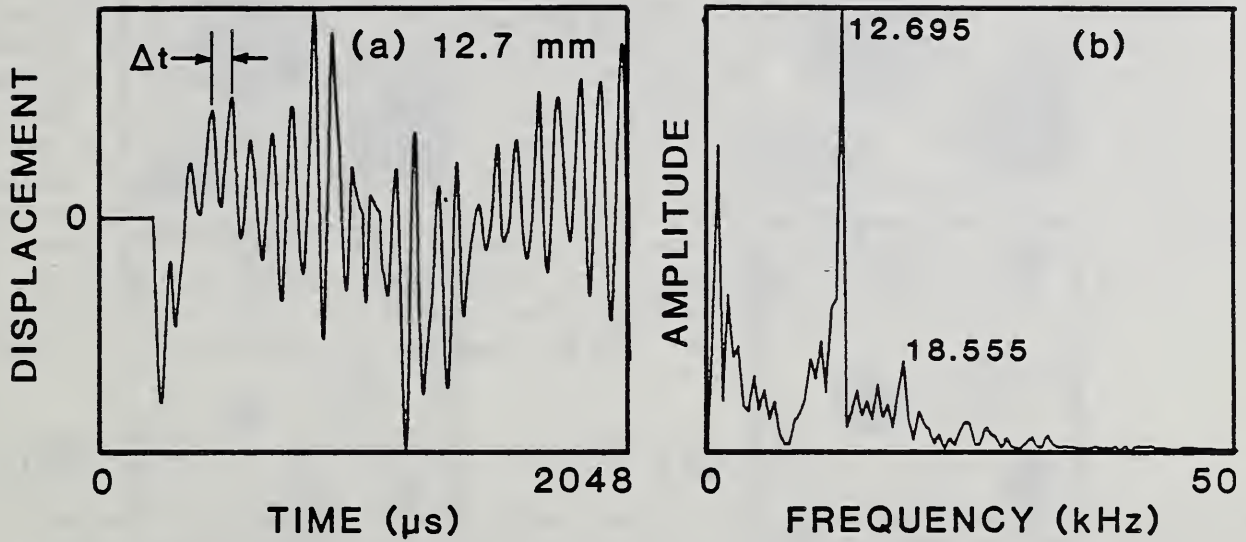
Figure 3.11   Response of a hardened concrete cylinder to impact
by a 12.7 mm ball (t_c = 60 us): a) surface displacement waveform;
and, b) frequency spectrum
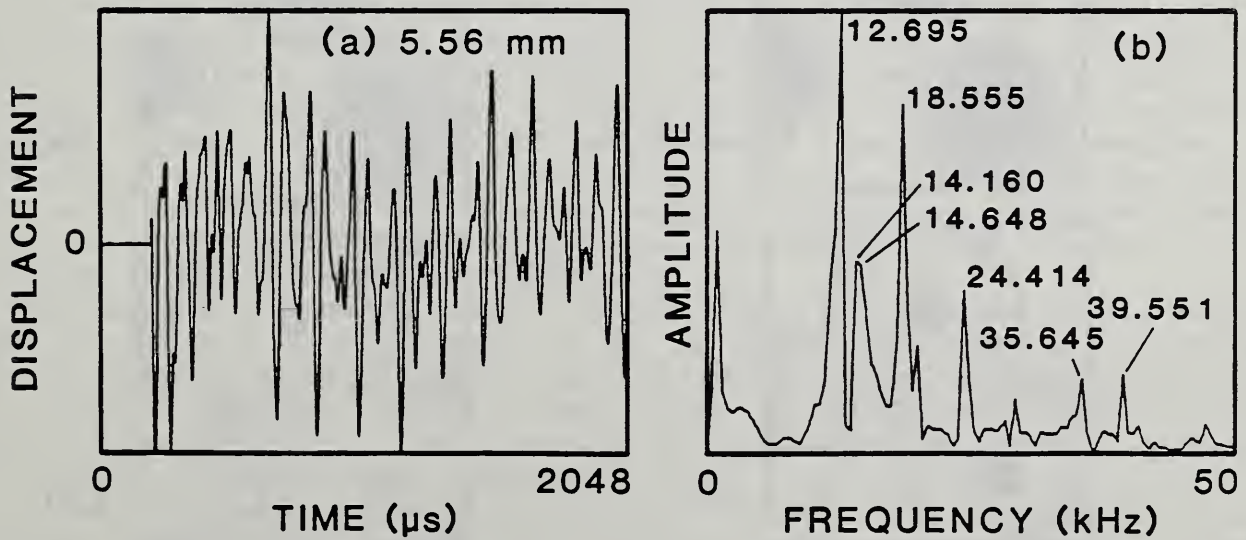
Figure 3.12   Response of a hardened concrete cylinder to·impact
by a 5.56 mm ball ('t_c = 30 us): a) surface displacement waveform;
and, b) frequency spectrum
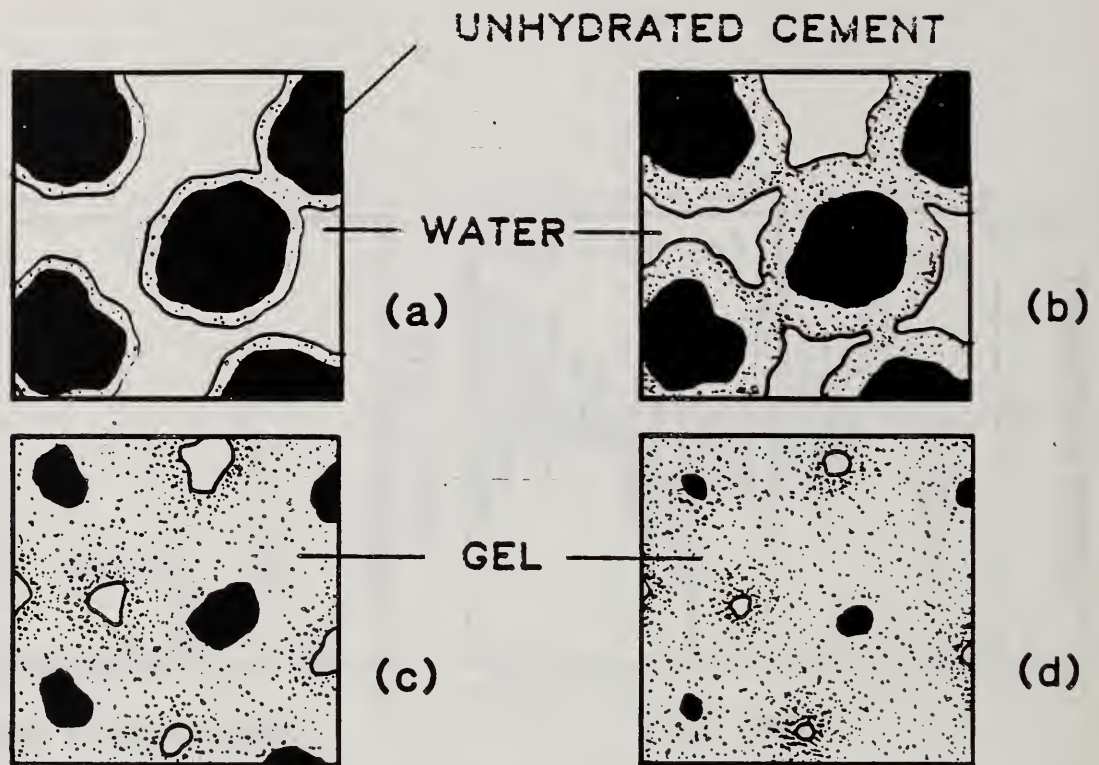
Figure 3.13   Structure of cement paste at various stages of
hydration: a) after initial mixing; b) post-induction period structure;
c) even later stage of hydration; and, d) advanced stage of hydration
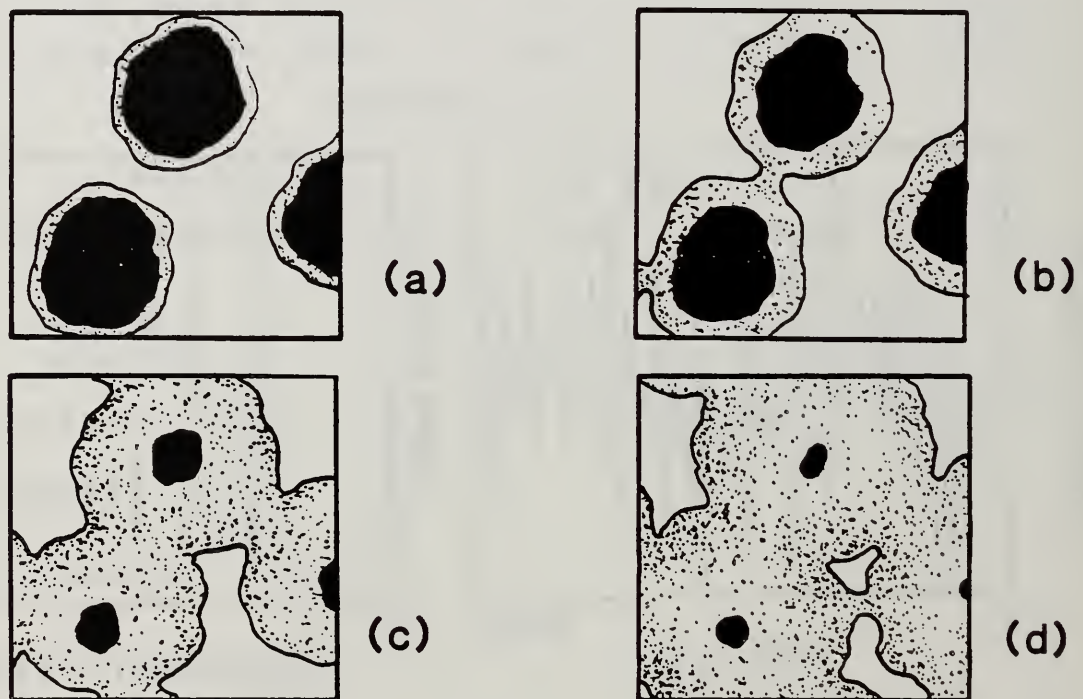
Figure 3.14   Structure of cement paste at various stages of hydration
- higher w-c ratio: a) after initial mixing; b) post-induction period
structure; c) even later stage of hydration; and, d) advanced stage
of hydration

28

CHAPTER 4
MEASUREMENT OF SETTING TIME

4.0 INTRODUCTION

The correlation between the development of P-wave velocity in concrete and setting time is presented in this chapter. The technique used to make the velocity measurements on early-age concrete is discussed in section 4.1. Results from initial experiments studying the relationship between P-wave velocity and penetration resistance on prepared mortars are discussed in section 4.2. In section 4.3, a simple model is used to explain how the P-wave velocity in concrete may be affected by the velocities in the paste and aggregate phases, and the relative proportions of each. Section 4.4 presents the results of velocity measurements on concrete specimens made with different w-c ratios, and with and without set-controlling admixtures. Lastly, two approaches for using the impact-echo method to measure the setting time of concrete are presented in section 4.5.

4.1 DEVELOPMENT OF MEASUREMENT TECHNIQUE

The basic principle of the impact-echo technique was discussed in section 3.1. This section discusses how the method was adapted for use on early-age concrete to monitor the development of P-wave velocity. The following discussion is applicable to both the concrete and prepared mortar specimens.

4.1.1 Experimental Set-up

Figure 4.1 is a schematic representation of the experimental set-up used to monitor the development of P-wave velocity in early-age concrete. Cylindrical specimens 152 mm (6.0 in.) in diameter by 160 mm (6.3 in.) deep were used in the study. Since the development of velocity had to be monitored at the earliest possible age it was necessary to make velocity measurements while the concrete was still fluid-like. It was not practical to attempt to generate stress waves by impact directly on fresh concrete, nor could the receiving transducer be placed directly on the fresh concrete surface. Therefore, 9.5-mm (0.37 in.) thick polycarbonate plates, the dimensions of which are given in Figure 4.2, were placed onto the surface of the fresh concrete to act as impact and receiver surfaces. The impact plate was placed at the center of the concrete surface, and the receiver plate placed at half the radius of the cylinder (see Figure 4.1).

The small steel spheres used to create impact were dropped from a height of 200 mm onto the impact surface. A 200 mm long plastic tube resting on the impact surface was used to control the drop height. The transducer rested on the receiver surface, with a thin lead strip inserted between the piezoelectric tip of the transducer and the polycarbonate plate to complete the electrical circuit of the transducer.

In order to make reliable measurements, good acoustic coupling had to be maintained between the concrete and the impact and receiver surfaces. Bleed water migrating to the surface of the specimen helped to maintain this coupling. For this reason, the fresh concrete was placed in the mold to a level 10 mm below the top rim of the mold, allowing room for the bleed water

to accumulate. Only a small amount of surface water was needed. For very wet mixtures exhibiting excessive bleeding, excess water was drawn from the surface to keep the transducer dry. As hydration proceeded, the cement paste began to stiffen and adhere to the impact and receiver surfaces. This adhesion was beneficial, leading to improved acoustic coupling between the specimen and polycarbonate surfaces. As the bleed water evaporated, additional water was added to the top surface to maintain good coupling. The specimen was covered with a plastic sheet when not being tested. The presence of small amounts of water on the surfaces of the specimens did not alter the P-wave velocities.

Impact and receiver plates of three different thicknesses were investigated: 3.2, 6.4, and 9.5 mm. For these thicknesses, no noticeable differences were observed in either the measured displacement waveforms or the frequency spectra. The 9.5 mm plate was selected and used throughout the testing, because it provided the greatest clearance between the receiving transducer and the specimen surface, which helped keep the transducer dry.

4.1.2 Signal Interpretation

A typical surface displacement waveform obtained from a specimen at an age of about 7.3 hours is shown in Figure 4.3 (a). This displacement waveform is easily interpreted in the time domain. The time interval between peaks in the waveform caused by P-wave arrivals is 270 us. Thus, the P-wave velocity C_p in the specimen calculated using eq. (3.11) is 1185 m/s. Displacement waveforms at earlier ages such as the one shown in Figure 4.3 (b) at 3.1 hours are not as easily interpreted because the signal is dominated by the resonance of the transducer (see section 4.1.4), and the P-wave arrivals are difficult to discern.

When the displacement waveforms shown in Figures 4.3 (a) and (b) are transformed into the frequency domain, as shown in Figures 4.4 (a) and (b), interpretation is greatly simplified. The frequency peak corresponding to the multiply reflected P-wave is identified in the figures. Using the resonant frequencies obtained from each figure, the P-wave velocity can be calculated according to eq. (3.13). For the spectrum shown in Figure 4.4 (a), C_p = 1188 m/s, which is the same result obtained above using eq. (3.11). For the spectrum shown in Figure 4.4 (b), C_p = 313 m/s. Throughout the testing, results were analyzed in the frequency domain, using eq. (3.13) to compute velocities.

The frequency peak attributed to resonance of the receiving plate-transducer assembly was reduced through the use of filters, as will be explained section 4.1.4. Other lower amplitude peaks present in the frequency spectra are due to higher modes of vibration excited by the impact.

4.1.3 Sampling Frequency and Voltage Range

The displacement waveforms shown in Figures 4.3 (a) and (b) are each composed of 1024 data points, recorded at a sampling frequency of 100 kHz (sampling interval of 10 us). Thus, the total duration of the record is 10240 us. From eq. (3.1), the frequency interval in the frequency spectrum is 0.098 kHz, which allowed the P-wave velocity to be computed to the nearest 30 m/s. Refining the displacement waveforms by increasing the sampling frequency to 200 kHz (sampling interval of 5 us) would increase the frequency interval to

0.195 KHz, which in turn would allow the velocities to be computed to the nearest 60 m/s. Therefore, the refinement to which the velocity can be computed is determined by the sampling frequency. The 10 us sampling rate was selected and used throughout the testing.

The displacement waveforms shown in Figures 4.3 (a) and (b) are plots of signal voltage versus time. The signal voltage is directly related to the amplitude of the displacements detected by the receiving transducer, large amplitude displacements appearing as large voltage signals. With increasing specimen age, the measured displacements in the specimens decreased. Therefore, the sensitivity of the measurement had to be increased to detect these smaller voltage signals. This was accomplished by reducing the voltage range of the oscilloscope. For this study, voltage ranges from $\pm$ 2.0 V to $\pm$ 0.1 V were used.

4.1.4 Transducer Resonance

The effect of the low frequency transducer assembly resonance is clearly seen as the dominant low frequency oscillation present in the surface displacement waveform in Figure 4.3 (b), and as the low frequency peak in the corresponding frequency spectrum in Figure 4.4 (b). The superposition of receiver resonance on the specimen response was one of the factors that made interpretation of displacement waveforms difficult at very early ages.

In the early age measurements, the peak in the frequency spectra attributed to resonance of the receiving plate-transducer assembly remained essentially constant, ranging from 0.293 kHz to 0.488 kHz. At later ages, this frequency peak increased slightly, varying between 0.391 and 0.684 kHz.

One way to reduce the effects of transducer resonance on displacement waveforms and frequency spectra is to filter the signal. In this study several filters were tried, and a variable high pass filter was found to give the best results. Using this filter, the frequency below which the signal was attenuated could be varied from 0 to 1.0 kHz.

For the 160 mm deep specimen used in the setting time tests, the effect of transducer resonance appeared as a low frequency peak in the frequency spectrum that was distinct from the peak corresponding to specimen resonance. This low frequency peak was ignored when interpreting the results.

4.2 PREPARED MORTAR TESTS

4.2.1 Objective and Scope

The objective of the initial phase of the study was to determine if a correlation existed between the development of P-wave velocity in prepared mortars, measured by the impact-echo technique, and initial and final setting as defined by ASTM C 403 (Standard Test Method for Time of Setting of Concrete Mixtures by Penetration Resistance). Three different mixture proportions were studied as described in Table 4.1. A total of nine experiments were conducted.

4.2.2 Materials

The prepared mortars were made using Type I portland cement, natural sand, and tap water. The sand was passed through a #4 sieve to remove any large particles that otherwise might have interfered with the penetration needles. Fineness modulus, specific gravity, absorption, and periodic moisture contents were determined according to applicable ASTM Standard Test Methods (C 136, C 128, C 566) (3). Material properties for the sand used in this part of the study are summarized in Table 4.2.

4.2.3 Specimen Preparation

The mortars were mixed in a 1.5 cubic foot capacity revolving drum mixer. The mixing procedure was as follows:

1. Thoroughly wet the mixing drum and allow it to drip dry in an inverted position for 1 minute.
2. Add sand and cement and dry mix for 30 seconds.
3. Add mixing water over a 1 minute period while drum is revolving.
4. Continue mixing for 1.5 minutes, cover the mixer opening, and allow mortar to rest for 1.5 minutes: then mix again for an additional 1.5 minutes.

After mixing, the mortar was placed into three cylindrical molds measuring 152 mm in diameter by 170 mm deep, according to the procedure prescribed in ASTM C 403. Mortar was placed to a depth of 160 mm in each mold. Two specimens were used for the penetration resistance tests: they were tested as prescribed in ASTM C 403, with successive penetration resistance tests made on alternate specimens. The impact surface, receiver surface, lead coupling strip and receiver were placed onto the third specimen approximately 1 hour after initial contact between cement and water.

The three specimens were the same size, and were exposed to the same temperature and humidity conditions. Hence, all specimens were assumed to be at the same stage of hydration at any given time.

Replicate tests were performed on different days. The temperatures of the specimens were not monitored in these initial experiments.

4.2.4 Results and Observations

In the following discussions, the four low w-c ratio (0.40) tests are referred to as ML1 through ML4, and the five high w-c ratio (0.55) tests as MH1 through MH5.

Figure 4.5 (a) shows the development of P-wave velocity for test ML2. Figure 4.5 (b) shows the corresponding results of the penetration resistance measurements. Superposed on Figure 4.5 (b) is a horizontal line at a penetration resistance of 500 psi. On each of these graphs, curves through the data were drawn by hand, and the "age" represents elapsed time after initial contact between cement and water.

Impact-echo velocity determinations were attempted at an age as early as 1.25 hours. As can be seen in Figure 4.5 (a), there was considerable scatter in the early measurements. In several of the earliest readings, it was impossible to determine which frequency in the spectrum corresponded to the

32

resonant frequency of the specimen. In these instances, no result was plotted. From this figure, it is seen that the early velocity measurements are scattered about a constant value up to an age of approximately $3^1/_2$ to 4 hours. After this period, the scatter in the measurements diminished, and the development of velocity in each specimen could be followed. At the start of the well-defined velocity gain curve, the velocity measurements in the test ML2 ranged from 350 m/s to 400 m/s.

It is not clear whether these earliest scattered measurements have physical meaning, or result from the experimental set-up. This initial period of scatter was also observed in the tests made on concrete specimens described in section 4.4. The significance of the scattered measurements was not investigated as part of this study.

Different high pass filters were being evaluated during the ML series tests. A set technique was adopted beginning with test MH4. This technique involved using a variable high pass filter, and is the technique used throughout the remainder of the setting time experiments. The filter was introduced after the resonant response of the cylinder had been clearly identified, and was used to filter frequencies lower than approximately one half the resonant frequency of the cylinder.

Figures 4.6 (a) and (b) show, respectively, the results of velocity and penetration resistance measurements on tests MH4 and MH5. Examination of Figure 4.6 (a) reveals that the well-defined velocity gain curve starts at an age between 3 and 4 hours. The corresponding P-wave velocities were approximately 250 m/s. During this same period, initial penetration resistance measurements ranged from 50 psi to 160 psi (Figure 4.6 (b)). A penetration resistance of 500 psi was achieved at approximately 4.8 hours in both tests. The corresponding P-wave velocity at 4.8 hours was approximately 375 m/s.

Figures 4.7 (a) and (b) show, respectively, the results of velocity and penetration resistance measurements of all four replicate ML test specimens. Similarly, Figures 4.8 (a) and (b) show results of replicates MH1 through MH3. From these figures, and Figures 4.6 (a) and (b), a consistent ranking of the penetration resistance and velocity curves is seen. In general, the test that showed the earliest time of initial setting measured by penetration resistance also showed the earliest development of P-wave velocity. Thus, the impact-echo technique appears to be sensitive to the same factors that affect the setting behavior as monitored by penetration resistance.

There is no apparent relationship between the development of P-wave velocity and final setting as defined by a penetration resistance of 4000 psi. In Figures 4.6 (a), 4.7 (a), and 4.8 (a) it is seen that at the time corresponding to a penetration resistance of 4000 psi, the velocity curves continue to increase.

It is useful to re-plot representative results from the low and high w-c ratio series together on the same graph. Figures 4.9 (a) and (b) show the velocity and penetration resistance results of series ML1, ML2, MH4, and MH5. The results of the impact-echo measurements revealed a difference in the rate of velocity increase between the low and high w-c ratio mortars. This difference was reflected in the slopes of the rising portions of the velocity curves, with the lower w-c ratio mortar exhibiting a greater slope than the higher w-c ratio mortar. The following discussion gives a possible explanation for this behavior.

33

As discussed in section 3.3, the cement grains of the lower w-c ratio paste were closer to each other compared with the higher w-c ratio paste. If hydration were proceeding at the same rate in both pastes, then the elastic modulus of the low w-c paste would probably develop faster, as a result of a greater degree of interlocking between hydration products and a lower porosity at any stage of hydration (refer to Figures 3.13 and 3.14).

A penetration resistance of 500 psi was reached at 3.9 and 3.6 hours for series ML1 and ML2 respectively, and at 4.8 hours for series MH4 and MH5. This difference in initial setting times (approximately 1 hour) between the low and high w-c ratio series was also reflected in the velocity measurements. As can be seen by the time separation between the corresponding velocity curves shown in Figure 4.9 (a), there is approximately a 1 hour difference in the velocity curves at the start of velocity gain. Thus, a correlation appears to exist between the time a penetration resistance of 500 psi was reached, and the time the P-wave velocity began to increase rapidly.

4.3 SERIES MODEL

Wave propagation in homogeneous elastic solids was discussed in Chapter 3. However, concrete is non-homogeneous because of large differences between the elastic properties of the aggregate and paste phases. The traditional series model can used to gain an understanding of how the velocity in the concrete may be affected by the velocities in the paste and aggregate phases separately. The model is described in section 4.3.1, followed by the results of an experiment performed to evaluate its validity in section 4.3.2.

4.3.1 Description of the Series Model

The series model is a simple approach for predicting the properties of a composite material based on the properties of the constituents. In the following discussion, the two constituent phases used to represent the concrete are the paste and the aggregate. The basis for choosing the series model is as follows. As a stress wave travels through the concrete, a single ray will alternately propagate through regions of paste and regions of aggregate. This is shown in Figure 4.10 (a). The path crossed by the ray can be replaced by an idealized series of paste and aggregate regions as shown in Figure 4.10 (b). This, in turn, can be replaced by the two-phase model shown in Figure 4.10 (c); hence the series model. Assuming the concrete is uniformly heterogeneous, each ray in the stress wave propagates through a similar two-phase model, and the entire stress wave can be represented as propagating through the series model shown in Figure 4.11.

The time required for a P-wave to travel through the concrete, $\Delta t'$, is taken as the summation of times required to travel through each phase individually, or

$$\Delta t' = \frac{L^p}{c_p{}^p} + \frac{L^a}{c_p{}^a} = \frac{L}{c_p{}^c} \tag{4.1}$$

34

where $C_p{}^c$, $C_p{}^p$, and $C_p{}^a$ are the velocities in the concrete, paste phase, and aggregate phase, respectively. The total path length L is the summation of the individual path lengths L^p in the paste phase and L^a in the aggregate phase. For a unit cube, L = 1, and L^p and L^a can be replaced by their fractional volumes V^p and V^a respectively. Equation 4.1 can then be written as

$$\frac{1}{C_p{}^c} = \frac{V^p}{C_p{}^p} + \frac{V^a}{C_p{}^a} \qquad (4.2)$$

For a given concrete mixture, the quantities V^p, V^a, and $C_p{}^a$ are constant. Only $C_p{}^p$, the velocity through the paste, varies as a function of time and temperature. Therefore, if the parameters V^p, V^a, and $C_p{}^a$ are known, and the development of $C_p{}^p$ is also known, the velocity in the concrete, $C_p{}^c$, can be calculated from the model.

Knudsen (22) has shown that, for concrete cured at a constant temperature, properties that are directly related to the extent of cement hydration can be represented by a hyperbolic expression of the form

$$A = \frac{A_u \left(K \left(t - t_o \right) \right)}{\left(1 + K \left(t - t_o \right) \right)} \qquad (4.3)$$

where A is the property that varies with the degree of hydration, evaluated at a time t, and A_u is the long term or limiting value of A. K is a constant related to the initial slope of the hyperbola, and t_o is an induction period before the property A begins to develop. A similar expression has been used to represent the strength gain of concrete as a function of maturity (11), which is the cumulative time-temperature history of the concrete. In this study it is assumed that velocity gain also obeys a hyperbolic relationship. However, because there is an initial velocity during the induction period the relationship is as follows:

$$C_p{}^p = \frac{\left(C_p^{up} - C_o \right) \left(K \left(t - t_o \right) \right)}{\left(1 + K \left(t - t_o \right) \right)} + C_o \qquad (4.4)$$

where C_p^{up} is the limiting paste velocity, and C_o the initial paste velocity at time t_o, when velocity gain starts. Using this hyperbolic expression, the development of velocity in the paste is as shown schematically in Figure 4.12 (a). The P-wave velocity in the aggregate remains constant with time, as is shown in Figure 4.12 (b). Thus, the resulting velocity in concrete for various aggregate contents, as predicted by eq. (4.2), is as shown in Figure 4.12 (c).

35

4.3.2 Experimental Evaluation of Series Model

The ability of the series model to predict the P-wave velocity in concrete was evaluated experimentally by monitoring the development of P-wave velocity in cement paste, and in concretes with controlled volumes of aggregate. Ordinary Type I portland cement was used in the experiment. The aggregate was a rounded gravel, ranging in size from 12.7 to 4.75 mm. The cement paste was mixed by hand first, to which controlled amounts of aggregate were then added. To minimize absorption of water from the paste, the aggregate was soaked in water for a period of 24 hours and surface dried with paper towels and an air stream just prior to use.

Three 152-mm diameter by 160-mm deep cylindrical specimens were made. One specimen was made with cement paste only. The remaining two specimens were made with approximately 40 and 60 percent aggregate by volume. The cylinders were kept in a water bath at room temperature in an attempt to keep the temperature of each as similar as possible. The temperature of each cylinder was monitored with a thermocouple placed in its center. The earliest velocity measurements were attempted at an age of 2.5 hours, and velocities were monitored to an age of 195 hours. Each cylinder was removed from the water bath while making velocity measurements and returned to the bath immediately afterwards.

Despite efforts to maintain each specimen at approximately the same temperature, the paste cylinder experienced a much greater temperature increase than either of the concrete specimens. Figure 4.13 shows the temperature of each specimen for the first 100 hours of the experiment. Because the initial temperature increase in the paste cylinder was much greater than either of the concrete specimens, it was at a more advanced stage of hydration at any given time. Results are therefore presented in terms of maturity instead of time. Maturity M can be expressed in equation form as

$$M = \int_0^t (T_t - T_o) \, dt \qquad (4.5)$$

where T_t is the temperature at any time t, and T_o is a datum temperature. In this experiment, T_o is taken as 5 °C, a value typical of Type I portland cements cured at about 20 °C (11). The approximate maturity of each specimen was calculated in discrete time increments, using the time and temperature data recorded in the experiment, according to the equation

$$M = \sum (T_a - T_o) \, \Delta t \qquad (4.6)$$

where T_a is the average temperature during the time interval Δt. At lower maturities, when the temperatures of the specimens were changing rapidly with age, the time interval Δt was 15 minutes. At higher maturities, when the temperature of each specimen remained relatively constant with age, Δt was

36

taken as 2 hours. Results are reported with time expressed in hours and temperature in $^{\circ}$C, hence M has the units $^{\circ}$C·hours.

The relationship between paste velocity and maturity is obtained by substituting maturity for age in eq. (4.4):

$$C_p^P = \frac{(C_p^{up} - C_o) K (M - M_o)}{1 + K (M - M_o)} + C_o \qquad (4.7)$$

where M_o is the maturity of the paste cylinder at the start of velocity gain.

To evaluate the series model, eq. (4.7) had to be fitted to the velocity-maturity data from the paste specimen. This was done as follows. First, the velocity-time results for each specimen were transformed into velocity-maturity results, using eq. (4.6) and a datum temperature of 5 $^{\circ}$C. Next, the limiting paste velocity is determined. At higher maturities,

$$M \simeq (M - M_o) \qquad (4.8)$$

and eq. (4.7) can be rearranged into the linear equation

$$\frac{1}{(C_p^P - C_o)} = \frac{1}{K (C_p^{up} - C_o)} \cdot \frac{1}{M} + \frac{1}{(C_p^{up} - C_o)} \qquad (4.9)$$

The y-intercept of eq. (4.9) is $(C_p^{up} - C_o)$. In this experiment, C_o was taken as 625 m/s because the measured data appeared to follow a hyperbolic relationship beyond this point. The best-fit of eq. (4.9) to the velocity-maturity results from the paste specimen was determined by linear regression. The regression was performed beginning with the results at highest maturity, and incrementally including one additional earlier measurement until the best-fit linear curve was obtained. The criterion used to determine how many data points to include was to use the number of points that produced the highest correlation coefficient. The results of the analysis are shown in Figure 4.14 (a). The best fit linear curve was obtained using 10 data points, resulting in a value of 2470 m/s for $(C_p^{up} - C_o)$.

Lastly, to determine K and M_o, eq. (4.7) was rearranged into a second linear equation

$$\frac{C_p^P - C_o}{((C_p^{up} - C_o) - (C_p^P - C_o))} = K M - K M_o \qquad (4.10)$$

The slope of the line is K and the x-intercept is M_o. As stated earlier, K is related to the initial slope of the hyperbola. Thus, a second linear

37

regression was performed using eq. (4.10), beginning with the data at lowest maturity, and incrementally including one additional later measurement until the best-fit linear curve was obtained. Again, the criterion was to use the number of points that produced the highest correlation coefficient. The results of the analysis are shown in Figure 4.14 (b). The best-fit linear curve was obtained using 21 data points, resulting in values for K and M_o of 0.005838 (°C·hours)$^{-1}$ and 157 °C·hours, respectively.

Once this relationship for the velocity in the paste specimen as a function of maturity was established, eq. (4.2), the series model, was used to predict the velocities in the concretes containing 40 and 60 percent aggregate by volume. In computing the predicted velocities in the concretes, the velocity in the aggregate was taken as 4850 m/s. This velocity is within the range of velocities (4300 to 5000 m/s) measured experimentally through large aggregate particles using the through transmission pulse velocity technique (3).

Figure 4.15 is a plot of the experimentally measured velocity in each specimen versus maturity. Superposed on the paste specimen results is the velocity predicted by eq. (4.7), using the values of (C_p^{up} - C_o), K, and M_o arrived at as described above. Superposed on the concrete specimens results are the velocities predicted by the series model (eq. 4.2). From Figure 4.15 it is seen that eq. (4.7) represents the velocity development in the paste well. Further, from Figure 4.15 it is seen that the series model gives a good prediction of the P-wave velocity in the concrete. Thus, the series model appears to adequately describe the influence of aggregate content on the velocity in the concrete. This information is useful in explaining some of the observations presented in the sections that follow.

4.4 CONCRETE AND SIEVED MORTAR TESTS

4.4.1 Objective and Scope

As stated in Chapter 1, one of the main objectives of this research project was to evaluate the usefulness of the impact-echo technique as a means of measuring the setting time of concrete. Results of impact-echo velocity tests performed on concrete are reported in this section. The results of these measurements are compared to initial setting times measured by penetration resistance.

Four different concrete mixtures were examined:

1. low w-c ratio concrete (approximately 0.39 after aggregate moisture corrections)
2. low w-c ratio concrete with an accelerator (0.39)
3. low w-c ratio concrete with a retarder (0.39)
4. high w-c ratio concrete (0.78)

A total of twelve experiments (three replicate tests of each mixture) were performed. Replicate tests were performed on different days.

For each test, four cylindrical specimens were prepared; one concrete specimen and three sieved mortar specimens. The concrete and sieved mortar was placed to a depth of 160 mm in each mold. The concrete specimen and one

sieved mortar specimen were used to monitor the development of P-wave velocities. The remaining two sieved mortar specimens were used to monitor the development of penetration resistance.

4.4.2 Materials

The concretes were made using Type I portland cement, rounded gravel with nominal maximum size of 19 mm (0.75 in.), sand with a fineness modulus of 2.12 and tap water. Fineness modulus, specific gravity, absorption, and periodic moisture contents were determined according to applicable ASTM Standard Test Methods (C 127, C 128, C 136, C 566) (3). Mixture proportions and material properties for the aggregates used in this part of the study are summarized in Tables 4.3 and 4.4 respectively. When a set-controlling admixture was used, the amount of mixing water was adjusted to account for the water content of the admixture. The accelerator used in the experiments conformed to ASTM C 494 (Standard Specification for Chemical Admixtures for Concrete) (3), Type C. The retarder used conformed to ASTM C 494, Types B and D. Admixtures were used at the dosages recommended by the manufacturer. The amount of each admixture used is listed in Table 4.3.

4.4.3 Specimen Preparation

The concretes were mixed in a 1.5 cubic foot capacity revolving drum mixer. The mixing procedure was as follows:

1. Thoroughly wet the mixing drum and allow it to dry in an inverted position for 1 minute.
2. Add coarse aggregate, fine aggregate, and cement and dry mix for 30 seconds.
3. Add mixing water over a two minute period while drum is revolving.
4. Continue mixing for an additional 3 minutes.
5. Perform slump test; ASTM C 143 (3) (results of the slump tests are reported in Table 4.5).
6. Briefly remix, cover the mixer opening, and allow the concrete to rest for 20 minutes elapsed time after initial contact between cement and water.

The concrete was allowed to rest for 20 minutes prior to the sieving operation to allow absorption of mixing water by the coarse and fine aggregate to take place. This was done to ensure similar w-c ratios in the paste phases of the concrete and the mortar sieved from the concrete.

Just prior to sieving, a portion of the fresh concrete was set aside to make the concrete specimen. The remainder was passed through a #4 sieve to remove large aggregate, as prescribed in ASTM C 403. A vibrator was used to aid in the sieving operation.

4.4.4 Results and Observations

As stated in section 4.4.1, four different concrete mixtures were examined: low w-c ratio concrete (approximately 0.39 after aggregate moisture corrections), high w-c ratio concrete (approximately 0.78 after aggregate moisture corrections), accelerated concrete, and retarded concrete. In the

39

following discussions, these four concrete mixtures are referred to as CL, CH, CA, and CR respectively. The CL, CA, and CR concretes all have the same w-c ratio (0.39); the only difference between each series was the use of the admixtures. The data from the impact-echo and penetration resistance tests performed on the CL, CH, CA, and CR series are presented in Appendix A.

4.4.4.1 Velocity Measurements on Concrete

In this section, the results of impact-echo velocity measurements on the low w-c ratio concrete series (CL) are discussed. Observations about the scatter in the velocity measurements, strength of the signals, and higher modes of vibration, are applicable to all the series tested (CL, CH, CA, and CR).

Figure 4.16 (a) shows the results of penetration resistance measurements on test CL2, one of the CL series replicates. From this figure, times of initial and final setting, as defined by ASTM C 403, were determined to be 4.4 and 5.6 hours, respectively. Figure 4.16 (b) shows the results of the velocity measurements made on the concrete and sieved mortar from test CL2. Superposed on Figure 4.16 (b) as dashed lines are the times of initial and final setting determined from the penetration resistance test.

As was found in the prepared mortar tests, there was considerable scatter in the earliest velocity measurements in both the concrete and sieved mortar specimens. Again this scatter appeared to be about a constant value. After this initial period of scatter, the velocity measurements became more clearly defined, and the development of velocity could be followed.

Figures 4.17 (a) through (l) show the frequency spectra for some of the impact-echo tests made on the concrete specimen shown plotted in Figure 4.16 (b). The frequency range shown in each spectrum is from 0 to 15 kHz. Noted on each frequency spectrum is the frequency peak used to compute the velocity plotted in Figure 4.16 (b).

As can be seen in Figures 4.17 (a) and (b), early frequency spectra were characterized by large amplitude low frequency peaks. As the concrete matured, the peak attributed to the resonance of the receiver became clearly visible as a single low frequency, high amplitude peak (Figures 4.17 (c) and (d)). As can be seen in Figure 4.16 (b), the velocity measurements are still scattered at this age (2.73 hours). Beginning at an age of 2.88 hours (Figure 4.17 (e)), the peak at 0.781 kHz attributed to the resonant response of the specimen could be clearly identified. Using eq. (3.13), the corresponding P-wave velocity was calculated as 250 m/s.

At the time of this earliest well-defined measurement the resonant response of the cylinder was weak; that is, the magnitude of the peak in the frequency spectrum due to the fundamental mode of vibration of the specimen was small relative to the peak attributed to transducer resonance. The fact that the earliest reliable measurements were associated with smaller amplitude frequency peaks (relative to the peak caused by the transducer) aided in identifying the reliable measurements.

Once the peak attributed to the resonant response of the specimen was clearly identified, the development of velocity could be easily followed. In Figure 4.16 (b) it is seen that at ages later than 2.88 hours, the scatter in the velocity development curve diminishes. Further, as hydration proceeded, the response of the cylinder became stronger. Higher modes of vibration

became more evident in the frequency spectra, as can be seen by the smaller amplitude, higher frequency peaks beginning in Figure 4.17 (i).

Figure 4.16 (b) shows that at any given time, the concrete exhibited a higher velocity than the sieved mortar. This is easily explained by the series model. Because the coarse aggregate had been removed from the sieved mortar, it had a lower aggregate-paste ratio than the concrete. If the paste phases were similar in both the concrete and sieved mortar at any given time (neglecting temperature differences discussed in section 4.4.4.4), then the concrete, containing a higher proportion of aggregate, would be expected to exhibit a higher velocity. Hence, the vertical separation between the concrete and sieved mortar velocity curves reflects the difference in aggregate content between the two specimens.

From Figures 4.16 (a) and (b) it is seen that at the time of initial setting (as defined by a 500 psi penetration resistance), the velocity development curves are already well-defined for both the concrete and sieved mortar. Further, as in the prepared mortar tests, it is seen that at the time of final setting (as defined by a 4000 psi penetration resistance) there are no discontinuities in the velocity curves.

Clearly, an advantage of the impact-echo method is that the development of P-wave velocity can be monitored for a longer period of time than can penetration resistance. It is impractical to continue penetration resistance tests much beyond a penetration resistance of 4000 psi. The material is beyond the stiffening or setting period and is gaining strength. However, impact-echo velocity measurements can still be made at these later ages, into the region of strength gain. This is discussed in detail in Chapter 5.

The results of all three replicate CL series tests are shown plotted together in Figures 4.18 (a) and (b). It is seen from these figures that in test CL3, setting began earlier than in tests CL1 and CL2. This earlier setting time was reflected by similar shifts in both the velocity and penetration resistance curves. Thus, as in the prepared mortar tests, the velocity measurement was influenced by the same factors that altered the setting time measured by the penetration resistance test. The test that showed the earliest time of initial setting as defined by penetration resistance also showed the earliest gain in P-wave velocity.

For replicate tests CL1 and CL3 the earliest well-defined velocity measurements were 281 m/s at 3.17 hours, and 313 m/s at 2.87 hours, respectively. As stated earlier, the times of these earliest reliable velocity measurements mark the end of the period during which there is considerable scatter in the measurements. At the time the measurements become clearly defined, the P-wave velocity begins to increase rapidly with age. The differences in the values of the initial velocity readings in each of the CL replicates are not significant. This is because of the velocity tests were made at discrete time intervals, whereas the velocity was increasing continuously (approximately 275 m/s per hour at the time of the earliest measurements). Further, as pointed out in section 4.1.3, the accuracy to which the velocity could be computed was limited by the sampling interval.

It is noted that the values of the earliest well-defined velocity measurements are less than the velocity of sound in air (343 m/s). The reason for this is unclear. It may be the result of inelastic or viscoelastic behavior in the very weak concrete, because the stress waves introduced by impact are transmitted through what is probably a sparsely interconnected microstructure.

41

A comparison was made of the time the P-wave velocity began to develop in each CL series concrete specimen with the time of initial setting (penetration resistance of 500 psi) of the corresponding sieved mortar specimen. For simplicity, the beginning of velocity gain in each concrete specimen was taken as the time a velocity of 300 m/s was achieved. Clearly, this is within the range of the earliest reliable measurements obtained experimentally. The times corresponding to velocities of 300 m/s in the concrete specimens were obtained by interpolation on curves hand drawn through the data points. A similar interpolation was made to determine the initial setting times corresponding to penetration resistances of 500 psi in the sieved mortars.

Initial setting occurred at 4.4 hours for tests CL1 and CL2, and at 3.9 hours for test CL3. The beginning of velocity development in the concrete specimens (300 m/s) occurred at 3.3, 3.1, and 2.9 hours for tests CL1, CL2, and CL3, respectively. Thus the difference between the time of initial setting and the beginning of P-wave velocity development in the concrete was approximately the same for each test (approximately 1.1, 1.3, and 1.0 hours for tests CL1, CL2, and CL3 respectively). Thus, on the average, the velocity in the concrete began to increase dramatically about 1.1 hours before initial setting of the corresponding sieved mortar.

A comparison was also made of the magnitude of the velocity in each concrete specimen at the time of initial setting in the corresponding sieved mortar specimen. By interpolation on the concrete velocity curves, velocities of 590, 620, and 590 m/s were obtained at the times of initial setting for tests CL1, CL2, and CL3, respectively. Thus, on the average, the velocity in each CL concrete specimen was approximately 600 m/s at the time of initial setting of the corresponding sieved mortar.

4.4.4.2 Influence of Set-Controlling Admixtures

Figures 4.19 (a) and (b) show the results of the penetration resistance and velocity measurements for the three replicate accelerated concrete tests. Initial setting occurred at 3.3 hours for test CA1, and at 3.6 hours for tests CA2 and CA3. As in the low w-c ratio concrete tests, the velocity in the accelerated concrete was about 300 m/s at the onset of velocity development. The velocity in each accelerated concrete specimen reached 300 m/s at 2.4, 2.7, and 2.6 hours for tests CA1, CA2, and CA3, respectively. Thus, as was found in the CL series, there was a consistent difference (approximately 0.9 hours for tests CA1 and CA2, and 1.0 hours for test CA3) between the time of initial setting, and the onset of velocity development in the accelerated concrete specimens.

The same analysis of the results of the three replicate retarded concrete tests, shown plotted in Figures 4.20 (a) and (b), lead to similar results. Initial setting occurred at 6.6, 6.3, and 6.4 hours for tests CR1, CR2, and CR3, respectively. The velocity in each corresponding concrete specimen reached 300 m/s at 5.1, 4.8 and 5.0 hours respectively. Thus the difference between the time of initial setting, and the onset of velocity development was the same for each test (approximately 1.5 hours for tests CR1 and CR2, and 1.4 hours for test CR3).

From the above results, it is seen that the time interval between the onset of P-wave velocity development and initial setting is shorter in the accelerated concrete series as compared to the retarded concrete series. This shorter time separation is explained by Figures 4.21 (a) and (b), which show

42

the results of penetration resistance and velocity measurements from tests CA3 and CR1. In these figures, the times of initial setting are indicated with dashed lines, and the times that 300 m/s velocities were reached in the concrete specimens are indicated with solid lines. From Figure 4.21 (b) it is seen that there was a more rapid rate of velocity increase in test CA3 as compared to test CR1. This is especially evident immediately after the beginning of velocity development in each test. Also, there is a slightly greater rate of increase of penetration resistance in the accelerated mortar as compared to the retarded mortar. At the onset of velocity development, the penetration resistances for tests CA3 and CR1 were about the same low value. Thus, because of the slower rate of increase in CA3, a longer time is needed to reach the 500 psi penetration resistance. As a result, for test CR1, a longer period of time elapsed between when the velocity in the concrete reached 300 m/s, and the penetration resistance in the sieved mortar reached 500 psi, as compared to CA3.

Again, it is useful to compare the velocity in each concrete specimen at the time of initial setting of the accompanying sieved mortar specimen. By interpolation on the velocity curves shown in Figure 4.19 (a), the velocities in the accelerated concrete specimens at the time of initial setting were the same; 700 m/s for test CA1, and 720 m/s for tests CA2 and CA3. By interpolation on the velocity curves shown in Figures 4.20 (a), the velocities in the retarded concrete specimens at the time of initial setting were approximately the same; 650, 770, and 680 m/s, for tests CR1, CR2, and CR3, respectively.

4.4.4.3 Influence of Changes in Water-Cement Ratio

Figures 4.22 (a) and (b) show the results of penetration resistance and velocity measurements for the three replicate high w-c ratio (0.78) concrete tests. Initial setting occurred at 5.6, 6.0, and 5.7 hours, for tests CH1, CH2, and CH3, respectively. As in the low w-c ratio tests, the velocity in the high w-c ratio concrete at the onset of velocity development was about 300 m/s. The velocity in each corresponding concrete specimen reached 300 m/s at 4.3, 4.8, and 4.5 hours, respectively. Thus, as was found in the CL, CA, and CR series, there was a consistent difference (approximately 1.3 hours for test CH1, and 1.2 hours for tests CH2 and CH3) between the C 403-time of initial setting and the onset of velocity development.

By interpolation on the velocity curves in Figure 4.22 (b), the velocity in each high w-c ratio concrete specimen at the time of initial setting was approximately the same; 520, 510, and 480 m/s, for tests CH1, CH2, and CH3, respectively. These velocities are lower than the velocities in the CL, CA, and CR concrete specimens at their respective initial setting times.

Figures 4.23 (a) and (b) show comparison of representative results from the low and high w-c ratio tests (tests CH1 and CL2). As was observed in the prepared mortar tests, the rate of velocity increase was different for the different w-c ratio mixtures. The initial setting time, and the time a P-wave velocity of 300 m/s was reached for each test are shown as dashed and solid lines, respectively, in the figures.

The time interval between the onset of velocity development in the concrete specimen and the time of initial setting of the sieved mortar was the same for both tests; 1.2 hours. This consistent 1.2 hour time difference is somewhat surprising, since the rates of velocity and penetration resistance

43

increase in the CH and CL mixtures were different. In section 4.4.4.2 it was shown that because these rates differed between the accelerated and retarded concretes, the time interval between the onset of velocity development and initial setting also differed. Accordingly, it might have been expected that the time interval between the onset of velocity development and initial setting would have been longer in test CH1 as compared to test CL2.

This apparent contradiction may be explained as follows. Most of the adjustment in mixture proportions to produce the high w-c ratio concrete was made by a volumetric replacement of some cement with fine aggregate. Thus the aggregate contents of the CH series concretes and sieved mortars were more similar to each other, than were the concretes and sieved mortars of the CL series, assuming the sieving operation was equally effective in both series. No attempt was made to determine the fractions of paste and aggregate in the sieved mortars. However, examination of Figure 4.23 (b) reveals a smaller vertical separation between the velocity curves for the CH1 concrete and sieved mortar, as compared to the CL2 concrete and sieved mortar. Recalling that this vertical separation may result from a difference in aggregate content further suggests that the aggregate contents of the CH series concretes and sieved mortars were more similar to each other than were those of the CL series. The effect of aggregate content on penetration resistance was not studied as a part of this investigation. However, it is reasonable to expect that the presence of more fine aggregate may have led to a higher penetration resistance for a given cement paste strength. Thus the initial setting time for the CH series sieved mortars would tend to be lower. This lower initial setting time would have reduced the time interval between the onset of velocity development in the concrete and the time of initial setting in the sieved mortar.

4.4.4.4 Specimen Temperatures

The temperatures of the concrete and sieved mortar specimens were monitored using thermocouples positioned at the center of the specimen. Using a data logger, the specimen temperatures were automatically sampled once every 30 seconds, and average temperatures computed and recorded every 15 minutes. Three sieved mortar specimens were prepared for each test (one for velocity measurements, and two for penetration resistance tests), with the temperature monitored in one mortar specimen considered as representative of all three.

Figures 4.24 (a), (b), and (c) show the temperatures of the concrete and sieved mortar specimens recorded from tests CL3, CA3, and CR1, respectively. Superposed on each figure as dashed lines are the initial setting times, and as solid lines the times the P-wave velocity in each concrete specimen reached 300 m/s.

The ratio of paste to aggregate was higher in each sieved mortar specimen than its corresponding concrete specimen. As a result, the sieved mortar specimens, containing a higher proportion of cement paste, exhibited a greater temperature rise than the concrete specimens.

The significance of this temperature difference at any given age depended upon the cumulative time-temperature (maturity) difference. For the tests shown in Figures 4.24 (a), (b), and (c), the difference in temperature between the concrete and sieved mortar specimens was not significant at the C 403-time of initial setting. Thus, up to this time, the paste phases of the concrete

44

and sieved mortar specimens were probably at approximately the same degree of hydration. This was typical for all CL, CA, and CR tests.

Figure 4.24 (d) shows the temperatures of the concrete and sieved mortar specimens recorded from test CH1. Again, superposed as dashed and solid lines, are the time of initial setting and the time the compression wave velocity reached 300 m/s in the concrete specimen. As can be seen, the concrete and sieved mortar specimens of test CH1 exhibited a lower temperature rise than the specimens of tests CL3, CA3, and CR1. This is because the high w-c ratio mixture contained less cement. Further, the largest temperature difference between the concrete and sieved mortar specimens in the high w-c ratio mixture was only 2 °C. Hence the temperature differences between the concrete and sieved mortar specimens were probably insignificant, and paste phases of both the concrete and sieved mortar specimens were at approximately the same degree of hydration throughout the duration of the test. This was typical of all CH series tests.

4.5 DEFINING SETTING TIME USING IMPACT-ECHO VELOCITY MEASUREMENTS

In section 4.4 it was observed that for a given concrete series, there was a consistent difference between the time of initial setting in sieved mortar specimens and the onset or beginning of velocity development in the concrete specimens. The onset of P-wave velocity development was taken as the time a velocity of 300 m/s was reached in each concrete specimen. It was also observed in section 4.4 that for a given concrete series, the velocities in the concrete specimens at the times of initial setting in the corresponding mortar specimens were approximately the same in each replicate test. These two observations suggest the following two approaches to defining the setting time of concrete using impact-echo velocity measurements:

1.   Defining setting at the time corresponding to the onset or beginning of P-wave velocity development in the concrete.
2.   Defining setting at the time a specified P-wave velocity is reached in the concrete.

These two approaches are shown schematically in Figure 4.25 as "1" and "2" respectively. This second approach is analogous to the way initial and final setting are defined by penetration resistance in ASTM C403.

The following sections explore each of these approaches in greater detail, examining the basis and implications of each.

4.5.1 Defining Setting Time at the Onset of P-Wave Velocity Development

Table 4.6 lists the C 403-time of initial setting for the mortar specimens, and the time at which a 300 m/s velocity was reached in the corresponding concrete specimens. Figure 4.26 is a plot of these two setting times for each test. From this figure it is seen that variations in initial setting times, measured by penetration resistance, were reflected by proportional variations in the times the velocities began to increase in each concrete specimen. The straight line superposed on the data was determined by linear regression, and the correlation coefficient is 0.9956. Thus there is a strong correlation between the time of initial setting and the onset of

45

velocity development. Therefore, by defining setting time as the onset of velocity development, it appears that different mixtures will show proportional changes in setting times measured by impact-echo and penetration resistance.

Defining the setting time of concrete as the time of the start P-wave velocity development is appealing, because setting is thus based on an actual physical change occurring in the cement paste, rather than on some arbitrary strength or stiffness that is changing continuously. Setting will mark the time the elastic modulus of the paste begins to increase dramatically. This dramatic increase is probably due to the interlocking of the hydrating cement grains in the developing microstructure, and may indicate the end of the induction period. A change in aggregate content should not alter the setting time measured in this way, because the time at which the elastic modulus begins to increase rapidly is determined by changes occurring in the paste.

The disadvantage to this approach is that the onset of velocity development is sometimes difficult to identify because the earliest measurements are weak. Further, the concrete is still weak at this age; at the onset of velocity development in the concrete, the penetration resistance in the accompanying sieved mortar is about 80 psi. Thus setting time defined by this approach may not have much practical significance insofar as being related to specific construction operations such as slipforming or finishing operations.

Defining the setting time at the onset of velocity development can be useful in the laboratory. The entire velocity development curve can be constructed, and the influence of different variables upon the time of setting and subsequent rate of velocity increase can be compared.

4.5.2 Defining Setting Time at a Specified P-Wave Velocity

A second approach to defining the setting time of concrete based on impact-echo velocity measurements is to use the time a specified P-wave velocity is reached. This approach to defining setting has several implications which are discussed in the following paragraphs.

For the CL, CA, and CR series (same mixture proportions), it is logical to assume, based on the series model, that at a given P-wave velocity in each concrete, the paste phase in each has the same elastic modulus. Thus, for a given mixture proportion, initial setting time based on a specified velocity should indicate when the paste has reached a given stage of hydration.

For two concrete mixtures with the same aggregate fractions but different w-c ratios, it is logical to assume that for the same P-wave velocity in both concretes, the paste phases have the same elastic modulus. However, to achieve the same elastic modulus in the pastes, the cement grains of the higher w-c ratio mixture would probably have to be at a more advanced stage of hydration. This is because the cement grains are further apart in a high w-c ratio mixture. If elastic modulus is dependent upon the degree and stiffness of interlocking between hydration products and the volume of voids, the higher w-c ratio mixture would therefore require a greater degree of hydration to achieve a given elastic modulus. In short, although the pastes may have the same elastic modulus at any given concrete velocity, the hydration will probably be more advanced in the higher w-c ratio concrete (see Figures 3.13 and 3.14).

46

Lastly, for two concrete mixtures of the same w-c ratio, but different aggregate fractions, a given P-wave velocity in both concretes would indicate the paste phases of each had different elastic moduli. The paste in the concrete with the lower aggregate content would have a higher elastic modulus (or probably a greater degree of hydration).

From the discussion above, it is seen that by selecting a target velocity to define the setting time of concrete, the paste phases of different concrete mixtures could be at different stages of hydration or have different elastic moduli. Setting time would be defined in terms of the composite elastic modulus of the material. If, however, setting was defined by a specific target velocity for a particular concrete mixture, then the paste phases of different batches of that mixture would have the same elastic modulus and degree of hydration at that velocity.

Table 4.6 also lists the times a target velocity of 670 m/s was achieved in each concrete specimen. This target velocity was taken as the average velocity of the CL, CA, and CR concrete specimens at the C 403-time of initial setting. Thus a target velocity of 670 m/s makes the two setting times approximately the same for the CL, CA, and CR series. Figure 4.27 is a plot of these two setting times. Because the setting times were made to be approximately the same, a line through the origin with a slope equal to 1 is drawn on the figure. As can be seen, the points from the CH series fall below this line. Thus by defining setting time by this second approach, concretes with different mixture proportions may not have proportional setting times measured by impact-echo and penetration resistance.

Defining the setting time of concrete at a specific target velocity may have more practical uses. A relationship can be established for a given concrete mixture between a specific P-wave target velocity and certain construction operations. Further, target velocities are easier to identify than the onset of velocity development.

The two approaches to using impact-echo velocity measurements to define the setting time of concrete could be used in combination. Initial setting time could be defined as the time of onset of P-wave velocity development, and final setting at some later target velocity. Then the time interval between initial and final setting might be used as an indication of the rate of hardening of the given mixture.

4.6 SUMMARY

The results of tests aimed at demonstrating the feasibility of using the impact-echo method to determine the setting time of concrete were presented in this chapter. The development of P-wave velocity was monitored and related to setting time measured by penetration resistance.

It was shown that very early-age velocity measurements were scattered, and that the scatter appeared to be about a constant velocity value. At the age the velocity measurements became well-defined, the velocity began to increase dramatically and the development of velocity could be easily followed.

It was demonstrated that there is a strong correlation between the C 403-time of initial setting and the onset of P-wave velocity development in concrete. This was demonstrated in two ways. First, for a given series, a consistent difference was found between the time the P-wave velocity began to

47

increase rapidly and the time of initial setting of the corresponding sieved mortar. Second, for a given series, the velocity in each concrete specimen was the same at the time of initial setting in its corresponding sieved mortar. It is also noted that the onset of velocity development occurred earlier than initial setting of the sieved mortar.

The impact-echo method was shown to be sensitive to changes in setting times caused by set-controlling admixtures. Variations in initial setting time, measured by penetration resistance, were reflected by proportional variations in the times the velocities began to increase dramatically in each concrete specimen.

Lastly, it was shown that the influence of aggregate content on the compression wave velocity in concrete could be described by a simple series model. The time of transit of a compression wave through the concrete could be taken equal to the summation of the time of transit through each phase individually.

Based on the observations summarized above, two approaches were presented for using the impact-echo method to define the setting time of concrete:

1. Defining setting time at the onset of velocity development;
2. Defining setting at the time a specified velocity value is reached.

The first approach defines setting based upon changes occurring in the cement paste. The second approach defines setting in terms of a composite elastic modulus for the concrete.

Table 4.1 Mixture proportions (by weight) for prepared mortar tests

Test	Sand	Cement	Water
ML1, ML2, ML3, ML4	2.4	1.0	0.40
MHI, MH2, MH3	3.0	1.0	0.55
MH4, MH5	2.7	1.0	0.55

Table 4.2 Material properties for prepared mortar tests

Cement:	Type I (ASTM C 150)
Natural Sand:	
Fineness Modulus	2.34
Bulk Specific Gravity (SSD Basis)	2.63
Absorption (SSD Basis)	1.4 %
Range of Moisture Contents	0.65 to 0.50 %

Table 4.3 Mixture proportions for concrete-sieved mortar tests

Test Series	Water (gm)	Cement (gm)	Coarse Aggregate (gm)	Fine Aggregate (gm)	Admixture (mL)
CL	425	1000	2091	1091	
CA	423*	1000	2091	1091	2.0
CR	423*	1000	2091	1091	2.6
CH	795	1000	2426	3558	

* Quantity of mixing water adjusted for water content of admixture

Table 4.4   Material properties for concrete-sieved mortar tests

Cement:	Type I (ASTM C 150)
Natural Sand:	
Fineness Modulus	2.12
Bulk Specific Gravity (SSD Basis)	2.65
Absorption (SSD Basis)	1.6 %
Range of Moisture Contents	0.50 to 0.40 %
Coarse Aggregate (Gravel):	
Bulk Specific Gravity (SSD Basis)	2.56
Absorption (SSD Basis)	0.7 %
Range of Moisture Contents	0.60 to 0.13 %

Table 4.5 Results of slump tests

Test	Slump (mm)
CL1	140
CL2	150
CL3	180
CA1	140
CA2	165
CA3	120
CR1	190
CR2	190
CR3	190
CH1	95
CH2	70
CH3	65

Table 4.6 Comparison of setting times

Test	Initial Setting Time (C 403) (hours)	Time to Reach 300 m/s (hours)	Time to Reach 670 m/s (hours)
CL1	4.4	3.3	4.7
CL2	4.4	3.1	4.6
CL3	3.9	2.9	4.1
CA1	3.2	2.4	3.2
CA2	3.6	2.7	3.5
CA3	3.6	2.6	3.5
CR1	6.6	5.1	6.7
CR2	6.3	4.8	6.1
CR3	6.4	5.0	6.4
CH1	5.6	4.3	6.3
CH2	6.0	4.8	6.8
CH3	5.7	4.5	6.7
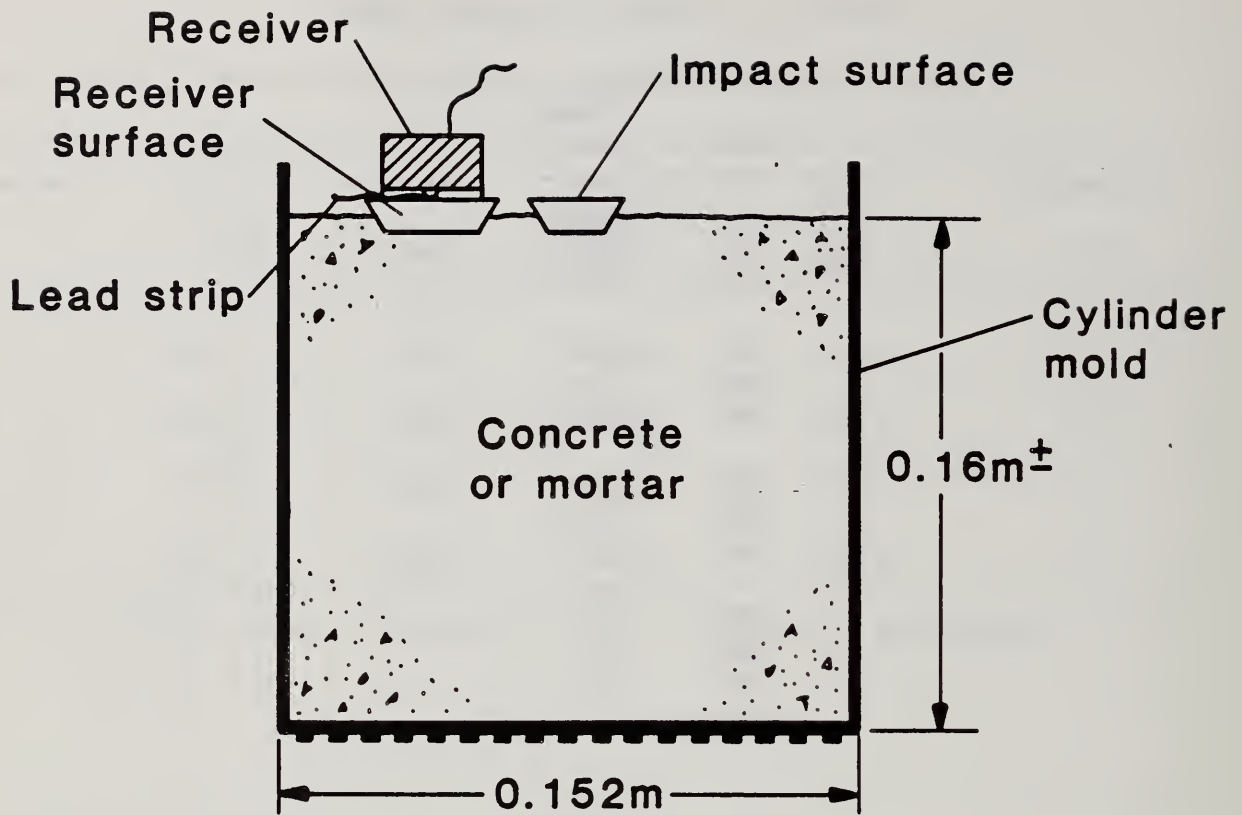
Figure 4.1   Schematic representation of experimental set-up used
to monitor the development of P-wave velocity in early-age concrete
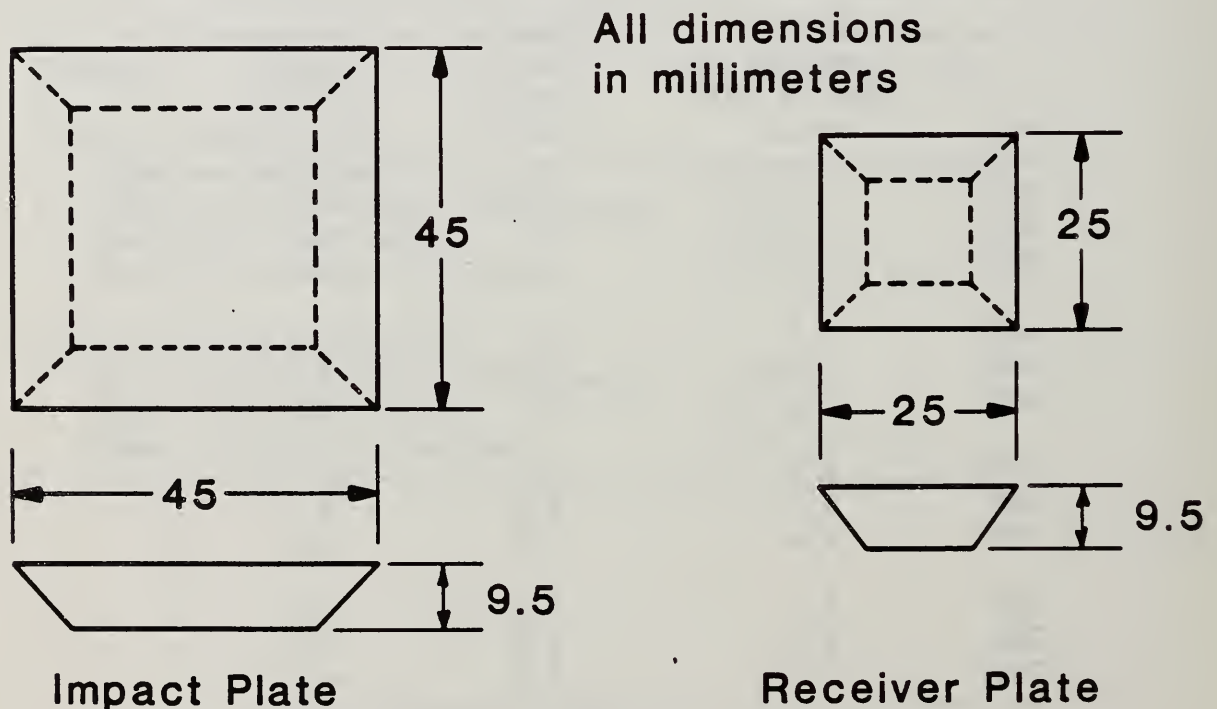
Figure 4.2   Impact and receiver plates
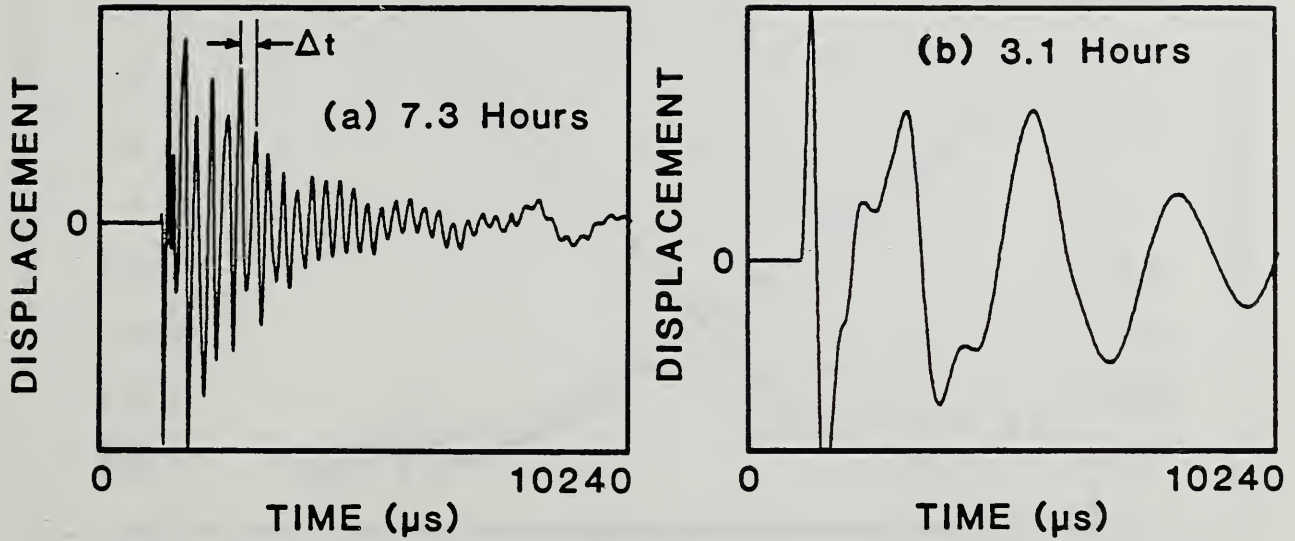
Figure 4.3   Typical surface displacement waveforms at ages of:
a) 7.3 hours; and, b) 3.1 hours
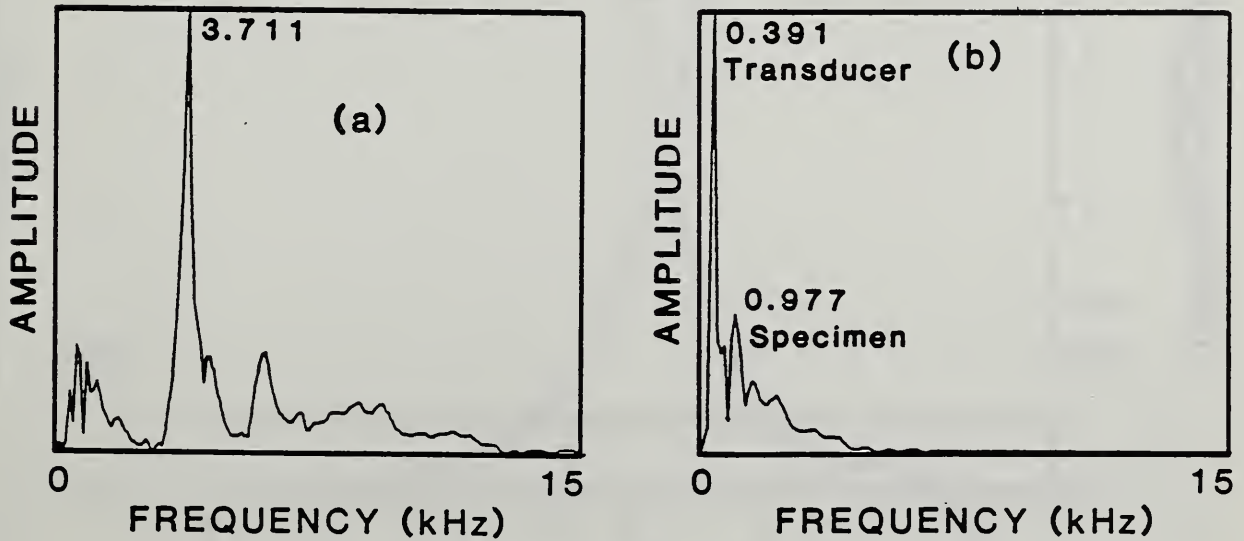
Figure 4.4   Frequency spectra of the waveforms shown in: a) Figure
4.3 (a); and, b) Figure 4.3 (b)

53
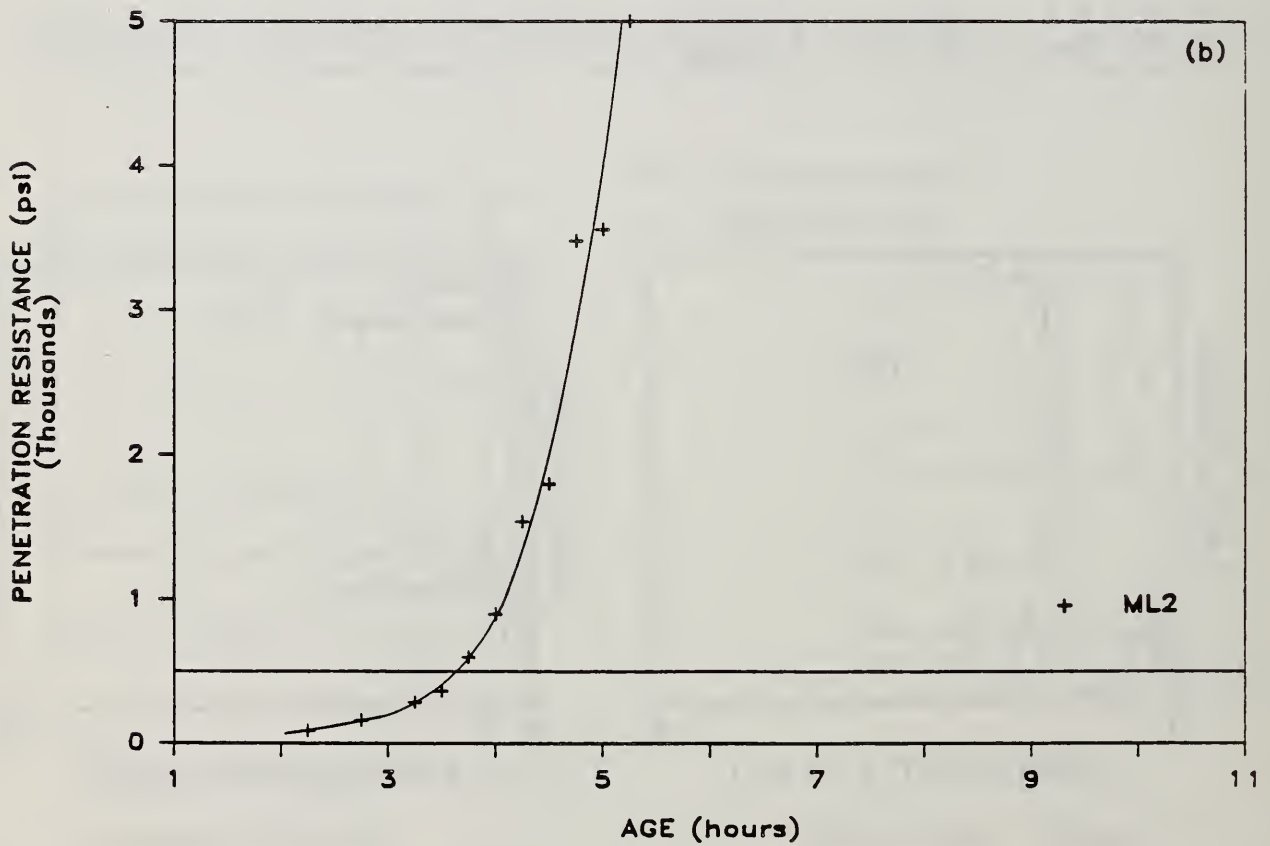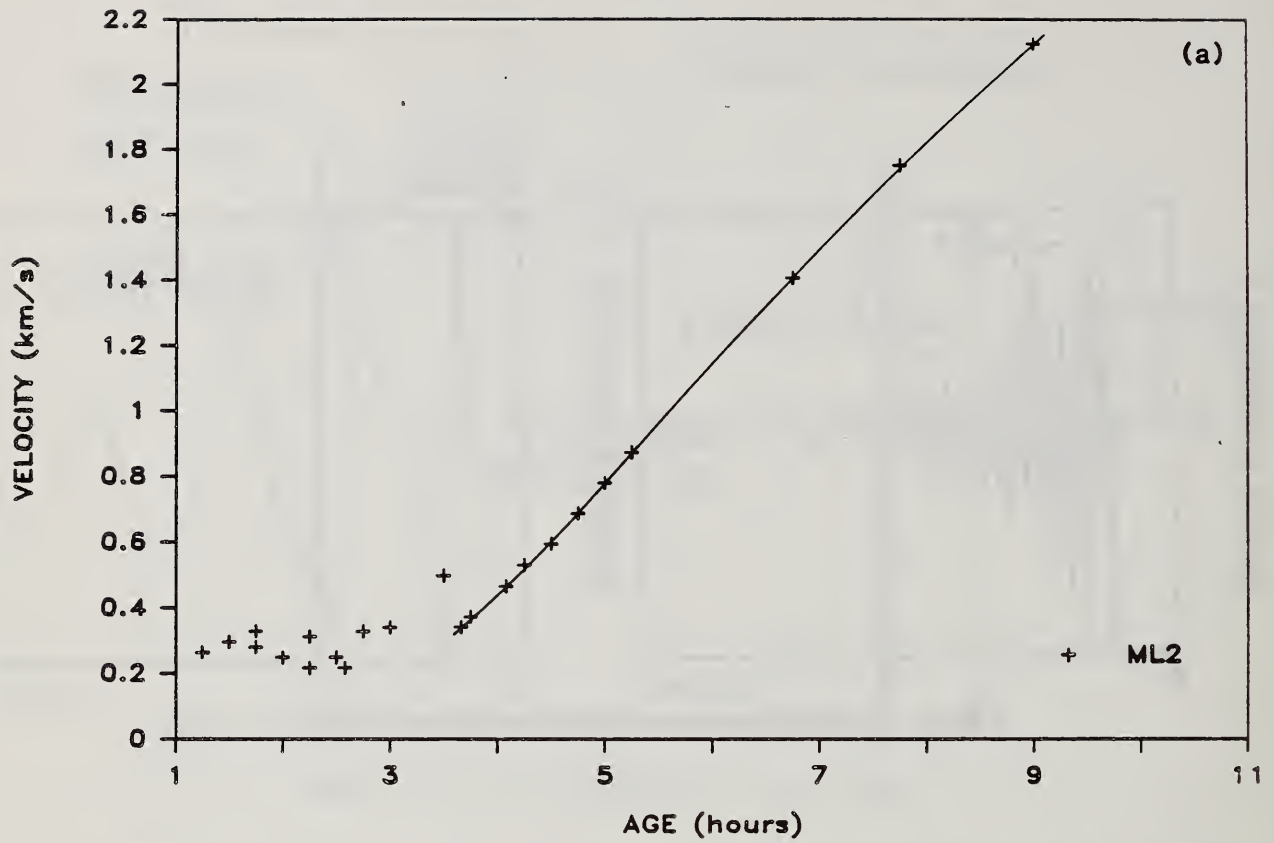
Figure 4.5   Results of prepared mortar test ML2: a) P-wave velocity
vs age; and, b) penetration resistance vs age
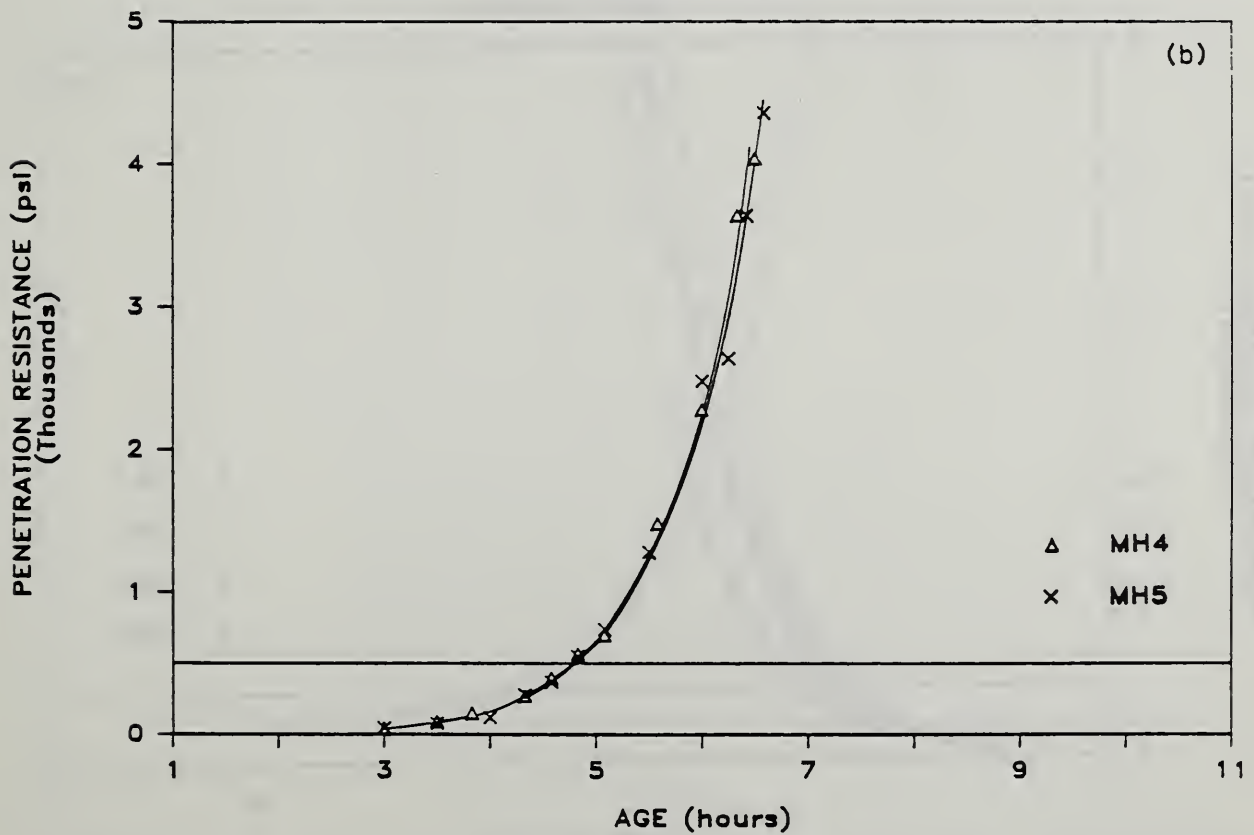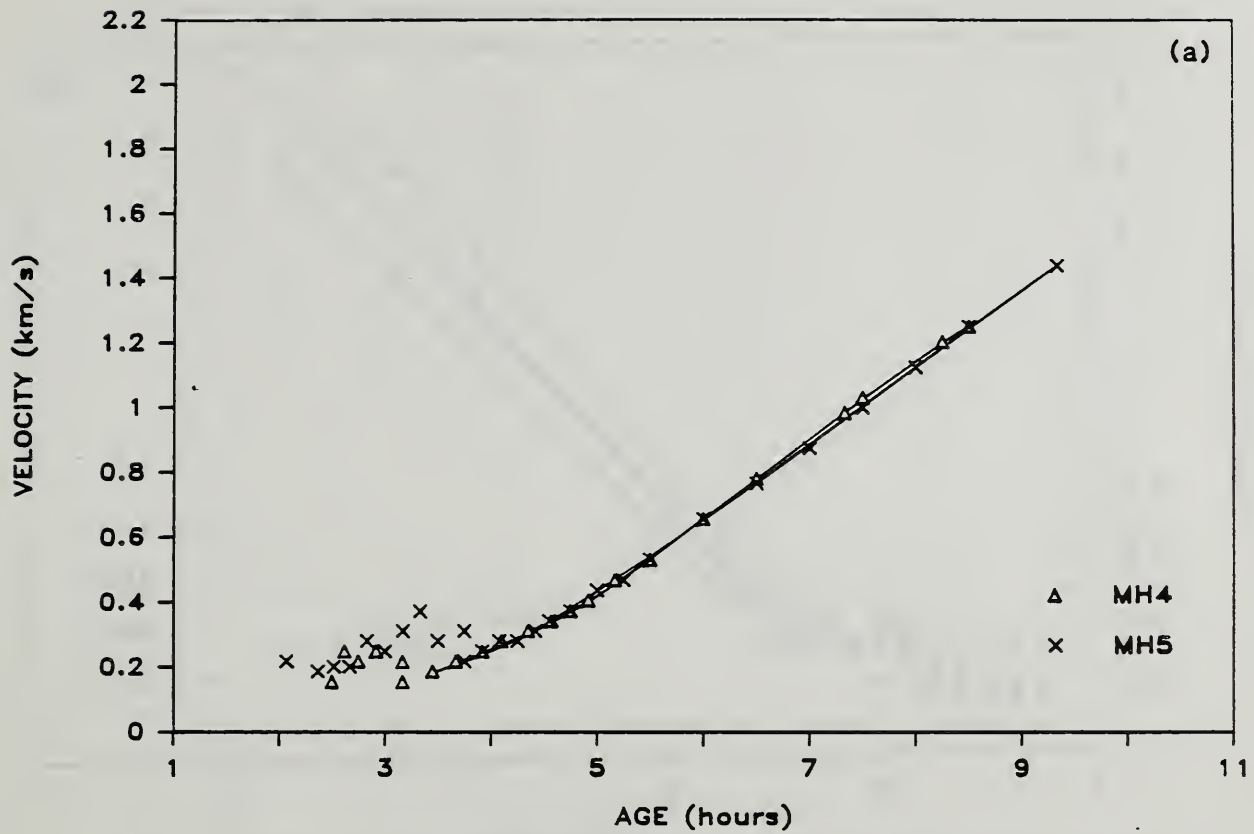
Figure 4.6   Results of prepared mortar replicates MH4 and MH5: a)
P-wave velocity vs age; and, b) penetration resistance vs age

55
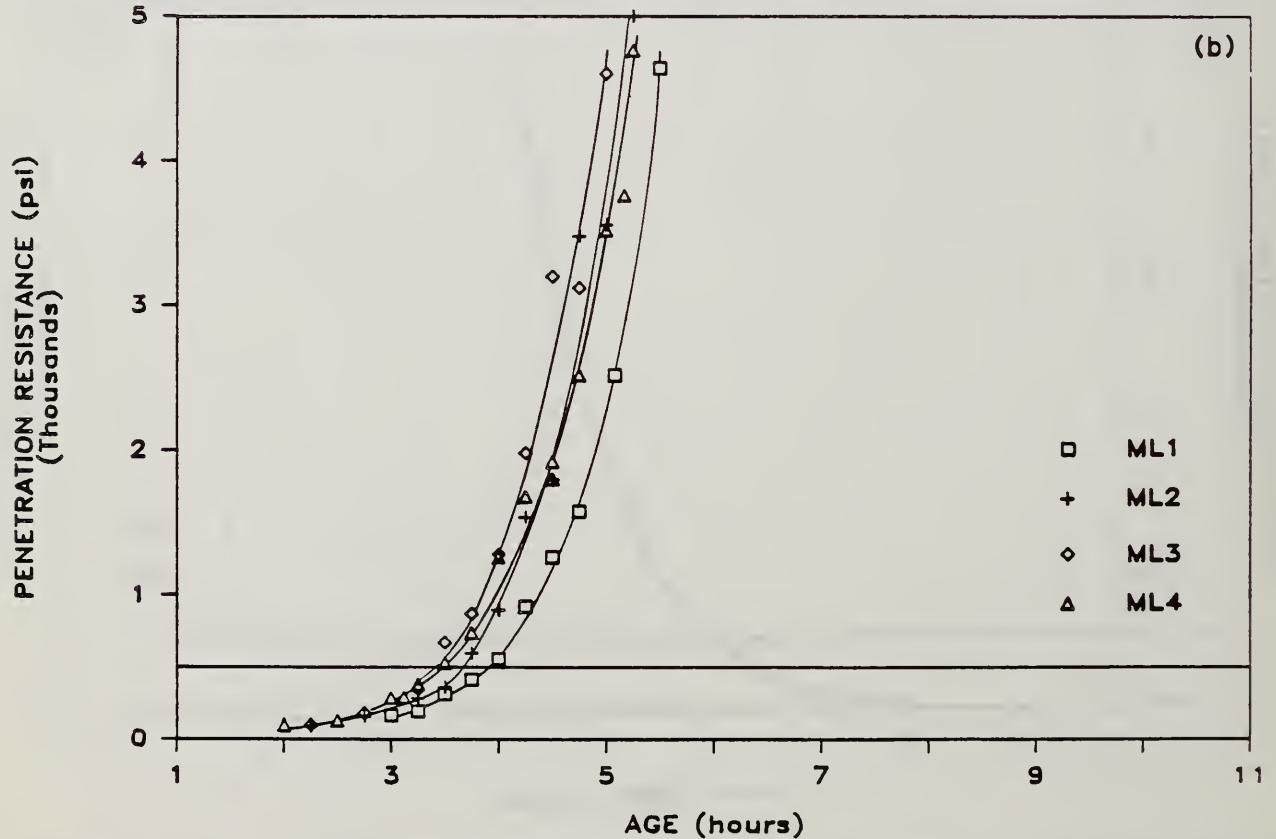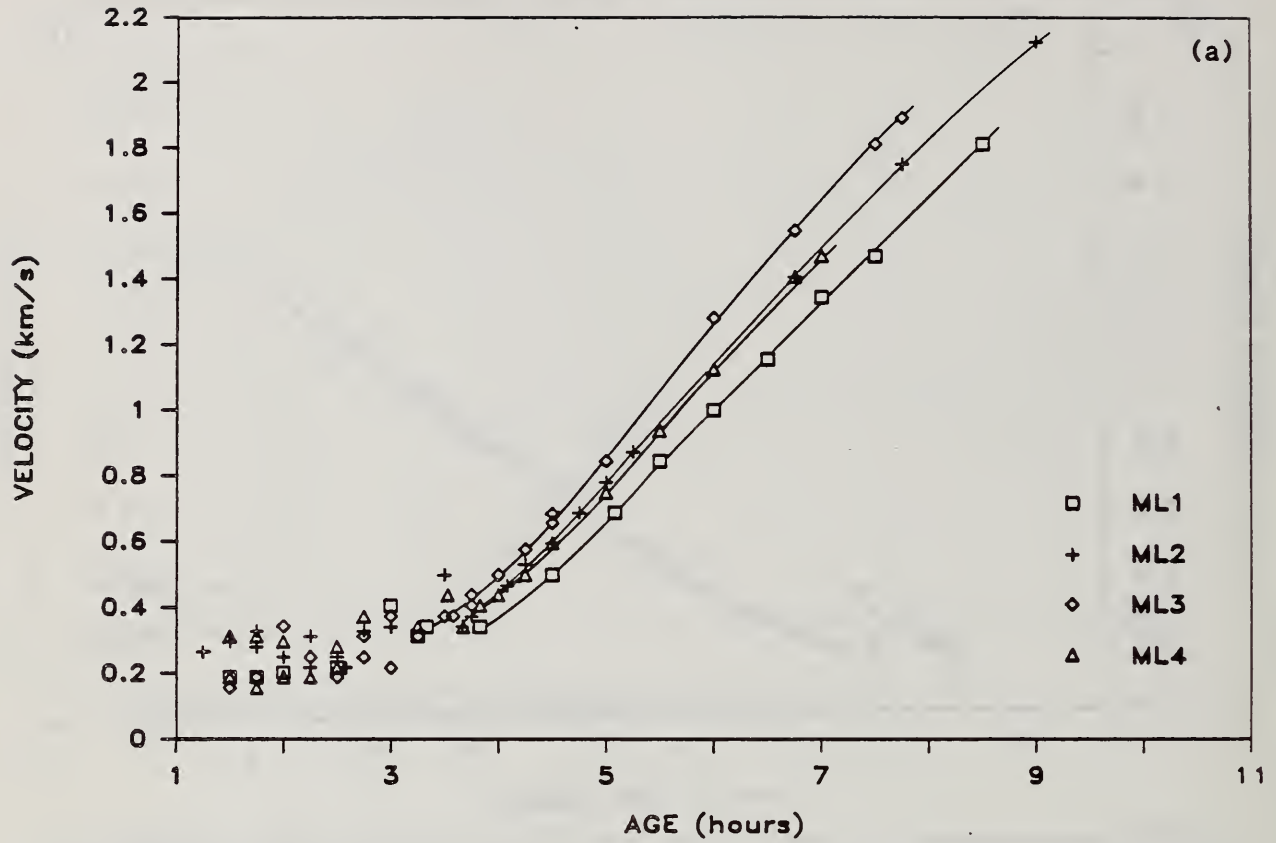
Figure 4.7   Results of prepared mortar replicates ML1 through
ML4: a) P-wave velocity vs age; and, b) penetration resistance vs
age

56
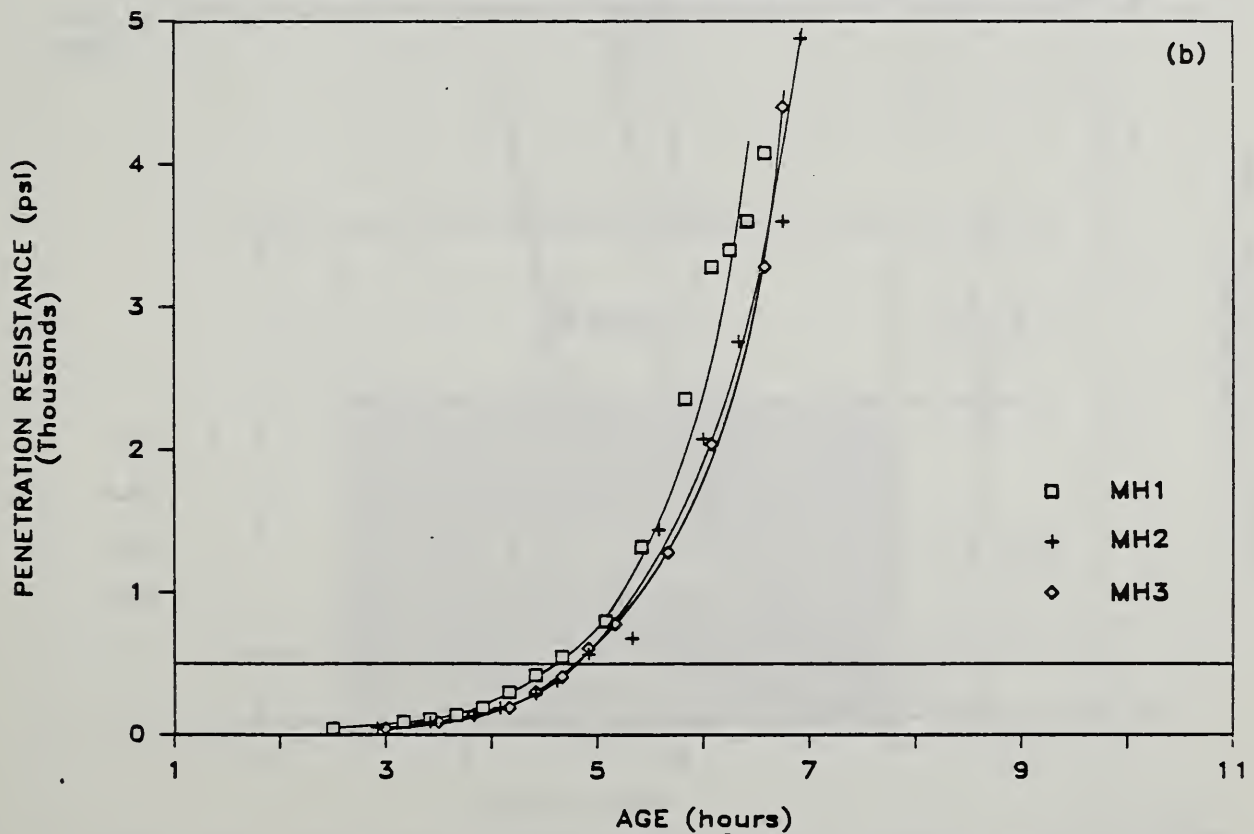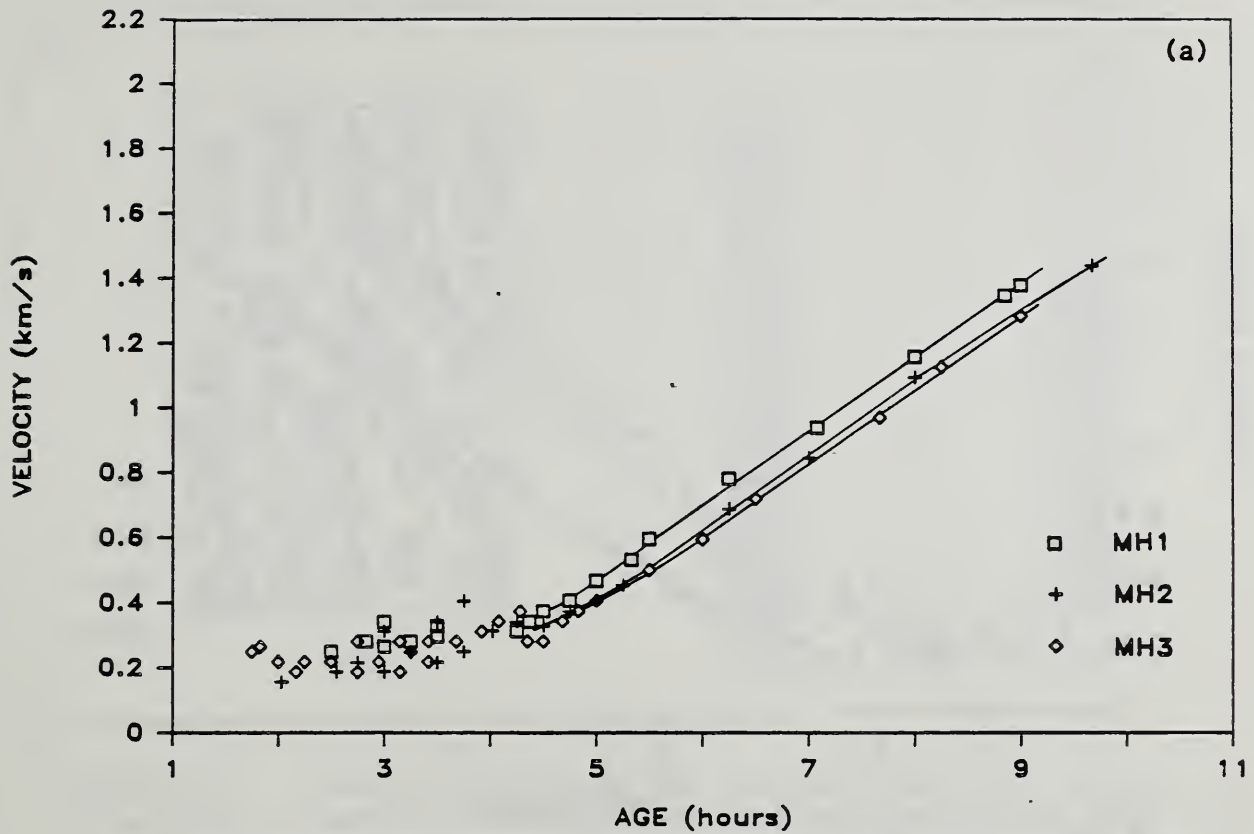
Figure 4.8   Results of prepared mortar replicates MH1 through MH3: a) P-wave velocity vs age; and, b) penetration resistance vs age

57
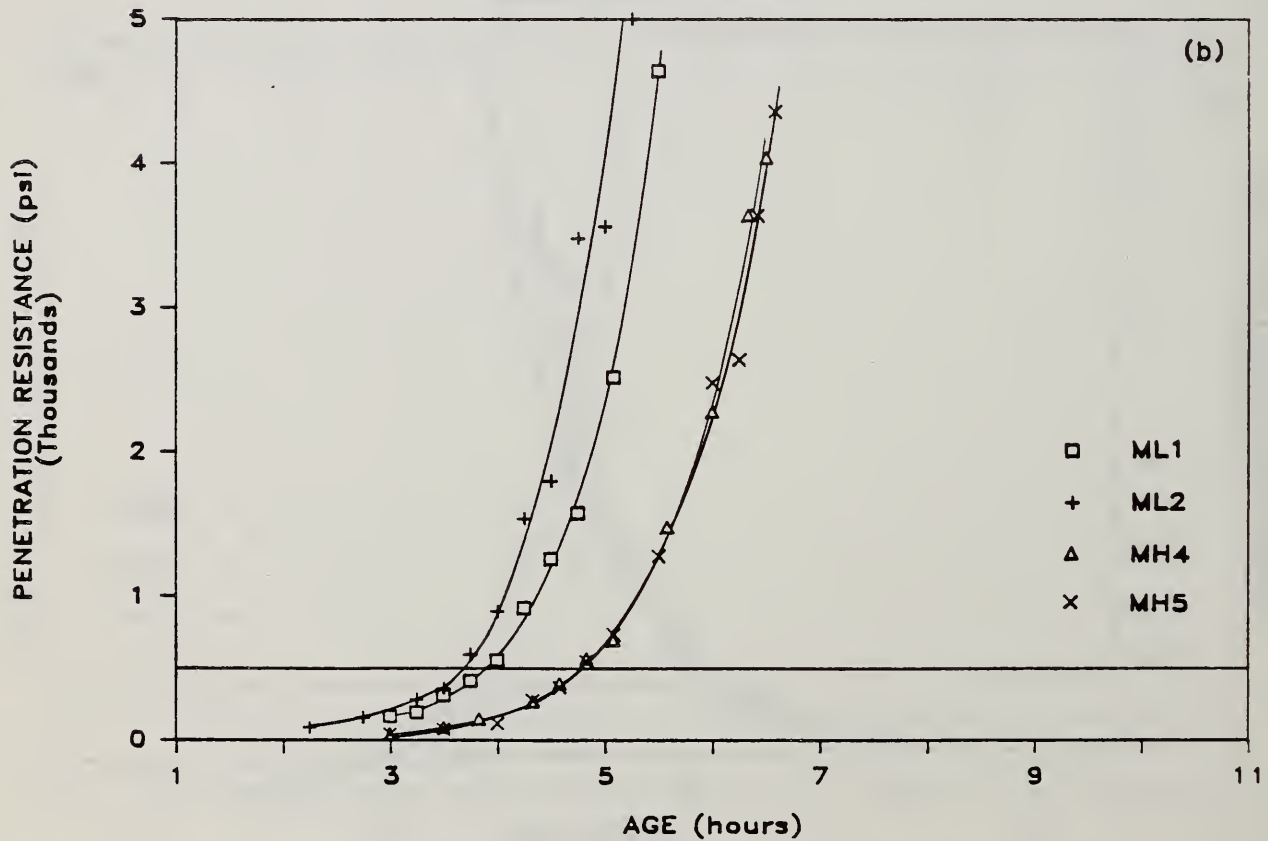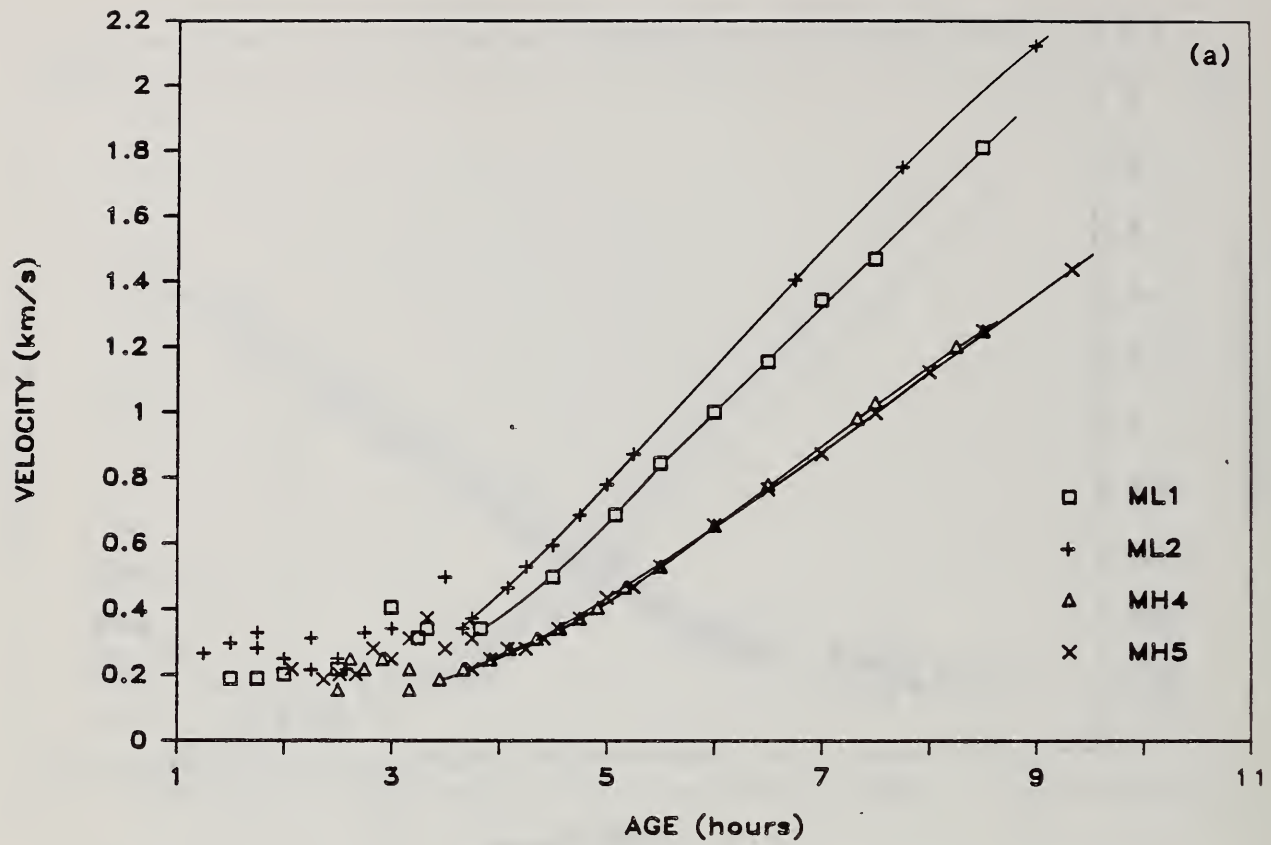
Figure 4.9   Results of prepared mortar tests ML1, ML2, MH4, and MH5: a) P-wave velocity vs age; and, b) penetration resistance vs age

58
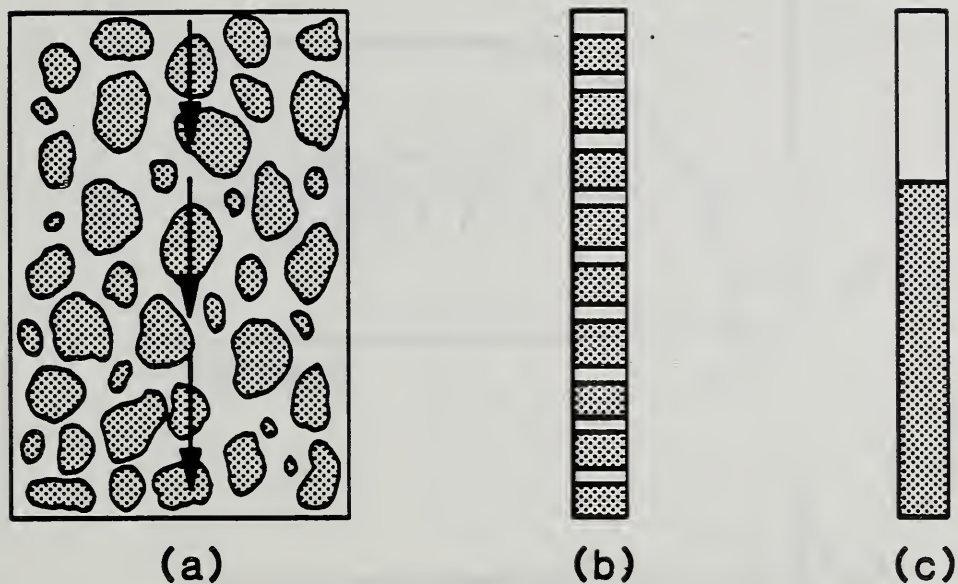
Figure 4.10   Description of the series model: a) Single ray propagating through the concrete; b) idealization of the path as a series of paste and aggregate regions; and, c) equivilant two-phase model
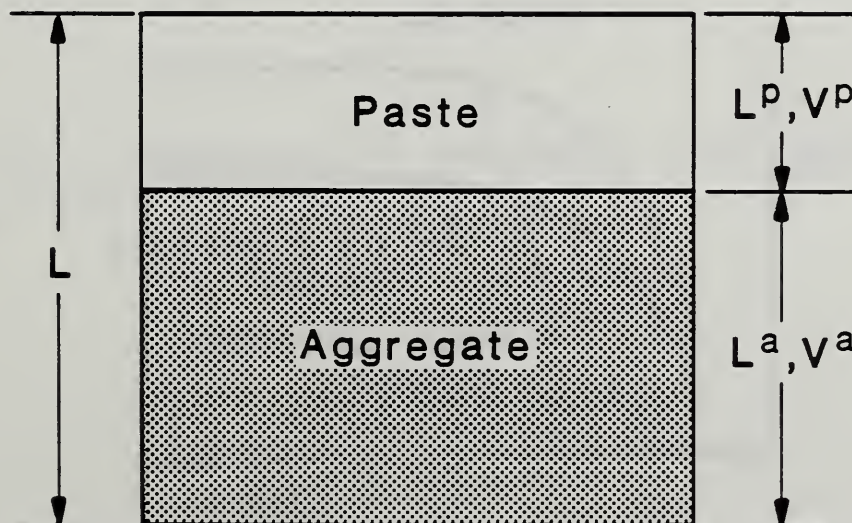
Figure 4.11   Two-phase series model, consisting of paste and aggregate phases, used to model the concrete
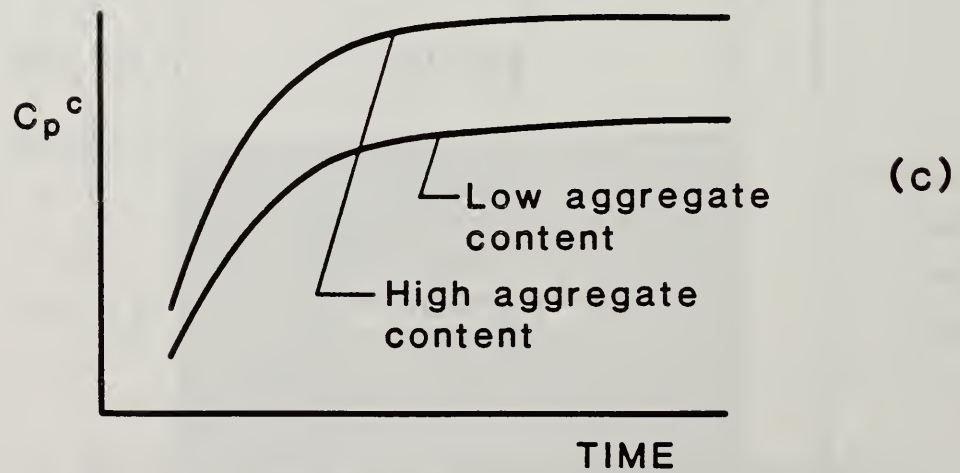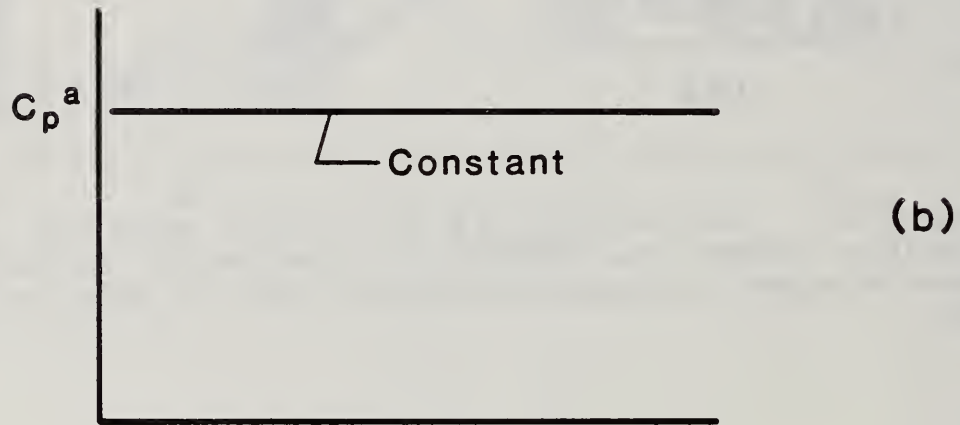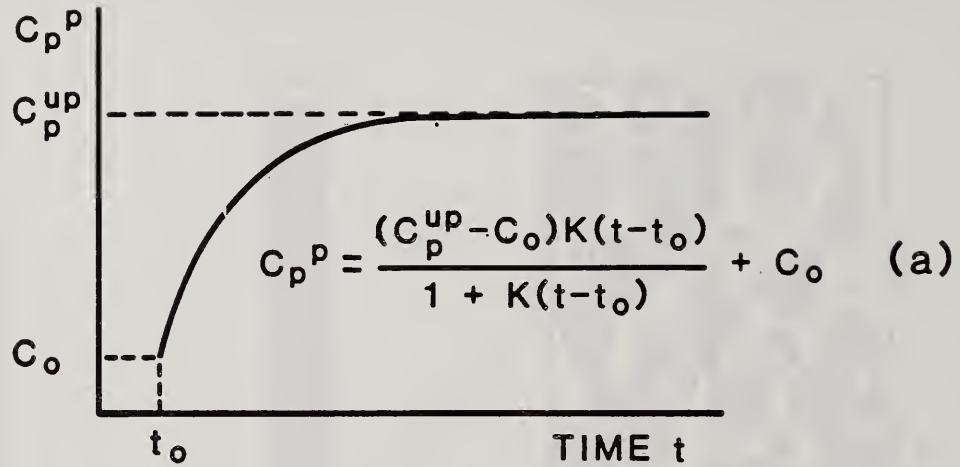
Figure 4.12   Gain in velocity in concrete with age: a) gain in velocity in the cement paste; b) constant velocity in the aggregate; and, c) gain in velocity in concrete predicted by Eq. 4.2 for different aggregate contents

60
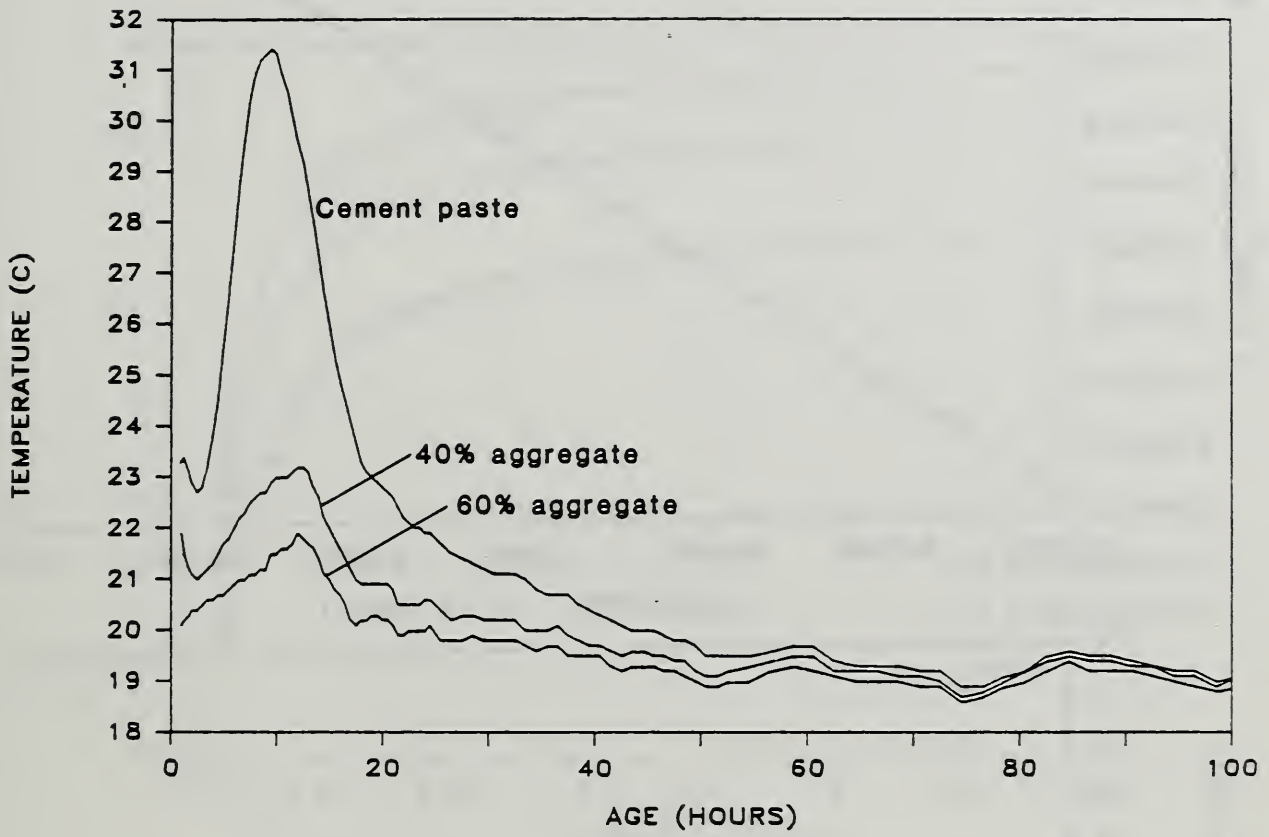
Figure 4.13   Temperatures of the cement paste, 40 % aggregate, and 60 % aggregate specimens vs age

61
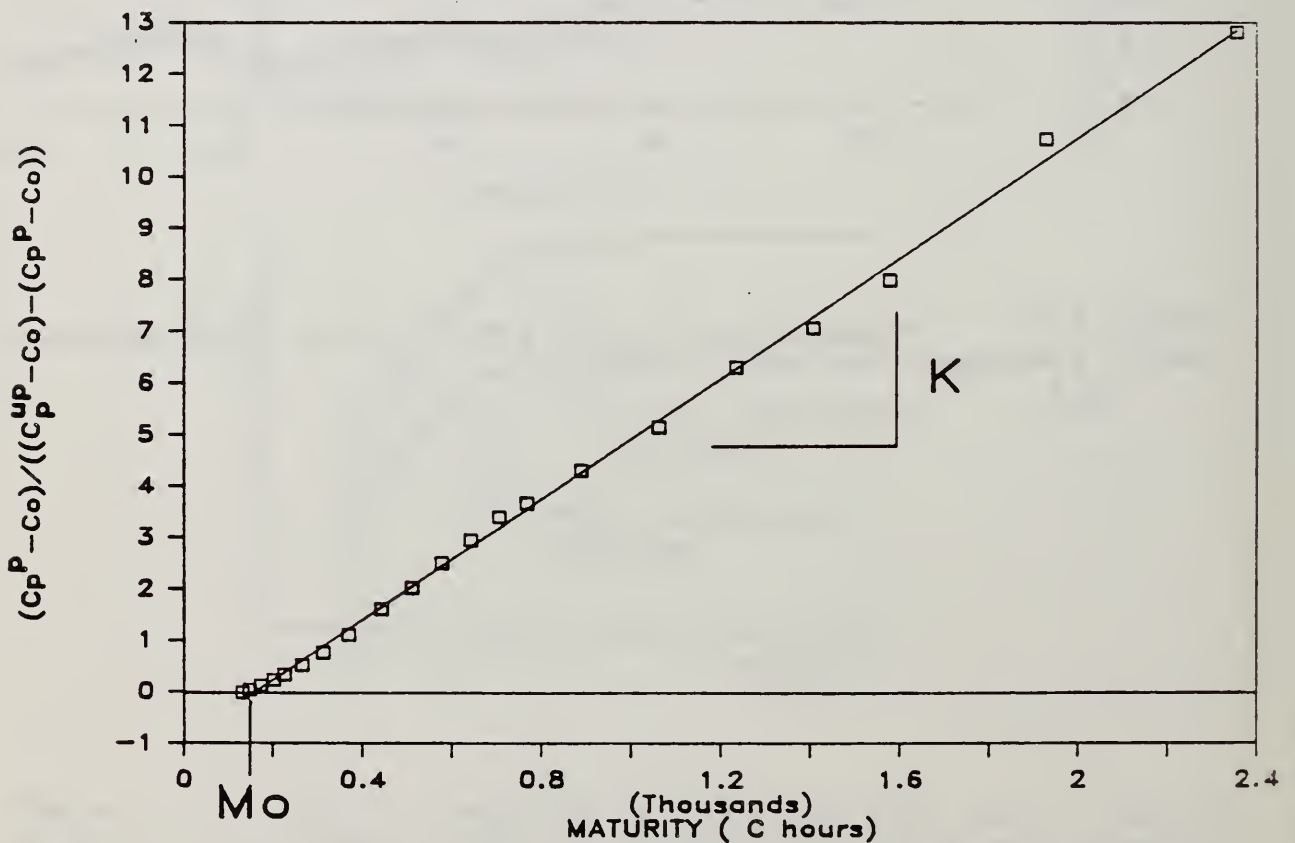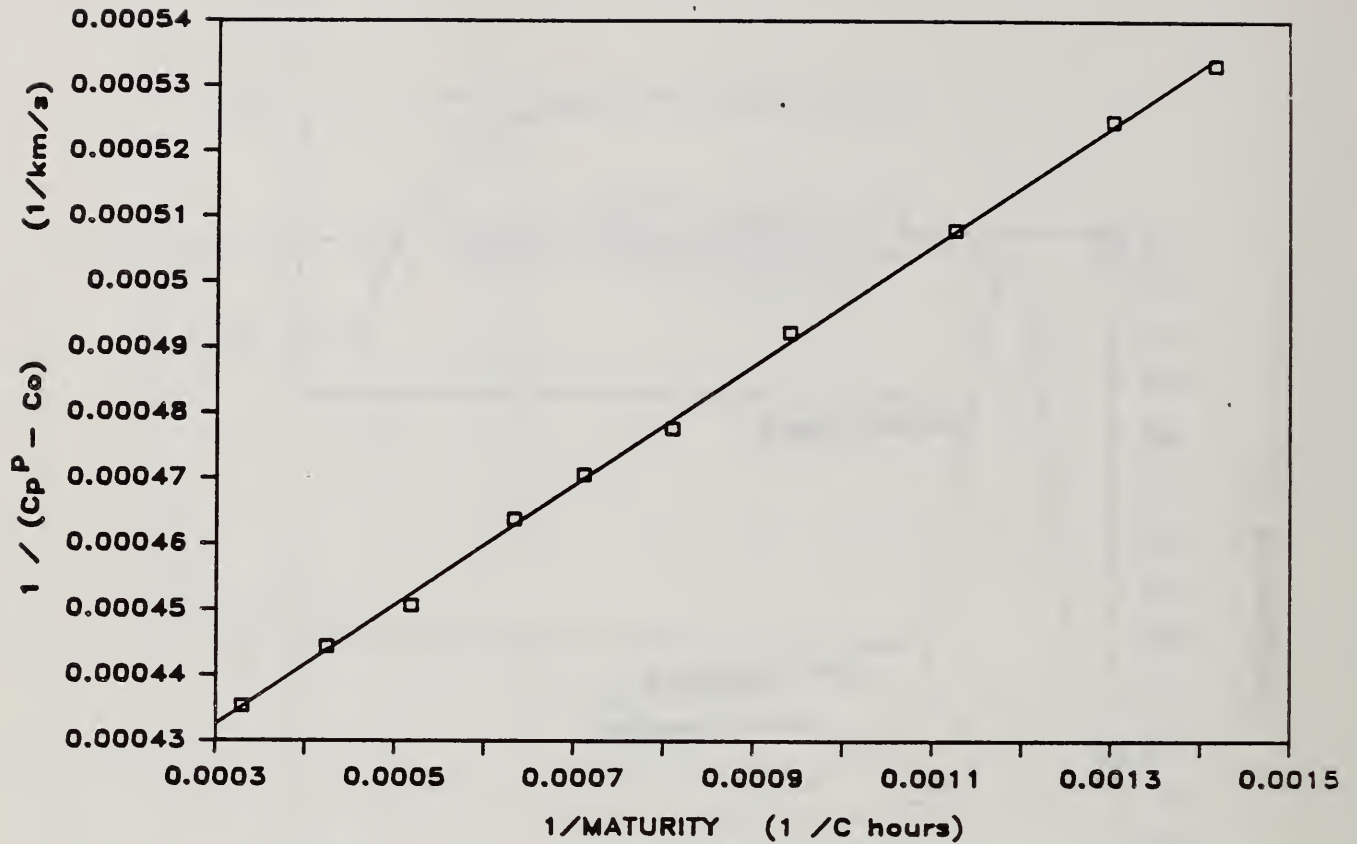
Figure 4.14   Linear regressions to determine $(C_p^{up} - C_o)$, K, and M_o: a) Equation 4.9; and, b) Equation 4.10
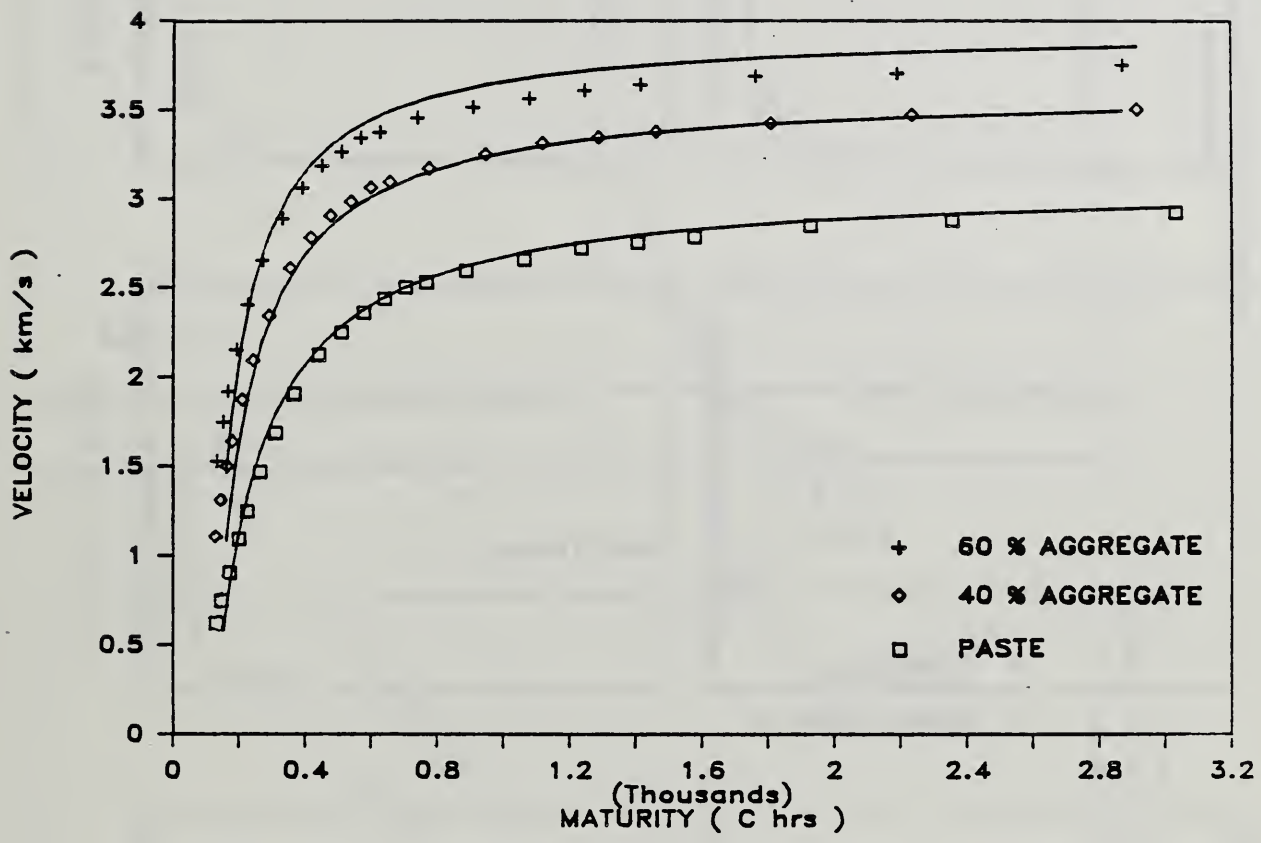
Figure 4.15   P-wave velocity vs maturity for the cement paste, 40 % aggregate, and 60 % aggregate specimens

63
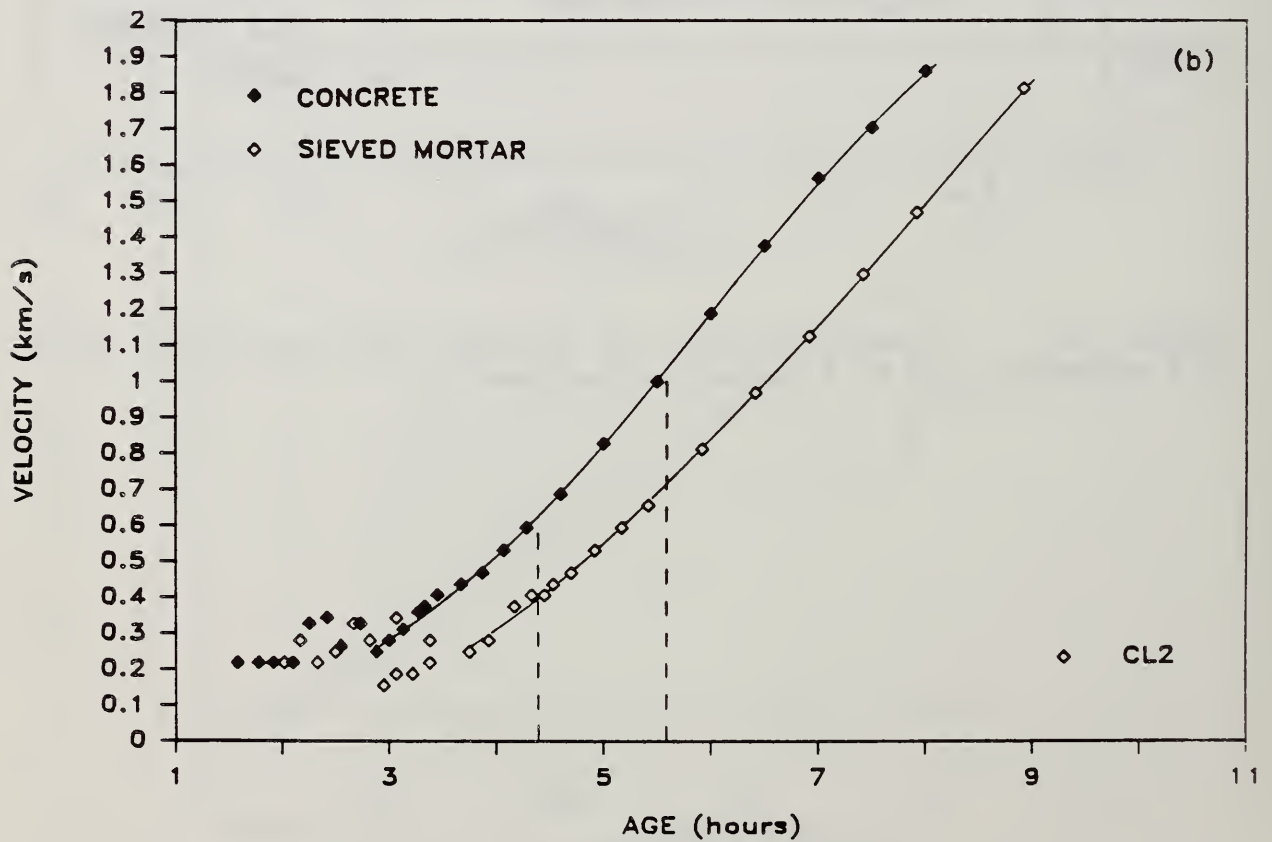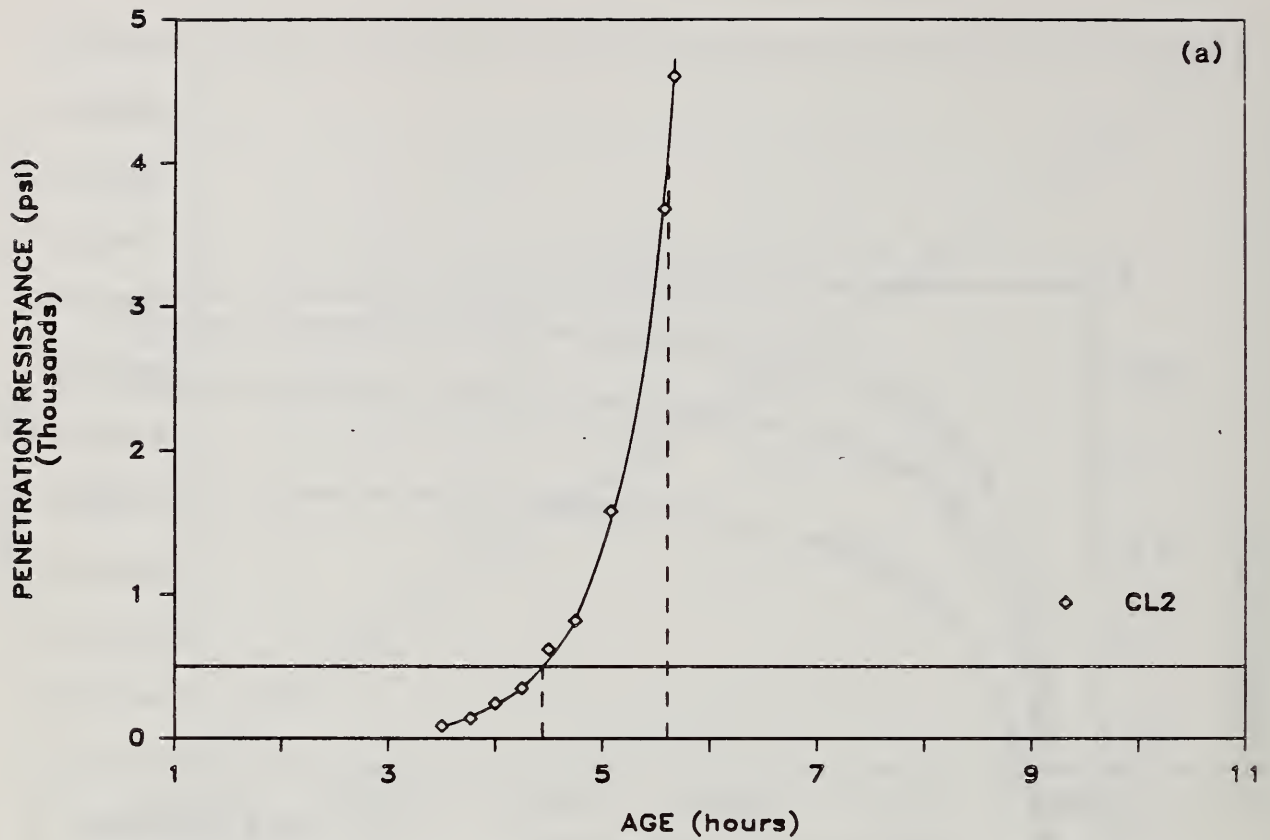
Figure 4.16   Results from test CL2 (low w-c ratio mixture): a) penetration resistance vs age; and, b) P-wave velocity vs age

64
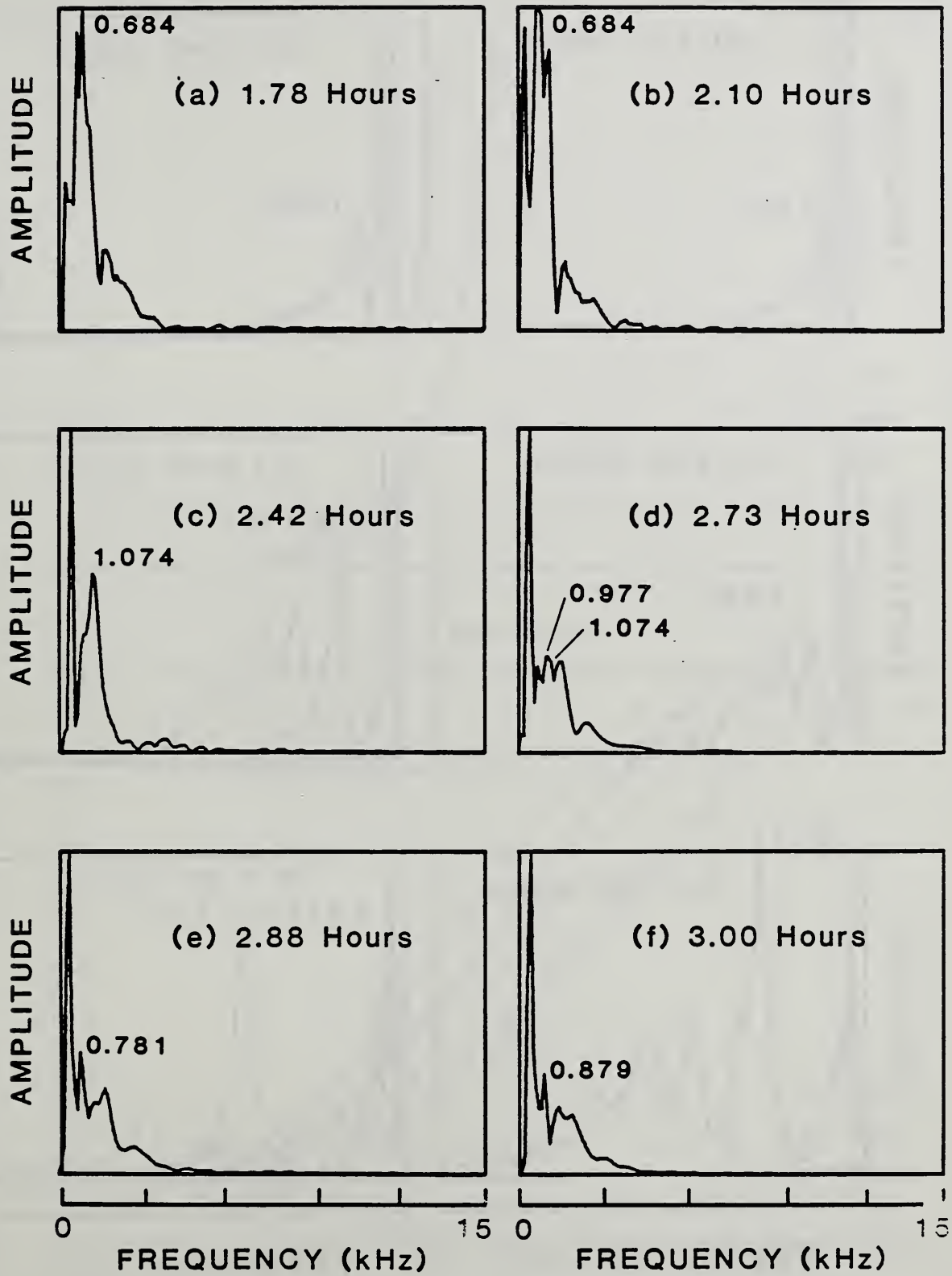
Figure 4.17   Frequency spectra from test CL2 at ages of: a) 1.78 hours; b) 2.10 hours; c) 2.42 hours; d) 2.73 hours; e) 2.88 hours; f) 3.00 hours;

65
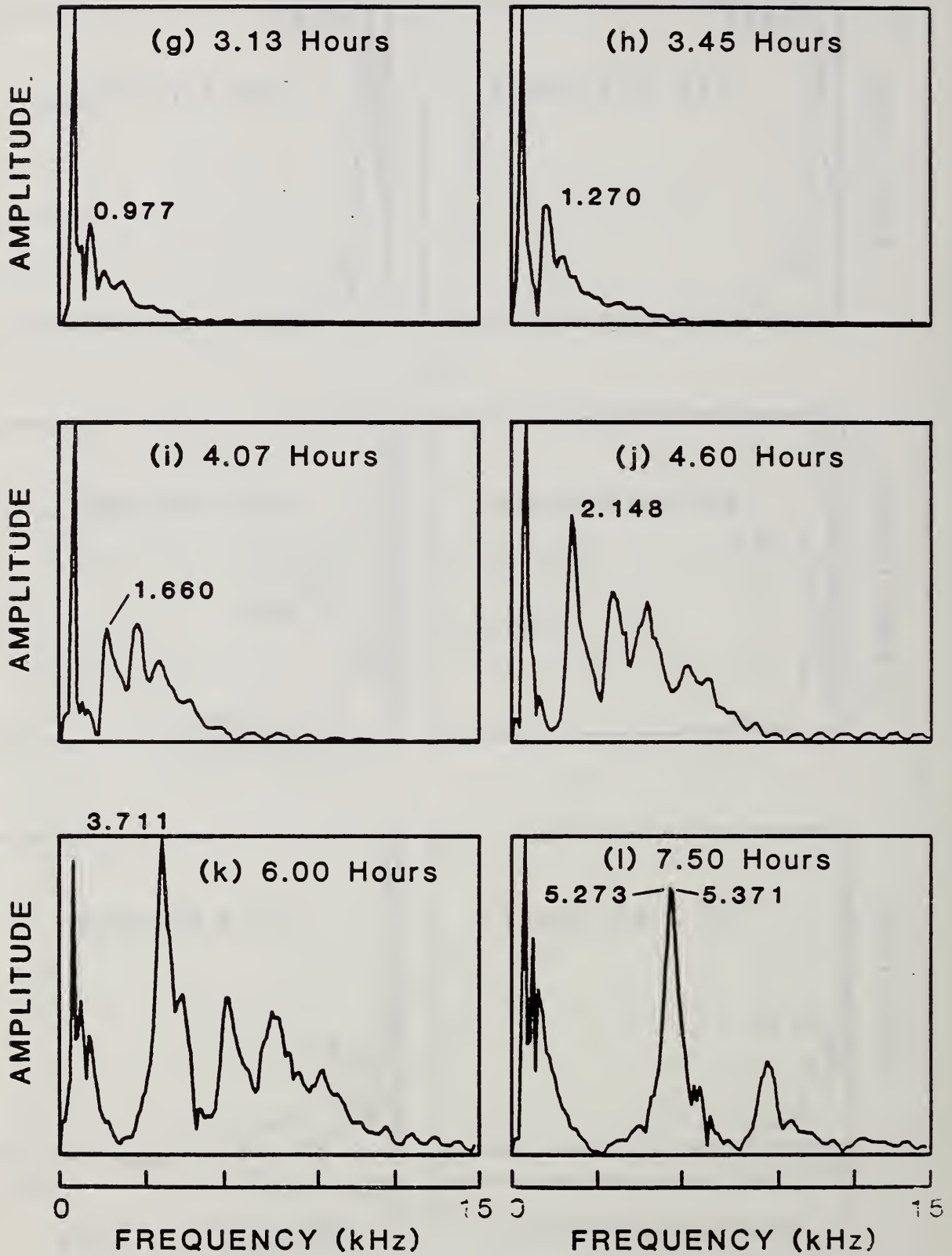
Figure 4.17 (continued) Frequency spectra from test CL2 at age of: g) 3.13 hours; h) 3.45 hours; i) 4.07 hours; j) 4.60 hours; k) 6.00 hours; and, l) 7.50 hours

66
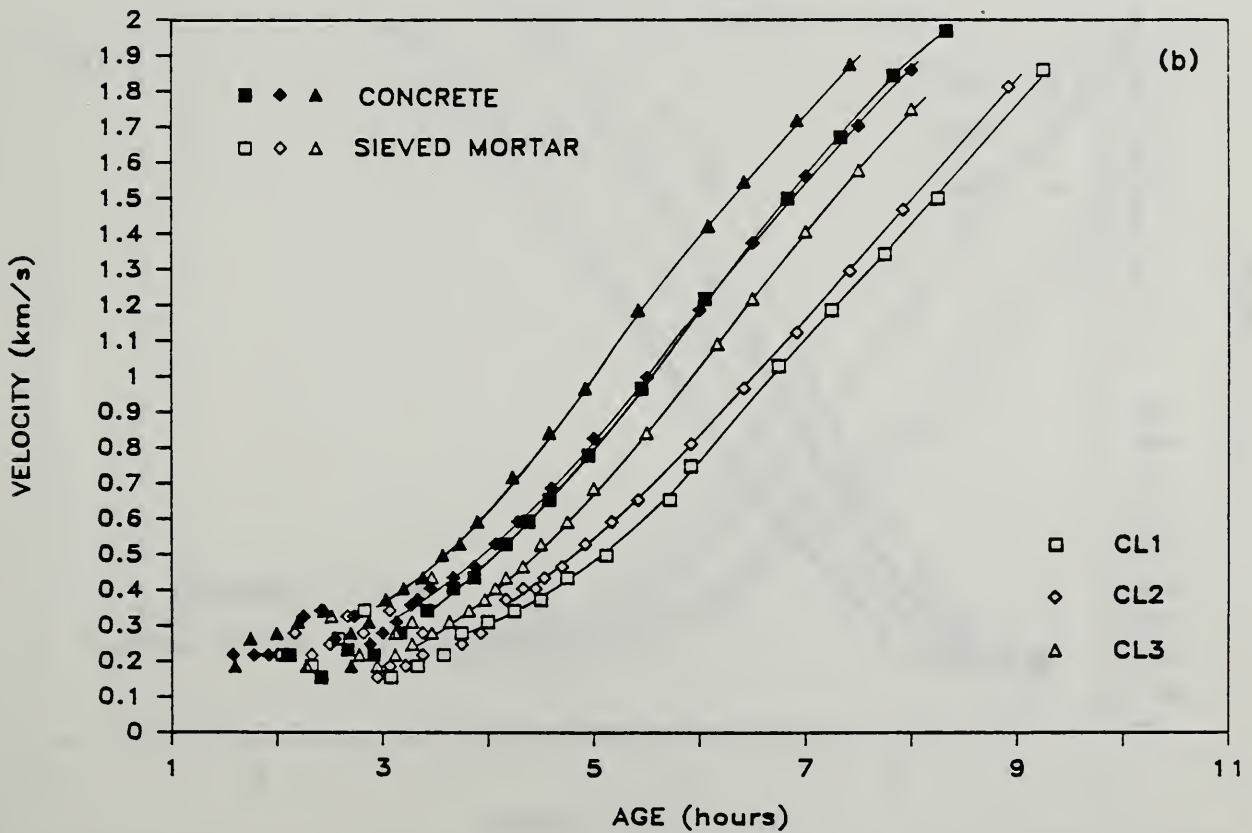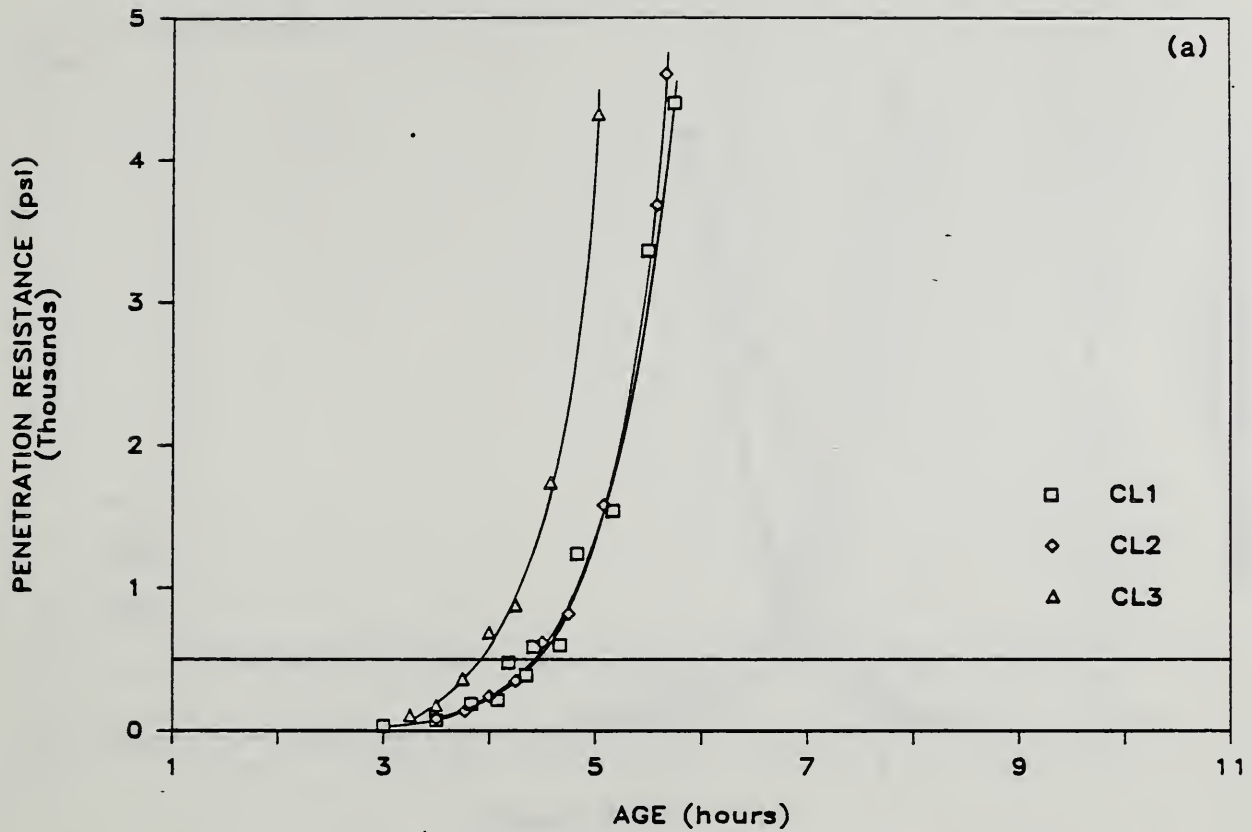
Figure 4.18   Results of replicate tests of a low w-c ratio mixture (tests CL1, CL2, and CL3): a) penetration resistance vs age; and, b) P-wave velocity vs age
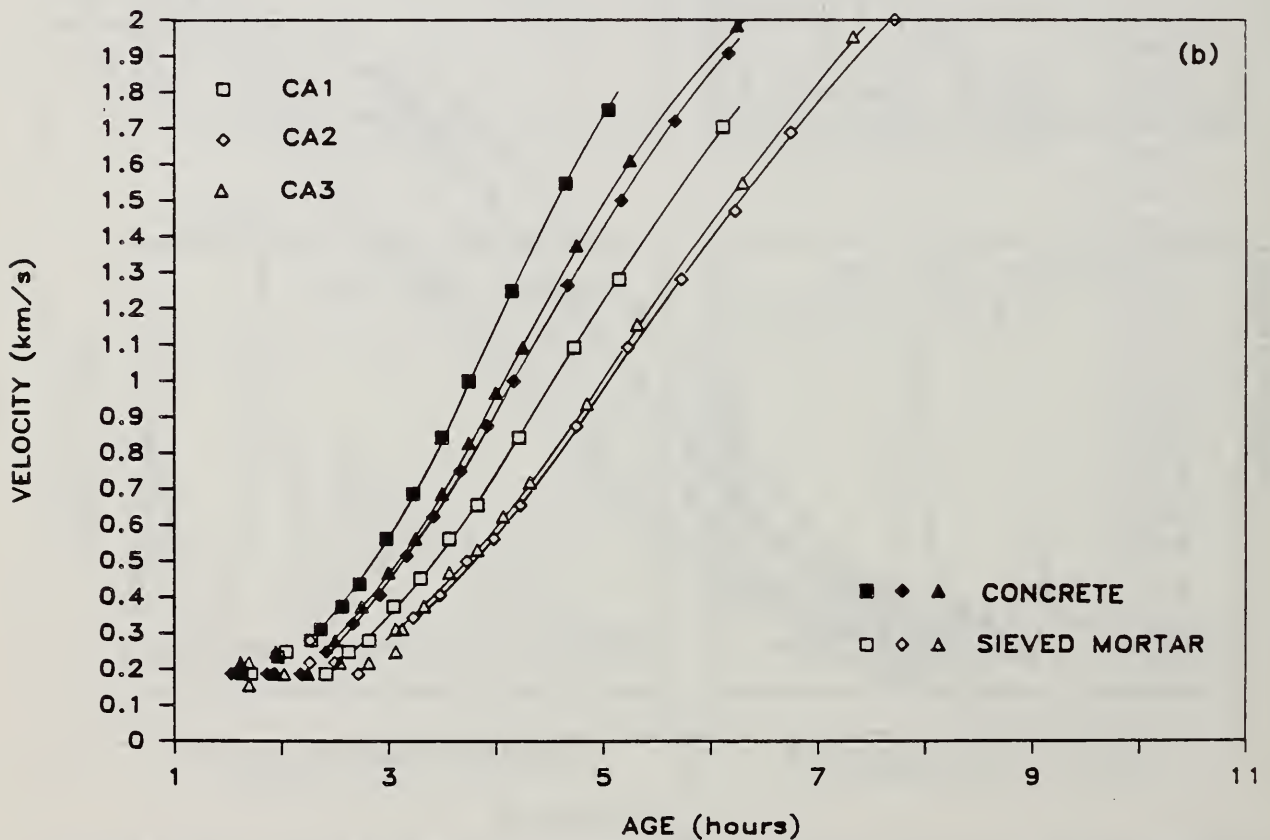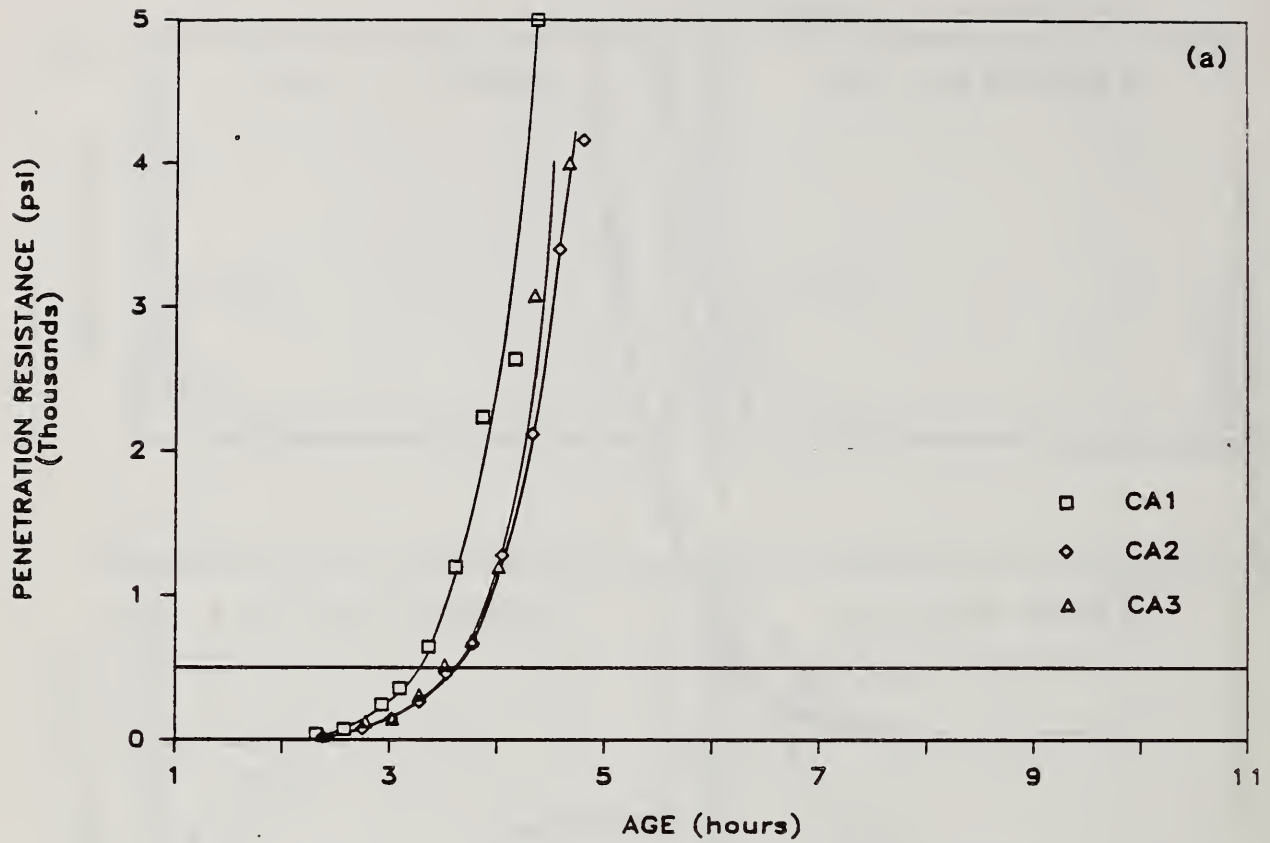
Figure 4.19   Results of replicate tests of an accelerated mixture
(tests CA1, CA2, and CA3): a) penetration resistance vs age; and,
b) P-wave velocity vs age
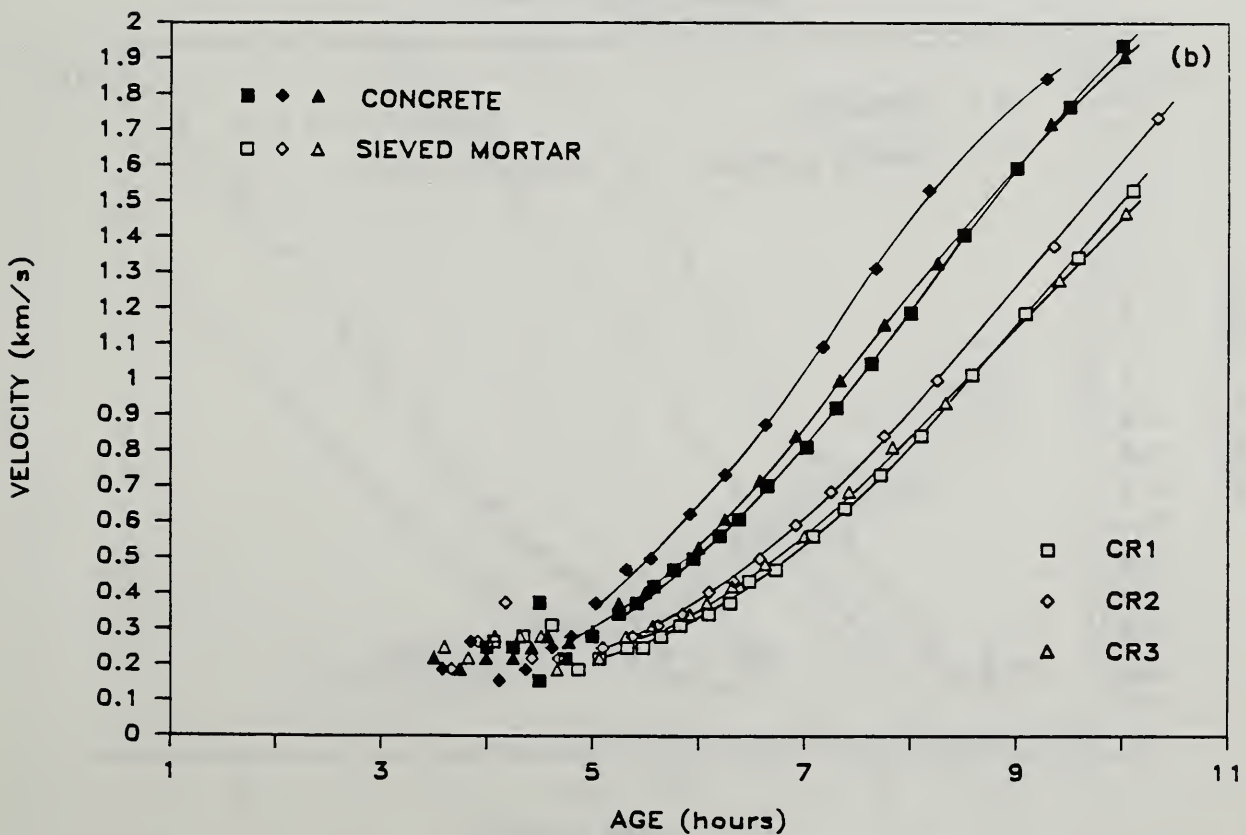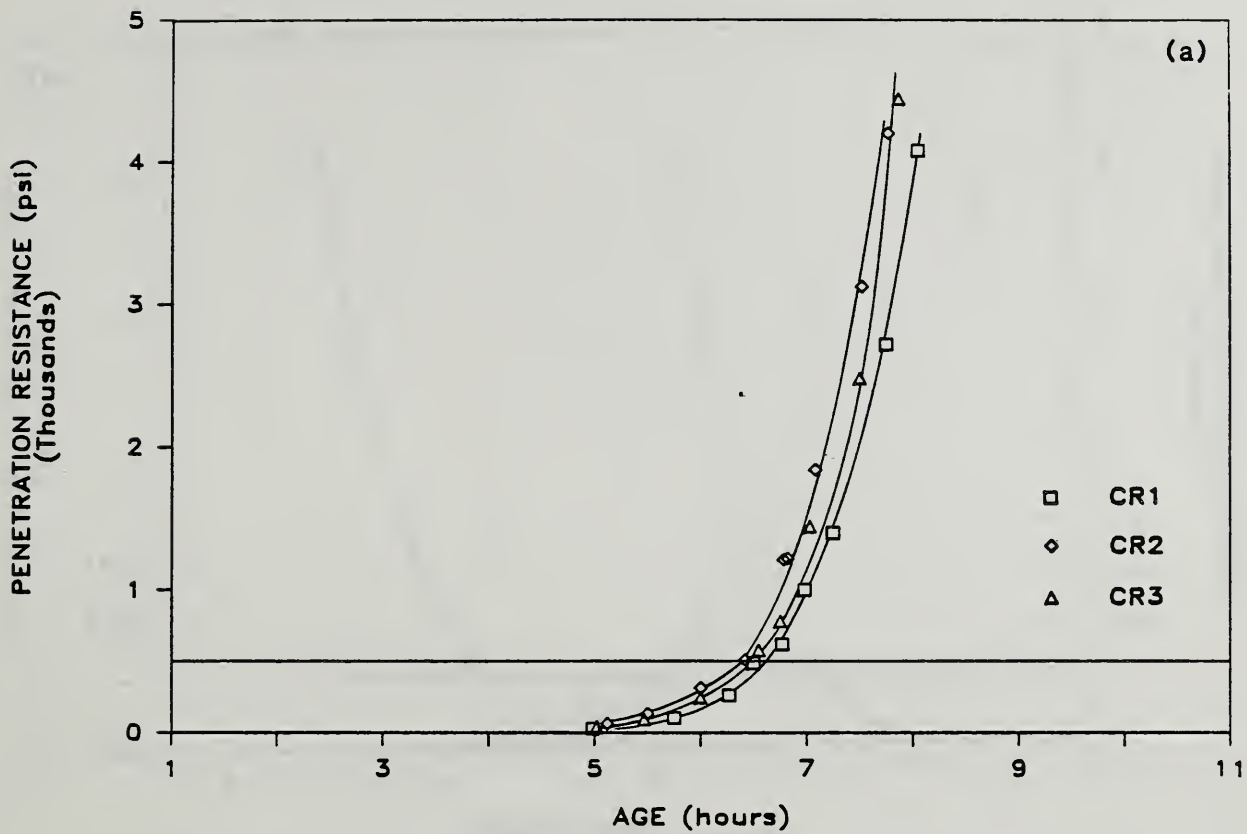
Figure 4.20   Results of replicate tests of a retarded mixture (tests CR1, CR2, and CR3): a) penetration resistance vs age; and, b) P-wave velocity vs age

69
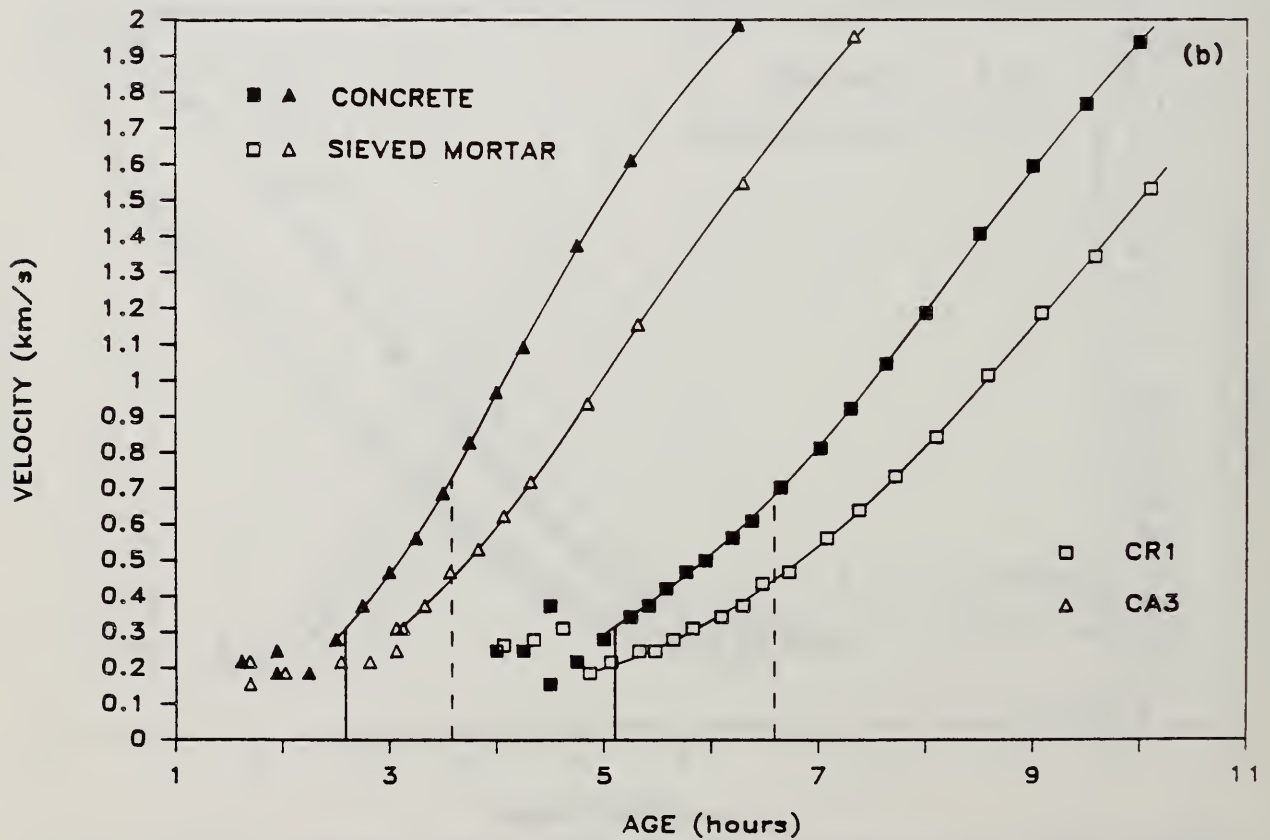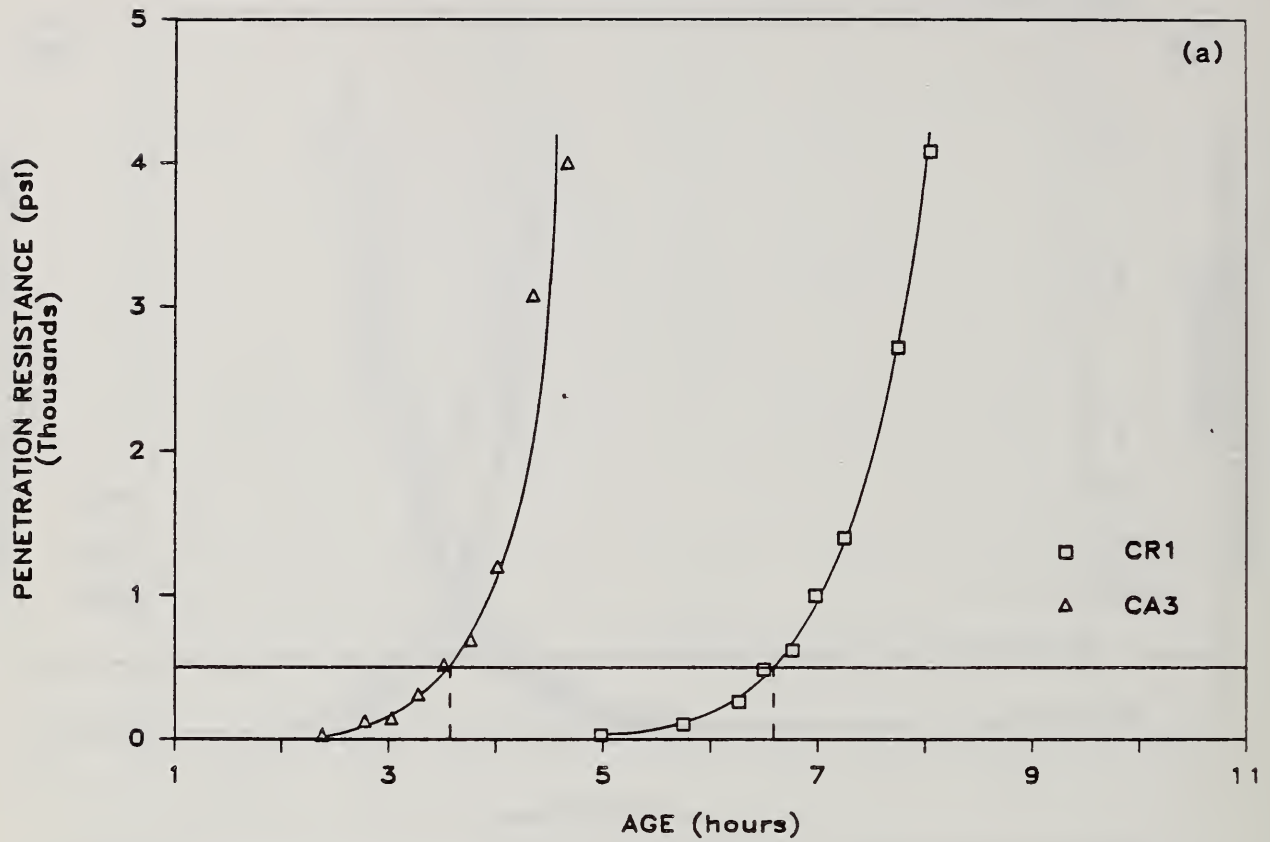
Figure 4.21   Results of tests CA3 and CR1: a) penetration resistance
vs age; and, b) P-wave velocity vs age
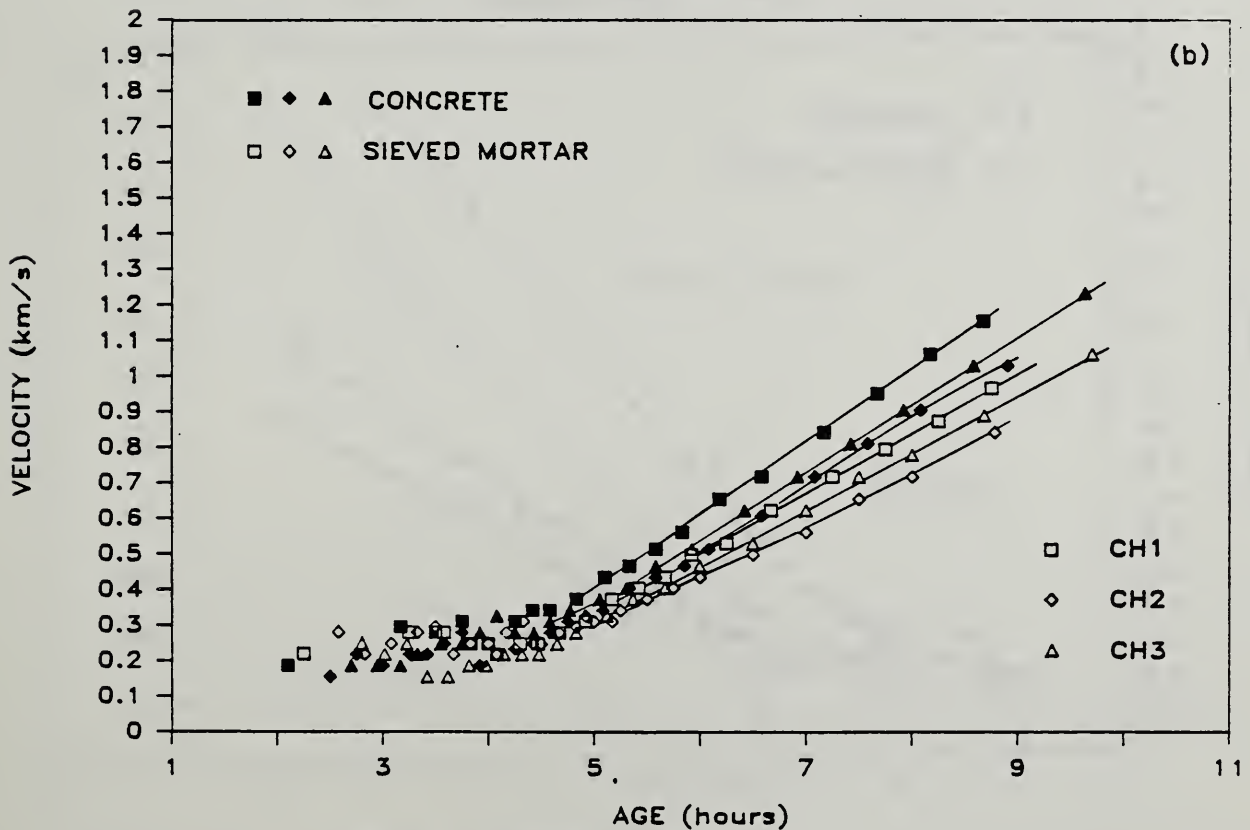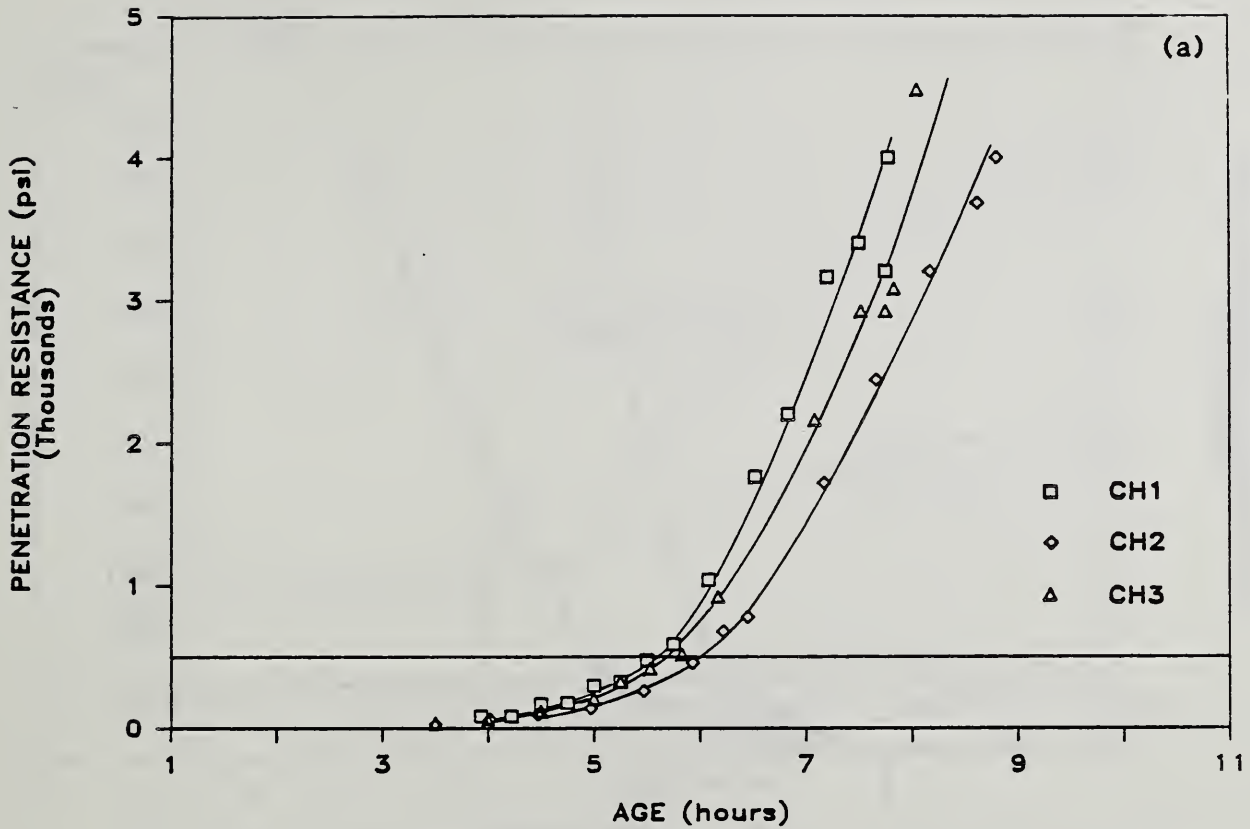
Figure 4.22   Results of replicate tests of a high w-c ratio mixture (tests CH1, CH2, and CH3): a) penetration resistance vs age; and, b) P-wave velocity vs age

71
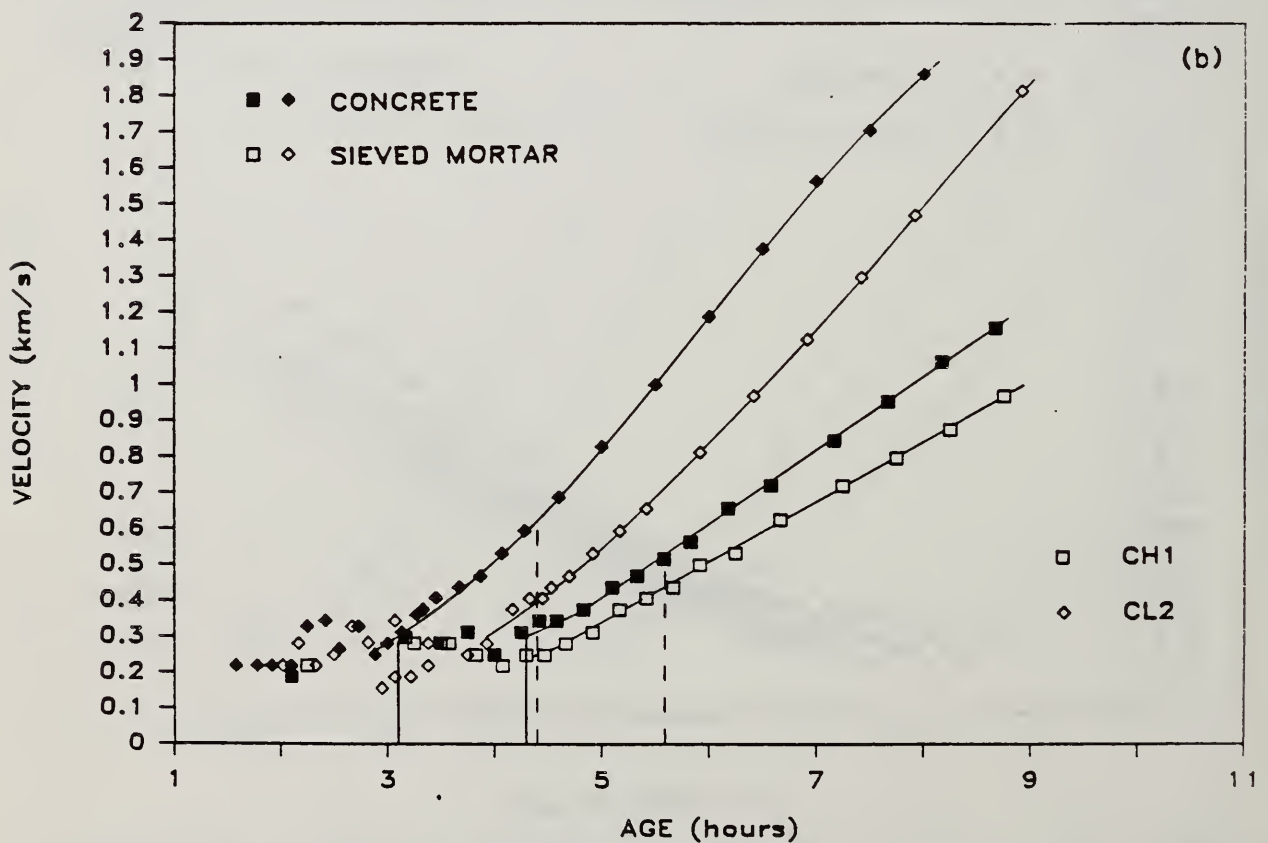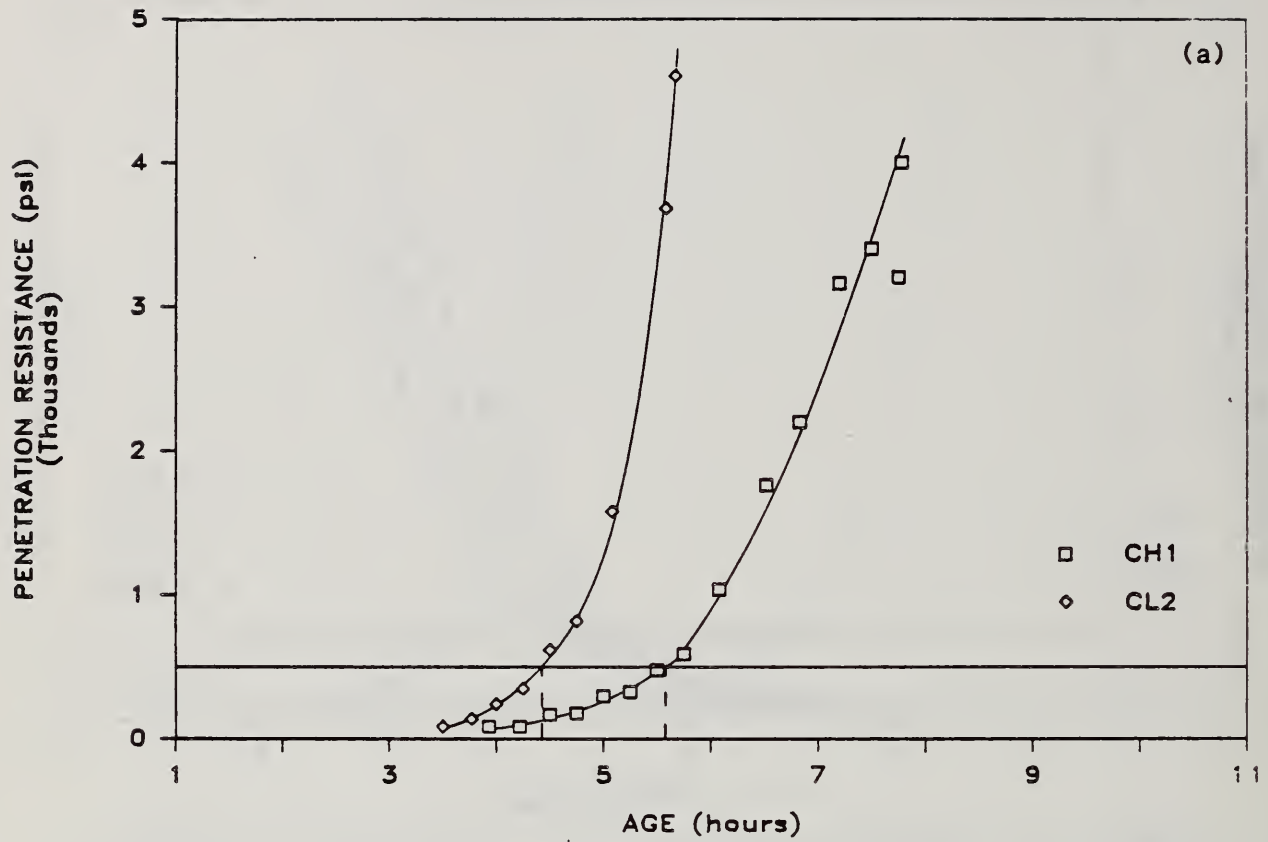
Figure 4.23 Results of tests CH1 and CL2: a) penetration resistance vs age; and, b) P-wave velocity vs age

72
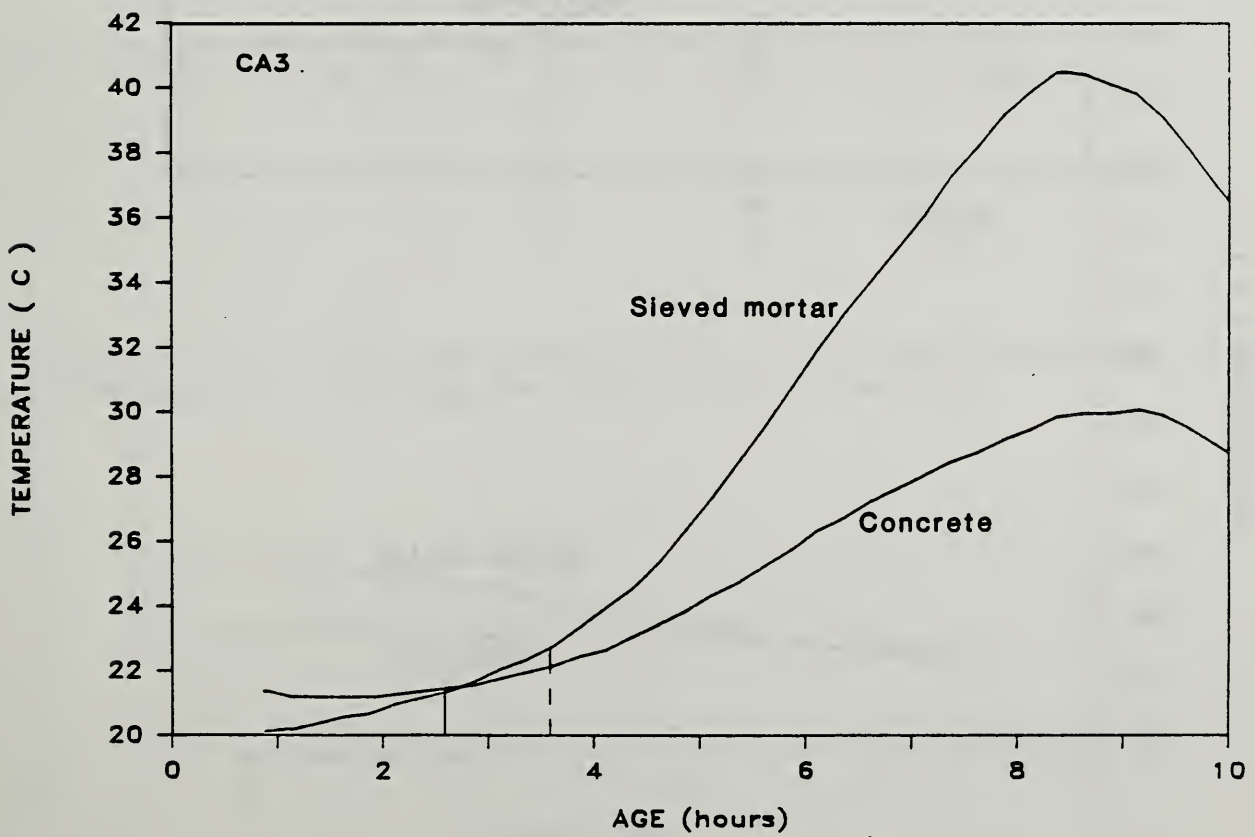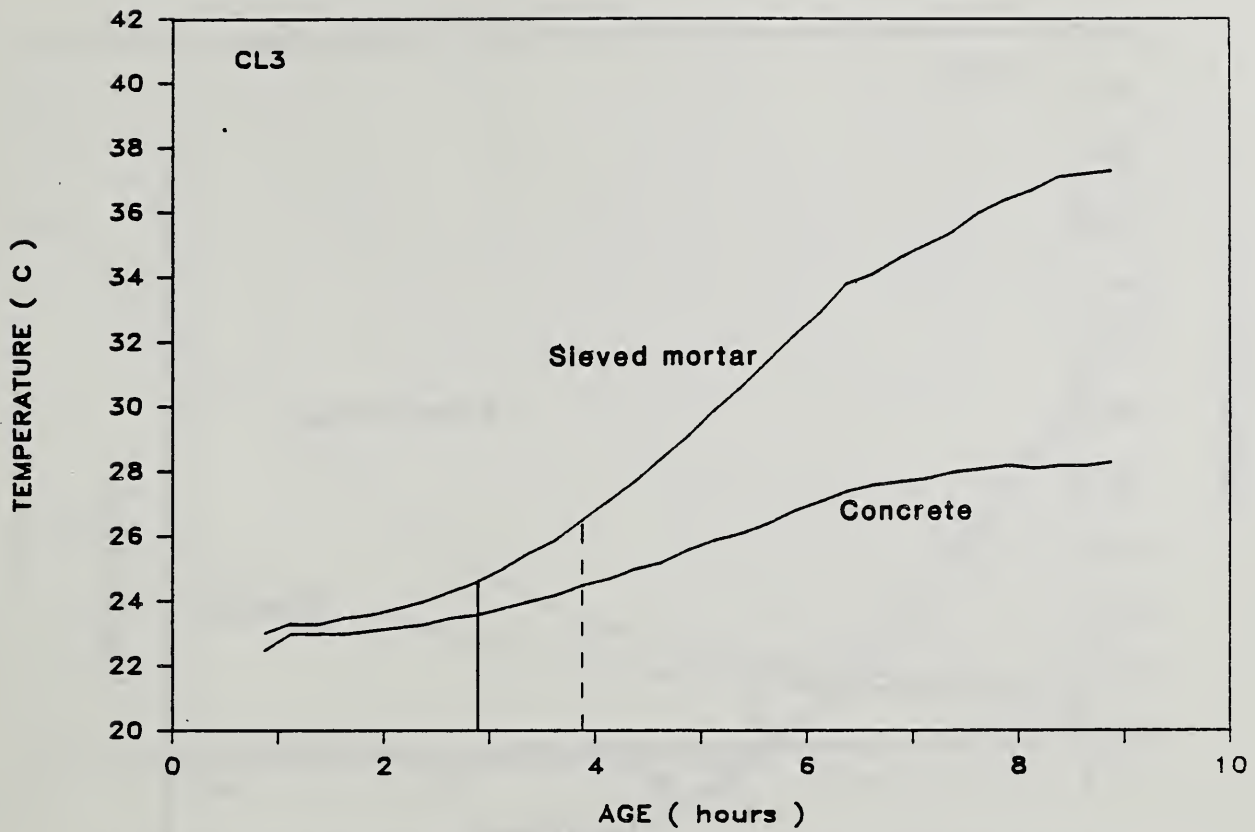
Figure 4.24   Specimen temperature vs age: a) test CL3; b) test
CA3

73
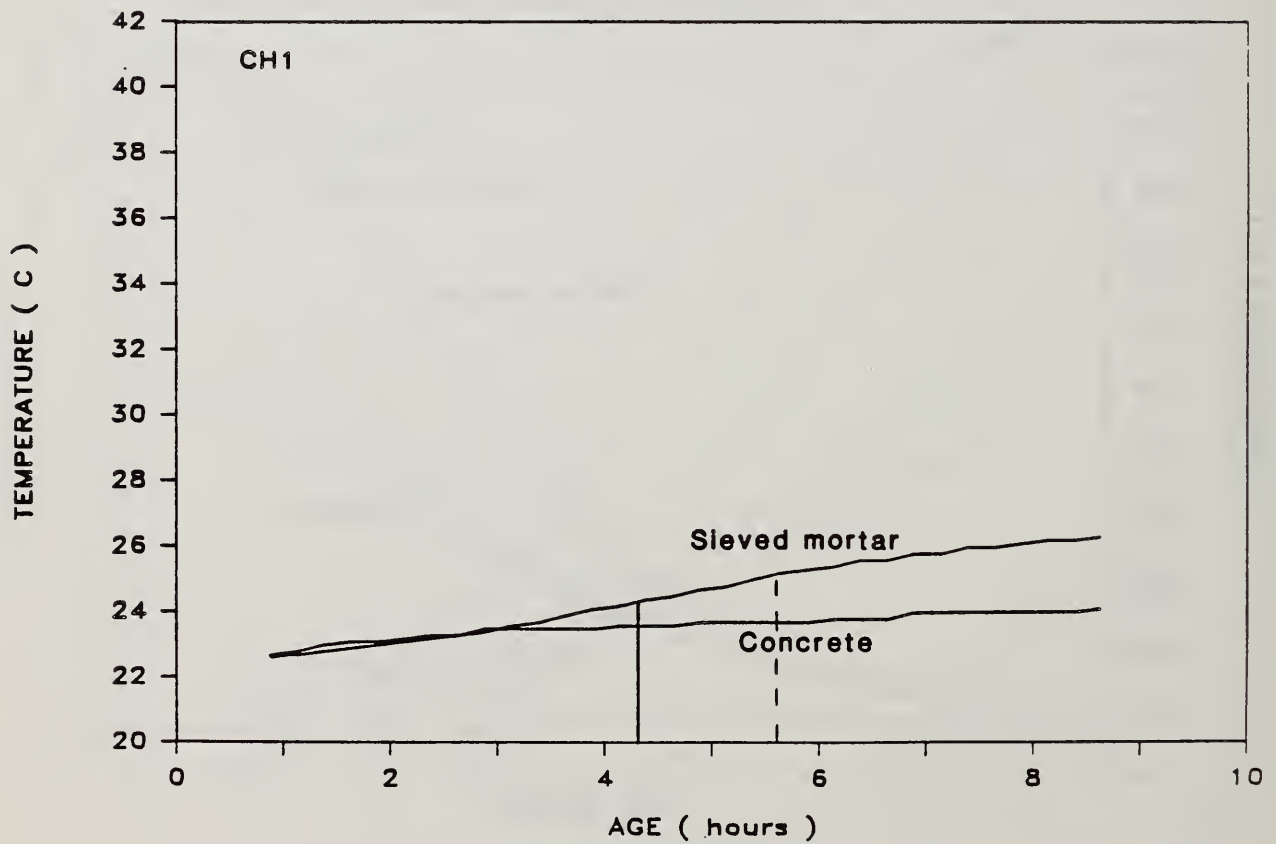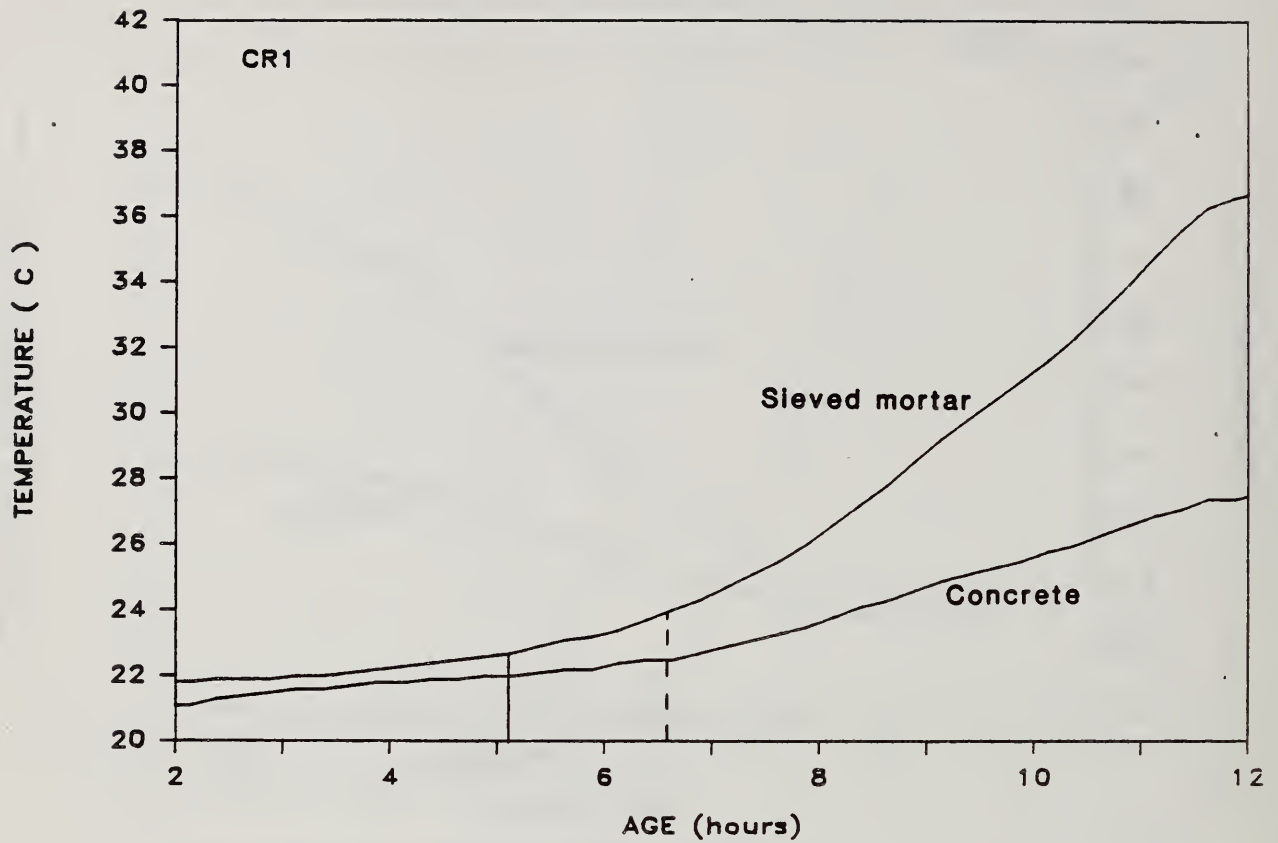
Figure 4.24 (continued) Specimen Temperature vs age: c) test CR1;
and, d) test CH1

74

Figure 4.25   Two approaches for using impact-echo velocity measurements for defining the setting time of concrete
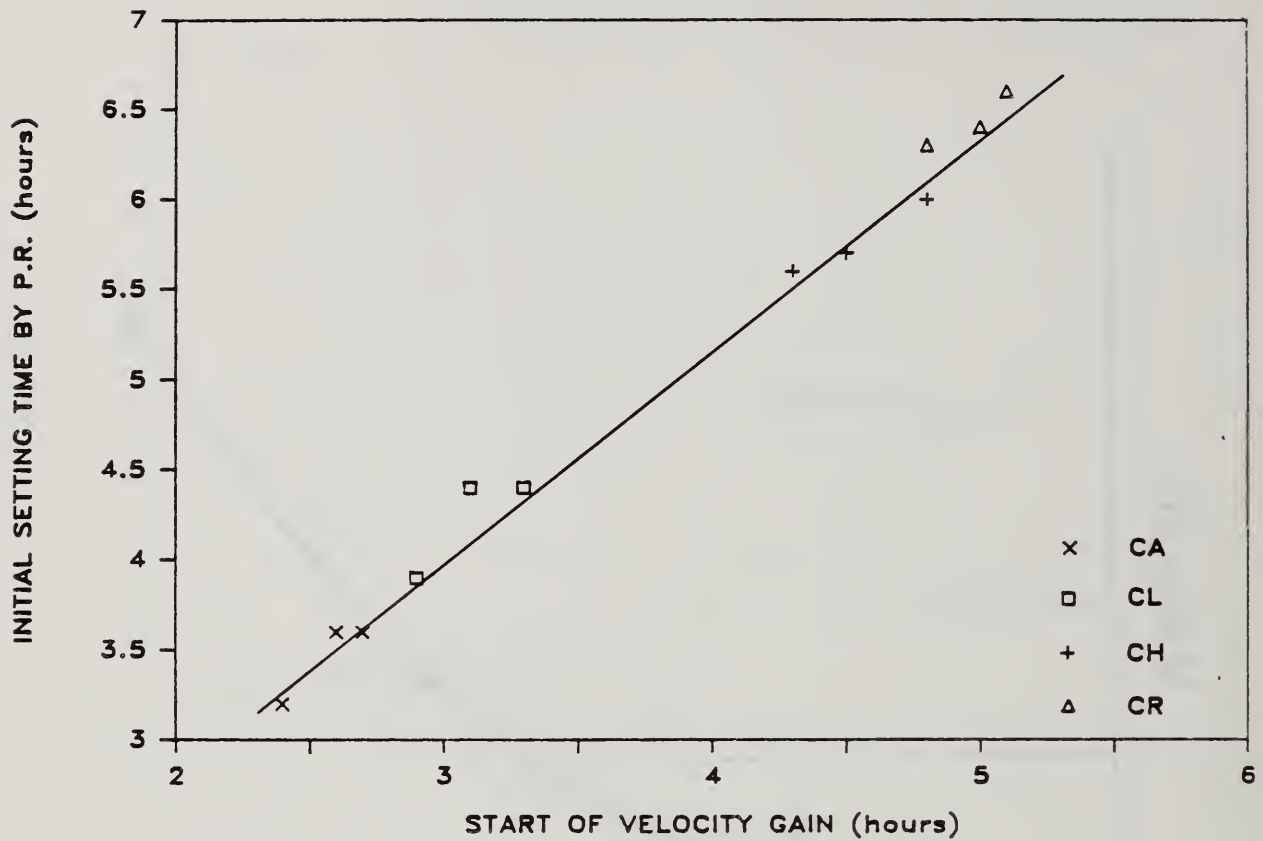
Figure 4.26   Comparison of setting times – penetration res: .
initial setting time vs start of velocity gain
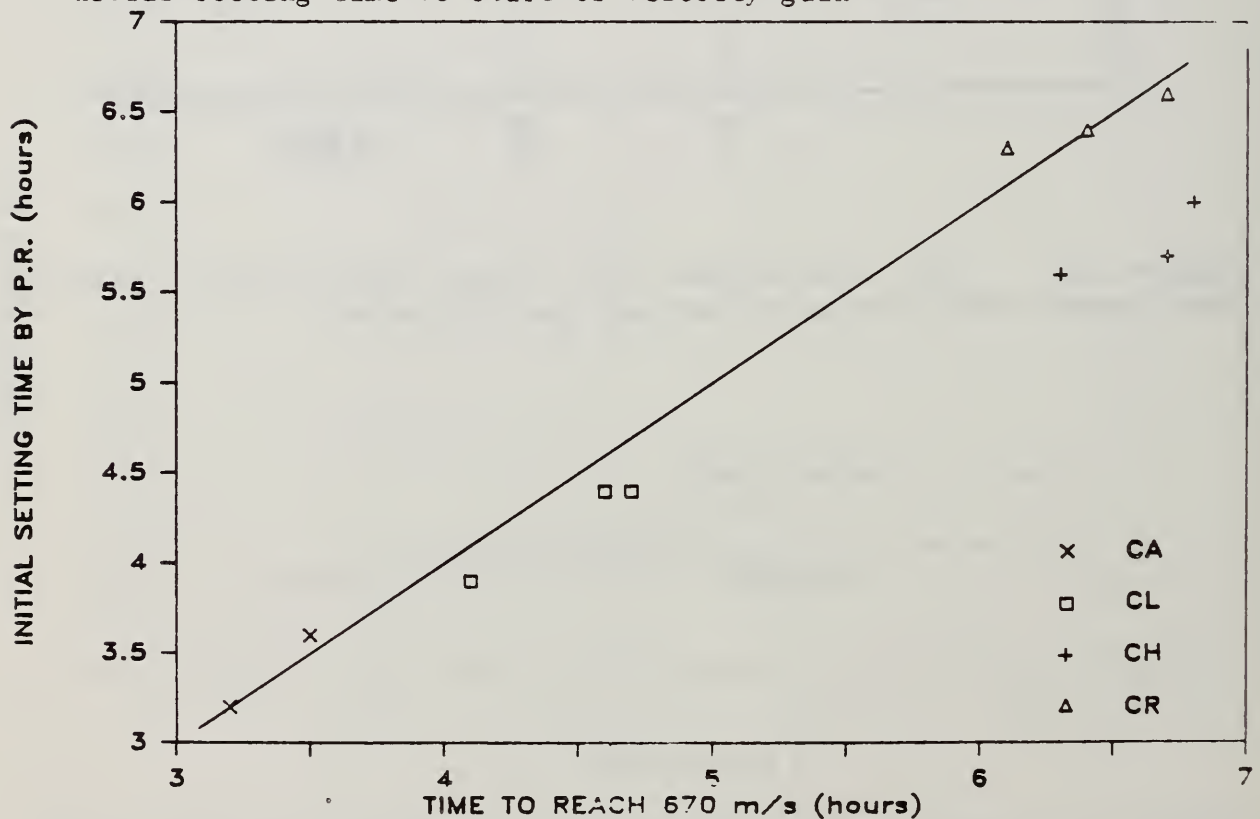
Figure 4.27   Comparison of setting times – penetration resistance
initial setting time vs target velocity of 670 m/s

76

CHAPTER 5
MEASUREMENT OF COMPRESSIVE STRENGTH

5.0 INTRODUCTION

As stated in Chapter 1, this research project had two main objectives. The first of these objectives, to evaluate the impact-echo technique as a means of measuring the setting time of concrete, was explained in Chapter 4. The second objective, to evaluate the impact-echo technique as a means of estimating the compressive strength of concrete, is discussed in this chapter. The findings presented are a first step towards an in-place strength estimation test based upon the measurement of P-wave velocity by the impact-echo method.

The general methodology for in-place strength estimation during construction is as follows (1). First, a relationship is established between concrete strength and the results of a specific in-place test. This is usually done in the laboratory for a given concrete mixture. Tests are performed at different maturity values and the resulting paired data are used to develop an empirical relationship, such as the one shown in Figure 5.1. Once established, this relationship is used to estimate the strength of the concrete in the structure, using the results of in-place tests performed on the structure.

In this study, the relationship between cylinder compressive strength and P-wave velocity was studied. The scope of the study is discussed further in section 5.1, followed by a description of the experimental set-up and testing procedures in section 5.2. Section 5.3 describes how the velocity and strength measurements were made. The anticipated relationship between strength and velocity is discussed in section 5.4, followed by the experimental results in section 5.5.

5.1 OBJECTIVE AND SCOPE

In order to reliably use the impact-echo technique as a means of estimating in-place strength, it is important to understand how the relationship between strength and impact-echo velocity is influenced by factors that are commonly encountered in construction practice. Such factors might include variations in curing temperatures, w-c ratio, and aggregate content, to name a few. Thus, as an integral part of evaluating the applicability of the impact-echo technique as a means of estimating compressive strength, the influence of each of these factors upon the strength-velocity relationship was examined. A comparison was made of the strength-velocity relationships for concretes made with the same mixture proportions, but water-cured at three different temperatures, approximately 10, 20, and 35 °C. A comparison was also made of the strength-velocity relationships for two concrete mixtures with the same aggregate content, cured at room temperature (approximately 20 °C), but having different w-c ratios (0.50 and 0.57). Lastly, a comparison was made of two concrete mixtures with the same w-c ratio, cured at room temperature, but with different agregate contents (67 and 72 percent by volume).

5.2 EXPERIMENTAL SET-UP AND PROCEDURES

5.2.1 Materials

The concrete specimens were made using Type I portland cement, graded rounded gravel ranging in size from 31.5 to 4.75 mm (1.25 to 0.187 in.), natural sand with a fineness modulus of 2.12, and tap water. Fineness modulus, specific gravity, absorption, and periodic moisture contents were determined according to the applicable ASTM Standard Test Methods (C 127, C 128, C 136, C 566) (3). Material properties are summarized in Table 4.4 (the materials used in the strength tests were the same as those used in the concrete and sieved mortar setting time tests).

5.2.2 Mixture Proportions

Three different mixture proportions were used in the study. The mixture proportions for each are given in Table 5.1. The basis of comparison used throughout the study was a 0.57 w-c ratio concrete, with a volumetric aggregate fraction of 0.67 (mixture 1), cured at 20 °C. To investigate the influence of changes in curing temperature, a total of four batches were made using this mixture. In the discussion to follow, the specimens cured at 20, 35, and 10 °C will be referred to as room-, hot-, and cold-cured specimens, respectively. In order to detect differences between the specimens cured at different temperatures that may actually have been caused by batch-to-batch variations, room-cured cylinders were also cast from the batches used to cast hot- and cold-cured cylinders. It was found that the strength-velocity relationships for the room-cured cylinders taken from all four batches were the same, i.e., there were no batch to batch differences between concretes. Hence the observations made in section 5.5.2 can be attributed solely to changes in curing temperatures.

The investigation of the influence of changes in w-c ratio was made using a second concrete mixture (mixture 2) with the same volumetric fraction of aggregate as the base mixture (0.67), but with a lower w-c ratio (0.50 as compared to 0.57). Two batches of this lower w-c ratio concrete were made and specimens were cured at room temperature.

Lastly, the investigation of the influence of changes in aggregate content was made using a concrete mixture (mixture 3) with the same w-c ratio as the base mixture (0.57), but containing a 5 percent increase in the volume fraction of aggregate. Two batches of this higher aggregate content mixture were made and specimens were cured at room temperature.

Table 5.2 presents a summary of the 8 batches, listing the number of specimens cast from each batch, the number of specimens cured at each temperature, and the aggregate content, w-c ratio, and slump of each batch.

5.2.3 Specimen Preparation

The concretes were mixed in a 1.5 cubic foot capacity revolving drum mixer. The mixing procedure was as follows:

1. Thoroughly wet the mixing drum and allow it to drip dry in an inverted position for 1 minute.

2. Add the coarse aggregate, fine aggregate, and cement, and dry mix for about 30 seconds.
3. Gradually add the mixing water while the drum is revolving. Cover the drum opening and continue mixing for approximately 8 minutes.
4. Perform the slump test (C 143) (3), then briefly re-mix the concrete.

The specimens were cast in 102 mm (4.0 in.) diameter by 203 mm (8.0 in.) deep cylindrical plastic molds. Concrete was added to each mold in two equal layers, each layer rodded 15 times with a 9.5 mm diameter rod with a rounded tip. The fresh concrete surfaces were then leveled off with a trowel.

Immediately after casting, the fresh concrete specimens were placed in lime-saturated curing baths at the specified temperatures. The water in each curing bath was raised to a level approximately 25 mm above the top surfaces of the specimens. Care was taken to ensure that the top surfaces were undisturbed and remained plane with the bottom surfaces.

Three curing baths were used, and were maintained at approximately 10, 20, and 35 °C. The temperatures of the room- and cold-curing baths were monitored using thermocouples. The temperature of the hot-curing bath was monitored using a glass thermometer. The room-curing bath remained relatively constant throughout the experiment, ranging from 18 to 23 °C. The hot-curing bath consisted of a metal tub fitted with a lid, that was placed in an oven maintained at approximately 35 °C. As a result, the temperature of the hot-curing bath also remained relatively constant throughout the duration of the experiment, ranging from 34 to 37 °C. The cold-curing bath consisted of a plastic tub, covered with insulation board, and kept outdoors in the winter climate. During the early part of the experiment, the temperature of the cold-curing bath ranged mostly from 5 to 12 °C. During one period at later ages (compressive strengths of approximately 21 MPa), the temperature of the cold curing bath fell as low as 0 C.

To facilitate stripping the specimens from the molds, each mold was lightly oiled prior to casting. In addition, each mold had a 6-mm diameter hole drilled in the center of its bottom, which was then covered with a masking tape. To strip the specimens from the molds, pressurized air was blown through this hole, forcing the cylinder from the mold. For very low strength specimens (2 to 7 MPa), the perimeter of the bottom surfaces of the specimens were damaged slightly by this operation. However, as described in the next paragraph, the specimens were capped prior to testing, filling in any damaged areas that otherwise might have reduced the measured compressive strength.

Prior to making the velocity measurement and subsequent compressive strength test, each cylinder was capped with a high strength sulfur mortar, as prescribed in ASTM C 617 (Standard Method of Capping Cylindrical Concrete Specimens) (3). It was difficult to cap the very low strength cylinders (2 MPa) because the capping material adhered more strongly to the capping plate than to the specimen.

5.3 SPECIMEN TESTING

For each concrete cylinder, the velocity was measured, then the compressive strength was determined. Hence each data record is the result of

a velocity measurement and a compression test on the same cylinder. The following sections discuss how the velocity and strength tests were made.

5.3.1 Velocity Measurement

The technique used to make the impact-echo measurements on the capped cylinders was similar to that used in the setting time study described in section 4.1. In the strength study, the capped surfaces of the specimens provided a smooth surface upon which to make the velocity measurements, without the need for any surface preparation. Stress waves were generated by the impact of a small steel sphere dropped from a height of approximately 0.2 m onto the center of the top surface of the capped specimen. The receiving transducer, located at half the radius, detected the resulting surface displacements. A thin lead strip was inserted between the piezoelectric tip of the transducer and the sulfur cap to complete the electrical circuit of the transducer.

In the measurements at the lowest maturities, the velocities through the concrete specimens were approximately 2100 m/s. The corresponding compressive strengths were approximately 2 MPa. For the specimens cured at room temperature, this was approximately 12 hours after mixing.

A typical displacement waveform and accompanying frequency spectrum obtained from a specimen with a compressive strength of 1.87 MPa are shown in Figures 5.2 (a) and (b). It is possible to interpret this signal in either the time or frequency domain, as was explained in section 4.1.2. The time interval between peaks in the displacement waveform, Δt, can be used to calculate compression wave velocity according to eq. (3.11). From Figure 5.2 (a), Δt was found to be 190 us. Using the nominal cylinder height T = 0.203 m, the P-wave velocity was calculated as C_p = 2 x 0.203 m / 190 us = 2140 m/s. Alternately, the 5.176 kHz peak in the frequency spectrum due to the fundamental response of the specimen can be used to calculate the velocity according to eq. (3.13). This leads to C_p = 2 x 0.203 m x 5.176 kHz = 2100 m/s.

Throughout the testing, results were analyzed in the frequency domain. Velocities were computed according to Eq 3.13. A 100 kHz sampling frequency (10 us sampling interval) was used to make the measurements, resulting in a 0.098 kHz frequency interval in the frequency spectra. Hence, for the 0.203 m specimen height used, the velocity could be computed to the nearest 40 m/s. Note that this is only 2 percent of the earliest velocity measurements made (2100 m/s).

Capping each specimen prior to making the velocity measurement caused a slight decrease in the measured velocity. This was attributed to the added thickness of the capping material. In terms of obtaining a true measure of the velocity through the concrete, it would have been better to cap the specimens after making the velocity measurement. However, this was not practical from a procedural viewpoint, because at the time of the earliest measurements, the velocity in the specimens was changing rapidly with time. Capping these early-age specimens was especially time consuming, thus the velocity would have changed appreciably before the strength could be determined. It was therefore decided to cap the cylinders prior to making the velocity measurements, introducing a shift (approximately 190 m/s) in the strength-velocity curve to a lower velocity value.

5.3.2 Compressive Strength Determination

Immediately after the velocity measurements were made, the cylinders were tested in compression as prescribed in ASTM C 39 (Standard Test Method for Compressive Strength of Cylindrical Concrete Specimens) (3). Each cylinder was loaded at a rate of approximately 0.15 MPa per second, and the maximum load sustained recorded to the nearest 0.45 kN. In computing the failure compressive stress of each specimen, f_c, the cross-sectional area was taken as 0.008 m^2, based on the nominal diameter of the cylinder.

5.4 ANTICIPATED COMPRESSIVE STRENGTH - VELOCITY RELATIONSHIP

It has been shown empirically in work by Pauw (26) that, for mature concrete, the modulus of elasticity of concrete E_c is proportional to the square root of compressive strength, or

$$E_c \ \alpha \ \sqrt{f_c} \tag{5.1}$$

Further, it has been shown from the physics of wave propagation that P-wave velocity through an elastic solid is proportional to the square root of the elastic modulus E, or

$$C_p \ \alpha \ \sqrt{E} \tag{5.2}$$

Assuming eq. (5.1) also applies to immature concrete, and from Eqs. 5.1 and 5.2, taking E as E_c, it is seen that

or,
$$C_p \ \alpha \ \sqrt[4]{f_c} \tag{5.3}$$

$$f_c \ \alpha \ (\ C_p \ )^4 \tag{5.4}$$

Thus it is expected that there may exist an approximately fourth power relationship between compressive strength and compression wave velocity. This fourth power relationship is shown schematically in Figure 5.3.

5.5 EXPERIMENTAL RESULTS

This section discusses the experimental results. Section 5.5.1 examines the general relationship between compressive strength and velocity, and describes two empirical curves used to represent this relationship. The discussion is presented using the data from the room-cured cylinders. Sections 5.5.2, 5.5.3, and 5.5.4 discuss, respectively, the influence of

changes in curing temperature, w-c ratio, and aggregate content, using the room-cured cylinders as a
reference for comparison. The strength-velocity data from all batches are presented in Appendix B.

5.5.1 Regression Model: Room-Cured Specimens

Figure 5.4 shows the experimental results for 33 concrete cylinders from mixture 1 cured at room temperature. In agreement with the discussion in section 5.4, the data appears to follow a power relationship. At lower velocities, the velocity is increasing rapidly relative to the strength. At higher velocities, the opposite is true; that is, relatively large gains in strength are accompanied by only small increases in velocity. It is also noted that there is little scatter in the data, thus there was minor batch-to-batch variability.

Two empirical equations were used to represent the strength velocity data shown in Figure 5.4. One equation used was the power relationship

$$f_c = a \, (C_p)^b \tag{5.5}$$

To determine the constants a and b, eq. (5.5) was transformed into a linear equation by taking its logarithm:

$$\log f_c = \log a + b \log C_p \tag{5.6}$$

The intercept (log a) and slope (b) were then determined by linear regression in log space. Figure 5.5 (a) shows the best-fit line (predicted line) of eq. (5.6) to the room temperature data, calculated using the method of least squares. The best-fit values of a and b were 0.063 and 4.44, respectively, and the standard error (in real space) was 2.18 MPa. It can be seen in Figure 5.5 (a) that in the center region of the graph the predicted line is consistently above the experimental data. Further, above a log velocity of 0.56, the predicted line falls below the experimental data. Thus, the simple power relationship does not appear to fit the data. This lack of fit is further demonstrated in Figure 5.5 (b), which is a plot of the residuals (difference between experimental and predicted values) from Figure 5.5 (a) as a function of the log of velocity. In the calculation of the best fit line, each data point was assumed to have equal importance. In addition, least-squares regression analysis assumes that the residuals (errors) have a normal distribution, with an average error of 0 (5). Thus, a predicted curve that fits the data will have residuals randomly scattered above and below the zero-residual line. Clearly, the residuals are not randomly scattered in Figure 5.5 (b). Hence, a simple power function does not appear to be an accurate description of the relationship between strength and velocity.

When transforming from log space back into real space, the residuals at higher velocities become larger relative to the residuals at lower velocities. This can be seen by comparing Figure 5.5 (c), which is a plot of the residuals in real space, with Figure 5.5 (b). Consequently, an equation

82

that fits the data will have a residual plot in real space that displays a fan-like pattern. The residuals will be randomly distributed about the zero-residual line, and increase in magnitude with increasing velocity. Residual plots in real space will be used to help interpret the results presented in later sections of this chapter.

Lastly, Figure 5.5 (d) shows the best-fit power curve (eq. 5.5) superposed onto the room-cured data. As was explained in the preceding development, it can be seen that in the range of velocities from 2900 to 3500 m/s, the power curve over-predicts strength, whereas above 3700 m/s, it under-predicts strength.

A second equation used to represent the strength-velocity data was

$$f_c = a \left(\frac{C_p}{n} + 1 \right)^b \tag{5.7}$$

Again, the equation was transformed into a linear equation by taking its logarithm:

$$\log f_c = \log a + b \log \left(\frac{C_p}{n} + 1 \right) \tag{5.8}$$

The constants a and b were determined by linear regression for incrementing values of n. The criterion for determining n was to increment n by 50 until the standard error remained unchanged in the third decimal place. The resulting best-fit values of a, b, and n were 0.079, 306.2 and 200, respectively, and the standard error in real space was 1.26 MPa.

Figures 5.6 (a), (b), (c), and (d) show, respectively, the linear fit in log space, the residuals in log space, the residuals in real space, and the fit in real space of eq. (5.7) to the room-cured cylinder data. Comparison of these figures with Figures 5.5 (a) through (d) reveals that eq. (5.7) agrees more closely with the experimental data than does eq. (5.5). As seen in Figure 5.6 (d), in the range from 2900 to 3500 m/s, the experimental data fall close to the best-fit line; above 3700 m/s, it passes through the data, rather than underestimating it as was the case with the simple power function given by eq. (5.5). The residuals in Figure 5.6 (b) show a random distribution about the zero-residual line, and in Figure 5.6 (c), the residuals in real space form the fan-like pattern described earlier. Lastly, as can be seen from Table 5.3, the standard errors obtained from Eqs. 5.5 and 5.7 respectively were 2.182 MPa and 1.261 MPa. Thus eq. (5.7) represents the strength-velocity data better than eq. (5.5). Therefore, eq. (5.7) was used to evaluate the results presented in the remainder of this chapter. It is noted that there may be other empirical functions that fit the data better than eq. (5.7). However, it is felt that eq. (5.7) fits the data reasonably well, and is satisfactory for the purpose of this study.

5.5.2 Curing Temperature Variation

5.5.2.1 Hot-Cured Specimens

The earliest tests of the hot-cured specimens were made 6 hours after initial mixing. The velocities through the concrete specimens were approximately 2080 m/s, and the corresponding strengths approximately 1.98 MPa.

Figure 5.7 (a) is a plot of the strength-velocity data for the hot-cured specimens. Superposed on the data is the best-fit curve (eq. 5.7) for the room-cured specimens, discussed in the previous section. Figure 5.7 (b) is a plot of the residuals of the hot-cured data about the room-cured curve in real space. From these figures it is seen that up to velocities of approximately 2800 m/s, the hot-cured data agrees well with the room-cured prediction curve. At velocities above 2800 m/s, the room-cured curve over-predicts the strength. For this concrete mixture, a velocity of 2800 m/s corresponds to a strength of about 6.1 MPa. Thus increasing the curing temperature from 20 to 35 °C alters the strength-velocity relationship at higher velocities. Above 2800 m/s, the hot-cured specimens exhibit lower strengths relative to the room-cured specimens for a given velocity.

5.5.2.2 Cold-Cured Specimens

The earliest test of a cold-cured specimen was made approximately 24 hours after initial mixing. The velocity in the concrete was 2000 m/s, and the corresponding strength was 1.59 MPa.

Figure 5.8 (a) shows the strength-velocity data for the cold-cured specimens. Superposed on the data is the best-fit curve to the room-cured specimens. Figure 5.8 (b) is a plot of the residuals in real space. As can be seen in the figures, good agreement was found between the cold-cured cylinders and the room-cured prediction curve. The residuals shown in Figure 5.8 (b) are randomly scattered about the best-fit curve along the entire length of the curve. Thus a decrease in the curing temperature from 20 to 10 °C did not alter the strength-velocity relationship.

5.5.3. Water-Cement Ratio Variation

Figure 5.9 (a) shows the strength-velocity data from the low w-c ratio cylinders, with the prediction curve of the room-cured (high w-c ratio) specimens superposed. Figure 5.9 (b) is a plot of the residuals of the low w-c ratio data about this prediction curve. It can be seen from these two figures that up to velocities of approximately 4000 m/s (strengths of 33 MPa), there is good agreement between the low and high w-c ratio results. Thus the change in w-c ratio did not alter the strength-velocity relationship for velocities below 4000 m/s. It is noted that 33 MPa is approximately the 28-day strength of the high w-c ratio mixture. Residuals were computed for the low w-c ratio mixture by extrapolating the best-fit high w-c ratio curve above 33 MPa.

The low w-c ratio concrete reached any given strength-velocity point at an earlier age than the high w-c ratio concrete. Thus even though the strength-age or strength-maturity relationships for the two concretes differed, the strength velocity relationships were the same below a velocity

84

of 4000 m/s. At velocities greater than 4000 m/s (strengths greater than 33 MPa), the prediction curve from the high w-c ratio concrete underestimates the strength of the low w-c ratio mixture.

5.5.4 Aggregate Content Variation

Figure 5.10 (a) shows the strength-velocity data from the high aggregate content concrete. Again, superposed on the figure is the best-fit curve of the room-cured (low aggregate content) specimens. Figure 5.10 (b) is a plot of the residuals of Figure 5.10 (a). It is seen that a change in aggregate content alters the strength-velocity relationship. Figure 5.10 (a) shows that an increase in aggregate content shifts the strength-velocity data to the right, resulting in a higher velocity at any given strength. This shift is evident along the entire length of the curve. This result is not surprising. In section 4.3 it was shown that the velocity through the concrete depends upon the velocities through the paste and aggregate phases, and the relative proportions of each. Increasing the aggregate content increases the proportion of higher elastic modulus material, thus increasing velocity. Increasing the aggregate content also increases the area of paste-aggregate interfaces, which may also influence strength. The 28-day strengths of both the low and high aggregate content mixtures were the same. Thus it appears that the velocity rather than the strength was influenced by the increase in aggregate content, resulting in a higher velocity for a given strength.

5.6 DISCUSSION AND SUMMARY

It was observed that at lower velocities, the velocity was increasing rapidly relative to strength, and at higher velocities, the opposite was true. It follows that the impact-echo method would therefore be a more sensitive strength estimator at lower velocities, because small changes in strength would be revealed by relatively large changes in velocity.

Figure 5.11 shows the velocity and strength data from the room-cured cylinders plotted versus the time after initial mixing. From this figure it is seen that most of the velocity gain occurred during the first day. The velocities at 1, 3, and 7 days were approximately 3200, 3600, and 3800 m/s, respectively. The corresponding strengths were approximately 10.4, 19.2, and 26.4 MPa, respectively. In Figure 5.6 (d), the measurements that were made at ages of 1, 3, and 7 days are identified. It is seen from Figure 5.6 (d) that for the given concrete mixture, cured at room temperature, the sensitive region of the strength-velocity relationship lasts for about 3 days (up to velocities of approximately 3600 m/s). The 28-day strength of the concrete was found to be 33.6 MPa, hence the strength at 3600 m/s represents approximately 60 percent of the 28-day strength. Clearly, this is within the range typically required for safe removal of formwork, or the transfer of prestressing.

It was shown that a decrease in curing temperature from 20 to 10 °C did not affect the strength-velocity relationship. It also was shown that at higher velocities, an increase in curing temperature from 20 to 30 °C did affect the strength-velocity relationship, resulting in a lower strength at a given velocity for the hot-cured specimens.

The reason for the lower strength at a given velocity for the hot-cured specimens might be as follows. The rate of hydration increases with an increase in curing temperature. It has been suggested by Verbeck and Helmuth that at higher temperatures, the rate of hydration may be too fast to allow the products of hydration to diffuse and precipitate uniformly throughout the interstitial space between cement grains (36). As a result, hydration product will concentrate close to the cement grains. This has two consequences. First, complete hydration may be prevented, because water cannot diffuse through the layer of hydration product to the unreacted cement. Second, the porosity of the cement paste will be non-uniform; the paste in the regions near the cement grains will be less porous than the paste further away from the grains. Verbeck and Helmuth suggested that even if hydration were complete, the non-uniform porosity would lead to a lower strength, because strength would be limited by the more porous portion of the paste. P-wave velocity may also be dependent upon porosity, but not upon the distribution of porosity. Thus, at any velocity, both the room- and hot-cured specimens may have the same porosity (same degree of hydration). However, the non-uniform distribution of porosity in the hot-cured specimens may lead to a lower strength at that velocity.

As a consequence, it may not be possible to employ accelerated curing to develop the strength-velocity correlation for a given batch, which could then be used to predict the strength of the concrete in the structure from that batch.

A significant change in w-c ratio was shown to influence the strength-velocity relationship only at higher strengths and velocities (33 MPa, 4000 m/s). This, however, is probably above the useful range anyway, because of the insensitivity of velocity to changes in strength at high velocities. Based on these results, small changes in w-c ratio due to normal batching variations would not be expected to alter the strength-velocity relationship, and the relationship derived from laboratory testing would be applicable.

Both the low and high w-c ratio mixtures were cured at room temperature. Thus the distribution of porosity was probably about the same in both mixtures, and the porosity influenced both the strength and velocity in the same manner in both mixtures.

The strength-velocity relationship was greatly influenced by a 5 percent increase in aggregate content. It was suggested that the velocity rather than the strength was influenced by the increase in aggregate content. The higher aggregate content mixture exhibited higher velocities at any given strength. It is therefore apparent that the correlation must be established for a given concrete mixture, and that control must be exercised over batching operations for the correlation to be useful.

Table 5.1   Mixture proportions for compressive strength tests

Mixture Number	Water (gm)	Cement (gm)	Coarse Aggregate 31.5 to 12.5 mm (gm)	12.5 to 4.75 mm (gm)	Fine Aggregate (gm)
1	570	1000	801	2185	1984
2	500	1000	743	2008	1754
3	574	1000	974	2632	2287

Table 5.2   Summary of strength test program

Batch	Mixture Number	Volumetric Aggregate Fraction	w-c Ratio	Slump (mm)	Number of Specimens	Number of Specimens cured at 10 C	20 C	35 C
1	1	0.67	0.57	195	15		15	
2	1	"	"	200	18		4	14
3	1	"	"	180	20	15	5	
4	1	"	"	180	19		9	10
5	2	0.67	0.50	90	14		14	
6	2	0.67	0.50	90	13		13	
7	3	0.72	0.57	25	14		14	
8	3	0.72	0.57	25	13		13	
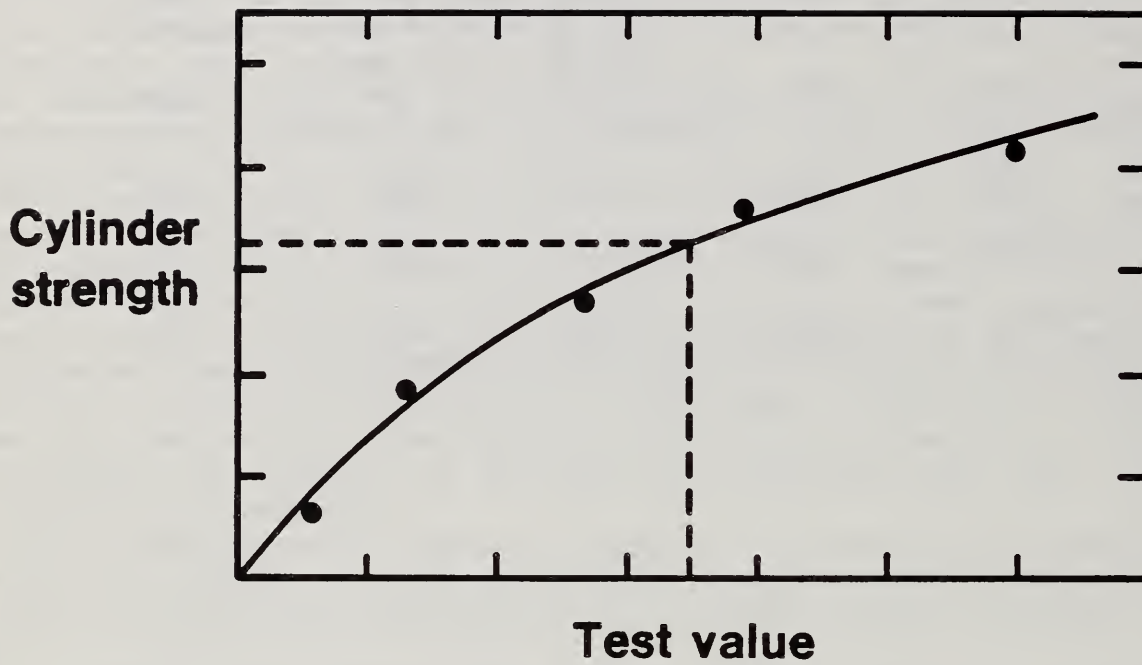
Figure 5.1   Methodology of in-place strength estimation (i)
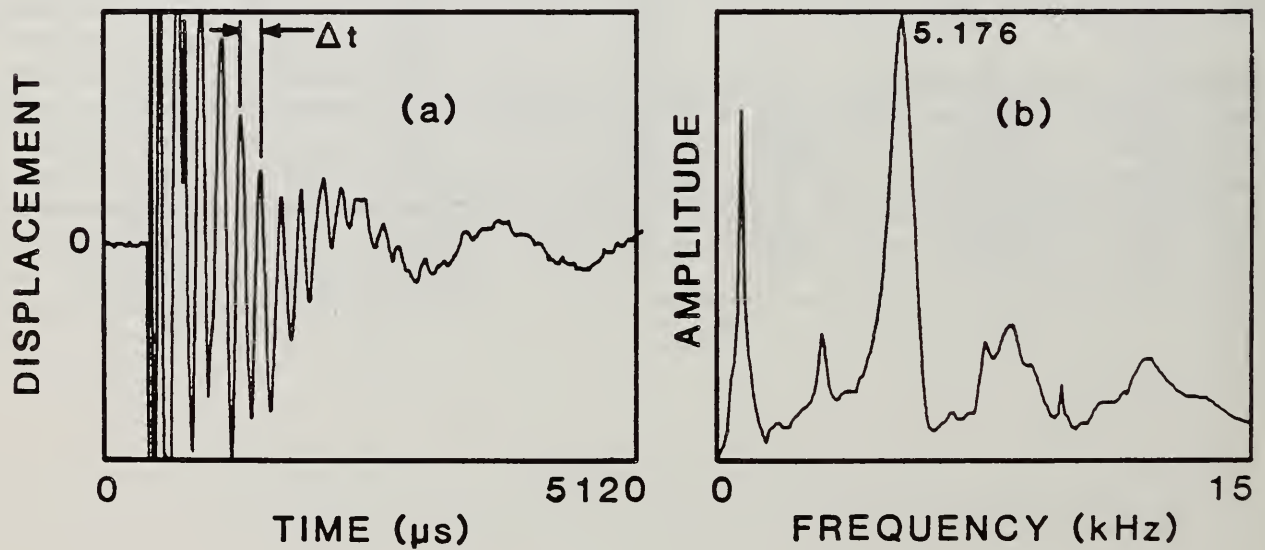
Figure 5.2   Typical velocity measurement: a) surface displacem
waveform; and, b) frequency spectrum
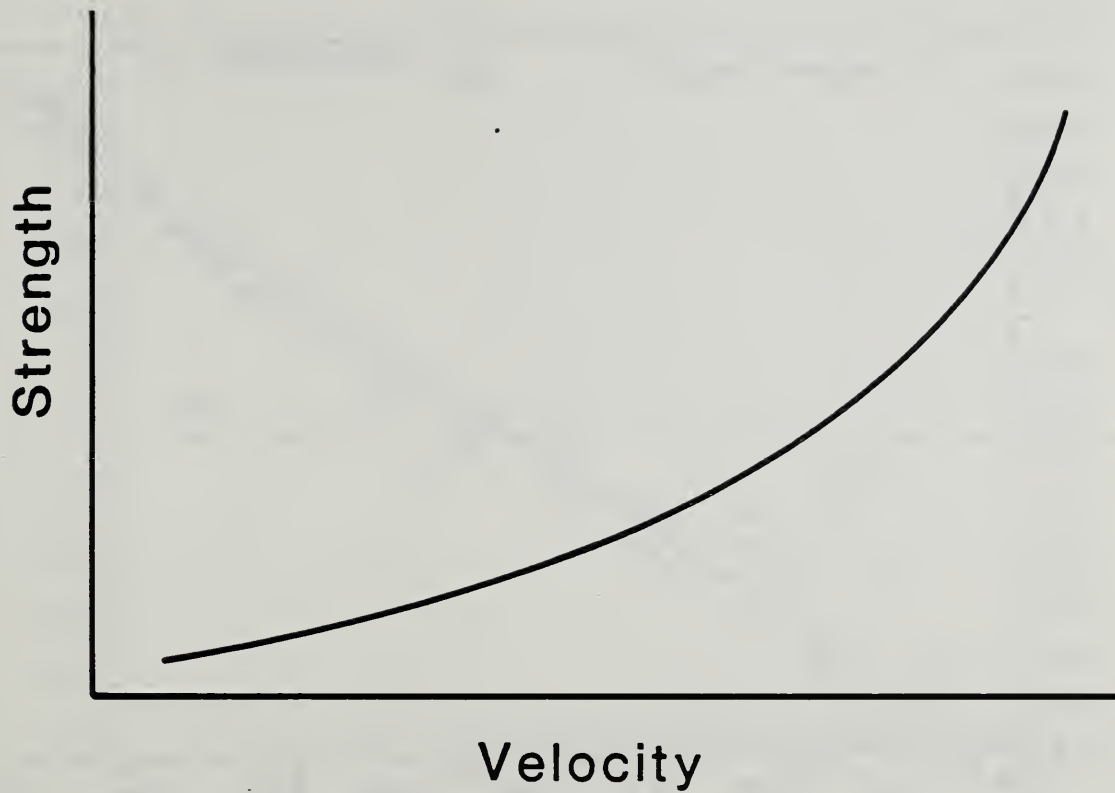
Figure 5.3   Anticipated fourth-power relationship between compressive strength and P-wave velocity
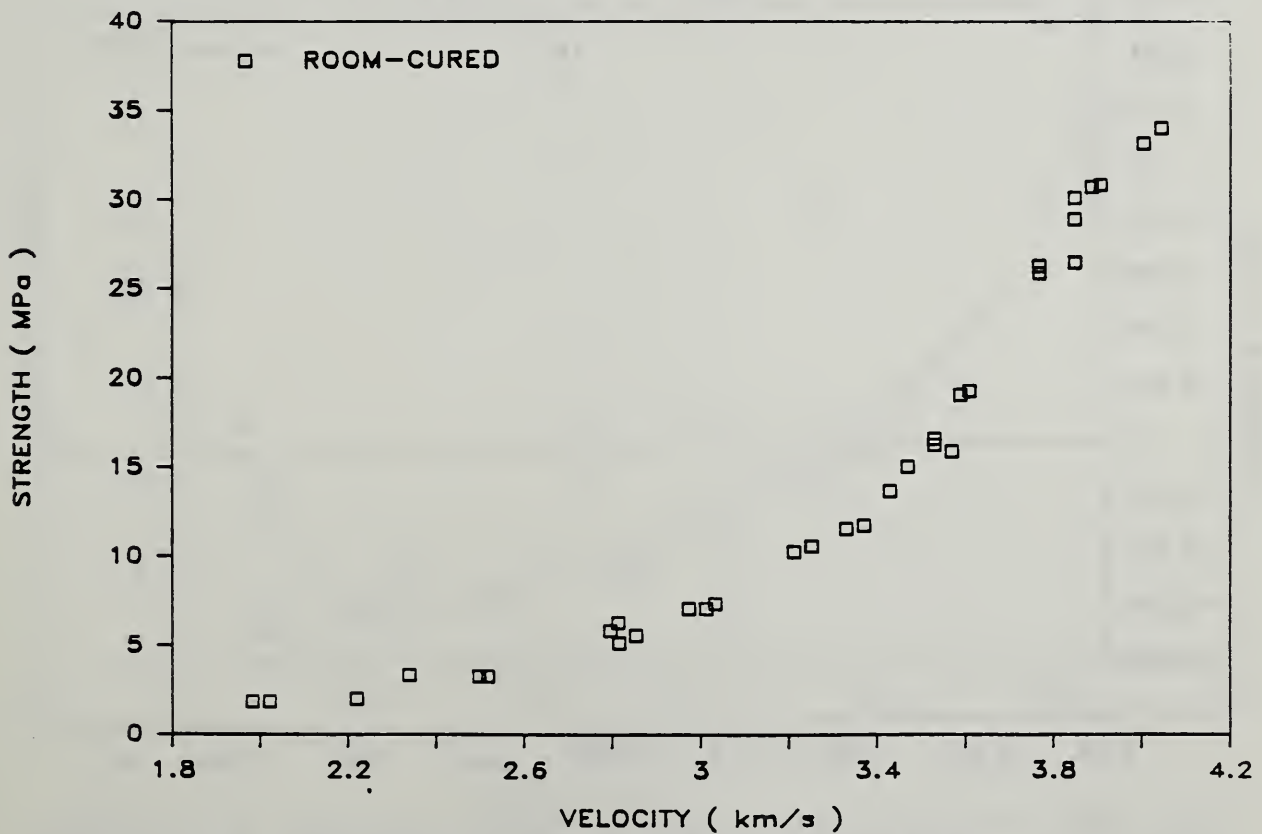
Figure 5.4   Room-cured specimens: strength vs velocity
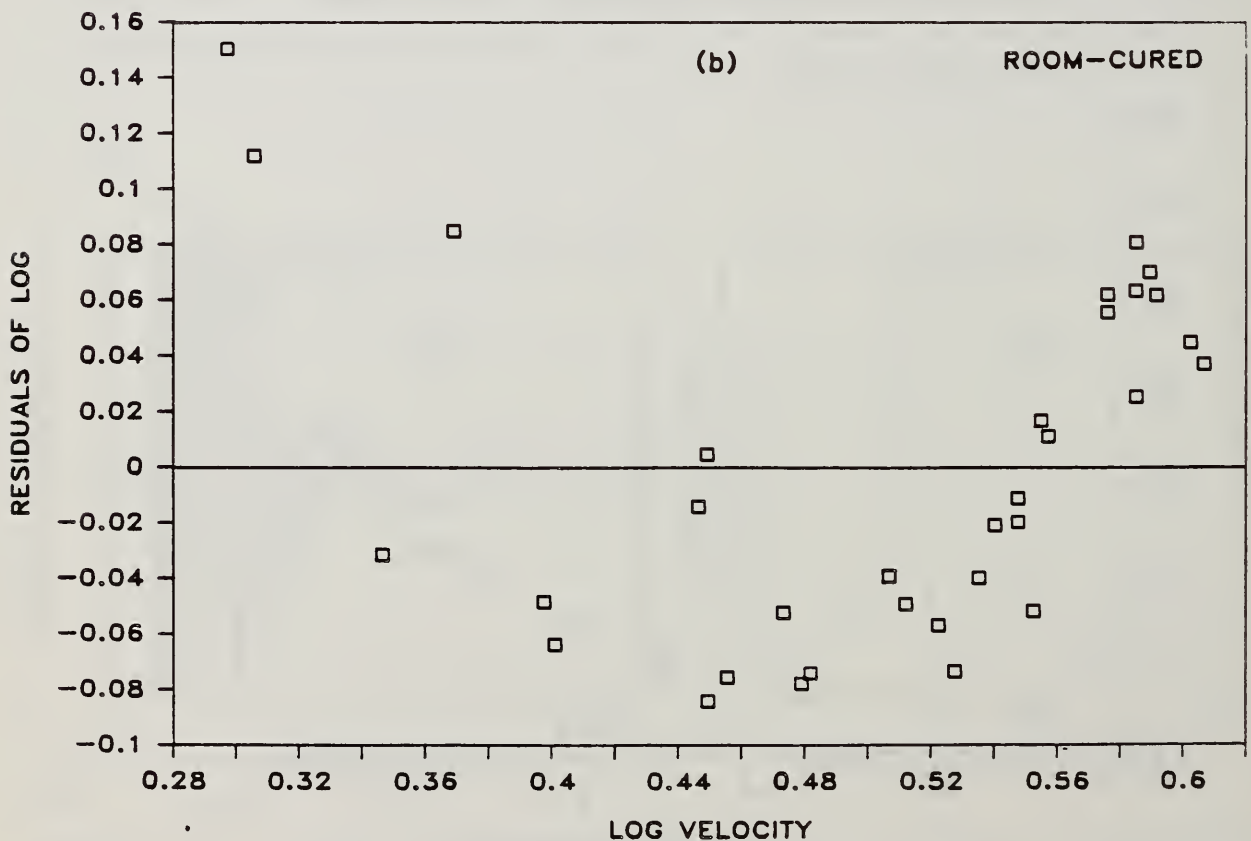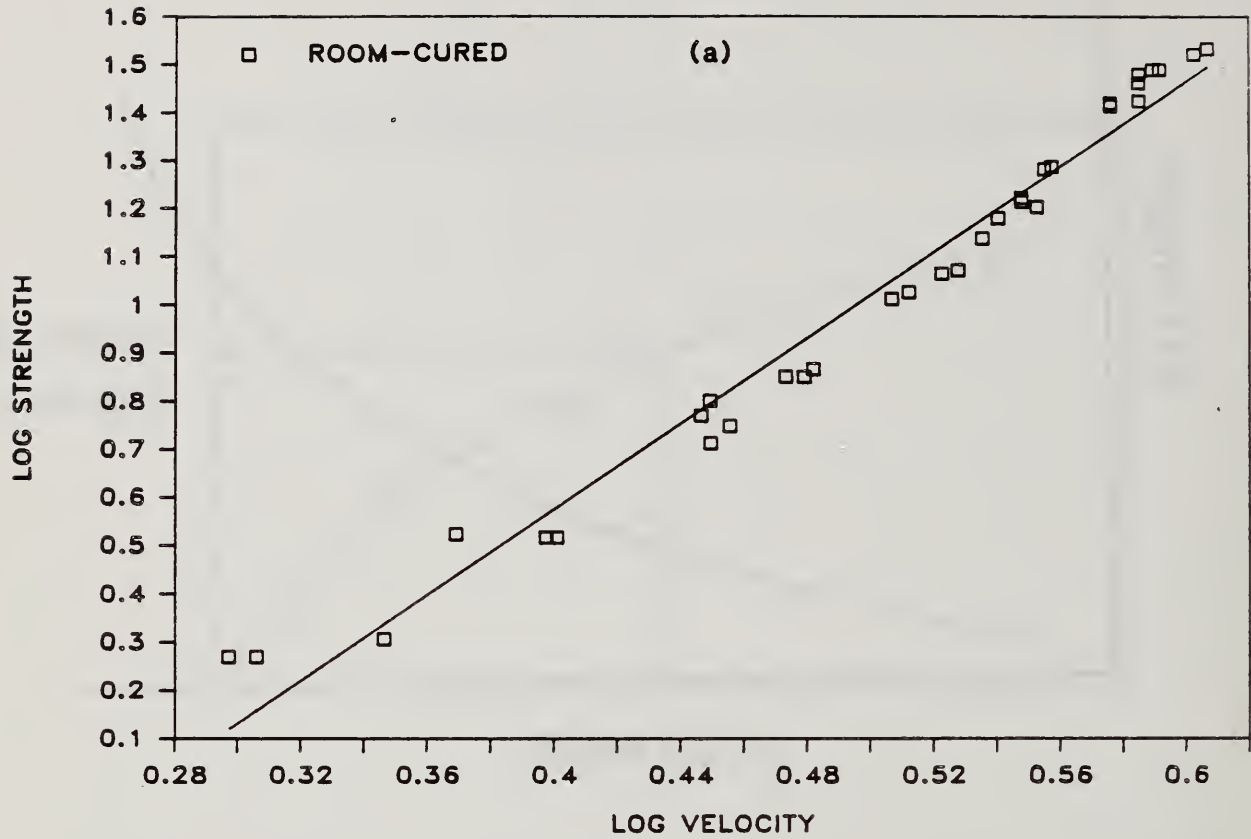
Figure 5.5   Results of regression analysis using Eq. 5.5: a) linear
fit of Eq. 5.5; b) residuals in log space

Figure 5.5 (continued) Results of regression analysis using Eq. 5.5: c) residuals in real space; and, d) best-fit of Eq. 5.5

91
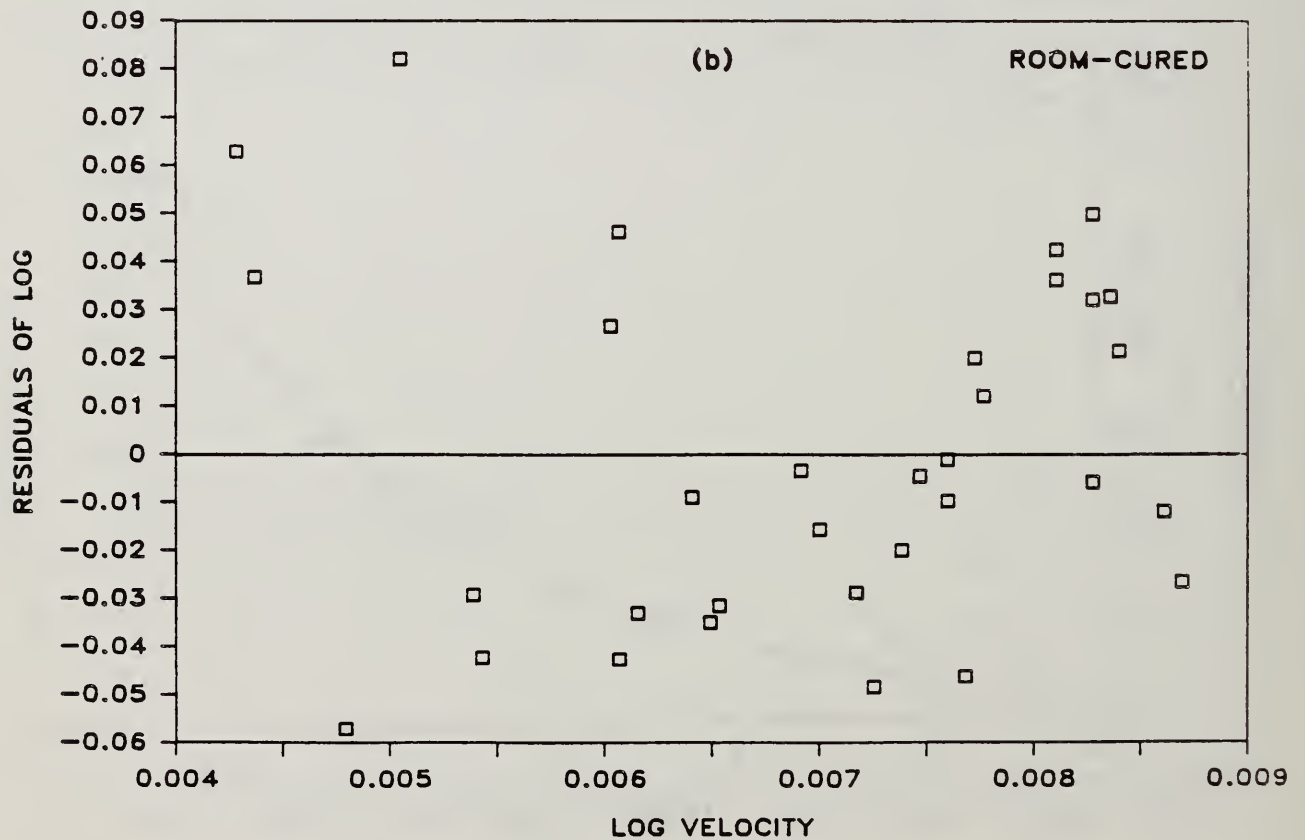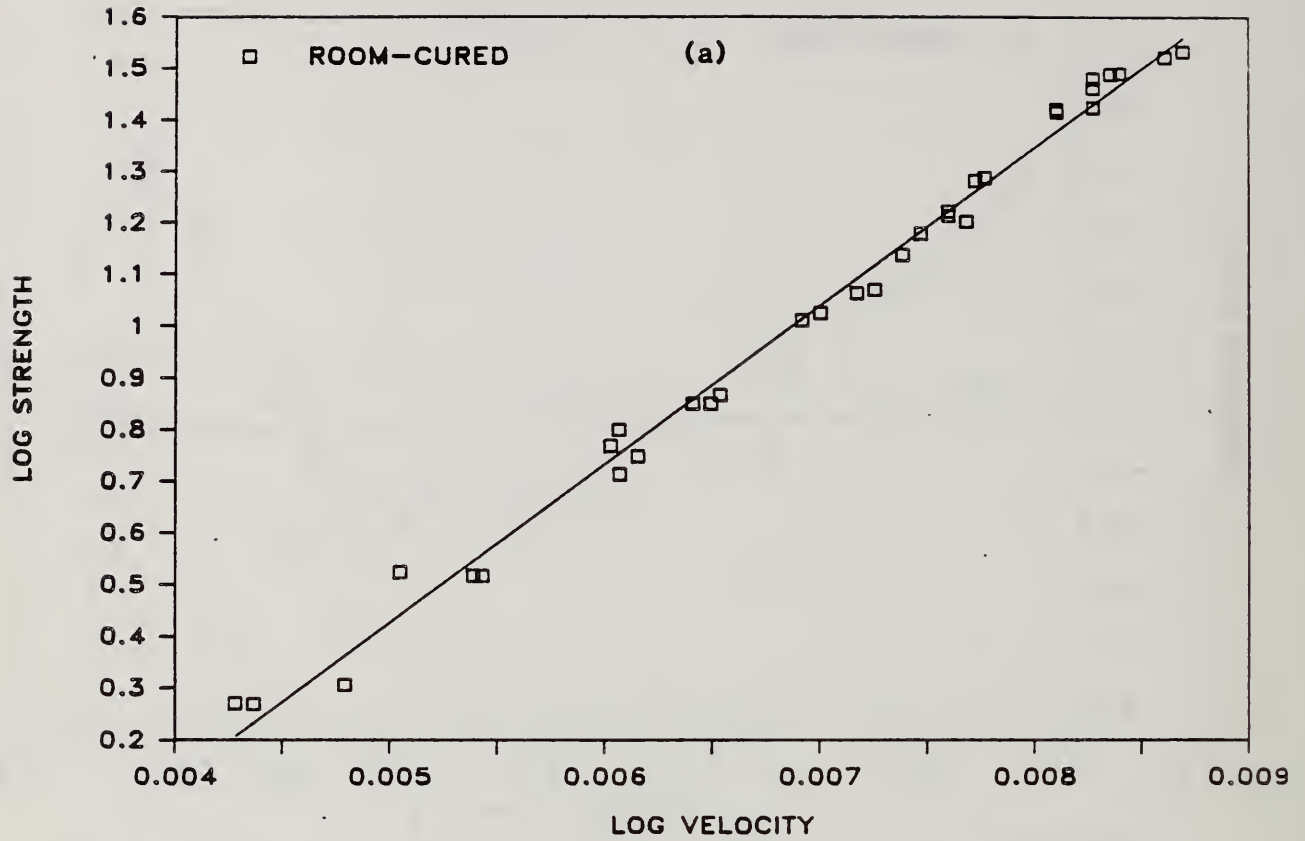
Figure 5.6   Results of regression analysis using Eq. 5.7: a) linear
fit of Eq. 5.7; b) residuals in log space
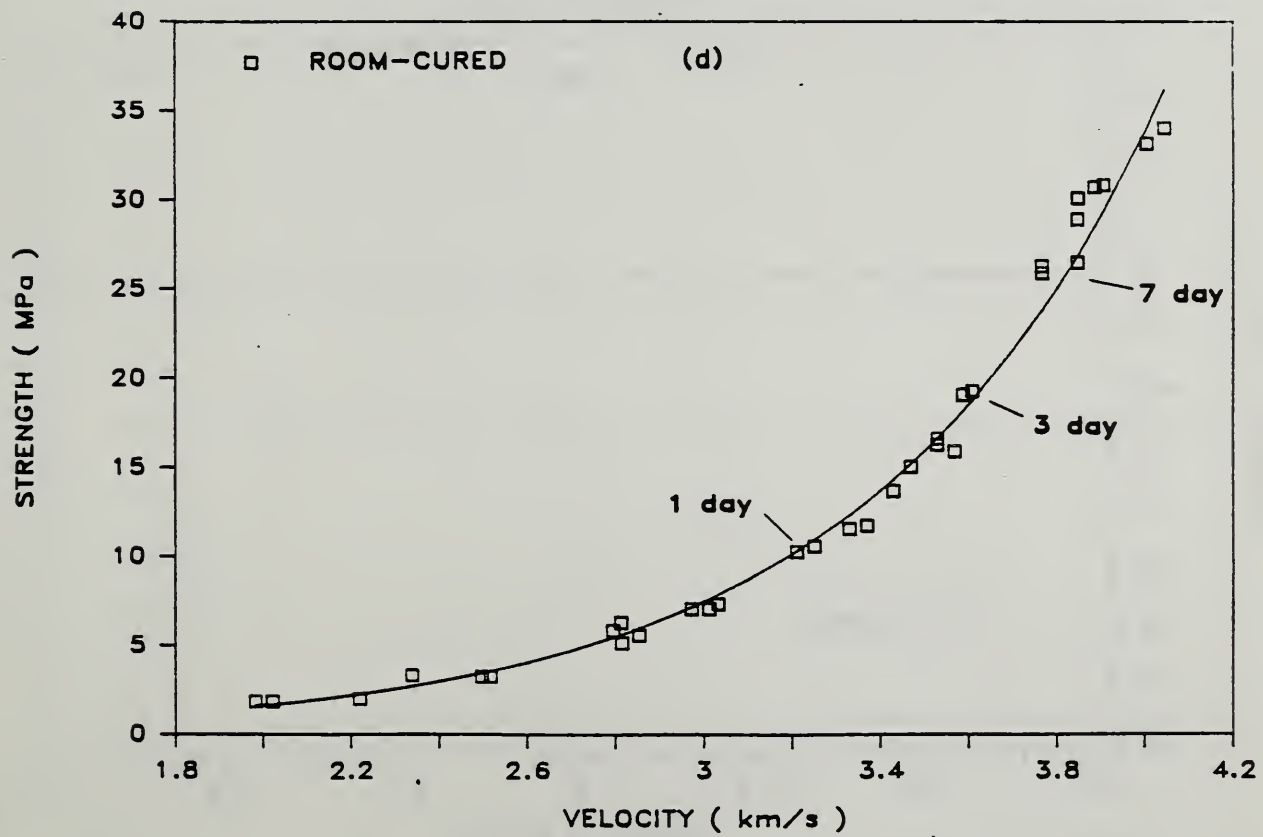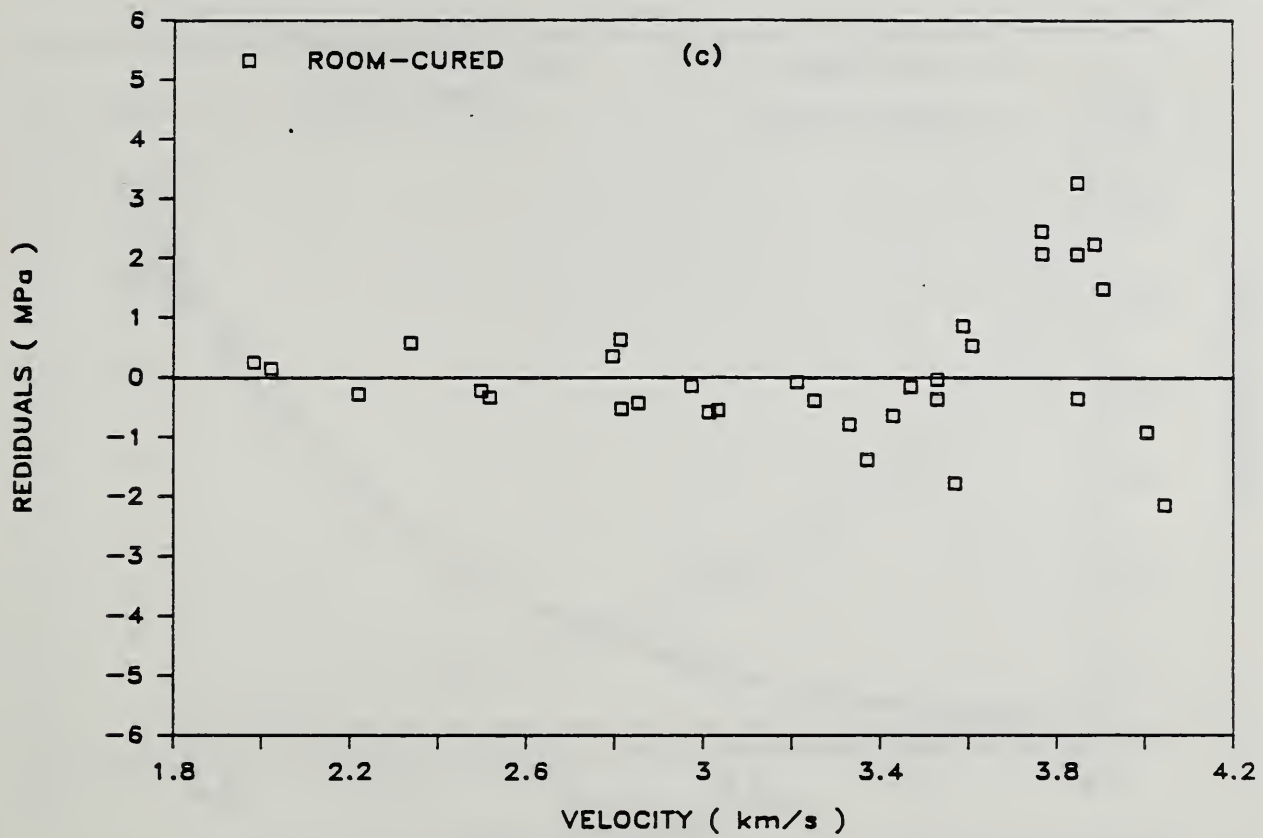
Figure 5.6 (continued) Results of regression analysis using Eq. 5.7: c) residuals in real space; and, d) best-fit of Eq. 5.7
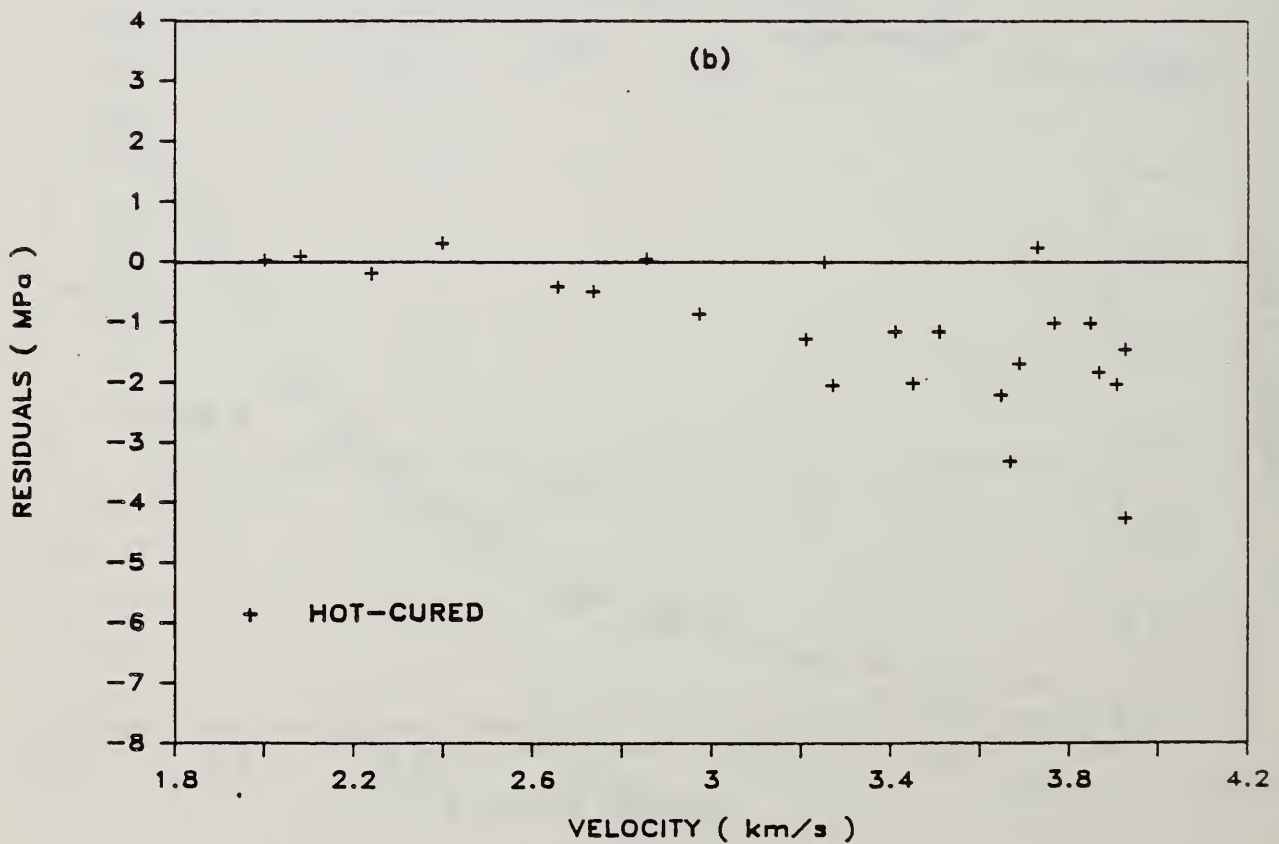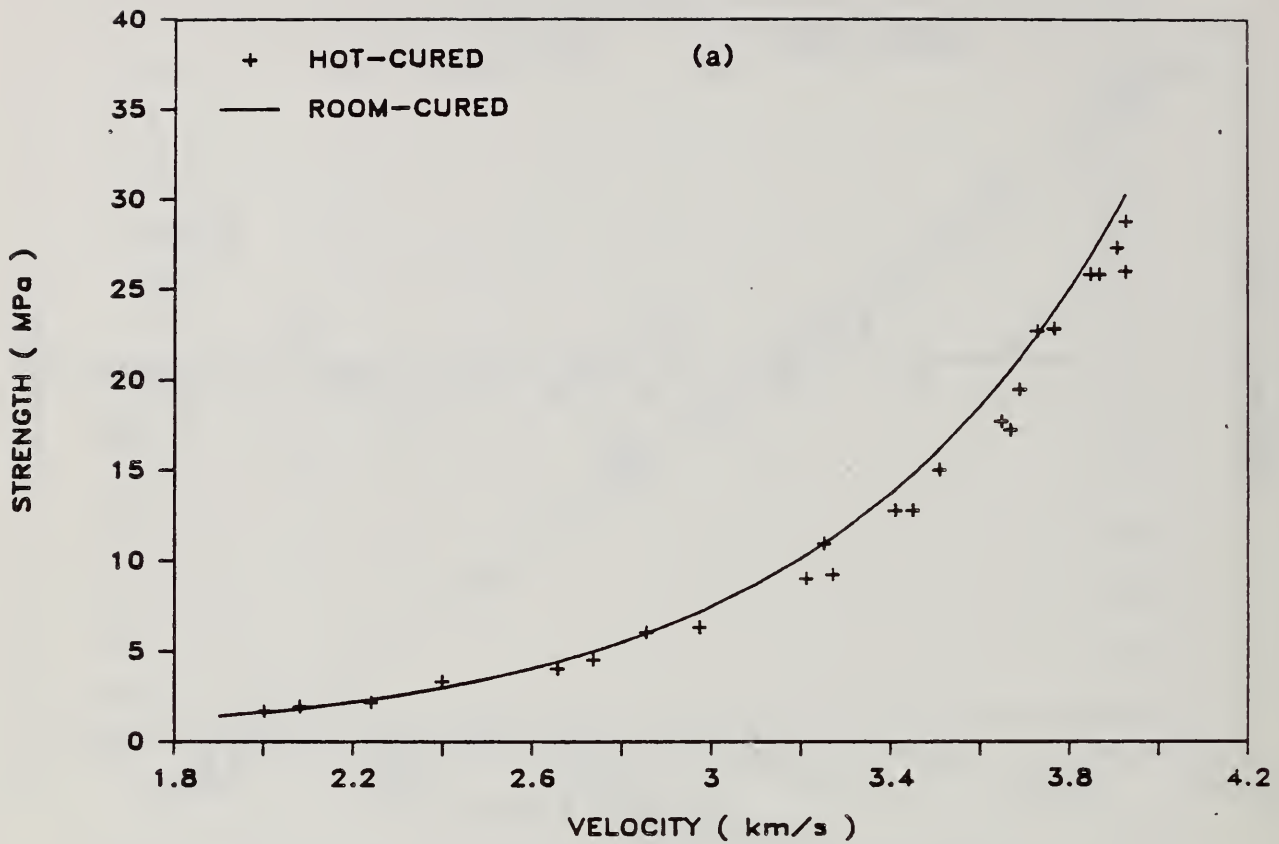
Figure 5.7   Hot-cured specimens: a) strength vs velocity; and, b) residuals in real space about best-fit of Eq. 5.7 to room-cured results
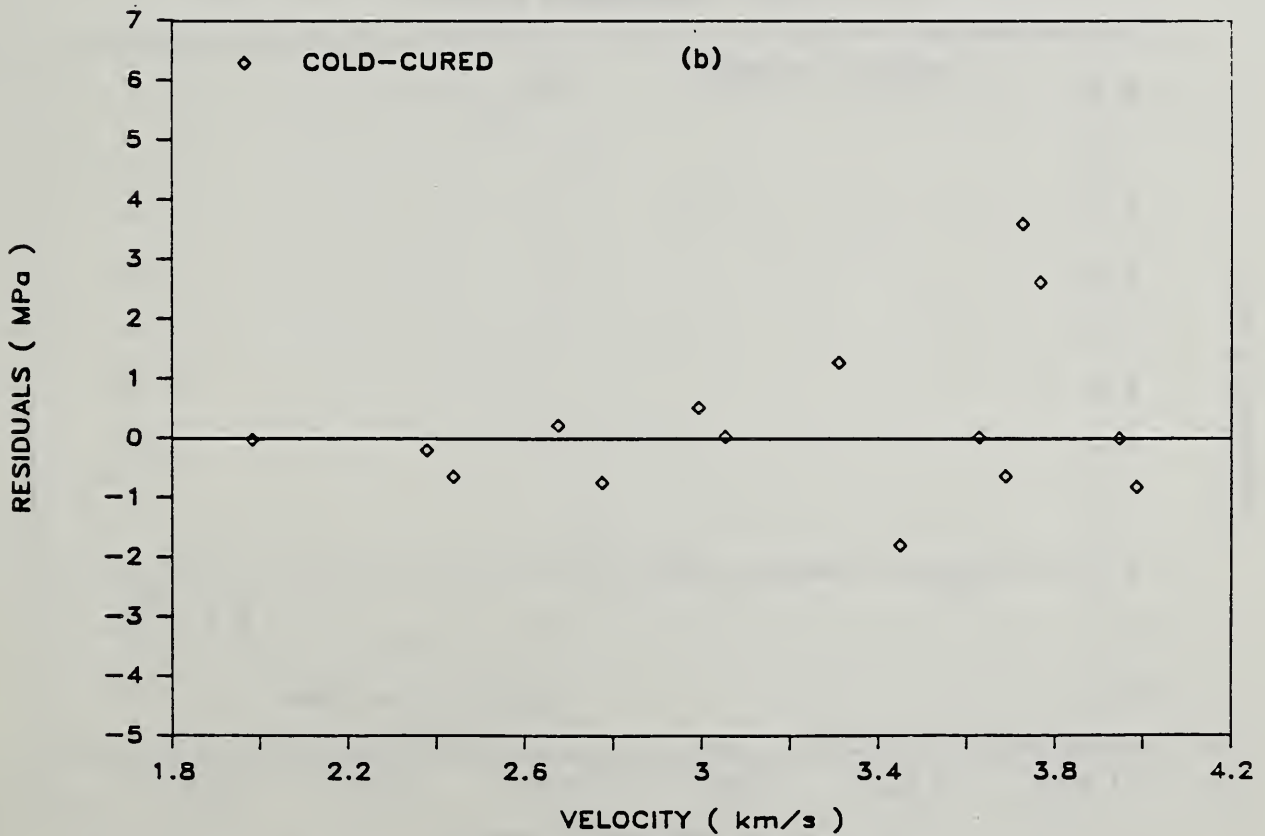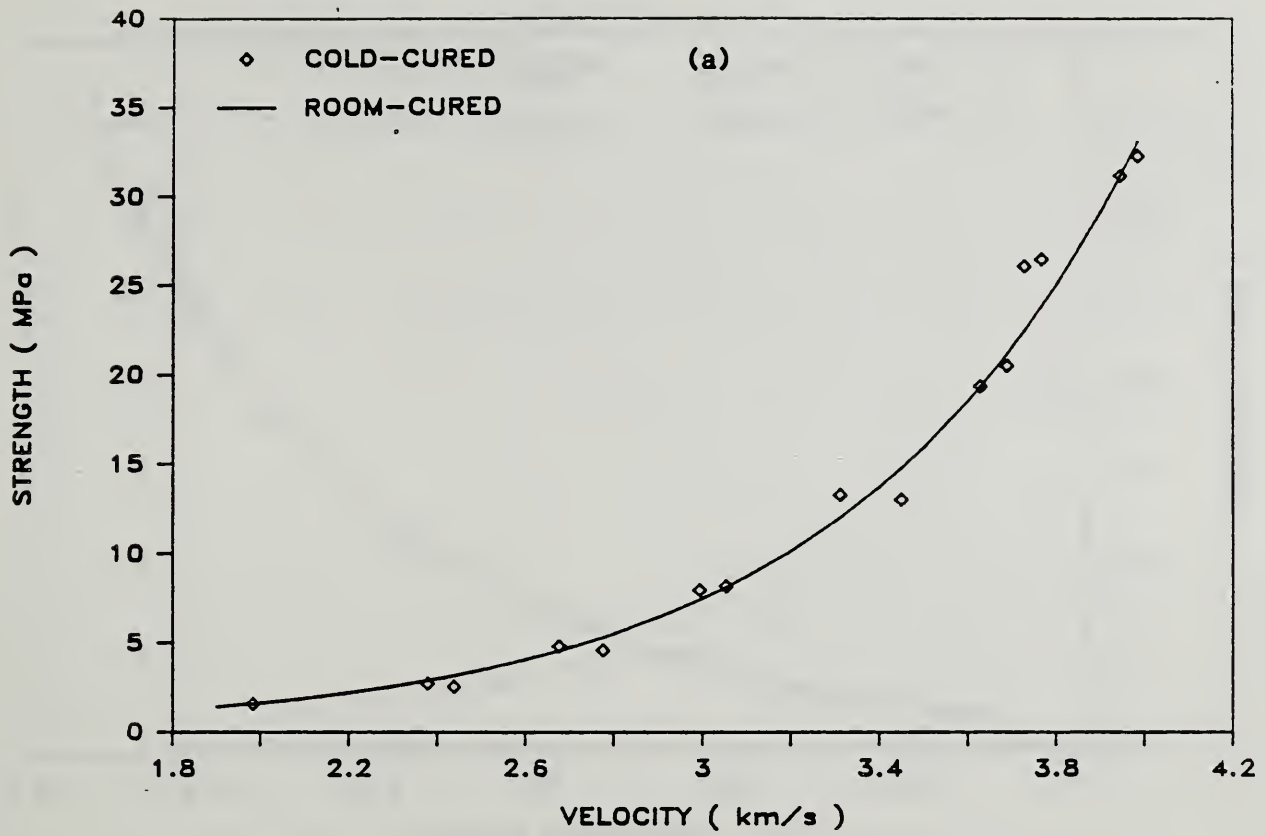
Figure 5.8   Cold-cured specimens: a) strength vs velocity; and, b) residuals in real space about best-fit of Eq. 5.7 to room-cured results

95
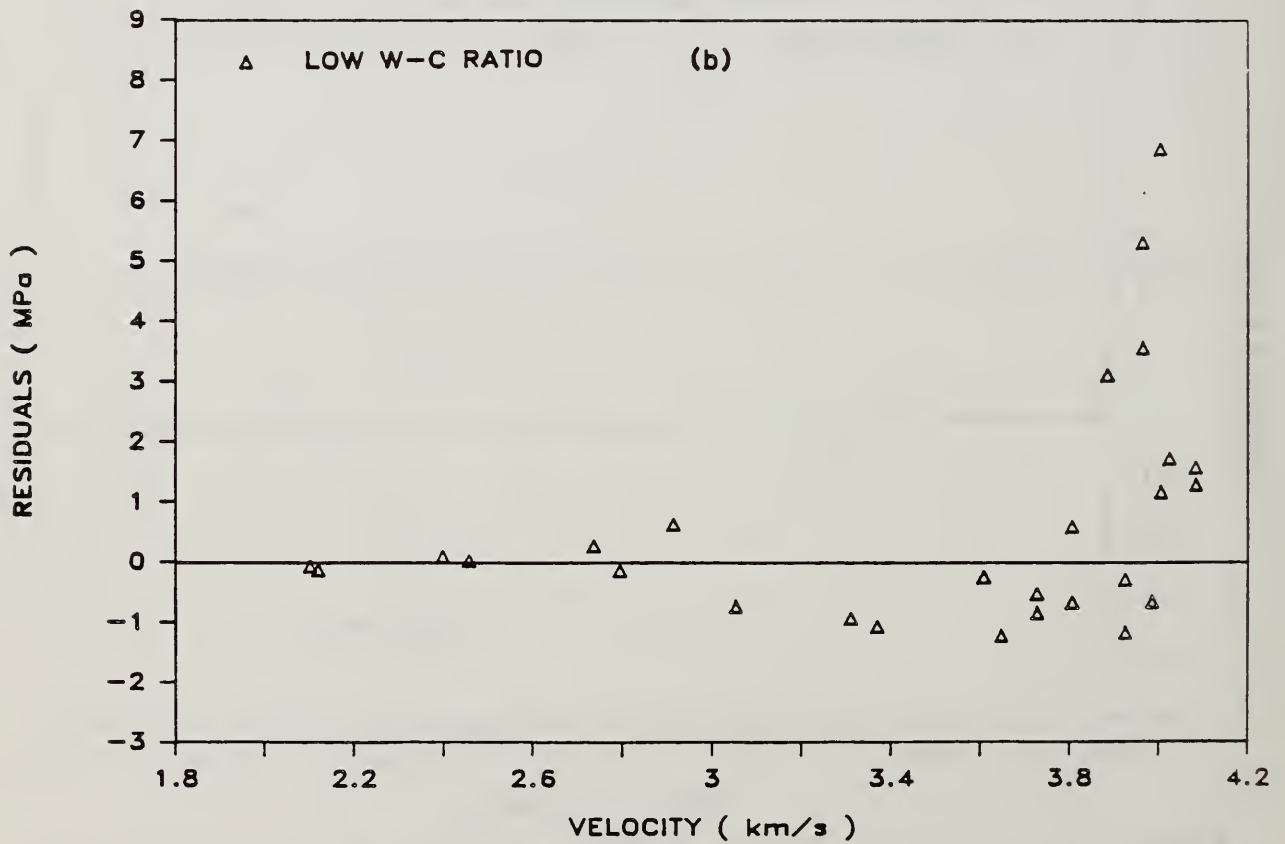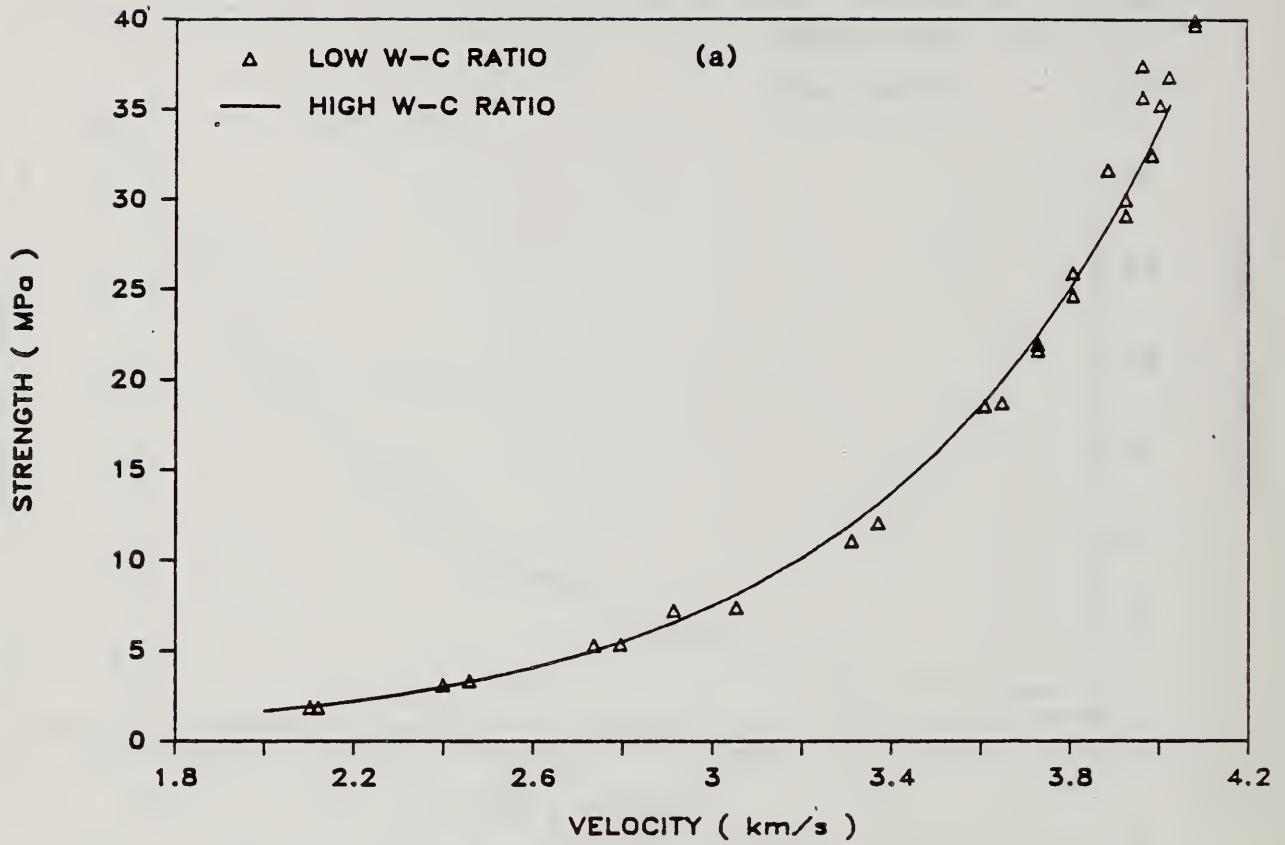
Figure 5.9 Low w-c ratio: a) strength vs velocity; and, b) residuals in real space about best-fit of Eq. 5.7 to high w-c ratio results

96
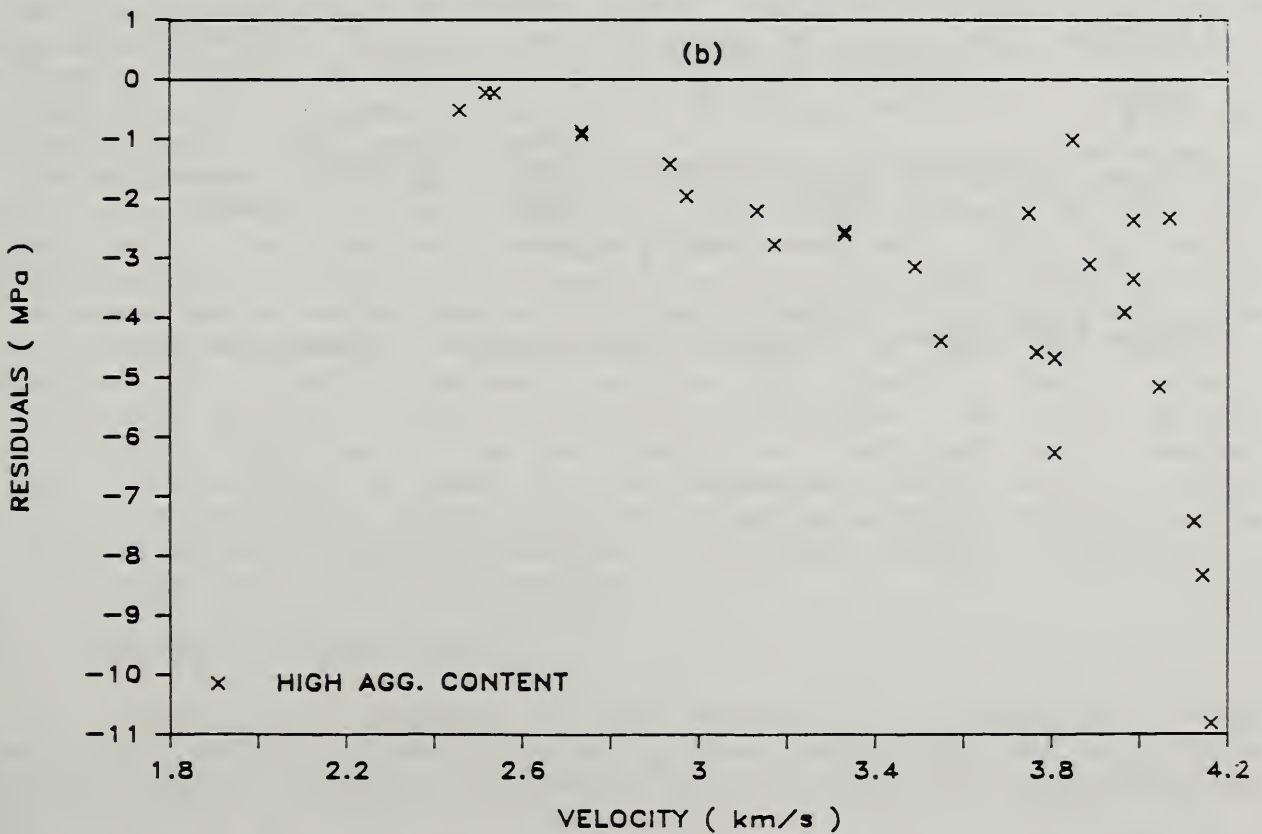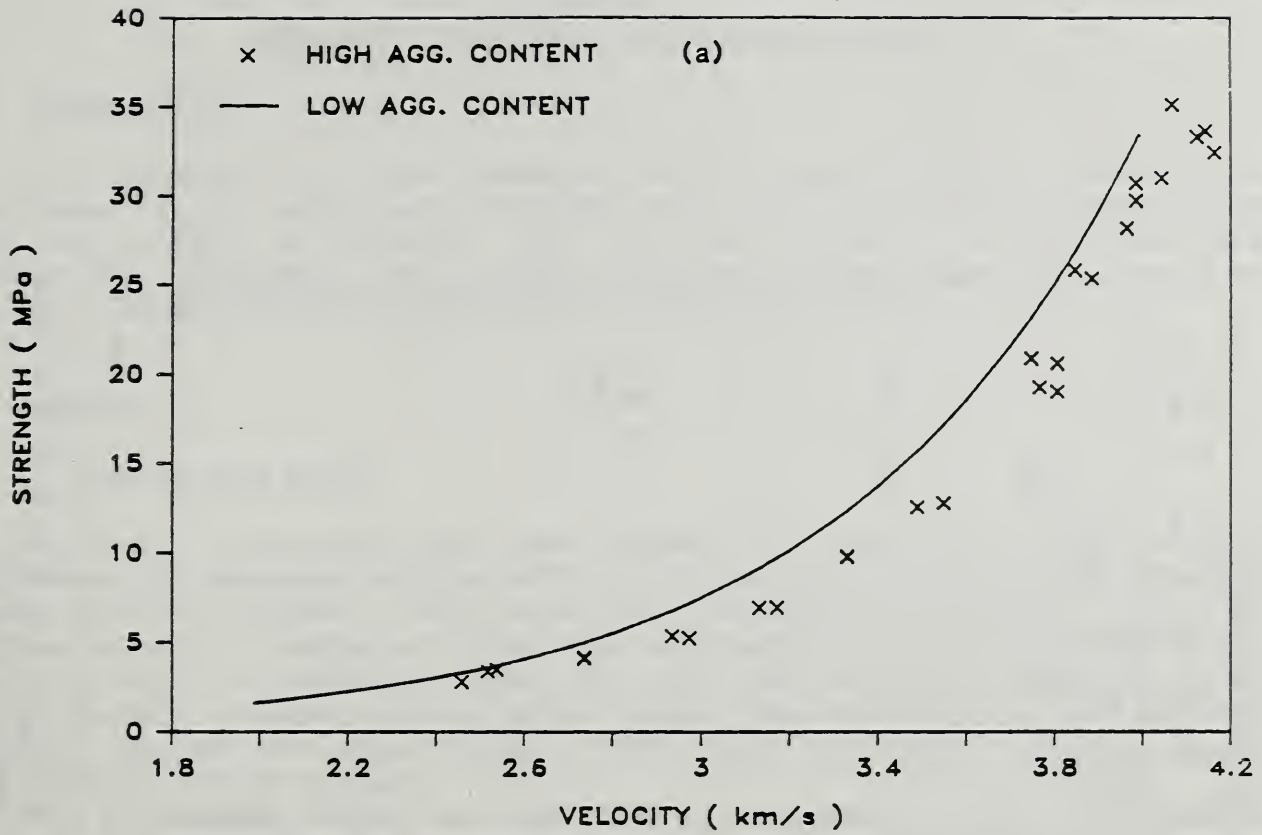
Figure 5.10 High aggregate content: a) strength vs velocity; and, b) residuals in real space about best-fit of Eq. 5.7 to low aggregate content results
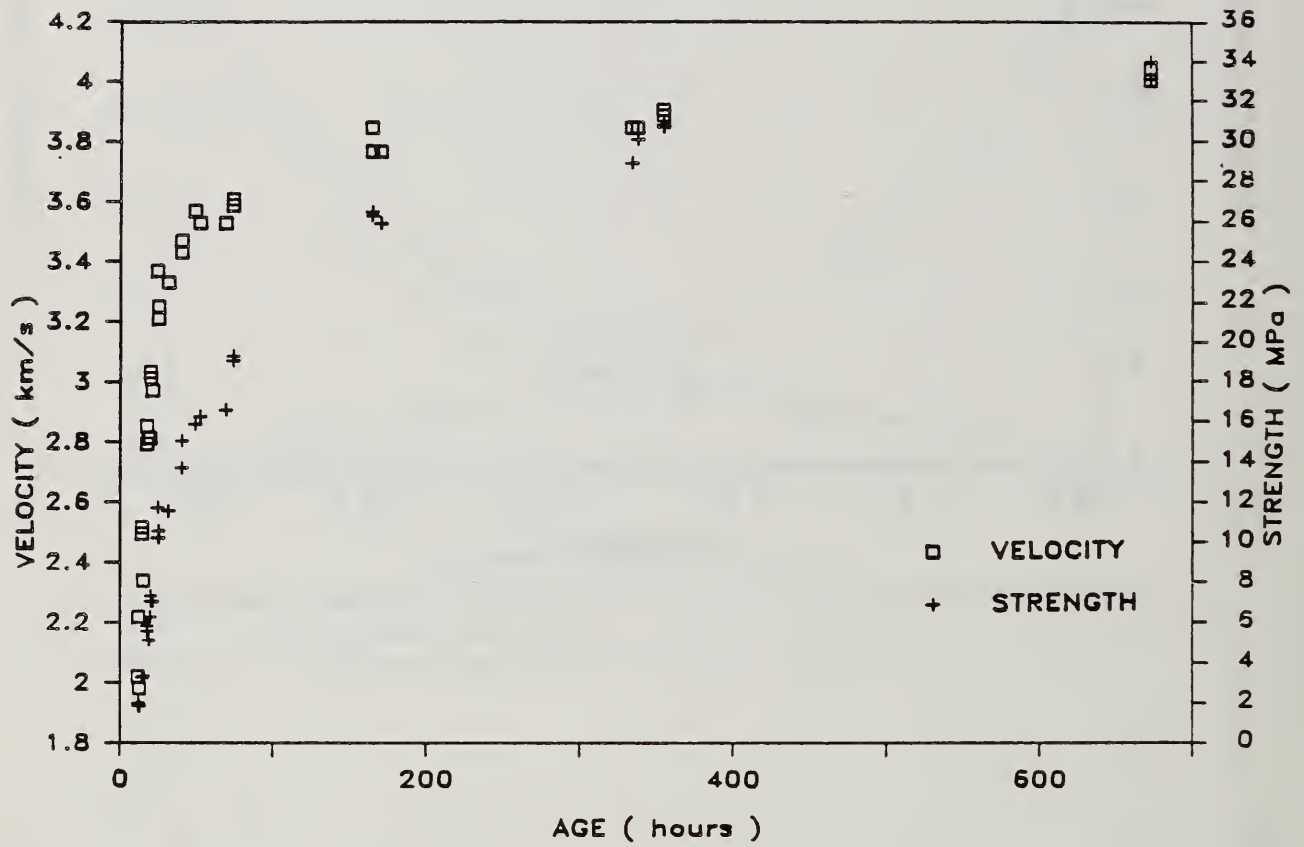
Figure 5.11 Room-cured specimens: velocity and strength vs age

CHAPTER 6
SUMMARY, CONCLUSIONS, AND FUTURE RESEARCH

6.0 INTRODUCTION

The objective of this research was to experimentally evaluate the usefulness of the impact-echo technique as a means of measuring the setting time and strength of concrete. The work was presented as the first step towards the development of reliable in-place setting time measurement and strength estimation tests based on the impact-echo method.

6.1 SUMMARY

6.1.1 Setting Time Study

A strong correlation was found between the onset of P-wave velocity development in concrete and the ASTM C 403-time of initial setting of mortar sieved from the concrete. This correlation was shown in two ways. First, for a given series, a consistent difference was found between the time the P-wave velocity began to increase rapidly and the time of initial setting in the sieved mortar. Second, for a given series, the velocity in each concrete specimen was at the same value at the time of initial setting of the corresponding sieved mortar.

The impact-echo method was also shown to be sensitve to the influences of set-controlling admixtures on setting times. Variations in the C 403-time of initial setting due to admixtures were reflected by proportional variations in the times the velocities began to increase in each specimen.

The influence of aggregate content on the P-wave velocity in concrete was described using a simple series model.

Two approaches for using the impact-echo method to define and measure the setting time of concrete were presented. The first approach is to define setting time at the onset of P-wave velocity development. This approach is appealing because setting is thus based on an actual physical change occurring in the cement paste, rather than an arbitrary strength or stiffness value that is changing continuously. Setting time defined in this way would be independent of aggregate content, because the onset of rapid velocity development depends upon changes occurring in the paste. The second approach is to define setting time at the time a specified P-wave velocity is reached. In this case setting is based on the composite elastic modulus of the concrete. By selecting a target velocity to define setting, the paste phases of different concrete mixtures could be at different stages of hydration, or have different elastic moduli at setting.

6.1.2 Compressive Strength Study

The relationship between cylinder compressive strength and P-wave velocity was studied. It was found that at lower velocities, the velocity was increasing rapidly relative to strength, and at later ages the opposite was true.

A decrease in curing temperature from 20 to 10 $^{\circ}$C did not affect the strength-velocity relationship. An increase in curing temperature from 20 to

99

35 °C did affect the relationship at higher velocities. Above a velocity of about 2800 m/s, the hot-cured specimens exhibited a lower strength at any given velocity. A significant change in w-c ratio was found to affect the strength velocity relationship only at higher velocities, and an increase in aggregate content led to a higher velocity at any given strength.

6.2 CONCLUSIONS

The work presented in this report clearly demonstrates that the impact-echo method is a feasible means of measuring the setting time and estimating the compressive strength of concrete.

Throughout this report, the results of the setting time and compressive strength studies were presented separately. However, some of the highest velocities measured in the setting time study were approximately 2000 m/s, and, as noted earlier, this is about where the lowest velocity measurements were made in the strength study. Thus the impact-echo method is a feasible means of monitoring the early-age properties of concrete from the time of initial casting to well into the region of strength gain.

Measurements can be attempted while the concrete is still fluid-like, so the setting behavior can be monitored. Although there is considerable scatter in data from the earliest attempts, the measurements soon become well-defined and the development of velocity can be easily followed. Two approaches were presented in this report for using these early measurements to define the setting time.

Velocity measurements can continue to be made as the concrete passes through the setting period and into the region of strength gain, and these later measurements can be correlated to compressive strength. Thus the same test can be used to measure the setting time and to estimate the strength of concrete.

It was seen that the velocity increases rapidly relative to the strength at lower velocities. Thus the method is a more sensitive strength estimator at lower velocities. For the concrete mixtures in this study, the sensitive region of the strength velocity relationship extended to velocities of about 3600 m/s, or compressive strengths of 19 MPa. This was seen to be about 60 % of the 28-day strength. Reliable estimates of strengths within this range could be used to improve construction safety and economy.

6.3 PRACTICAL APPLICATIONS

In its current state, the impact-echo technique described in this report can be used as a means of monitoring the setting time of concrete in the laboratory. The method can be used to evaluate admixture performance in concrete and may be incorporated into performance acceptance standards. Further, the technique may be useful as a means of non-destructively monitoring changes in the elastic modulus of concrete cylinders caused by deterioration due to freeze-thaw or alkali-aggregate reactivity.

The most important practical applications for the impact-echo method will come when it is developed into a reliable field technique for measuring the setting times and estimating the strength of concrete in-place. Impact-echo velocity measurements may have many uses in the concrete construction

industry. For example, measurements may be useful as a means of determining formwork removal times, the start and termination of curing operations, transfer of prestressing, rate of slipforming, rate of concrete placement and finishing times. Further, impact-echo velocity measurements may be useful as a means of quality control when set-controlling admixtures are being used, or as a means of detecting flash or false setting.

6.4 FUTURE RESEARCH

The experiments described in this report were performed on small cylindrical mortar and concrete specimens. Only a limited number of variables were examined. Future work should study additional parameters such as air content, other admixtures, cement types, fly ash, and different aggregates, to gain more experience with the technique.

The next step towards a reliable field technique is to perform impact-echo tests on actual structural elements such as slabs, walls, columns, and beams. Measurements on these structures may be more complicated than measurements performed on cylinders for two reasons. First, complicated modes of vibration may be excited by the impact, making determination of the P-wave velocity more difficult. Second, the energy imparted by the impact will no longer be confined to a small volume of concrete as in a cylinder. Thus different impact sources may have to be evaluated for testing actual structural elements. Both plain and reinforced concrete structures need to be examined to study the possible influence of reinforcing steel, and the possible influence of different types and stiffnesses of formwork needs to be evaluated.

It was explained in section 3.2.1.1 that the P-wave velocity is higher in large plate structures than in thin rod structures such as cylinders. The magnitude of this difference in early-age concrete, and how it changes as the concrete matures, needs to be examined. This is necessary if strength-velocity relationships established using cylinders in the laboratory are to be used to predict strength in the field.

In addition to measuring the setting time of concrete and estimating strength, the technique presented in this thesis may have applications in other related areas as well. It was also explained in section 3.2.1.1 that P-, S-, and R-waves travel with different velocities, and that the relative velocities of each can be expressed in terms of Poisson's ratio (eqs. 3.7 and 3.8). Thus, information about the relative velocities of each wave type may provide a means of measuring Poisson's ratio of concrete at a very early age. Lastly, early-age velocity measurements may be used in conjunction with the electron microscope to study the structure of hydrating cement paste.

CHAPTER 7
REFERENCES

1. American Concrete Institute, Committee 228, "In-place Methods for Determination of Strength of Concrete," in preparation.

2. American Society for Testing and Materials, 1985 Annual Book of Standards, Philadelphia, Vol. 4.01, Cement; Lime; Gypsum.

3. American Society for Testing and Materials, 1985 Annual Book of Standards, Philadelphia, Vol. 4.02, Concrete and Mineral Aggregates.

4. Arndt, W. J., Discussion of "Dynamic Testing of the Soniscope Apparatus," Proceedings, 29th Annual Meeting Highway Research Board, 1949, pp. 181-183.

5. Bethea, R. M., Duran, B. S., and Boullion, T. L., Statistical Methods for Engineers and Scientists, 2nd ed., Marcel Dekker, Inc., New York, 1985, 698 pp.

6. Bullock, R.E., and Whitehurst, E. A., "Effect of Certain Variables on Pulse Velocities Through Concrete," Highway Research Board, Bulletin 206, Effects of Concrete Characteristics on the Pulse Velocity - A Symposium, 1959, pp. 37-41.

7. Bye, G. C., Portland Cement Composition, Production and Properties, Pergamon Press, Oxford, 1983, pp. 94-98.

8. Byfors, J., Plain Concrete at Early Ages, Swedish Cement and Concrete Research Institute, Stockholm, 1980, 464 pp.

9. Byfors, J., "Pulse Velocity Measurements for Indication of the Compressive Strength at Early Ages," International Conference on Concrete of Early Ages, Vol. 1, April, 1982, pp. 117-122.

10. Carino, N.J., and Sansalone, M., "Pulse-Echo Method for Flaw Detection in Concrete," National Bureau of Standards Technical Note 1199, July, 1984, 33 pp.

11. Carino, N. J., "The Maturity Method: Theory and Application," Cement, Concrete, and Aggregates, Vol. 6, No. 2, 1984, pp. 61-73.

12. Casson, R. B. J., and Domone, P. I. J., "Ultrasonic Monitoring of the Early Age Properties of Concrete," International Conference on Concrete of Early Ages, Vol. 1, April, 1982, pp. 129-135.

13. Cheesman, W. J., "Dynamic Testing of Concrete with the Soniscope Apparatus," Proceedings, 29th Annual Meeting Highway Research Board, 1949, pp. 176-181.

14. Cheesman, W. J., Discussion of "Use of the Soniscope for Measuring the Setting Time of Concrete," Proceedings of the American Society for Testing Materials, Vol. 51, 1951, pp. 1176-1180.

15. Cheesman, W. J., "Soniscope Studies of Concrete During the Setting Period," Hydro Research News, Vol. 3, No. 3, July-Sept., 1951, pp. 8-11.

16. Elvery, R. H., and Ibrahim, L. A. M., "Ultrasonic Assessment of Concrete Strengths at Early Ages," Magazine of Concrete Research, Vol. 28, No. 97, Dec., 1976, pp. 181-190.

17. Goldsmith, W., Impact: The Theory and Physical Behavior of Colliding Solids, Edward Arnold Press, Ltd., 1965, pp. 24-50.

18. Hutchinson, J.R., "Vibrations of Solid Cylinders," Journal of Applied Mechanics, ASME, Vol. 47, Dec., 1980, pp. 901-907.

19. Jones, R., "The Non-Destructive Testing of Concrete," Magazine of Concrete Research, Vol.2, 1949, pp. 67-76.

20. Jones, R., "A Non-Destructive Method of Testing Concrete During Hardening," Concrete & Constructional Engineering, April, 1949, pp. 127-129.

21. Jones, R., "Testing of Concrete by Ultrasonic-Pulse Technique," Proceedings, 32nd Annual Meeting, Highway Research Board, 1953, pp. 258-275.

22. Knudsen, T., "On Particle Size Distribution in Cement Hydration," Proceedings of the 7th International Congress on the Chemistry of Cement, Vol. 2, Paris, 1980, pp. 170-175.

23. Kolsky, H., Stress Waves in Solids, Dover Publications, Inc., New York, 1963.

24. Krautkramer, J., and Krautkramer, H., Ultrasonic Testing of Materials, 3rd ed., Springer-Verlag, Heidelberg, 1983, 667 pp.

25. McMahon, G. W., "Experimental Study of the Vibrations of Solid, Isotropic, Elastic Cylinders," The Journal of the Acoustical Society of America, Vol. 36, No. 1, Jan., 1964, pp. 85-92.

26. Pauw, A., "Static Modulus of Elasticity of Concrete as Affected by Density," Journal of the American Concrete Institute, Vol. 32, No. 6, Dec., 1960, pp. 679-687.

27. Philleo, R. E., "Comparison of Results of Three Methods for Determining Young's Modulus of Elasticity of Concrete," Journal of the American Concrete Institute, Vol. 26, No. 5, Jan., 1955, pp. 461-472.

28. Powers, T. C., "Structure and Physical Properties of Hardened Portland Cement Paste," Journal of the American Ceramic Society, Vol. 1, No. 1, Jan., 1958, pp 1-6.

29. Proctor, T. M., Jr., "Some Details on the NBS Conical Transducer," Journal of Acoustical Emission, Vol. 1, No. 3, pp. 173-178.

30. Richart, F. E., Jr., Woods, R. D., and Hall, J. R., Jr., Vibrations of Soils and Foundations, Prentice-Hall, Inc., Englewood Cliffs, 1970, Chapter 5.

31. Sansalone, M., "Flaw Detection in Concrete Using Transient Stress Waves," PhD Thesis, Cornell University, June 1986, 220 pp.

32. Stearns, S. D., Digital Signal Analysis, Hayden Book Co., Inc., Rochelle Park, 1975, 280 pp.

33. Sturrup, V.R., Vecchio, F. J., and Caratin, H., "Pulse Velocity as a Measure of Concrete Compressive Strength," Non-Destructive Testing, ACI SP-82, pp. 201-227.

34. Timoshenko, S., and Goodier, J., Theory of Elasticity, 3rd ed., Mcgraw-Hill Book Co., New York, 1970, 567 pp.

35. Tuthill, L. H., and Cordon, W. A., "Properties and Uses of Initially Retarded Concrete," Journal of the American Concrete Institute, Vol. 27, No. 3, Nov., 1955, pp. 273-286.

36. Verbeck, G. J., and Helmuth, R. H.,"Structures and Physical Properties of Cement Paste," Proceedings of the Fifth International Symposium on the Chemistry of Cement, Part 3, Vol. 3, Tokyo, 1968, pp. 1-32.

37. Viktorov, I.A., Rayleigh and Lamb Waves, Trans. W.P. Mason. Plenum Press, New York, 1967, 154 pp.

38. Whitehurst, E. A., "Use of the Soniscope for Measuring the Setting Time of Concrete," Proceedings of the American Society for Testing Materials, Vol. 51, 1951, pp. 1166-1176.

APPENDIX A — Setting Time Data

Elapsed Time (hours)	Frequency (kHz)	Cp (km/s)
CL1 CONCRETE		
2.12	0.684	0.219
2.42	0.488	0.156
2.67	0.733	0.235
2.92	0.684	0.219
3.17	0.879	0.281
3.42	1.074	0.344
3.67	1.270	0.406
3.87	1.367	0.437
4.17	1.660	0.531
4.38	1.856	0.594
4.58	2.051	0.656
4.95	2.441	0.781
5.45	3.027	0.969
6.05	3.809	1.219
6.83	4.688	1.500
7.33	5.225	1.672
7.83	5.762	1.844
8.33	6.152	1.969
9.33	7.031	2.250
CL1 SIEVED MORTAR		
2.05	0.684	0.219
2.33	0.586	0.188
2.58	0.830	0.266
2.83	1.074	0.344
3.08	0.488	0.156
3.33	0.586	0.188
3.58	0.684	0.219
3.75	0.879	0.281
4.00	0.977	0.313
4.25	1.074	0.344
4.50	1.172	0.375
4.75	1.367	0.437
5.12	1.563	0.500
5.72	2.051	0.656
5.92	2.344	0.750
6.75	3.223	1.031
7.25	3.711	1.188
7.75	4.199	1.344
8.25	4.688	1.500
9.25	5.811	1.860
CL2 CONCRETE		
1.58	0.684	0.219
1.78	0.684	0.219
1.92	0.684	0.219
2.10	0.684	0.219
2.25	1.026	0.328
2.42	1.074	0.344
2.55	0.830	0.266
2.73	1.026	0.328
2.88	0.781	0.250
3.00	0.879	0.281
3.13	0.977	0.313
3.27	1.123	0.359
3.33	1.172	0.375
3.45	1.270	0.406
3.67	1.367	0.437
3.87	1.465	0.469
4.07	1.660	0.531

Elapsed Time (hours)	Frequency (kHz)	Cp (km/s)
4.28	1.856	0.594
4.60	2.148	0.687
5.00	2.588	0.828
5.50	3.125	1.000
6.00	3.711	1.188
6.50	4.297	1.375
7.00	4.883	1.563
7.50	5.322	1.703
8.00	5.811	1.860
9.00	6.641	2.125
CL2 SIEVED MORTAR		
2.02	0.684	0.219
2.17	0.879	0.281
2.33	0.684	0.219
2.50	0.781	0.250
2.67	1.026	0.328
2.82	0.879	0.281
2.95	0.488	0.156
3.07	0.586	0.188
3.07	1.074	0.344
3.22	0.586	0.188
3.38	0.684	0.219
3.38	0.879	0.281
3.75	0.781	0.250
3.93	0.879	0.281
4.17	1.172	0.375
4.33	1.270	0.406
4.45	1.270	0.406
4.53	1.367	0.437
4.70	1.465	0.469
4.92	1.660	0.531
5.17	1.856	0.594
5.42	2.051	0.656
5.92	2.539	0.812
6.42	3.027	0.969
6.92	3.516	1.125
7.42	4.053	1.297
7.92	4.590	1.469
8.92	5.664	1.812
CL3 CONCRETE		
1.60	0.586	0.188
1.75	0.830	0.266
2.00	0.879	0.281
2.20	0.977	0.313
2.45	1.074	0.344
2.70	0.879	0.281
2.70	0.586	0.188
2.87	0.977	0.313
3.03	1.172	0.375
3.20	1.270	0.406
3.38	1.367	0.437
3.57	1.563	0.500
3.73	1.660	0.531
3.90	1.856	0.594
4.23	2.246	0.719
4.58	2.637	0.844
4.92	3.027	0.969
5.42	3.711	1.188
6.08	4.444	1.422

Elapsed Time (hours)	Frequency (kHz)	Cp (km/s)
6.42	4.834	1.547
6.92	5.371	1.719
7.42	5.859	1.875
7.92	6.299	2.016
9.02	7.178	2.297
CL3 SIEVED MORTAR		
2.08	0.684	0.219
2.28	0.586	0.188
2.52	1.026	0.328
2.78	0.684	0.219
2.95	0.586	0.188
3.12	0.879	0.281
3.12	0.684	0.219
3.28	0.781	0.250
3.28	0.977	0.313
3.47	0.879	0.281
3.47	1.367	0.437
3.63	0.977	0.313
3.82	1.074	0.344
3.97	1.172	0.375
4.07	1.270	0.406
4.17	1.367	0.437
4.33	1.465	0.469
4.50	1.660	0.531
4.75	1.856	0.594
5.00	2.148	0.687
5.50	2.637	0.844
6.17	3.418	1.094
6.50	3.809	1.219
7.00	4.395	1.406
7.50	4.932	1.578
8.00	5.469	1.750
9.08	6.836	2.188
CH1 CONCRETE		
2.10	0.586	0.188
3.17	0.928	0.297
3.50	0.879	0.281
3.75	0.977	0.313
4.00	0.781	0.250
4.25	0.977	0.313
4.42	1.074	0.344
4.58	1.074	0.344
4.83	1.172	0.375
5.10	1.367	0.437
5.33	1.465	0.469
5.58	1.612	0.516
5.83	1.758	0.563
6.18	2.051	0.656
6.58	2.246	0.719
7.17	2.637	0.844
7.67	2.979	0.953
8.17	3.320	1.062
8.67	3.613	1.156
CH1 SIEVED MORTAR		
2.25	0.684	0.219
3.25	0.879	0.281
3.58	0.879	0.281
3.83	0.781	0.250

Elapsed Time (hours)	Frequency (kHz)	Cp (km/s)	Elapsed Time (hours)	Frequency (kHz)	Cp (km/s)	Elapsed Time (hours)	Frequency (kHz)	Cp (km/s)
4.08	0.684	0.219	6.00	1.367	0.437	5.00	0.879	0.281
4.30	0.781	0.250	6.50	1.563	0.500	5.25	1.074	0.344
4.47	0.781	0.250	7.00	1.758	0.563	5.42	1.172	0.375
4.67	0.879	0.281	7.50	2.051	0.656	5.58	1.319	0.422
4.92	0.977	0.313	8.00	2.246	0.719	5.77	1.465	0.469
5.17	1.172	0.375	8.78	2.637	0.844	5.95	1.563	0.500
5.42	1.270	0.406				6.20	1.758	0.563
5.67	1.367	0.437	**CH3 CONCRETE**			6.38	1.905	0.610
5.92	1.563	0.500	2.70	0.586	0.188	6.65	2.197	0.703
6.25	1.660	0.531	2.95	0.586	0.188	7.02	2.539	0.812
6.67	1.953	0.625	3.17	0.586	0.188	7.30	2.881	0.922
7.25	2.246	0.719	3.33	0.684	0.219	7.63	3.272	1.047
7.75	2.490	0.797	3.55	0.781	0.250	8.00	3.711	1.188
8.25	2.734	0.875	3.75	0.781	0.250	8.50	4.395	1.406
8.75	3.027	0.969	3.92	0.879	0.281	9.00	4.981	1.594
			4.08	1.026	0.328	9.50	5.518	1.766
CH2 CONCRETE			4.25	0.879	0.281	10.00	6.055	1.938
2.50	0.488	0.156	4.43	0.879	0.281	11.00	6.984	2.235
2.75	0.684	0.219	4.58	0.977	0.313	12.55	8.203	2.625
3.00	0.586	0.188	4.77	1.074	0.344			
3.25	0.684	0.219	5.05	1.172	0.375	**CR1 SIEVED MORTAR**		
3.42	0.684	0.219	5.30	1.270	0.406	4.07	0.830	0.266
3.58	0.781	0.250	5.58	1.465	0.469	4.35	0.879	0.281
3.75	0.879	0.281	5.92	1.612	0.516	4.62	0.977	0.313
3.92	0.586	0.188	6.42	1.953	0.625	4.87	0.586	0.188
4.08	0.684	0.219	6.92	2.246	0.719	5.07	0.684	0.219
4.25	0.733	0.235	7.42	2.539	0.812	5.33	0.781	0.250
4.42	0.781	0.250	7.92	2.832	0.906	5.48	0.781	0.250
4.58	0.879	0.281	8.58	3.223	1.031	5.65	0.879	0.281
4.75	0.977	0.313	9.63	3.858	1.235	5.83	0.977	0.313
4.92	1.026	0.328				6.10	1.074	0.344
5.08	1.074	0.344	**CH3 SIEVED MORTAR**			6.30	1.172	0.375
5.33	1.270	0.406	2.80	0.781	0.250	6.48	1.367	0.437
5.58	1.367	0.437	3.02	0.684	0.219	6.73	1.465	0.469
5.85	1.465	0.469	3.23	0.781	0.250	7.08	1.758	0.563
6.08	1.612	0.516	3.42	0.488	0.156	7.38	2.002	0.641
6.58	1.905	0.610	3.62	0.488	0.156	7.72	2.295	0.734
7.08	2.246	0.719	3.82	0.586	0.188	8.10	2.637	0.844
7.58	2.539	0.812	3.98	0.586	0.188	8.58	3.174	1.016
8.08	2.832	0.906	4.15	0.684	0.219	9.08	3.711	1.188
8.90	3.223	1.031	4.32	0.684	0.219	9.58	4.199	1.344
			4.48	0.684	0.219	10.10	4.785	1.531
CH2 SIEVED MORTAR			4.65	0.781	0.250	11.08	5.859	1.875
2.58	0.879	0.281	4.83	0.879	0.281	12.65	7.764	2.484
2.83	0.684	0.219	5.12	1.026	0.328			
3.08	0.781	0.250	5.37	1.172	0.375	**CR2 CONCRETE**		
3.33	0.879	0.281	5.67	1.270	0.406	3.58	0.586	0.188
3.50	0.928	0.297	6.00	1.465	0.469	3.85	0.830	0.266
3.67	0.684	0.219	6.50	1.660	0.531	4.12	0.488	0.156
3.83	0.781	0.250	7.00	1.953	0.625	4.37	0.586	0.188
4.00	0.781	0.250	7.50	2.246	0.719	4.62	0.781	0.250
4.17	0.879	0.281	8.00	2.441	0.781	4.80	0.879	0.281
4.33	0.977	0.313	8.68	2.783	0.891	5.03	1.172	0.375
4.50	0.781	0.250	9.70	3.320	1.062	5.32	1.465	0.469
4.67	0.879	0.281				5.55	1.563	0.500
4.83	0.928	0.297	**CR1 CONCRETE**			5.92	1.953	0.625
5.00	0.977	0.313	4.00	0.781	0.250	6.25	2.295	0.734
5.17	0.977	0.313	4.25	0.781	0.250	6.63	2.734	0.875
5.25	1.074	0.344	4.50	0.488	0.156	7.17	3.418	1.094
5.50	1.172	0.375	4.50	1.172	0.375	7.67	4.102	1.313
5.75	1.270	0.406	4.75	0.684	0.219	8.17	4.785	1.531

Elapsed Time (hours)	Frequency (kHz)	Cp (km/s)	Elapsed Time (hours)	Frequency (kHz)	Cp (km/s)	Elapsed Time (hours)	Frequency (kHz)	Cp (km/s)
9.28	5.762	1.844	7.42	2.148	0.687	CA2 SIEVED MORTAR		
10.25	6.738	2.156	7.83	2.539	0.812	1.93	0.586	0.188
			8.33	2.930	0.938	2.27	0.684	0.219
CR2 SIEVED MORTAR			9.40	4.004	1.281	2.27	0.879	0.281
3.67	0.586	0.188	10.03	4.590	1.469	2.50	0.684	0.219
3.92	0.830	0.266	12.87	7.617	2.437	2.72	0.586	0.188
4.18	1.172	0.375				3.23	1.074	0.344
4.43	0.684	0.219	CA1 CONCRETE			3.48	1.270	0.406
4.68	0.684	0.219	1.63	0.586	0.188	3.73	1.563	0.500
5.10	0.781	0.250	1.97	0.733	0.235	3.98	1.758	0.563
5.38	0.879	0.281	2.37	0.977	0.313	4.23	2.051	0.656
5.62	0.977	0.313	2.57	1.172	0.375	4.75	2.734	0.875
5.85	1.074	0.344	2.73	1.367	0.437	5.23	3.418	1.094
6.10	1.270	0.406	2.98	1.758	0.563	5.73	4.004	1.281
6.33	1.367	0.437	3.23	2.148	0.687	6.23	4.593	1.470
6.58	1.563	0.500	3.50	2.637	0.844	6.75	5.273	1.687
6.92	1.856	0.594	3.75	3.125	1.000	7.72	6.250	2.000
7.25	2.148	0.687	4.15	3.906	1.250	8.75	7.324	2.344
7.75	2.637	0.844	4.65	4.834	1.547			
8.25	3.125	1.000	5.05	5.469	1.750	CA3 CONCRETE		
9.35	4.297	1.375	6.10	6.836	2.188	1.62	0.684	0.219
10.33	5.420	1.734	7.98	8.496	2.719	1.95	0.586	0.188
						1.95	0.781	0.250
CR3 CONCRETE			CA1 SIEVED MORTAR			2.25	0.586	0.188
3.50	0.684	0.219	1.72	0.586	0.188	2.50	0.879	0.281
3.75	0.586	0.188	2.05	0.781	0.250	2.75	1.172	0.375
4.00	0.684	0.219	2.28	0.879	0.281	3.00	1.465	0.469
4.25	0.684	0.219	2.42	0.586	0.188	3.25	1.758	0.563
4.43	0.781	0.250	2.63	0.781	0.250	3.50	2.148	0.687
4.58	0.879	0.281	2.82	0.879	0.281	3.75	2.588	0.828
4.78	0.830	0.266	3.05	1.172	0.375	4.00	3.027	0.969
5.00	0.928	0.297	3.30	1.416	0.453	4.25	3.418	1.094
5.25	1.172	0.375	3.57	1.758	0.563	4.75	4.297	1.375
5.50	1.270	0.406	3.83	2.051	0.656	5.25	5.030	1.610
5.75	1.465	0.469	4.22	2.637	0.844	6.25	6.201	1.984
6.00	1.660	0.531	4.73	3.418	1.094	7.27	7.227	2.313
6.25	1.905	0.610	5.15	4.004	1.281	8.27	8.008	2.563
6.58	2.246	0.719	6.12	5.322	1.703			
6.92	2.638	0.844	8.00	7.617	2.437	CA3 SIEVED MORTAR		
7.33	3.125	1.000				1.70	0.488	0.156
7.75	3.613	1.156	CA2 CONCRETE			1.70	0.684	0.219
8.25	4.151	1.328	1.53	0.586	0.188	2.03	0.586	0.188
9.32	5.371	1.719	1.87	0.586	0.188	2.55	0.684	0.219
10.02	5.957	1.906	2.18	0.586	0.188	2.82	0.684	0.219
12.78	8.203	2.625	2.42	0.781	0.250	3.07	0.781	0.250
			2.67	1.026	0.328	3.07	0.977	0.313
CR3 SIEVED MORTAR			2.92	1.270	0.406	3.13	0.977	0.313
3.60	0.781	0.250	3.17	1.612	0.516	3.33	1.172	0.375
3.83	0.684	0.219	3.42	1.953	0.625	3.57	1.465	0.469
4.08	0.879	0.281	3.67	2.344	0.750	3.83	1.660	0.531
4.32	0.879	0.281	3.92	2.734	0.875	4.07	1.953	0.625
4.52	0.879	0.281	4.17	3.125	1.000	4.32	2.246	0.719
4.67	0.586	0.188	4.67	3.955	1.266	4.85	2.930	0.938
5.07	0.684	0.219	5.17	4.688	1.500	5.32	3.613	1.156
5.32	0.879	0.281	5.67	5.371	1.719	6.30	4.834	1.547
5.57	0.977	0.313	6.17	5.957	1.906	7.33	6.104	1.953
5.92	1.074	0.344	6.67	6.494	2.078	8.28	7.373	2.359
6.08	1.172	0.375	7.67	7.324	2.344			
6.32	1.319	0.422	8.68	8.057	2.578			
6.63	1.514	0.484						
7.00	1.758	0.563						

Elapsed Time (hours)	Penetration Resistance (psi)	Elapsed Time (hours)	Penetration Resistance (psi)	Elapsed Time (hours)	Penetration Resistance (psi)
CL1		CH2		6.82	1220
3.00	36	3.50	30	7.08	1840
3.50	76	4.02	64	7.52	3120
3.83	192	4.47	98	7.77	4200
4.08	220	4.97	144		
4.18	480	5.47	264	CR3	
4.35	390	5.93	460	5.02	42
4.42	590	6.22	680	5.47	96
4.67	600	6.45	780	6.00	248
4.83	1240	7.17	1720	6.55	580
5.17	1540	7.66	2440	6.75	780
5.50	3360	8.17	3200	7.03	1440
5.75	4400	8.62	3680	7.50	2480
		8.80	4000	7.87	4440
CL2					
3.50	88	CH3		CA1	
3.77	140	3.50	36	2.32	42
4.00	244	4.00	66	2.58	76
4.25	350	4.50	122	2.93	248
4.50	620	5.00	208	3.10	360
4.75	820	5.25	328	3.37	650
5.08	1580	5.53	420	3.62	1200
5.58	3680	5.83	520	3.87	2240
5.67	4600	6.17	920	4.17	2640
		7.08	2160	4.37	5000
CL3		7.52	2920		
3.25	110	7.75	2920	CA2	
3.50	180	7.83	3080	2.38	22
3.75	364	8.05	4480	2.75	78
4.00	690			3.02	152
4.25	880	CR1		3.28	268
4.58	1740	4.98	30	3.53	460
5.03	4320	5.75	106	3.78	670
		6.27	264	4.05	1280
CH1		6.50	490	4.33	2120
3.93	88	6.77	620	4.58	3400
4.22	88	6.98	1000	4.80	4160
4.50	172	7.25	1400		
4.75	180	7.75	2720	CA3	
5.00	300	8.05	4080	2.38	30
5.25	330			2.78	130
5.50	480	CR2		3.03	148
5.75	590	5.12	64	3.28	316
6.08	1040	5.50	134	3.52	520
6.52	1760	6.00	316	3.77	690
6.83	2200	6.42	510	4.02	1200
7.20	3160	6.78	1210	4.35	3080
7.50	3400			4.67	4000
7.75	3200				
7.78	4000				

APPENDIX B – Strength Data

Batch	Frequency (kHz)	Cp (km/s)	fc (MPa)	Batch	Frequency (kHz)	Cp (km/s)	fc (MPa)
ROOM-CURED SPECIMENS							
1	4.981	2.022	1.87	3	8.496	3.449	13.30
1	5.469	2.220	2.03	3	8.155	3.311	13.28
1	6.152	2.498	3.29	3	8.936	3.628	19.37
1	6.201	2.518	3.29	3	9.082	3.687	20.52
1	6.885	2.795	5.87	3	9.180	3.727	26.06
1	7.031	2.855	5.60	3	9.277	3.766	26.45
1	7.471	3.033	7.35	3	9.815	3.985	32.26
1	7.422	3.013	7.08	3	9.717	3.945	31.17
1	7.910	3.211	10.26				
1	8.008	3.251	10.59	**LOW W-C RATIO SPECIMENS**			
1	8.545	3.469	15.09	5	5.176	2.101	1.87
1	8.447	3.429	13.72	5	5.225	2.121	1.87
1	8.789	3.568	15.91	5	6.885	2.795	5.38
1	8.691	3.529	16.30	5	6.738	2.736	5.32
1	9.277	3.766	25.90	5	8.155	3.311	11.08
2	5.762	2.339	3.35	5	8.301	3.370	12.07
2	6.934	2.815	5.16	5	9.180	3.727	21.62
2	8.300	3.370	11.74	5	9.180	3.727	21.95
2	9.473	3.846	30.12	5	9.668	3.925	29.96
3	4.883	1.982	1.87	5	9.668	3.925	29.08
3	6.930	2.814	6.31	5	9.766	3.965	35.66
3	7.324	2.974	7.08	5	9.863	4.004	35.23
3	8.691	3.529	16.63	5	10.059	4.084	39.94
3	9.473	3.846	28.92	5	9.863	4.004	40.93
4	8.203	3.330	11.58	6	6.055	2.458	3.35
4	8.838	3.588	19.09	6	5.908	2.399	3.13
4	8.887	3.608	19.31	6	7.520	3.053	7.41
4	9.473	3.846	26.50	6	7.178	2.914	7.24
4	9.277	3.766	26.28	6	8.984	3.648	18.71
4	9.619	3.905	30.84	6	8.887	3.608	18.55
4	9.570	3.885	30.73	6	9.375	3.806	25.90
4	9.863	4.004	33.14	6	9.375	3.806	24.64
4	9.961	4.044	34.02	6	9.815	3.985	32.43
				6	9.570	3.885	31.60
HOT-CURED SPECIMENS				6	9.766	3.965	37.42
2	4.932	2.002	1.70	6	9.912	4.024	36.82
2	5.127	2.082	1.98	6	10.059	4.084	39.67
2	5.518	2.240	2.19				
2	5.908	2.399	3.35	**HIGH AGGREGATE CONTENT SPECIMENS**			
2	6.543	2.656	4.06	7	6.250	2.538	3.51
2	6.738	2.736	4.55	7	6.201	2.518	3.40
2	7.324	2.974	6.36	7	7.324	2.974	5.27
2	7.031	2.855	6.09	7	7.227	2.934	5.38
2	7.910	3.211	9.05	7	8.203	3.330	9.77
2	8.057	3.271	9.27	7	8.203	3.330	9.82
2	8.008	3.251	10.97	7	9.375	3.806	19.04
2	8.643	3.509	15.03	7	9.277	3.766	19.26
2	9.082	3.687	19.48	7	9.570	3.885	25.40
2	9.668	3.925	26.01	7	9.473	3.846	25.84
4	8.496	3.449	12.78	7	9.815	3.985	30.73
4	8.398	3.410	12.78	7	9.961	4.044	31.00
4	9.033	3.667	17.23	7	10.018	4.067	35.12
4	8.984	3.648	17.72	7	10.156	4.123	33.31
4	9.180	3.727	22.72	8	6.055	2.458	2.80
4	9.277	3.766	22.83	8	6.738	2.736	4.17
4	9.522	3.866	25.84	8	6.738	2.736	4.12
4	9.473	3.846	25.84	8	7.813	3.172	6.97
4	9.619	3.905	27.32	8	7.715	3.132	6.97
4	9.668	3.925	28.81	8	8.740	3.548	12.78
				8	8.594	3.489	12.56
COLD-CURED SPECIMENS				8	9.375	3.806	20.63
3	4.883	1.982	1.59	8	9.229	3.747	20.90
3	5.859	2.379	2.74	8	9.766	3.965	28.20
3	6.006	2.438	2.58	8	9.815	3.985	29.74
3	6.836	2.775	4.61	8	10.205	4.143	33.
3	6.592	2.676	4.83	8	10.254	4.163	32.
3	7.520	3.053	8.18				
3	7.373	2.993	7.96				

U.S. DEPT. OF COMM. BIBLIOGRAPHIC DATA SHEET (See instructions)	1. PUBLICATION OR REPORT NO. NBSIR 87-3575	2. Performing Organ. Report No.	3. Publication Date JULY 1987

4. TITLE AND SUBTITLE

Measurement of the Setting Time and Strength of Concrete
by the Impact-Echo Method

5. AUTHOR(S)

Stephen P. Pessiki and Nicholas J. Carino

6. PERFORMING ORGANIZATION (If joint or other than NBS, see instructions) NATIONAL BUREAU OF STANDARDS U.S. DEPARTMENT OF COMMERCE GAITHERSBURG, MD 20899	7. Contract/Grant No. 8. Type of Report & Period Covered

9. SPONSORING ORGANIZATION NAME AND COMPLETE ADDRESS (Street, City, State, ZIP)

National Bureau of Standards
Department of Commerce
Gaithersburg, MD 20899

10. SUPPLEMENTARY NOTES

☐ Document describes a computer program; SF-185, FIPS Software Summary, is attached.

11. ABSTRACT (A 200-word or less factual summary of most significant information. If document includes a significant bibliography or literature survey, mention it here)

Tests were performed to evaluate the feasibility of using the impact-echo method to determine setting time and monitor strength development of concrete. In the impact-echo method, the test object is subjected to point impact and the surface displacement adjacent to the impact point is monitored. From the measured displacement waveform and the thickness of the object, the P-wave velocity is determined. Changes in the P-wave velocity with time reveal information about the development of mechanical properties. Setting time tests were made on concrete mixtures of two water-cement ratios and with and without set-controlling admixtures. A strong correlation was found between the time of initial setting of mortars sieved from the concrete, as determined by penetration resistance (ASTM C 403), and the time when the P-wave velocity began to increase. Two approaches for using the impact-echo method to define the setting time of concrete are presented. Tests were performed to examine the relationship between P-wave velocity, as determined by the impact-echo method, and the compressive strength of concrete. At early ages (up to about 3 days at standard temperature), the relationship was independent of curing temperature and water cement ratio. It is concluded that the impact-echo method is a promising technique for nondestructively monitoring the development of mechanical properties in concrete from initial setting to ages of several days.

12. KEY WORDS (Six to twelve entries; alphabetical order; capitalize only proper names; and separate key words by semicolons)

concrete; compressive strength; early-age; impact-echo method; nondestructive testing; mortar; setting time; wave propagation.

13. AVAILABILITY	14. NO. OF PRINTED PAGES
☒ Unlimited ☐ For Official Distribution. Do Not Release to NTIS ☐ Order From Superintendent of Documents, U.S. Government Printing Office, Washington, D.C. 20402.	121
☒ Order From National Technical Information Service (NTIS), Springfield, VA. 22161	15. Price $18.95

NBSIR 87-3576

The ABC's of Standards-Related Activities in the United States

Maureen A. Breitenberg

U.S. DEPARTMENT OF COMMERCE
National Bureau of Standards
Standards Code and Information
Office of Product Standards Policy
Gaithersburg, MD 20899

May 1987

U.S. DEPARTMENT OF COMMERCE

NATIONAL BUREAU OF STANDARDS

NBSIR 87-3576

The ABC'S OF STANDARDS-RELATED ACTIVITIES IN THE UNITED STATES

Maureen A. Breitenberg

Foreword

The Standards Code and Information Program in the NBS Office of Product Standards
Policy from time to time develops and publishes standards-related documents as a
service to producers and users of standards and certification systems, both in
the government and in the private sector. This report has been designed as an
introduction to standardization, certification, and laboratory accreditation for
those not fully familiar with these fields and their interrelationships. We hope
that this material will be informative and will also serve to stimulate wider and
more profitable applications of standardization. In addition, the interested
reader may wish to take further advantage of other available publications and
services provided by this office, some of which are described in the appendix.

                    Donald R. Mackay
                    Manager, Standards Code and Information
                    Office of Product Standards Policy

Table of Contents

Acknowledgements

Abstract

This report provides an introduction to voluntary standardization, product certification and laboratory accreditation for a reader who is not fully familiar with these topics. It highlights some of the more important aspects of these fields; furnishes the reader with both historical and current information on these topics; describes the importance and impact of the development and use of standards; and serves as background for using available documents and services.

Key Words: Certification; inspection; laboratory accreditation; standardization; standards; testing

Introduction

> "The inch is a standard of measurement.
> Money is a standard of exchange.
> Words are standards of communication.
> Traffic lights are safety standards.
> Octane numbers of gasoline are quality standards.
> 'No more than 1% shrinkage' is a performance standard." 1/

As the above indicates, standardization has a major impact on our lives, yet most people know little about the process or about the standards themselves. They know that camera film marked ISO 100 is likely to give good results in a camera with the film speed set at 100, but few understand that the ISO 100 marking on the package means that the film conforms to a standard established by the International Organization for Standardization (ISO), an international organization that writes standards. Few people question that three-holed notebook paper will align with the three rings in most notebooks, yet such confidence would not be possible without standards. While driving we are on the lookout for hexagonal, not round or square-shaped stop signs, just as we know that inverted triangles indicate where traffic should yield. These are just a few of the thousands of standards that impact on our lives.

Because standards have such an impact, it is important to have some familiarity with what they are and how they are developed and used. This paper is designed to be an introduction to some of the more significant aspects of standards development, product certification, and laboratory accreditation. It will also discuss some of the benefits and problems associated with these processes. The interested reader is encouraged to increase his knowledge of the field by taking advantage of other available publications and services described in the appendix.

Background

A standard was defined by the National Standards Policy Advisory Committee as:

> "A prescribed set of rules, conditions, or requirements concerning definitions of terms; classification of components; specification of materials, performance, or operations; delineation of procedures; or measurement of quantity and quality in describing materials, products, systems, services, or practices." 2/

Though often unrecognized, standards can help to assure health and safety and to increase the quality of life. Standards are vital tools of industry and commerce. They often provide the basis for buyer-seller transactions, hence they have tremendous impact on companies and nations, and even on the economic fabric of the world market.

In the United States alone, approximately 30,000 current voluntary standards have been developed by more than 400 organizations. These do not include a much greater number of procurement specifications (developed and used by Federal, State, and local procurement authorities), as well as mandatory codes, rules and regulations containing standards developed and adopted at Federal,

1

State, and local levels. In addition, numerous foreign national, regional and international organizations produce standards of interest and importance to U.S. manufacturers and exporters.

There are numerous international organizations that produce standards. The International Organization for Standardization (ISO) probably produces the largest number of International Standards, having issued approximately 6,000 standards. ISO's work is carried out through some 2,300 technical bodies in which more than 20,000 experts from all over the world participate annually in the development of ISO standards.

The international General Agreement on Tariffs and Trade (GATT) has as one of its major components the Agreement on Technical Barriers to Trade (usually referred to as the Standards Code). The framers of the Standards Code recognized that standards and standards-related activities can seriously hinder the free flow of goods in international commerce. The Code established, for the first time, some requirements for the procedures by which standards are developed, adopted, and used and for the systems which determine conformity with such standards.

The Trade Agreements Act of 1979 implemented the Standards Code in the United States. Federal agencies are required under the Act to:

"-Not engage in standards activities that are prepared, adopted or applied to create, or have the effect of creating, unnecessary obstacles to the foreign trade of the United States;

-Ensure that imported products are treated no less favorably than domestic products;

-Use international standards, if appropriate, as a base for developing new standards;

-Develop standards based on performance rather than design criteria, if appropriate; and

- Allow foreign suppliers access to their certification systems on the same basis as access is permitted to domestic suppliers." 3/

Historical Notes on Standardization

The history of standardization is both fascinating and demonstrative of the scope and variety of such activities. A predecessor of the American National Standards Institute (ANSI) noted that one of the first known attempts at standardization in the Western world occurred in 1120. King Henry I of England ordered that the ell, the ancient yard, should be the exact length of his forearm, and that it should be used as the standard unit of length in his kingdom. 4/

That history also notes that, in 1689, the Boston city fathers recognized the need for standardization when they passed a law making it a civic crime to manufacture bricks in any size other than 9x4x4. The city had just been destroyed by fire, and the city fathers decided that standards would assure rebuilding in the most economic and fastest way possible. 5/

Eli Whitney is sometimes referred to as "the Father of Standardization" in the area of interchangeability, having originated and implemented the concept of mass production in the United States in 1780. He was awarded a contract to produce 10,000 muskets by then Vice-President Thomas Jefferson. Though standardized parts had been successfully used in other parts of the world, Whitney brought the concept to this country when he divided the manufacturing process into individual steps and put different groups to work on each step of the process. All parts of the same type were copied from a model musket and were made to be interchangeable. Subsequently, when he appeared before Congress with a collection of assorted parts and proceeded to assemble ten working muskets by selecting the required parts at random, Congress was convinced of the benefits of mass production made possible by standardization. 6/

Standards are known to have existed as early as 7000 B.C. when cylindrical stones were used as units of weight in Egypt. However, the great blaze in downtown Baltimore in February 1904 and other, similar catastrophes provided tragic and undeniable evidence of the importance of standards. While the fire in Baltimore burned, fire engines from as far away as New York rushed to the scene only to discover that their hoses would not fit Baltimore hydrants. Those "alien" fire engines were useless! The inferno burned for more than thirty hours, destroying 1526 buildings covering more than seventy city blocks. All electric light, telephone, telegraph, and power facilities were also razed. 7/ In contrast, 23 years later, help from 20 neighboring towns saved Fall River, Massachusetts from destruction since hydrants and hose couplings had been standardized in these communities. 8/

As late as 1927, a color-blind motorist had as good (or as bad) a chance as anyone else when trying to interpret traffic signals. Purple, orange, green, blue, yellow, and red lights greeted him as he drove from state to state. In some states, green meant "Go," in others "Stop." Red, not yellow, lights meant caution in New York City. In 1927 a national code for colors was established through the work of the American Association of State Highway Officials, the National Bureau of Standards and the National Safety Council. 9/ Imagine the chaos that would occur during rush hour in any major U.S. city today if newcomers and tourists did not know what traffic signals meant!

Probably the most significant standard ever developed in the United States, however, was the railroads' standard track gage. This standard, now used in Great Britain, the U.S., Canada and much of continental Europe, enables railroad rolling stock to cross the country. 10/

It was the Second World War, however, that brought the urgency of extending domestic standardization to the international level. Allied supplies and facilities were severely strained because of the incompatibility of tools, replacement parts, and equipment. The War highlighted the need for standards aimed at reducing inventories and increasing compatibility.

Types of Standards

Standards may be classified in numerous ways, some of which are described here. ISO Draft Guide 2 differentiates eight types based on purpose. 11/ A basic standard has a broad ranging effect in a particular field, such as a standard for metal which affects a range of products from cars down to screws. Terminology

standards define words permitting representatives of an industry or parties to a transaction to use a common, clearly understood language. Testing standards define the test methods to be used to assess the performance or other characteristics of a product. Product standards establish qualities or requirements for a product (or related group of products) to assure that it will serve its purpose effectively. Process standards specify requirements to be met by a process, such as an assembly line's operation, in order to function effectively. Service standards, such as for servicing or repairing a car, establish requirements to be met in order to achieve the designated purpose effectively. Interface standards, such as the point of connection between a telephone and a computer terminal, are concerned with the compatibility of products. The last type provides a listing of data requirements for a product or service for which values need to be obtained.

Standards may also be classified by the intended user group. These classifications range from company standards, meant for use by a single industrial organization, to international standards. International standards are developed and promulgated by international governmental and non-governmental organizations, such as the North Atlantic Treaty Organization's (NATO's) Military Agency for Standardization (governmental) and the ISO (non-governmental). International standards may be voluntary or mandatory in nature. A harmonized standard, on the other hand, can be either an attempt by a country to make its standard compatible with an international, regional or other standard or it can be an agreement by two or more nations on the content and application of a standard, the latter of which tends to be mandatory. Harmonized standards may also be identical in content to other standards. There are still other classifications such as industry standards, developed and promulgated by an industry for materials and products related to that industry; and military or government standards, such as those designed to be used by the Department of Defense or by the Federal Government. These should not be confused with Federal and Military Specifications, used by the Federal Supply Services in the General Services Administration and by the Department of Defense respectively. Specifications are a set of conditions and requirements that provide a detailed description of a procedure, process, material, product, or service for use primarily in procurement and manufacturing. 12/

Another distinction among standards is the manner in which they specify requirements. Those standards that describe how a product is supposed to function are called performance standards. In contrast, design standards define characteristics or how the product is to be built. For example, a performance standard for water pipe might set requirements for the pressure per square inch that a pipe must withstand, along with a test method to determine if a specimen meets the requirement. On the other hand, the specification that a pipe be made of a given gage of copper would characterize a design standard. The distinction, however, between these two types of standards is not always clear cut. It is possible to include two different requirements within the same standard, one of which is stated in terms of performance and the other in terms of design. For example, in a standard for copper pipe, requirements for the pipe can be specified in terms of its performance (being able to withstand a given amount of pressure), but the same standard may require that the pipe's flanges or couplings meet specific design requirements.

Design standards may be appropriate, as in testing methods where the need for comparability may outweigh other considerations. In general, however, performance standards, though usually more difficult to write and enforce, tend to be less restrictive than design standards, and more likely to encourage innovation. For that reason, signatories to the Standards Code are encouraged to write technical regulations and standards in terms of performance, rather than design, characteristics.

Still another classification scheme distinguishes between voluntary standards, which by themselves impose no obligations regarding use, and mandatory standards. A mandatory standard is generally published as part of a code, rule or regulation by a regulatory government body and imposes an obligation on specified parties to conform to it. However, the distinction between these two categories may be lost when voluntary consensus standards are referenced in government regulations, effectively making them "mandatory" standards. Voluntary consensus standards may also become "quasi-mandatory" due to conditions in the marketplace. For example, the health care industry is sensitive to the need to have available the safest products to ensure patient safety and to protect manufacturers, vendors and health care providers against lawsuits. Informed buyers of health care products will frequently insist that products meet all appropriate voluntary consensus standards. If they wish to compete effectively, manufacturers of such products are obliged to conform to such standards.

It is clear, then, that standards cover a broad range of types and serve a wide variety of purposes.

Private Standards Organizations in the U.S.

The need for safe and economical structures, such as roads and bridges, led to the founding of the International Association for Testing and Materials in 1896. Its mission was to develop standardized test methods. Two years later, the American Section of this organization was formed and became the forerunner of the American Society for Testing and Materials, now known as ASTM. Since becoming an independent organization in 1902, ASTM has continued to grow and now produces the largest number of non-governmental, voluntary standards in the United States.

In 1918, ASTM was one of five private, technical society originators of the American Engineering Standards Committee, later to be known as the American Standards Association (ASA), and subsequently as the American National Standards Institute (ANSI). ANSI today serves as the coordinator of voluntary standards activities in the United States and as the agency that approves standards as American National Standards. ANSI is also the coordinator and manager of U.S. participation in the work of two non-governmental, international standards organizations, ISO and the International Electrotechnical Commission (IEC).

Another of the major private standards organizations, the American Society of Mechanical Engineering (ASME), was founded in 1880 and first issued the ASME Boiler Code in 1914. Today that Code is mandatory not only in the United States, but in many other countries throughout the world. In 1952, a forerunner of ANSI stated: "Probably no other single standard in America has done more for national safety than the ASME Boiler Code." 13/ The ASME Boiler Code may be the most widely used voluntary standard in the world.

The founding of the Society of Automotive Engineers (SAE) in 1910 led to the pioneering efforts of the American automotive industry to achieve substantial inter-company technical standardization. Most drivers now take these efforts for granted when choosing motor oils by SAE designations (such as 10W-40) without being aware of the full significance and background of the detailed standards development process.

Most consumers also take for granted the familiar UL mark on a range of products from electrical appliances to fire extinguishers. The Underwriters Laboratories (UL), founded in 1894, is not only a major standards writer, but also operates non-profit testing laboratories whose mission is to investigate products and materials with respect to hazards that might affect life or property and to list those items which appear to pose no significant hazards.

The work of other major standards organizations, although equally vital, tends to be less well known outside the standards community. For example, the National Fire Protection Association (NFPA) has for more than three quarters of a century produced the National Electrical Code, used in building construction, and many other standards affecting our safety from fires and other hazards. We accept without conscious thought the safety of aircraft unaware of the standards produced by the Aerospace Industries Association of America (AIA) for guidance and control systems and many other items. The Association of American Railroads' (AAR) standards similarly affect our railroads. Even the quality and size of paper is standardized through the work of the Technical Association of the Pulp and Paper Industry (TAPPI).

In all, more than 400 organizations develop voluntary standards of many different types for a broad range of services, products, and tests. Some organizations, such as ANSI and ASTM, are primarily concerned with standards. Others are trade associations interested in all matters affecting their members. The Electronic Industries Association, for example, has been a standards developer in the areas of electrical and electronic products and components since 1926.

Many professional and technical organizations are also standards developers. The Institute of Electrical and Electronics Engineers (IEEE), which traces back to 1884, maintains more than 500 standards with 800 more under development. IEEE is responsible for the National Electrical Safety Code, widely used by governments and regulatory agencies for electric supply and communications installations. Still other standards developers are primarily research and testing bodies, such as the National Sanitation Foundation (NSF), which develops standards for products from a health and sanitation perspective. The Factory Mutual Research Corporation (FM), another standards developer, is a "product listing" type of organization, as is UL.

In addition, building code organizations, such as the Building Officials and Code Administrators International (BOCA), the International Conference of Building Officials (ICBO), and the Southern Building Code Congress International (SBCCI), are involved in standards development. These organizations are composed of building, construction, zoning, and inspection officials; they have developed model building codes adopted by thousands of State and local governments.

The broad range of organizations participating in standards development reflects the impact standards have on a vast spectrum of interests and disciplines.

Standards Development Procedures

Two of the most widely used procedures for assuring consensus in the development of standards are the committee and the canvass methods.

Committee Method. Committee standards are subject to wide review and consideration by all interested parties. The requirements of this process vary among organizations. In some organizations, consensus may be defined as an agreement of at least 51% of the participants. Other organizations may also include requirements for due process, appeals procedures, the mandatory consideration of negative votes or comments, and for "committee balance." Balance is achieved when all parties having an interest in the outcome of a standard have an opportunity to participate and where no single interest can dominate the outcome. Standards organizations differ widely in the emphasis placed on each of these requirements. Organizations which emphasize all four factors, in addition to the achievement of substantial agreement among participants, produce standards that are more likely to be adopted and used.

Canvass method The "canvass" method is frequently used by an organization that has prepared a standard under its own internal procedures. To gain greater stature and acceptance of the drafted standard, the developer may then submit it to balloting by a set of organizations representing a variety of interests, such as manufacturers, consumers, government, and others. Any objections or comments from organizations on the "canvass list" must be addressed and satisfactorily resolved. Changes in a proposed standard, as well as any unresolved objections and the developing organization's rationale for its response, must be resubmitted to the "canvass list." It is crucial that all interested groups be included on the list. Two problems sometimes arise: the response level may be low and consumers and others on the "canvass list" may have difficulty commenting on a standard, because they did not participate in the initial drafting and may not understand the reasons for or implications of particular provisions.

Benefits and Problems of Standardization

On the whole, the benefits of standardization far outweigh the difficulties and potential for abuse. Standards promote understanding between buyer and seller and make possible mutually beneficial commercial transactions. Product attributes cannot always be evaluated by individual purchasers by inspection or even from prior experience. However, a product's conformance to accepted standards readily provides an efficient method of conveying complex information on the product's suitability. Architects use standards in a shorthand manner when drafting plans for buildings; purchasing agents can also use standards as an easy way of communicating their needs to potential suppliers. In a host of situations standards are or may be used to replace large quantities of complex information.

Standards underlie mass production methods and processes. They promote more effective and organized social interaction, such as the example of the standardized colors for traffic lights and many other widely accepted conventions. Standards are essential in efforts to improve product safety and a to clean up the environment. Standardized and interchangeable parts can reduce inventory requirements and facilitate product repairs. They can also promote

7

fair competition by facilitating the comparison of prices of standardized commodities.

In general, standards permit society to make more effective use of its resources and allow more effective communication among all parties to particular activities, transactions, or processes. Indeed, standards are crucial to every form of scientific and industrial process. Without standards, the quality of life would be significantly reduced.

No system, particularly one as complex and diverse as the U.S. voluntary standards system, is without problems. In a recent case of great significance, the United States Supreme Court on May 17, 1982, rendered its decision in favor of Hydrolevel, a manufacturer of low-water fuel cutoff devices, in the case of American Society of Mechanical Engineers (ASME) v. Hydrolevel. It found ASME liable for conspiring to restrain trade since two subcommittee officers, serving as volunteers but acting in the name of ASME, issued a misinterpretation of a standard and produced an adverse effect on the competitiveness of the plaintiff. Similarly, the Federal Trade Commission held hearings on standards and certification and uncovered "substantiated complaints of individual standards and certification actions that have, in fact, unreasonably restrained trade or deceived or otherwise injured consumers." 14/

In part, problems result from the sometimes substantial costs of participation in standards development, making it difficult (if not impossible) for small firms and non-industry representatives to be active in the process. The standards themselves may cause problems if highly technical in nature. It is frequently difficult, if not impossible, to get qualified consumer representatives to participate actively. This seriously complicates the attempts to achieve balanced representation by all interests concerned.

Other problems may occur when a standard undergoes review and revision. Unless the original writers of the standard participate in its revision, the reviewers may not be able to understand how the document was prepared, what was eliminated from consideration, and the reasons or assumptions underlying decisions and the resultant provisions. Problems can also occur in the application of specific provisions if the intent behind them is unclear. Rationale statements, which sometimes accompany a standard, are specifically designed to define the purpose and scope of the standard, to explain the criteria used in developing its requirements and to provide all other relevant information at the disposal of the developers. However, the use of rationale statements is not yet extensive. 15/

Certification

"The first time a craftsman claimed that his product met a commonly accepted standard, the most basic form of certification came into being." 16/ Today product certification schemes range from the simple to the complex. The hallmarking of precious metals was an early form of certification. Many early attempts, most unsuccessful, were also made to certify weights and measures to provide a uniform basis for the exchange of goods. Now there are over 100 private organizations and over 60 Federal programs in the United States which certify products ranging from electrical cords to kitchen cabinets. In addition, many certification programs are operated at the state and local level. Consumers see evidence of the extensiveness of certification when they note the Underwriters' Laboratory (UL) certification mark on many products ranging from coffee potsto fire extinguishers; the U. S. Department of Agriculture

8

(USDA) mark on meats, poultry and other agricultural products; and the International Wool Secretariat's Woolmark and Woolmarkblend on wool or wood blend textile goods. These are only a few of the many certification programs which are conducted in the United States.

Product certification is intended to confirm that a particular product conforms to one or more specified standards, thus providing the user with explicit or implicit information about the characteristics and/or performance of the product. Certification is a method for increasing a buyer's confidence in a product and for furnishing product information.

In the U.S., if a manufacturer or supplier attests to the fact that his product meets one or more standards, the process is called self-certification. This process is also known as a manufacturer's declaration in other parts of the world. The manufacturer's capability, integrity, and reputation determine the degree of confidence that can be placed in self-certification.

Third-party certification is the term applied to the process by which an organization, independent of either the manufacturer or supplier, assesses the product's conformance to one or more standards. A manufacturer's overall quality control program may also be examined as part of the certification process. A quality control program is a series of activities designed to assure that quality is being maintained at all phases of production. There are hundreds of third-party certification programs in the United States operated by Federal, State, and local governments and by many private organizations. Third-party certification programs differ greatly from one another, and the degree of confidence in the resultant certification depends on the program's type and comprehensiveness.

The methods used in third-party certification programs can be classified as follows:

o Type-testing/Initial Inspection - This assures that the manufacturer's design specifications can produce a product that conforms to a particular standard. Products from a production run are not inspected or tested, and there is no information on whether products from a production run also consistently meet the specification.

o Audit-Testing - In this procedure, test samples are selected at random from the marketplace. Extensive testing is usually required to provide adequate assurance that products meet the desired standard.

o Surveillance of the Manufacturing Process - Assessment of a manufacturer's production and control processes can, at relatively low cost, provide assurance that the manufacturer's quality control procedures are adequate.

o Field Investigations - Alleged failures of products under use conditions are investigated to determine the cause of failure and to suggest appropriate corrective action.

9

o <u>Batch-testing</u> - A sample of products is selected from a production batch and tested for conformance to the standard. If the sampling procedure and the sample size are adequate, batch-testing makes it likely that all products in that batch conform to the standard. It does not, however, ensure that a specific untested product in the batch will meet the standard nor does it furnish information on the quality of products produced in earlier or subsequent batches. Batch testing is used in many certification programs for building products, such as those for energy conservation.

o <u>100 Percent Testing</u> - Each individual product is tested to determine if it meets the designated standard. If the testing procedures are adequate, the procedure provides the highest possible level of assurance that the product conforms to a particular standard. It is also usually the most expensive method and can be applied only where the test has no adverse effect on the product. <u>17</u>/

Many programs apply two or more of these methods in their certification process. The choice of methods depends on the needs of both the buyer and the seller and the nature of the product. The methods chosen can greatly affect both the cost of the program and the level of confidence that can be ascribed to it. ANSI and ISO have each developed criteria to evaluate certification programs. ANSI has also developed a program to accredit certification schemes which meet its criteria, but only two programs have been accredited to date.

Laboratory Accreditation

Laboratory accreditation is a process for evaluating testing facilities and designating those laboratories judged competent to perform specific tests using standard test methods, where available. The National Voluntary Laboratory Accreditation Program (NVLAP) in the National Bureau of Standards, Department of Commerce, and the American Association for Laboratory Accreditation (AALA) are the two largest accreditation agencies in the United States. There are many other Federal, State and local government programs, as well as many private sector laboratory accreditation programs. Some of these include: the Department of Defense's (DOD) programs for accrediting laboratories which test products which will later be sold to DOD; the State of Massachusetts programs for accrediting concrete testing laboratories and laboratories which test solid fuel burning appliances; and the National Kitchen Cabinet Association's (NKCA) accreditation program for laboratories which test kitchen cabinets as part of the NKCA's certification program. <u>18</u>/

It should be emphasized that laboratory accreditation assesses the <u>capability</u> of a laboratory to conduct testing, generally using standard test methods. The accreditation process should not be confused with certification nor with the validation of a certification, which is "an action by a third party to assure that the producer (or certifier) is adhering to the requirements of a given certification program." <u>19</u>/ Laboratory accreditation neither reviews nor assesses products, nor does it check the tests conducted on specific products or product batches. In addition, laboratories may be accredited to conduct tests (such as EPA's accreditation program for laboratories testing drinking water) in fields where no certification program exists.

Laboratory accreditation, however, can affect the quality of certification programs by requiring evidence that a certifying laboratory has competent personnel, adequate equipment, and sufficient knowledge of the testing

10

procedures for which accreditation is sought. Also, laboratory accreditation is assuming increased importance in trade. As countries seek acceptance of their test data by trading partners, they must assure that the data comes from competent laboratories. Laboratory accreditation can help to provide that assurance.

Summary

Standardization, product certification, and laboratory accreditation are closely linked. In many developing countries, all three activities are conducted by the same organization. Certification programs are communication tools designed to reduce the cost of exchanging information between buyer and seller. The quality of the information conveyed depends on both the competence of the testing laboratory selected and the adequacy and appropriateness of the standards against which the product is to be evaluated. Certification can result in widespread consumer deception if performance characteristics or test methods contained in the standard are insufficient to assure adequate product performance or if the testing laboratory is incompetent or has biases which affect the reporting of test results.

Considering the number of standards in existence and the variety of fields covered by private sector standards development and certification organizations, the United States has one of the most developed and complex standardization and certification systems in the world. Furthermore, the number of Federal, State, and local government standardization and certification activities and the large volume of standards, regulations, and procurement specifications that these agencies have developed, result in an immense impact of standardization and related activities on almost every aspect of life in the United States. Not only are considerable resources invested in this country in such activities every year, but purchasers (consumers) depend on standards and certification to ensure that products purchased are safe and perform satisfactorily. Recognition of the impact of standards and certification on trade, as evidenced by the Standards Code, is also increasing. Society depends on standardization and related activities for its existence.

APPENDIX

Information Available from
The Standards Code and Information (SCI) Program
National Bureau of Standards
Administration Building, Room A629
Gaithersburg, MD 20899
(301) 975-4040

o <u>Directory of International and Regional Organizations Conducting
Standards-Related Activities</u> (NBS SP 649)
   Directory contains information on 272 international and regional organizations
which conduct standardization, certification, laboratory accreditation, or other
standards-related activities. Volume describes their work in these areas, as
well as the scope of each organization, national affiliations of members, U.S.
participants, restrictions on membership, and the availability of any standards
in English.

o <u>Standards Activities of Organizations in the United States</u> (NBS SP 681)
   The directory summarizes the standardization activities of more than 750
organizations in the United States, including Federal and State agencies and
approximately 420 private sector groups that develop standards. It also contains
listings of State procurement offices, sources of standards documents and
information, a subject index and related listings that cover acronyms and
initials, defunct bodies and organizations with name changes.

o <u>Private Sector Product Certification Programs in the United States</u> (NBS SP 703)
   This directory presents information from 109 private sector organizations in
the United States which engage in product certification activities. Entries
describe the type and purpose of each organization, the nature of the activity,
products certified, standards used, certification requirements, availability and
cost of services, and other relevant details.

o <u>Federal Government Certification Programs for Products and Services</u>
   (NBS SP 714)
   This directory presents information on 61 U.S. Government certification
programs for products and services. Entries describe the scope and nature of
each certification program, testing and inspection practices, standards used,
methods of identification and enforcement, reciprocal recognition or acceptance
of certification, and other relevant details.

o <u>KWIC Index</u> (Computer Output Microform (COM) produced)
   The KWIC Index contains the titles of more than 25,000 U.S. voluntary product
and engineering standards. A standard can be located by means of any significant
or key word in the title. Key words are arranged alphabetically. A standard with
five key words, for example, would therefore be listed in five different places.
To purchase microfiche copies of the 1985 revision of the Index, contact the
National Technical Information Service, 5285 Port Royal Road, Springfield, VA
22161; (703) 487-4600. Use order no. PB86-154408; cost is $13.50 for purchasers
in the U.S.

o tbt news
    This newsletter provides information on government programs and available
services established in support of the GATT Agreement on Technical Barriers to
Trade (Standards Code). tbt news reports on the latest notifications of proposed
foreign regulations; bilateral consultations with major U.S. trade partners;
programs of interest to U.S. exporters; and availability of standards and
certification information. Subscription is free upon request.

o Technical Barriers to Trade
    This booklet explains the basic rules of the international Agreement on
Technical Barriers to Trade negotiated during the Tokyo Round of the Multilateral
Trade Negotiations (MTN), and describes Title IV of the U.S. Trade Agreements Act
of 1979 which implements the United States' obligations under the Agreement. The
Agreement, popularly known as the Standards Code, was designed to eliminate the
use of standards and certification systems as barriers to trade. The booklet
describes the functions of the Departments of Commerce and Agriculture, the
Office of the U.S. Trade Representative, and the State Department in carrying out
the U.S.'s responsibilities.

o "GATT Standards Code Activities"
    This brochure gives a brief description of NBS' activities in support of the
Standards Code. These activities include operating the U.S. GATT inquiry point
for information on standards and certification systems; notifying the GATT
Secretariat of proposed U.S. regulations; assisting U.S. industry with
trade-related standards problems; responding to inquiries on foreign and U.S.
proposed regulations; and preparing reports on the Standard Code.

o Report to the United States Congress on the Agreement on Technical Barriers to
Trade - "Standards Code"
    This 2nd triennial report describes the programs and activities established to
implement the Standards Code in the United States by the four responsible U.S.
government agencies: Office of the U.S. Trade Representative; Department of
Commerce (National Bureau of Standards, International Trade Administration);
Department of Agriculture and Department of State.

o Free handout material on the Office of Product Standards Policy's (OPSP), the
National Center for Standards and Certification Information's (NCSCI) and GATT
activities, and standards-related information such as: Government sources of
specifications and standards, use of the KWIC index, foreign and international
standards bodies, U.S. standards organizations, State purchasing offices, NCSCI
fact sheet and its certification rules activity, and OPSP publications list
(bibliography).

In addition to general inquiry services, the following assistance is also
available:

o GATT Hotline
    A telephone hotline provides current information received from the GATT
Secretariat in Geneva, Switzerland, on proposed foreign regulations which may
significantly affect trade. The recorded message is updated weekly and gives the
product, country, closing date for comments (if any) and Technical Barriers to
Trade (TBT) notification number. The hotline number is (301) 975-4041 (not
toll-free).

13

o <u>Assistance to U.S. and foreign exporters</u> -- Current regulations and certification information for the manufacture of products in the U.S. for export are obtained from foreign countries. To aid foreign exporters, NCSCI provides directory information on State offices prepared to respond to queries concerning conditions to be met by goods for sale in their state, as well as standards and certification information for export to the U.S.

FOOTNOTES

1/ USA Standards Institute, "What is ... a Standard? the USA Standards Institute? a USA Standard?," USA Standards Institute, New York, New York, p. 1.

2/ National Policy on Standards for the United States and a Recommended Implementation Plan, National Standards Policy Advisory Committee, Washington, D.C.,December, 1978. p. 6.

3/ International Trade Administration, The Tokyo Round Agreements: Technical Barriers to Trade - Volume 4, Dept. of Commerce, Washington, D.C., September 1981.

4/ American Standards Association, "Through History with Standards" in Rowen Glie (ed.), Speaking of Standards, Cahner Books, Boston, MA, 1972, p. 38.

5/ Ibid., p. 42.

6/ Ibid., p. 44.

7/ Rexmond C. Cochrane, Measures for Progress: A History of the National Bureau of Standards, National Bureau of Standards, U.S. Department of Commerce, Washington, D.C., pp. 82-86, 1974.

8/ American Standards Association, p. 60.

9/ Ibid., p. 68.

10/ Ibid., p. 50.

11/ International Organization for Standardization, draft revision of ISO Guide 2, "General terms and their definitions concerning standardization, certification and testing laboratory accreditation," July 1985.

12/ W. E. Andrus, Jr., Draft NBS Glossary of Terms for Product Standardization, Product Certification and Laboratory Accreditation, U.S. national Bureau of Standards, Dept. of Commerce, 1974.

13/ American Standards Association, p. 48.

14/ Bureau of Consumer Protection, Standards and Certification: Final Staff Report - April 1983, Federal Trade Commission, Washington, D.C., April, 1983, p. 2.

15/ David A. Swankin, Rationale Statements for Voluntary Standards -- Issues, Techniques, and Consequences, National Bureau of Standards, Dept. of Commerce, Gaithersburg, MD, November, 1981.

16/ International Organization for Standardization, Certification: Principles and Practice, International Organization for Standardization, Geneva, Switzerland, 1980, p. 7.

17/   Douglas B. Thomas, <u>NVLAP Glossary of Terms for Laboratory Accreditation,</u> <u>Product Certification and Standardization</u>, U.S. National Bureau of Standards, Washington, D.C.   1980.

18/   Charles W. Hyer, <u>Principal Aspects of U.S. Laboratory Accreditation</u> <u>Programs</u>, National Bureau of Standards, Gaithersburg, MD 20899, October 1984.

19/   Ibid. 21.

U.S. DEPT. OF COMM. **BIBLIOGRAPHIC DATA** **SHEET** (See instructions)	1. PUBLICATION OR REPORT NO. NBSIR 87-3576	2. Performing Organ. Report No.	3. Publication Date May 1987

4. TITLE AND SUBTITLE

The ABC's of Standards Related Activities in the United States

5. AUTHOR(S)

Maureen A. Breitenberg

6. PERFORMING ORGANIZATION (If joint or other than NBS, see instructions) **NATIONAL BUREAU OF STANDARDS** **U.S. DEPARTMENT OF COMMERCE** **GAITHERSBURG, MD 20899**	7. Contract/Grant No. 8. Type of Report & Period Covered Final

9. SPONSORING ORGANIZATION NAME AND COMPLETE ADDRESS (Street, City, State, ZIP)

10. SUPPLEMENTARY NOTES

☐ Document describes a computer program; SF-185, FIPS Software Summary, is attached.

11. ABSTRACT (A 200-word or less factual summary of most significant information. If document includes a significant bibliography or literature survey, mention it here)

This report provides an introduction to voluntary standardization, product certification and laboratory accreditation for a reader who is not fully familiar with these topics. It highlights some of the more important aspects of these fields; furnishes the reader with both historical and current information on these topics; describes the importance and impact of the development and use of standards; and serves as background for using available documents and services.

12. KEY WORDS (Six to twelve entries; alphabetical order; capitalize only proper names; and separate key words by semicolons)

certification; inspection; laboratory accreditation; standardization; standards; testing

13. AVAILABILITY	14. NO. OF PRINTED PAGES
☒ Unlimited ☐ For Official Distribution. Do Not Release to NTIS ☐ Order From Superintendent of Documents, U.S. Government Printing Office, Washington, D.C. 20402.	23
☒ Order From National Technical Information Service (NTIS), Springfield, VA. 22161	15. Price $9.95